



Corso di dottorato di ricerca in:
Scienze Biomediche e Biotecnologiche

Ciclo 32°

Titolo della tesi

Unveiling the extracellular APE1 role in hepatocellular carcinoma
tumor biology

Dottoranda

Giovanna Mangiapane

Supervisore

Prof. Gianluca Tell

Anno 2020

Abstract

Tumor cells can develop drug resistance via repair mechanisms that counteract the DNA damage from chemotherapy or radiation therapy. The Apurinic/apyrimidinic endonuclease 1 (APE1) is an enzyme involved in the DNA base excision repair (BER) pathway. It confers resistance to chemotherapy or radiotherapy treatments in different kind of tumors like breast, hepatocellular carcinoma (HCC) and lung for this reason it could be considered as a possible target for novel anticancer strategies. Many other non-repair activities are ascribable to APE1, such as the cell response to oxidative stress, the regulation of gene expression and miRNA processing. There are also consistent recent evidences concerning the secretion of APE1, for which elevated intracellular protein levels in cancer are linked to poor prognosis. It was in fact, demonstrated that APE1 is a non-classically secreted protein, and its extracellular release is regulated by the acetylation of K6/K7 residues of the N-Term domain. No data regarding secreted APE1 are still available in HCC. In this study we proved that serum secreted APE1 (sAPE1) could be considered as a diagnostic biomarker in hepatocellular carcinoma (HCC). We provided indications about sAPE1 biological role in HCC, elucidating sAPE1 paracrine function in the regulation of IL-6 and IL-8 mRNA expression. We elucidated also the mechanisms responsible for APE1 secretion using a HCC cell line. Our findings suggest a role of extracellular APE1 as a paracrine pro-inflammatory molecule, and provide a characterization of the APE1 exogenous function, which may modulate the inflammatory status in cancer microenvironment, contributing in the evolution of HCC.

According to previous evidences about APE1 involvement in oncogenic miRNA processing under genotoxic stress, we also provide new indication about its role in miRNAs biology, elucidating its important contribute in miRNA expression/processing regulation and also in miRNA sorting in EVs, which could have great implication in tumor progression and in chemoresistance processes.

Index

<u>Introduction</u>	5
APE1 general overview... ..	6
APE1 gene description and transcriptional regulation.....	6
APE1 protein structure and functions... ..	7
APE1 N-terminal region... ..	9
APE1 redox activity	11
APE1 C-terminal region and its enzymatic activities... ..	13
APE1 as a regulator of gene expression	15
Indirect mechanisms of APE1 gene expression regulation... ..	15
Direct mechanisms of APE1 gene expression regulation... ..	15
The non-canonical APE1 functions	17
Identification of APE1 protein partners to comprehend the non-canonical role of the protein.....	17
APE1 role in controlling gene expression through miRNA processing... ..	19
The APE1 protein partner hnRNPA2B1 is involved in miRNAs assembly in EV	22
APE1 role in RNA metabolism and rRNA quality control.....	25
APE1 non-canonical role in maintaining genome stability through the recognition of abasic or deoxy riboG embedded in DNA.....	25
APE1: a prognostic marker in different tumors... ..	26
Altered APE1 subcellular localization: an important feature in cancer cells.....	27
APE1 in hepatocellular carcinoma (HCC)	28

Extracellular APE1.....	29
APE1 post-translational modifications are responsible for its own extracellular release.	30
Exosomes overview	31
Exosomes biogenesis and characterisation	31
Exosomes content	34
Exosomes and cancer	35
Exosomes and cancer therapy.....	36
<u>Aims of the study</u>	37
<u>Results</u>	39
Chapter 1	40
Serum APE1 (sAPE1) a prognostic biomarker in HCC.....	40
Chapter 2	46
Study of extracellular APE1 role in tumor biology.....	46
Extracellular vesicles characterization from JHH-6 cell line	46
APE1 protein is present in EVs of different cell lines.....	48
APE1 can be efficiently detected in NBI-isolated vesicles	55
EVs APE1 protein is enzymatically active	58
APE1 regulates steady-state levels of intracellular- and EV-sorted RNA content.....	62
Secretion of APE1 p33 form is stimulated by doxorubicin treatment in JHH-6 cell line and by CDDP treatment in A549 cells	68
Soluble rAPE1 triggers SASPs factors expression.....	76
Soluble rAPE1 promotes the activation of IL-8 promoter through NF- κ B transcription	

factor.....	80
Activation of IL-8 gene expression induced by soluble rAPE1 depends on ATM and on the APE1-redox function.....	82
Chapter 3.....	84
Characterization of APE1-hnRNPA2B1 interaction	84
Chapter 4.....	92
Analysis of miRNA expression profiles in hepatocellular carcinoma cells APE1-depleted.....	92
<u>Conclusion</u>	96
<u>Future perspectives</u>.....	103
<u>Material and methods</u>.....	104
Cell culture and treatments.....	105
Viability assay... ..	105
Extracellular vesicles (EVs) isolation	106
Exosome quantification and characterization... ..	106
Exosome extracts preparation (EXE)... ..	107
Whole cell extracts preparation (WCE)... ..	107
Nuclear cell extracts preparation (NCE)	107
Western blot analysis	108
Comassie brilliant blue staining	108
Cell transfection and immuno-purified protein production	109
Co-immunoprecipitation.....	109
siRNA transfection	110

Gene expression analysis.....	111
Description of modified DNA and RNA substrates used in this study	112
Recombinant proteins	113
Serum APE1 quantification	113
Amplified luminescent proximity homogeneous assay (alpha)	114
Enzymatic activity assays	114
Study of IL-8 promoter activity	115
Extracellular vesicle proteolytic activity	115
Proximity ligation assay... ..	116
miRNA targets functional enrichment analysis	116
Statistical Analyses... ..	117
<u>Bibliography</u>	118
<u>Abbreviations</u>	141
<u>List of Publications</u>	145

Introduction

APE1 general overview

Apurinic/Apyrimidinic endonuclease 1/Redox factor 1 (APE1/Ref1), is very well known enzyme that has a great impact in cell viability. It mainly co-operates with other DNA repair proteins for the maintenance of genome stability, being a main actor of the *Base Excision Repair pathway* (BER), but it is also known as master regulator of cellular responses to oxidative stress¹. The importance of this enzyme is due to its pleiotropic activity. Beside the two previously described functions, many other non-canonical roles of the protein have been already characterized¹. In particular, APE1 is a main player in controlling the redox homeostasis, participates in RNA metabolism, RNA stability and decay², and has also influence in the regulation of *microRNA* (miRNA) in quality of DROSHA partner for the miRNA processing³.

Although its multiple functions seem disconnected from each other, APE1 characteristic is to coordinate different activities promoting multiple responses for maintaining cells sustainability.

APE1 is overexpressed in many different tumors and it can support cell proliferation and induce tumor chemoresistance phenomena, for this reason is considered as a good target for cancer therapy.

In the following paragraphs at first will be deeper described APE1 gene and the multiple canonical and non-canonical APE1 functions, later APE1 contribution in cancer will be provided.

APE1 gene description and transcriptional regulation

APE1 gene, called APEX1 is located into chromosome 14q11.2. It is a ~ 3000bp gene constituted of 5 exons interspersed by four small introns. All the exons are translated except for the first one⁴. APEX1 is a TATA less gene, and has multiple *transcription start sites* (TSS) located 130bp upstream the first splice junction¹. The activation of APEX1 gene transcription occurs constitutively at basal levels and also before and during the S-phase of the cell cycle. The transcription is dependent by Sp1 binding

sites. Two Sp1 binding sites, called respectively Sp1-1 and Sp1-2, are located in the proximal promoter region of the gene. The first one is located upstream the CCAAT box and the second one is downstream the TSS. Sp1-1 site is required for the basal APEX1 gene expression, while Sp1-2 is required for the transcription coordinated to cell cycle⁵. The activation of gene transcription is also induced in mild oxidative stress condition. Sub-toxic ROS doses indeed induce the transcription of APEX1 gene and stimulate a sort of “adaptive response” for the following stresses exposure⁶. APEX1 repression on the contrary is regulated by three *negative calcium responsive elements* (nCaRE) elements, that are located ~2000bp upstream into the promoter region, which function is related to a self-negative regulation of APEX1 gene transcription mediated by APE1 protein itself⁷. Also p53 protein seems to have a role in the repression of the APEX1 gene. Even if no p53 binding sites have been found in the promoter of the gene, and no mechanisms have been elucidated yet, it is hypothesised that p53 could indirectly repress APEX1 gene expression, interacting with Sp1 located into Sp1-1 region and inhibiting therefore the basal transcription of the gene⁸.

APE1 protein structure and functions

APE1 is a monomeric protein of 318 amino-acids, consisting of an unstructured portion of 33-35 amino-acids at the N-terminal region and a structured globular portion from residue 44 to residue 318, consisting of two domains, the first one, called N-terminal domain core, from amino-acid 44 to 146 and from 295 to 318, and the second one, called C-terminal domain core, from amino-acid 137 to 260. Every domain is made of six β -sheets surrounded by α -helices which form a four layered α - β sandwich⁹ (Figure1). Actually the information about the tri-dimensional structure of the protein is partial because the X-ray crystallographic structure was performed in the truncated form, lacking of the first 39 unstructured amino-acids¹. For this reason, nowadays there is no a complete description about the interaction of the unstructured N-terminal region with the globular portion and as a consequence of this lacking information no details

about a possible regulation of APE1 activity promoted by the N-terminal region is provided¹.



Figure 1: X-ray crystallographic structure of APE1 truncated form. The interaction with the abasic DNA (green) is also shown ¹⁰.

The N-terminal region is composed by the first 127 residues. The 1-33 amino-acid residues contain the *nuclear localization signal* (NLS). This region is involved in protein-protein interaction and RNA-protein interaction. The residues from 34 to 127 are deputies to the redox activity¹¹, while the C-terminal region is in charge for the endonuclease activity of the enzyme¹² (Figure 2).

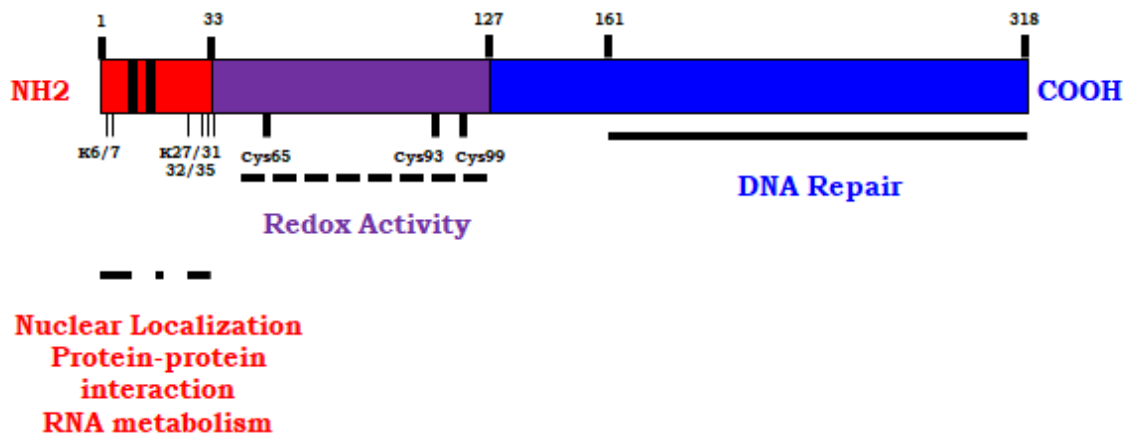


Figure 2: Representation of APE1 protein regions. In red the first 33 amino-acid residues deputies to protein-protein interaction and to RNA-protein interaction. In black are indicated the NLS. In purple the region from aa 34 to aa 127 involved in the redox activity, in blue the C-terminal domain responsible for the endonuclease activity. Regulatory lysine and cysteine residues are also illustrated.

APE1 N-terminal region

It seems that the unstructured N-terminal region of the proteins has an important role in controlling the activity of the enzyme, because of its capability to interact with other protein partners and with RNA¹¹. While the C-terminal region of the protein is structurally conserved in the species during the evolution, the N-terminal domain doesn't and just among mammalian species seems to be conserved with an homology that rises the 90%¹³. The N-terminal region is responsible for the modulation of the multiple APE1 activities¹¹, because of its competence to interact with other proteins like *X-ray repair cross complementing 1* (XRCC1)¹⁴ and *nucleophosmin 1* (NPM1)¹⁵. The refinement of APE1 function, could be determinate by *post translational modifications* (PTMs) that fall into the N-terminal region¹¹. The acetylation for instance of the residues K6 and K7 and the ubiquitination of the residues K24, K25, and K27 are accountable respectively for the PTEN transcriptional regulation¹⁶, and for the APE1 cytosolic localization and degradation mediated by MDM2¹⁷. The acetylation is actually the only PTM find out in vivo¹⁸. This modification promotes a neutralization of the positive charge of the N-tail, determining a conformational variation of APE1.

Due to this conformational change, APE1 is much more prone to interact with chromatin and less inclined to interact with its protein partners. This event was very well characterized studying the dynamic of APE1 and NPM1 interaction¹⁹. The interaction between these two proteins occurs through the K27, K31, K32, K35 residues of APE1 protein. If acetylation of these residues occurs, as demonstrated under genotoxic stresses, the interaction between the two protein fails. As a consequence of this event, APE1 is delocalized from nucleoli and is released into the nucleus, where it can exert the repair activity with a better efficiency^{19 20}. This is a very suitable example of APE1 PTMs that affect its functions according to the biological conditions. Furthermore, the acetylation at the N-terminal region seems to be part to the BER pathway because in its absence an accumulation of AP site in the genome and an increase of sensitivity to stress occurs²⁰. The most glaring PTM that occurs in the N-tail is its cleavage. The loss of the first 33 amino-acid residues of the protein determinates the loss of the NLS and the cytosolic accumulation of the protein as a consequence. The cleavage does not completely abolish APE1 nuclear presence¹, suggesting that other events affect APE1 cellular distribution¹. What is sure is that this PTM affects the usual APE1 protein-protein interactions, while the endonuclease activity of the protein is emphasized¹¹. Nowadays the proteases able to cleave APE1 have not yet been identified, even if during pro-apoptotic stimuli the serine protease Granzyme A is suspected to do it, because of its capability to bound APE1 present in *endoplasmic reticulum-associated complex* (SET)²¹. The N-tail of the protein is important also for supporting cell growth, due to its capacity to interact with RNA molecules. APE1 in fact exerts through these interactions the RNA quality control and the post-transcriptional regulation of gene expression¹¹.

APE1 redox activity

As mentioned before, the APE1 region that lies between amino-acid 34 to amino-acid 127 is involved in the redox activity of the protein¹, which simply exerts the reduction of some TFs conferring their activation. The redox domain takes place in a loop at the N-terminal central core of the globular protein. The identified residues that absolve redox activity are located in a hydrophobic pocket within the core, for this reason probably the protein acquires conformational adjustments which allow the redox reactions^{22,23}. APE1 is a redox factor different from the others because of its capability to makes intermolecular disulphide bounds and to make a complex with *thioredoxin* (TRX) through the formation of mixed disulphide bounds²². The *cysteine* (Cys) residues, responsible for redox activity, that can change their oxidative state through the formation of disulphide bridges or through their switch into a thiol state are the Cys65, Cys93, and Cys99²² (Figure3). The cysteine 65 acts as a nucleophilic cysteine which favours the reduction of TFs disulphide bridges, the residues Cys93 and Cys99 instead act as a resolving disulphide bounds, which are made upon APE1 oxidation²². Three are the possible hypothesised mechanisms by which APE1 could promote the reduction of the TFs. The first one is called the *recruitment model*, where APE1 acts as a bridge between the oxidised TF and the reducing agent. The second one is called the *conformational change model*, in which APE1 promotes some conformational changes to the TFs that allow an exposure of the reducible residues to the reducing agents. The third one is called the *oxidation barrier model*, where APE1 stabilizes the reduced state of TFs through a direct formation of hydrogen bound with the thiol group of the TFs¹. As already mentioned before, APE1 is able to reduce different transcription factors, such as AP-1, p53, NF- κ B, and HIF-1 α through a thiol-based mechanism²³. Due to the variety of TFs that APE1 is able regulate, it can induce pro-apoptotic, but also pro-proliferative signalling, according to the different cellular conditions¹. The different TFs regulated by APE1 have a peculiar role in the progression of many tumors, for this reason the inhibition of APE1 redox function could significantly be taken in

consideration alone or better in combination with other chemotherapy treatments²⁴. E3330, is the most specific APE1 redox inhibitor that actually is in clinical trial for cancer treatment²⁴. It is a quinone that specifically promotes the disulphide bound of Cys65 and Cys93 of the protein, keeping the protein in an oxidised state preventing its role in redox regulation^{23,25}. This small molecule inhibitor is now used in clinical trials²⁴.

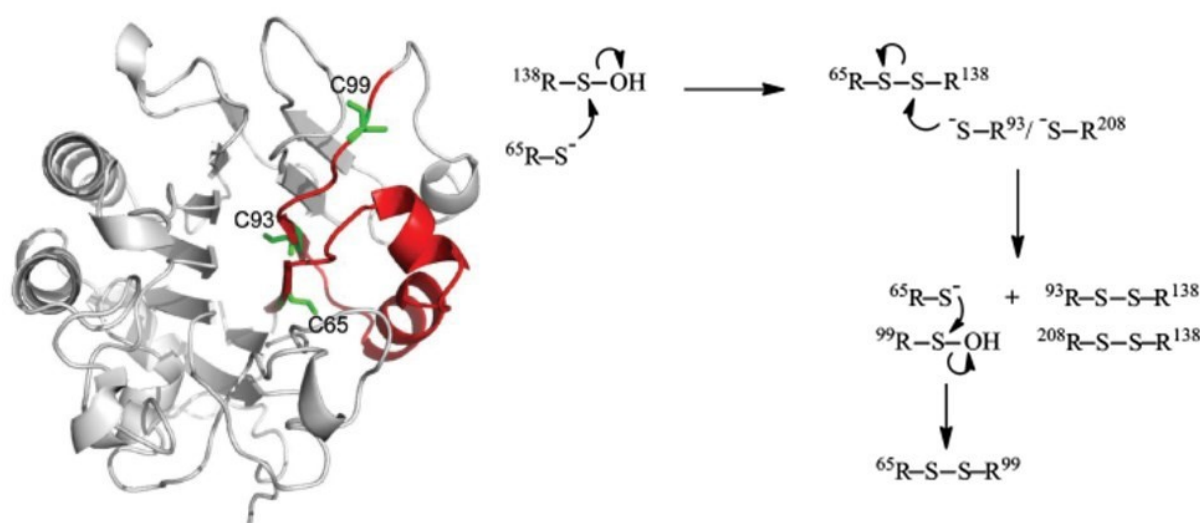


Figure 3: APE1 ribbon representation where cys residues involved in redox activity are represented. The disulphide bonds formation is shown in the reaction scheme on the left²².

APE1 C-terminal region and its enzymatic activities

The C-terminal domain of the protein is deputy for the endonuclease activity. APE1 is mainly known as a DNA repair protein which participates to BER. BER pathway is a DNA repair process, activated as a consequence of the presence of alkylation or oxidative lesions in DNA that could be caused by endogenous or exogenous stresses, such as chemotherapy treatments²⁶. It is specifically involved in the recognition and the following substitution of damaged nucleotides embedded in DNA. This process is characterized by the high coordination of 5 reaction steps and two different sub-pathways are delineated for its execution (Figure 4). The first one is called *Single Nucleotide Base Excision Repair* (SN BER) and is characterized by the substitution of a single damaged nucleotide with an undamaged one through a template directed DNA synthesis²⁷. The second one is called *Long Patch Base Excision Repair* (LP BER), where the damaged nucleotide together with two or more surrounding nucleotides are substituted²⁷. According to the activated sub-pathways different players are involved once the generation of a nick into the DNA is completed. As soon as DNA damage occurs, mono or bi-functional glycosylases recognize the damaged deoxyribonucleotide and remove the injured base, generating a deoxy abasic site. The deoxy abasic site is later recognized and processed by APE1, whose function is to remove the deoxy abasic site, generating a nick on the DNA backbone that is subsequently filled by the activity of DNA polymerase β (Pol β), and sealed by the activity of the complex XRCC1-DNA ligase III (LigIII) if the repair occurs through the SN BER, when instead the repair occurs through the LP BER, Polymerase δ (Pol δ) or Polymerase ϵ (Pol ϵ) together with *proliferating cell nuclear antigen* (PCNA) are deputies to fill the gap, generating a 2-12 nucleotide stretch. *Flap endonuclease 1* (FEN1) later removes the excess of nucleotides and *Ligase I* (LigI) seals the nick²⁶.

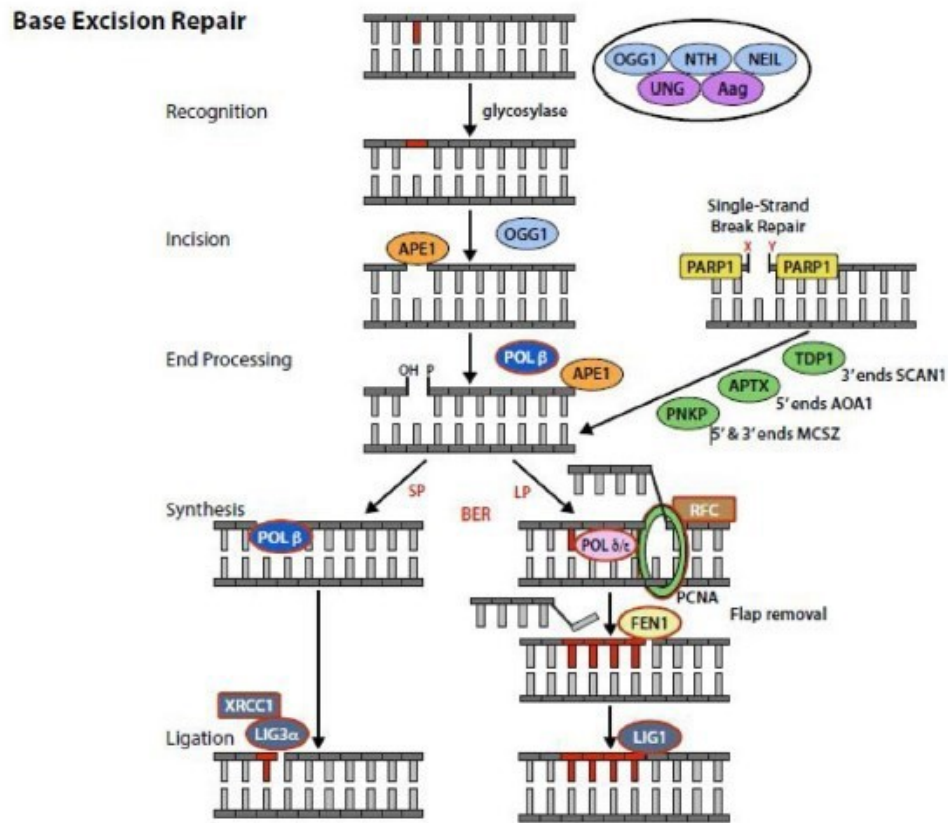


Figure 4: Cartoon of BER. All five reaction steps are illustrated, pointing out both SP and LP ²⁸.

APE1 not only removes deoxy-abasic sites embedded in DNA, but exerts also enzymatic activities upon non-canonical substrates. It in fact, possesses endonuclease activity on abasic single stranded RNA, weak 3'-5' exoribonuclease activity, and it also takes part to the *nucleotide incision repair pathway* (NIR)²⁹. NIR pathway is an APE1 enzymatic activity recently discovered. In this process, APE1 directly removes specific damaged by oxidative stress bases such as, 5-hydroxy-2 -deoxyuridine, 5,6-dihydro-2 -deoxyuridine, bypassing the action of the glycosylases. The N-tail of the protein is essential for this repair pathway, because NIR activity is strongly reduced in APE1 lacking of the first 33 amino-acids (APE1^{NA33})³⁰. Therefore, others non canonical APE1 substrates were recently characterized by our laboratory. APE1 in fact, is able to remove ribo-abasic sites and deoxy-ribonucleotides embedded in DNA²⁹. All of these activities strengthen the importance of APE1 in the maintenance of genome stability.

APE1 as a regulator of gene expression

One of the non-repair activity exerted by APE1 and supported by post-translational modification is the regulation of gene expression. APE1 in fact can act as a co-activator or as a co-repressor of gene transcription through redox dependent and redox independent mechanisms and also through indirect and direct mechanisms²⁶.

Indirect mechanisms of APE1 gene expression regulation

The indirect mechanism of gene expression regulation is related to APE1 capability to modify the redox status of many TFs, promoting their activation, as already described. Nowadays numerous are the identified TFs regulated by APE1 such as p53, NF- κ B, PEBP-2, CREB, HIF-1 α , AP-1, Egr-1³¹⁻³³ and the majority of them have a relevant role in controlling cell proliferation and apoptosis, confirming APE1 important role in the maintenance of cellular homeostasis^{16,33,34}.

Direct mechanisms of APE1 gene expression regulation

Besides the indirect way to participate in gene regulation, recent evidences about a direct mechanism of controlling gene transcription have been found. In particular, it seems that APE1 can regulate gene expression also through epigenetic modifications³⁵. One example is related to its capability to interact with specific promoter regions of the regulated genes called nCaRE³⁶. The nCaRE-sequences are DNA regulatory regions which APE1 interacts with through its N-terminal domain³⁶. They are sequences characterized by having ALU repeats and are used to be in correspondence of many gene promoters³⁷. APE1 interacts with these regions together with other proteins like the *Heterogeneous nuclear ribonucleoprotein L* (hnRNPL), PARP1 and Ku70/80³⁶. Examples of negative regulation of gene expression mediated by APE1 through its interaction with nCaRE-sequences are the inhibition of *parathyroid hormone* (PTH),

renin and Bax transcription^{36,38-40}. On the contrary, one example of positive regulation through nCaRE-sequences is the activation of SIRT1 gene upon oxidative stress. APE1 lies in the nCaRE-sequences of the promoter of SIRT1. During genotoxic stress, oxidised deoxy-nucleotides located in this region are recognized and repaired by APE1. The endonuclease activity of the protein, probably favours important chromatin changes at level of the promoter that allows the transcription of the gene³⁶. Other example of direct regulation of gene expression mediated by the endonuclease action of APE1 upon oxidised guanine located in G-quadruplex structures of some gene promoter it has been recently described. This mechanism it has been elucidated for the activation of VEGF gene. Oxidative stress causes the oxidation of guanine present in G-quadruplex. First intervenes the glycosylase OGG1 to remove the injured base and later APE is recruited in correspondence of the a-basic site. It seems that APE1 role in this context is much more associated to the recruitment of the transcription factor machinery to the gene promoter rather than for the execution of its endonuclease activity upon the generated a-basic site⁴¹. The aforementioned examples suggest that the activation of DNA repair processes could be an instrument for the regulation of gene expression for better controlling the sustainability of living cells⁴¹. Noteworthy, sometimes both direct and indirect mechanisms intervene together. This is what happens during the activation of VEGF transcription in hypoxic conditions of solid tumors⁴². Under hypoxic conditions HIF-1 is activated by APE1 through a redox-dependent manner. Therefore, the oxidative stress induced by hypoxia causes the oxidation of guanine located in correspondence of *hypoxic response element* (HRE) of the VEGF gene. The originated 8-oxoguanine are recognised by OGG1, and later APE1 exerts the endonuclease activity. The originated single strand breaks cause the modification of VEGF promoter topology which favours the activation of gene transcription⁴².

The non-canonical APE1 functions

After the description of the canonical APE1 functions, an overview about the non-canonical APE1 roles will be offered to the reader.

Identification of APE1 protein partners to comprehend the non-canonical role of the protein

APE1 interactome analysis shows the plethora of APE1 protein partners offering a general overview of APE1 contribution to cell sustainability, DNA repair and regulation of gene expression. Through the analysis of APE1 protein partners is much more immediate to comprehend not only its contribution in canonical function but also in its non-canonical ones. APE1 is able to interact with 103 proteins species³. Analysing APE1 interactors, five functional annotation clusters have been delineated, and consequently APE1 participates in the following five biological pathways: RNA processing, DNA Repair, *Double Strand Breaks* (DSB) repair, Transcriptional Regulation and Apoptosis. These clusters are not independent each other, but many factors participate in more than one group (Figure 5), interconnecting different pathways^{3,26}. This analysis gives information about the multifunctional role of APE1, which is not only associated to DNA Repair pathway and transcriptional regulation, but is also able to contribute in RNA processing, and RNA metabolism, due to its capability to interact with ribonucleoproteins like hnRNPK and factors involved in miRNA processing like SFPQ⁴³. The majority of APE1 protein partners that has been found (~60%), contributes to the RNA processing³. Moreover, has been also observed that the interaction between APE1 and many protein partners is mediated by RNA molecules, suggesting that APE1 could have a strong influence in RNA metabolism³.

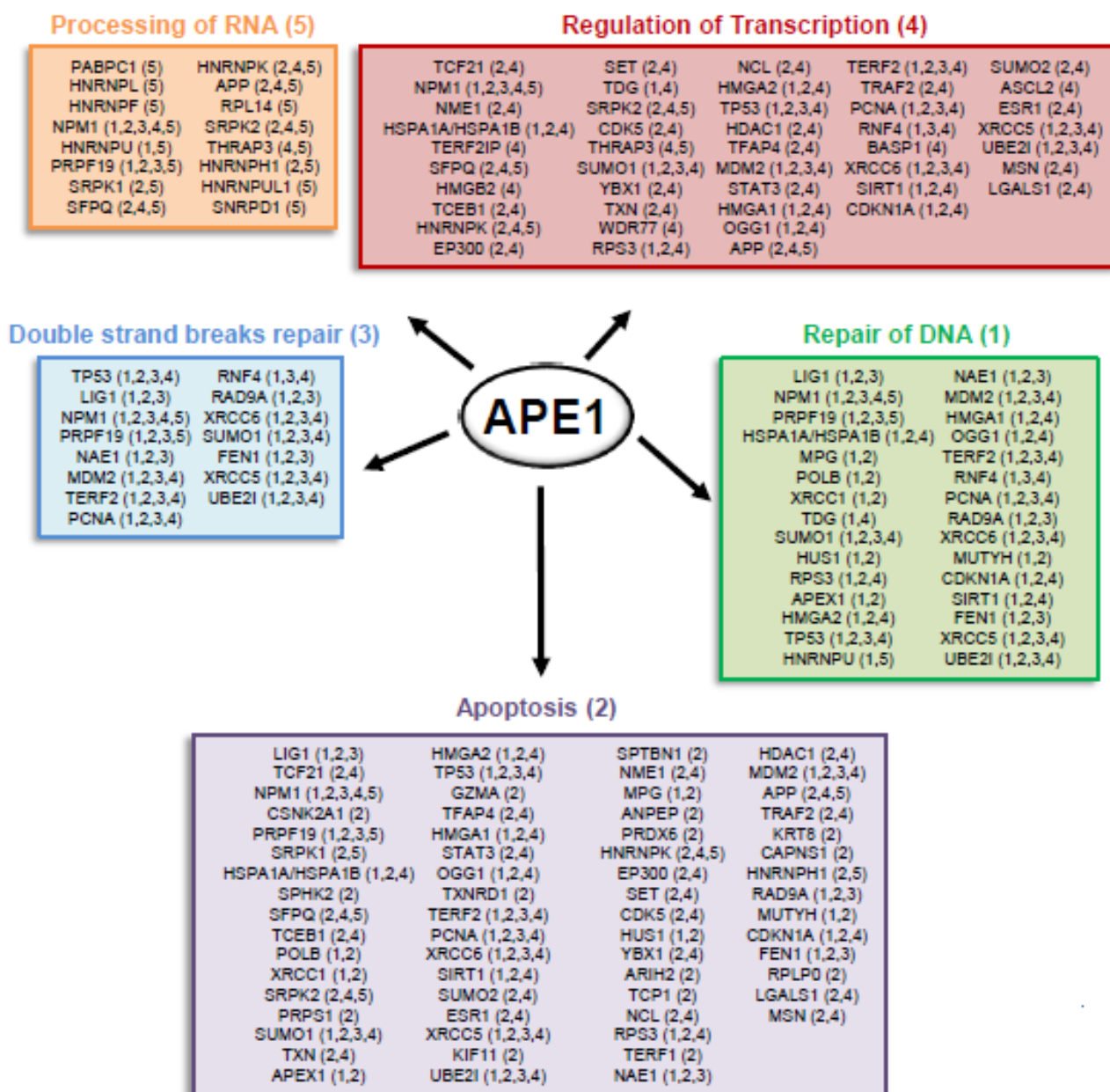


Figure 5: Functional annotation clusters of APE1 interactors. APE1 is represented as the fulcrum of the interactome and proteins partners are listed in five charts corresponding to the biological pathways³.

APE1 role in controlling gene expression through miRNA processing

One of the first non-canonical APE1 functions is its capability to interact with damaged abasic RNA and to process it⁴⁴. APE1 in fact is able to recognize and interact with RNA through its N-terminal domain and possesses 3' RNA phosphatase, 3' exoribonuclease activity⁴⁵ and also endoribonuclease activity on abasic sites containing RNA. The endoribonuclease activity is due to its capability to cleave abasic single stranded RNA contributing to the RNA decay. This activity of the protein has been observed in mRNA molecules, for instance in c-myc mRNA⁴⁶, but also in microRNAs such as miR-21 and miR-10b⁴⁴, giving suggestions about a duplex APE1 role in controlling post-translational regulation, not only directly affecting the mRNA half-life, but also through the control of microRNAs^{3,44}.

MicroRNAs are small non coding RNA molecules ~ 23nt long, in charge to post-translational regulation of gene expression. These molecules in fact through a base pairing with the mRNA targets prevent their translation and cause their degradation. MicroRNAs undergo maturation processes. They are transcribed by *RNA Polymerase II* (Pol II) and are organized in a stem and loop RNA structure having unpaired 3' and 5' ends. The RNase III Drosha, together with the RNA binding protein *DiGeorge critical region 8* (DGCR8) are delegate to cleave the unstructured tails of the pri-miRNA, originating the pre-miRNA hairpin precursor. The pre-miRNA is later exported from nucleus to cytoplasm through *Exportin-5 protein* (XPO-5), where another RNase III, called Dicer, processes the pre-miRNA in a mature 22nt RNA duplex miRNA. Just the complementary strand of the target mRNA is finally loaded into the *RNA induced silencing complex* (RISC), which has the function to guide base pairing between the new synthesized miRNA with its own mRNA target. *Argonaute* (AGO) proteins at the end of the process are the effectors for the translational repression and mRNA decay^{47,48}.

RNA molecules can be modified upon oxidative stress. The oxidation events are not random in the transcriptome but some RNAs are much more susceptible than others.

In Alzheimer's disease for example, oxidation events upon certain mRNAs strongly contribute to the pathogenesis of the illness impairing protein synthesis⁴⁹.

Recent evidences suggest also that microRNAs can be modified by oxidative stress. The oxidation events can make microRNAs prone to recognize their own target. Worthy of note is the case of microRNA 184 (miR-184), that becomes able to recognize its targets Bcl-xL and Bcl-w inducing apoptosis⁵⁰ after oxidative modifications events that occur in its own sequence. Moreover, sometimes oxidative modifications which occurs to miRNA molecules are responsible for modulating their activity promoting an exchange of targets⁴⁷.

Recently our laboratory found APE1 contribution in the regulation of miRNA processing. Nanostring analyses performed in knock down APE1 HeLa cell lines showed that the absence of the protein caused a substantial dysregulation of mature microRNAs, suggesting APE1 peculiar role in their regulation.

Moreover, experiments performed upon HeLa cell lines subjected to genotoxic stress through hydrogen peroxide (H₂O₂) treatment, showed an up-regulation of many microRNAs, among them the miR-221 and miR-222. Because of miRNA 221 and 222 are responsible for the post-translational regulation of the tumor-suppressor PTEN, which transcription is regulated by APE1¹⁶, our laboratory decided to proper characterize this regulation trying to discover the hypothetic APE1 role in the regulation of modified oxidised miRNAs. APE1 is overexpressed in many tumors and the analysis of its interactome suggested its important contribution in the regulation of gene expression through the miRNA processing. The obtained results showed that APE1 is responsible for regulating the onco-miR 221 and 222 who interact with. It seems in fact that under genotoxic stress APE1 intensifies its interaction with the RNase III Drosha, which is deputy for the processing of pri-miRNA (Figure 6). The endonuclease activity of APE1 protein seems indispensable for the processing of these two pri-miRNAs, because treating the cells with the inhibitor of APE1 endonuclease activity compound 3 (#3) an accumulation of pri-miRNA 221 and 222 was observed,

demonstrating the impairment of pri-miR processing when this activity of the protein is compromised. All of these data suggested that APE1 has a role in regulating PTEN expression not only directly acting to the transcription but also through post-transcriptional regulation, in particular controlling miRNA 221 and 222 processing and/or stability during genotoxic stress³. This mechanism could be probably extended to many APE1 targets strengthening the importance of APE1 role in RNA metabolism³.

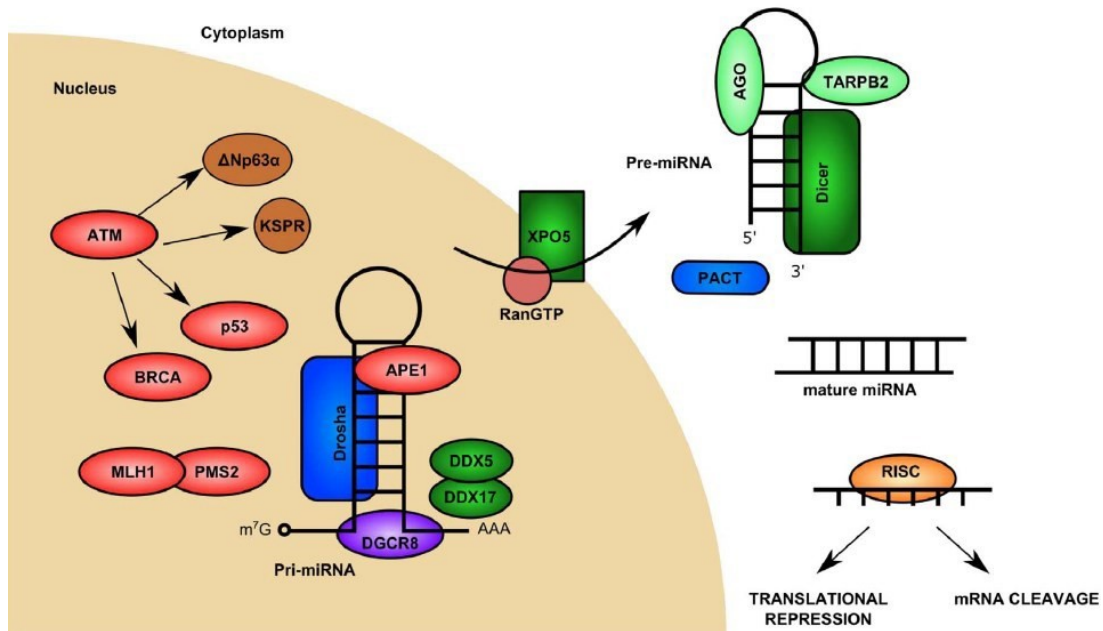


Figure 6: Cartoon illustrating APE1 putative role in controlling miRNA processing. APE1 could take part together with Drosha in processing of newly transcribed oxidised pri-miRNAs²⁶.

The APE1 protein partner hnRNPA2B1 is involved in miRNAs assembly in EVs

APE1 is able to interact with different ribonucleoproteins, as already mentioned before. The ribonucleoproteins belong to a family of more than 20 polypeptides, which range size goes from 34 to 120kDa⁵¹. Their heterogeneous nature makes them able to absolve different functions. They interact with DNA and mostly with RNA, through their RNA recognition motifs, taking part to a series of nuclear processes such as telomere maintenance, transcription, DNA replication and repair, pre-mRNA splicing and nucleus-cytosol mRNA export⁵¹.

According to interactome analysis, one APE1 protein partner is the ribonucleoprotein SNRPD, also called hnRNPA2B1³. hnRNPA2B1 is composed by two different isoforms hnRNP A2, of 341 amino-acids, and B1 of 353 amino-acids, both transcribed by HNRNPA2B1 gene and characterized by having two tandem RNA recognition motifs followed by a Glycine reach region consisting of an *arginine/glycine-rich* (RGG) box and a M9 domain. The last one is a non-canonical NLS, indispensable for the nuclear localization of both subunits. hnRNPA2B1 protein is structured in a tetramer consisting of three A2 and one B1 subunits and is involved in many activities in particular in *alternative splicing* (AS) regulation⁵¹⁻⁵⁴, RNA degradation, microRNAs sorting^{55,56}. hnRNPA2B1 deregulation is a feature of many diseases such as cancer⁵⁷, *amyotrophic lateral sclerosis* (ALS)⁵³ and other neurodegenerative disorders such us *multisystem proteinopathy* (MSP). MSP consists in muscles, brain and moto-neuron degenerations, due to mutations occurrence in RGG box of the protein which cause the formation of fibrils structures between the mutated subunits (*self-seed fibrils*) and also between the mutated and the wild type ones (*cross-seed fibrils*). These fibrils are later accumulated in cellular stress granules and are probably responsible for neuro-degenerative diseases initiations⁵⁸. hnRNPA2B1 is overexpressed in many tumor like breast cancer, glioblastoma and lung cancer, where is considered a biomarker for early stage of tumor detection, because is responsible to induce Sp1 protein synthesis

through its ability to interact with Sp1 5'UTR mRNA and to promote the CAP independent translation of the transcript^{57,59–61}. hnRNPA2B1 is involved in exons inclusion of many AS mRNAs in the whole transcriptome^{53,54}. An alteration of AS provokes many cellular disorders such as cancer⁵⁴ and ALS. In ALS for instance, a depletion of hnRNPA2B1 causes the synthesis of a shorter *D-amino acid oxidase* (DAO), an enzyme involved in serine metabolism, which works less efficiently as a consequence of an altered splicing event and is responsible for ALS excitotoxicity⁵³. HnRNPA2B1 is also able to recognizes UAGG motifs in 3'UTR of many central nervous system transcripts⁵³ and through targeting of 3'UTR RNAs motifs, is able to promote RNAs decay⁵⁵. Moreover, HnRNPA2B1 has an important role for miRNA processing⁶². The protein in fact, recognizes *N*⁶-methiladenosine (m⁶A), an RNA specific modification, and directly interacting with DGCR8, induces the processing of the pri-miRNAs carrying this modification⁶² (Figure 7).

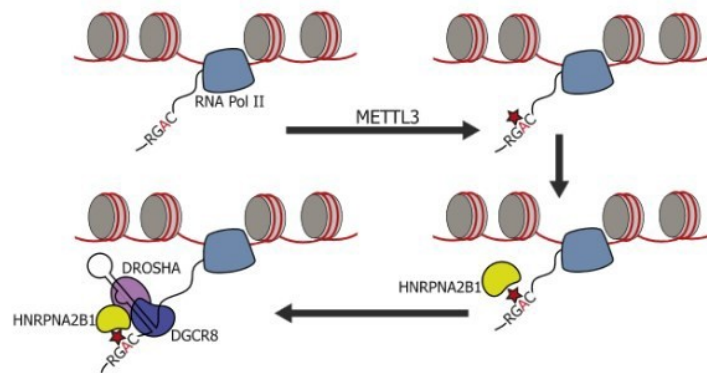


Figure 7: Representation of hnRNPA2B1 miRNA processing regulation. hnRNPA2B1 recognizes m⁶A upon new synthesized pri-miRNAs and interacting together with DGCR8 facilitates the processing process⁶².

HnRNPA2B1 is not only important for promoting a regulated miRNA processing but is also involved in promoting miRNAs sorting into exosomes (Figure 8). The miRNAs selected carry a specific motifs called EXO motifs, a short GGAG sequence, which is recognised by a sumoylated hnRNPA2B1, which is in charge of loading the selected miRNAs into the particles⁵⁶.

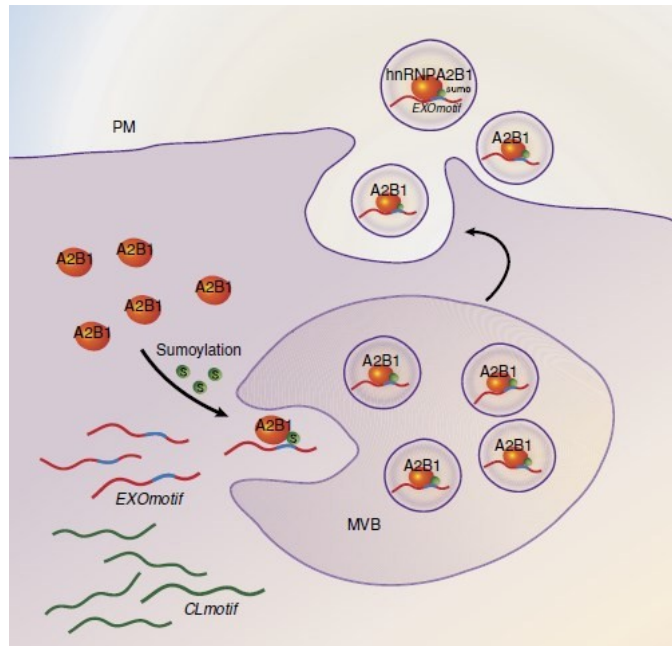


Figure 8: Representation of miRNA sorting process exerted by hnRNPA2B1. Sumoylated hnRNPA2B1 is able to recognize EXO motifs of selected miRNAs and participates in their loading into exosomes⁵⁶.

HnRNPA2B1 has also important role in the regulation of gene expression of clustered genes flanked by DSBs hot spots. The DSBs hot-spots are extended regions 50-250kb long, where hnRNPA2B1 and *Poly ADP Ribose Polymerase 1* (PARP1) interact and participate for their transcriptional regulation⁶³. The DSBs hot-spots seem to be a peculiar chromatin organization for rDNA, where the transcription is controlled by H₃K₄me₃ epigenetic marker, which occurs in correspondence of the CTCF binding sites. Also in correspondence of rDNA DSBs hot-spots hnRNPA2B1 interaction occurs, suggesting its contribution in rDNA expression through epigenetic modifications⁶⁴.

Among its numerous functions hnRNPA2B1 offers also a contribution in telomere maintenance, because it favours telomere elongation promoting telomere G-quadruplex unfolding and allows DNA template and RNA telomerase components interactions⁵¹.

Because of the multiple roles of this protein, many of them in common with APE1 functions, in future it will be interesting to unveil if these two proteins participate together in some cellular processes.

APE1 role in RNA metabolism and rRNA quality control

APE1 takes part also in rRNA quality control. Studies performed on inducible APE1 kd HeLa cell line, demonstrated that under genotoxic stress a greater accumulation of oxidised RNA species is observed. Moreover, in basal conditions, APE1 down-regulated cells showed an impairment of cell growth due to an inefficacy of translational machinery and a reduction of the total cellular protein amount⁶⁵. These relevant evidences suggest that APE1 exerts the role of RNA cleansing factor for genotoxic stress and that has a role also in controlling the quality of transcribed RNAs before their translation. APE1 localizes in nucleoli interacting with NPM1. Seems that the interaction APE1-NPM1 inhibits the ribonuclease activity of the protein, and actually nothing is known about the hypothetic role of this protein complex during normal conditions. When oxidative stress occurs, the protein is released from nucleoli to the nucleoplasm where it can exert the DNA damage response^{15,65}. For all these reasons NPM1 seems to have an important role in controlling APE1 functions and BER modulation⁶⁶.

APE1 non-canonical role in maintaining genome stability through the recognition of abasic or deoxy riboG embedded in DNA

Ribonucleotides triphosphate (rNTPs) cellular amount is much higher compared to *deoxyribonucleotide triphosphate* (dNTPs) one (~ 40-350-fold higher in cycling cells) because cells need a greater quantity for transcription^{67,68}. During normal condition there is a default frequency of *ribonucleotides monophosphate* rNMPs incorporation into DNA that was estimated around ~ 100milions of residues per cell cycle²⁹. These events of incorporation are much more frequent under genotoxic stress because the production of reactive oxygen species promotes the oxidation of *deoxyribonucleotide triphosphate* (dNTPs) in rNTPs⁶⁹. The incorporation of rNMPs in genomic DNA causes a topological distortion of the sequence, giving rise to genome stability issues^{67,70}. The

enzyme RNase HII is involved in the recognition and removal of rNMPs incorporated in DNA through *ribonucleotides excision repair* (RER) pathway⁷¹. Studies demonstrated that RNase HII is not able to remove abasic rNMPs embedded in DNA. Our group recently found that APE1 is the only enzyme able to do it, having also a weak activity upon oxidised rNMPs embedded in DNA, opening a new scenario about APE1 contribution in controlling genome stability²⁹.

APE1: a prognostic marker in different tumors

Due to its pleiotropic activity in controlling genome stability, regulating gene expression and controlling RNA quality, APE1 actively intervenes in several cellular mechanisms, for this reason its dis-regulation is associated to different pathologies such as neurodegenerative and cardiovascular disorders and above all to cancer^{1,72}. Numerous are the evidences in literature asserting APE1 overexpression as a prognostic factor in many tumor such as prostate cancer, hepatocellular carcinoma, lung carcinoma, oral squamous carcinoma, prostate cancer and ovarian adenocarcinoma^{73–80}. APE1 overexpression in fact is associated with deregulated cancer cell proliferation and with the activation of chemoresistance mechanisms, for all of these reasons it is considered as a good target for anticancer therapy¹. APE1 overexpression is a frequent event, which occurs in many neoplastic diseases, probably because a dis-regulation of APE1 gene expression occurs during cell transformation¹. APE1 is a ubiquitous protein, which can show different subcellular distribution according to cell types. It is mainly located in nuclei⁸¹, particularly into nucleoli together with its interactor NPM1, where probably can perform the rRNA quality control. During oxidative stress, as explained before, it comes out from nucleoli and it is distributed into nucleoplasm, where it can exert the DNA repair activity⁶⁵. But there are also evidences about APE1 cytoplasm localization and this distribution has been found in cells having high metabolic and proliferative rate. Even if there is no still explanation about APE1 role in cytosol, it is supposed that probably could contribute

in DNA repair into the mitochondrial compartment⁸², and also could be responsible for ROS reduction in endoplasmic reticulum through *Rac Family Small GTPase1* (Rac1) inhibition^{31,83}. Noteworthy, in many kind of cancer like breast, ovarian, lung and hepatocellular carcinoma, its overexpression and its cytosol localization are markers of poor prognosis and shorter overall survival⁸⁴. In hepatocellular carcinoma for instance, these features could be associated to an adaptive response to chronic oxidative stress, that could support hepato-carcinogenesis and also tumor progression^{75,84}. Further studies need to be performed to comprehend APE1 role in “unusual” cellular compartment in order to understand its contribution in tumor biology.

Altered APE1 subcellular localization: an important feature in cancer cells

As already mentioned, APE1 subcellular localization is a dynamic finely regulated event^{1,65}. An overexpression and a dis-localization of the enzyme is registered in many tumor as explained before, like breast cancer and hepatocellular carcinoma and it is also considered a prognostic factor. For *Acute myeloid leukemia* (AML) instead, a kind of blood tumor in which APE1 is expressed at normal extents, what is interesting is a frequent genetic mutation of NPM1 gene, that causes both APE1 and NPM1 dislocation. This mutation was found in OCI-AML3 cells, which show abnormal APE1 cellular distribution, due to a frameshift mutation in *C-term* (CTD) of NPM1. This common dominant genetic alteration causes conformational changes in the third helix of NPM1-CTD, that gives rise to a greater aggregation propensity and also confers a modest toxicity of the protein⁸⁵. Due to this mutation, NPM1 is dislocated into cytosol (NPM1c⁺). Because NPM1 is indispensable to held APE1 into nucleus, as a consequence of this mutation also APE1 is dislocated into cytosol. In this kind of tumor the impairment of APE1 correct localization, causes deficit in DNA repair, and OCI-

AML3 for this reason are more sensitive to chemotherapy treatment, compared OCI-AML2, which not bring NPM1 mutation, confirming APE1 contribution in chemoresistance^{15,85}.

APE1 in hepatocellular carcinoma (HCC)

Hepatocellular carcinoma is the second cause of cancer lethality over the world. The incidence of this disease is constantly growing and 40.710 it has been the estimation of new cases in 2017⁸⁶. Moreover, many studies for comprehending the biology and the prevention for this kind of tumor are still needed. HCC onset can be determined by an inflammatory status triggered by many possible causes, for instance viral infections such as *chronic hepatitis B* (HBV) and *C* (HCV), chronic alcohol consumption, cirrhosis, *non-alcoholic steatohepatitis* (NASH), some genomic alterations and neoplastic dysplasia^{87,88}. Chronic inflammation causes cirrhotic tissue formation, which trigger to dysplasia focus formation that can acquire malignancy features, and becoming cancer. Different grade of this disease have been identified. From a *low-grade dysplastic nodules* (LGDN), the transformation can proceed in an intermediated status call *high grade dysplastic nodule* (HGDN) which culminates in the advanced stage defined HCC. Due to the severity of the disease and to its high incidence, the individuation of HCC biomarkers for its prognosis, are needed. For this purpose, transcriptomic studies on different tumor stage specimens⁸⁷, and also on circulating miRNAs and protein biomarkers have been performed⁸⁹⁻⁹¹. In HCC APE1 is upregulated in terms of protein and transcript levels. APE1 amount is higher in low differentiated tumors compared to the high differentiated ones and it seems to have a protective role against oxidative stress, safeguarding cells for triggering apoptosis process through BAX inhibition⁷⁵. Besides APE1 upregulation, cytosolic localization is also considered as a prognostic marker for HCC. This is a peculiar feature of cancer cells since normal cells retain APE1 in nucleus compartment. Moreover, higher level of cytosolic APE1 were found in poorly differentiated tumors, compared to the well differentiated ones, and patients

having high cytosolic APE1 levels showed lower overall survival. For all of these reasons APE1 can be considered as a prognostic biomarker for HCC⁸⁴. Information about the possible function of cytosolic APE1 in this kind of cancer are still missing and our laboratory is making efforts for better characterize and comprehend this phenomenon and its contribution in the HCC tumor biology.

Extracellular APE1

APE1, as already explained, is a negative prognostic factor in many tumor, due to its capability to promote cell proliferation and also chemoresistance mechanisms for instance through the induction of the drug efflux transporter protein MDR1 expression⁹². The first evidences about APE1 presence in serum samples came out in 2011, when autoantibodies for the protein were detected in sera of Lupus erythematosus patients⁹³. Because of its predictive role in cancer, and of the necessity to find new tumor prognostic biomarkers, the Dong Wang group together with his collaborators, started to look APE1 in sera samples and surprisingly they found higher APE1 levels in sera of *not small cell lung cancer* NSCLC patients compared to controls⁹⁴. They also noticed that APE1 could be defined as a predictive biomarker for the patient's response to platinum-based chemotherapy⁹⁵, because its higher levels in tissue and sera are responsible for a decreased sensitivity to treatments. The obtained evidences studying NSCLC regarding APE1 as a serological biomarker for the disease are also confirmed in other tumor types for instance in bladder cancer⁹⁶. It would be now useful to unveil the extracellular APE1 function. Regarding this point recent studies suggested that APE1 could participate in inflammatory response because its secretion is induced in monocyte after inflammatory stimuli, and its role could be connected to the inflammatory response induction through NF κ B activation, which is responsible for IL-6 gene transcription^{97,98}. Would be not the first time in which a DNA repair protein can act as a *senescence-associated secretory phenotype* (SASP) factor. SASP are immune-modulatory factors such as IL-6 and IL-8, but also growth factors, survival

molecules that can act as autocrine proteins strengthening the senescence phenotype and also as paracrine factors stimulating *epithelial to mesenchymal transition* (EMT) and tumor progression⁹⁹.

Another evidence suggested also that secreted hyper-acetylated APE1 can induce the initiation of apoptotic process *via receptor for advanced glycation end product* (RAGE) activation in *triple negative breast cancer* cells (TNBC)¹⁰⁰. The authors in this case excluded the possibility of a downstream NFκB pathway activation *via* RAGE. Further investigation will be useful for comprehending extracellular APE1 role, which could be connected to tumor progression.

APE1 post-translational modifications are responsible for its own extracellular release

In the last 6 years, literature offered some interesting indications regarding APE1 extracellular release. Before then, a software called Secretome 2.0¹⁰¹, which offers a prediction of the secreted proteins plethora, individuated APE1 as an un-canonical secreted protein.

APE1 is a protein which shuttling from cytoplasm to nuclei was observed in response to oxidative and nitrosative stress¹⁰². Its localization is regulated by the N-term of the protein, where acetylation events mediated by *p300 histone acetyl transferase* (HAT) can occur¹⁰³. Many are the proteins which secretion is mediated by acetylation occurrence, on example is the *high mobility group-1 protein* (HMGB1)¹⁰⁴. In 2013 the same release mechanism it has been proposed for APE1, whose extracellular release seems to be based on the occurrence of N-terminal K6 and K7 lysine residues acetylation¹⁰⁵. In this work the authors demonstrated that an inhibition of *histone deacetylases* (HDAC) mediated by *trichostatin A* (TSA) promotes APE1 secretion. The same group offered the first indication about APE1 presence in plasma sample of lipopolysaccharide-

induced endotoxemic rats¹⁰⁶, offering a first explanation about the extracellular APE1 role and defining the protein as a serological biomarker for endotoxemia.

The acetylation upon N-terminal domain is a modification having important relevance not only for APE1 secretion but also for cancer progression. It was recently demonstrated how acetylation events are correlated in sustaining cell proliferation in NSCLC¹⁰³. Acetylation occurrence in the N-terminal domain of the protein in fact, not only protects the protein from cleavage, but it is also indispensable for promoting APE1 role in the regulation of gene expression for supporting cancer cell proliferation. In tumor tissues indeed, this post translational modification seems to arise with higher efficiency compared to normal tissues in which APE1 proteolysis greatly occurs¹⁰⁷. These evidences suggest a mechanism by which APE1 is a promoter of cell proliferation in tumor through acetylation events which prevent its cleavage¹⁰⁷.

Exosomes overview

Exosomes are nanovesicles, whose dimension range is approximately from 20 to 100nm. They originate from the fusion of endosomal *multivesicular bodies* (MVBs) with the plasma membrane and the consequent release of new generated particles in to the extracellular compartment. Deeper information about exosomes characterization and function are still needed. There are already some indications about the potentiality of these microvesicles to act as a carrier of proteins and nucleic acids, that are later accepted by the recipient cells and affect their metabolism^{108,109}.

Exosomes biogenesis and characterisation

MVBs are constituted of many *intraluminal vesicles* (ILVs), originated by MVB membrane invaginations. The ILVs formations can occurs through different mechanisms and information about the regulation of these different processes and the

possible differences between the cargo selection promoted is still missing¹¹⁰. The first mechanism proposed involves lipid rafts in MVBs membrane, which can promote the ILVs formations. The lipid rafts are constituted by ceramide, that is generated by the protein *neutral sphingomyelinase 2* (nSMase2). nSMase2 hydrolyses sphingomyelin in ceramide, which confers negative MVBs membrane folding and the consequent ILVs formation and inclusion into MVB¹¹¹.

The ILVs formation could be also promoted by the *Endosomal Sorting Complex Required for Transport* (ESCRT), which manages a cargo selection. ESCRT complex is constituted by five complexes ESCRT-0, ESCRT-I, ESCRT-II, ESCRT-III and Vps4¹¹² (Figure 9). ESCRT-0 recognizes ubiquitinated proteins, which are later recruited by ESCRT-I and ESCRT-II complexes, generating a dense zone of cargo proteins, in the meantime the invagination of MVB membrane occurs. ESCRT-III is required for the assembly of the ILVs content through the de-ubiquitination of the cargo, and thanks to its spiral shape it restricts the ILVs neck and it concludes the formation of the ILVs, where the proteins are seized. Once the ILVs is generated, the protein cargo is sorted inside the new vesicles and the ATPase Vps4 complex fulfils the disassembly of the ESCRT-III complex and the release of the ILV inside MVB occurs¹¹². Once formed MVBs can be fused together with lysosomes or can be released such as exosomes outside the cell through the plasma membrane. Actually there are no indications about the regulation of the MVBs shunting and the possible differences of protein content between “degradative” MVBs and “secretory” MVBs^{113–115}. The secretory MVBs are transported in proximity of plasma membrane along microtubules by kinesin. Different RAB proteins, according to different cellular types (normal or tumor cells), are responsible for MVBs docking to the plasma membrane^{116–118}. Subsequently, *soluble N-ethylmaleimide-sensitive component attachment protein receptor* (SNARE) proteins promote the exosomes extracellular release^{119,120}.

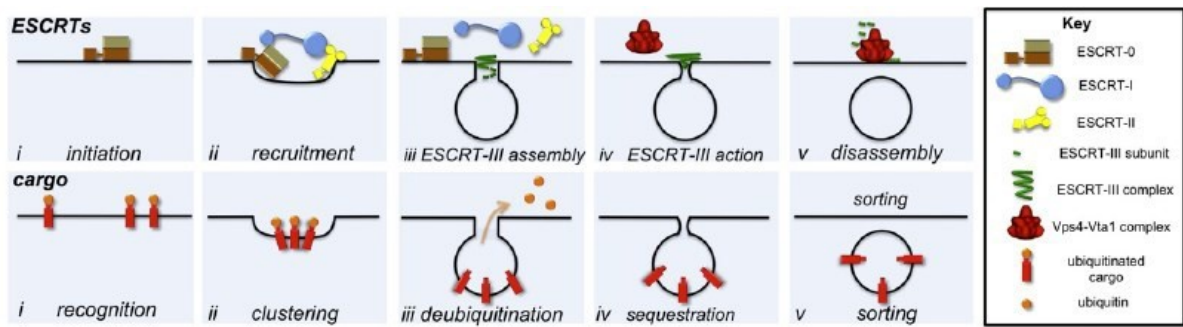


Figure 9: ESCRT-mediated ILV formation. Ubiquitinated cargo is recognised by ESCRT-0. ESCRT-I and ESCRT-II are recruited and dense protein cargo is formed followed by membrane invagination. Subsequently ESCRT-III deubiquitinates the protein cargo, which is now sequestered and it restricts the neck of the new formed vesicles. Vsp4-complex disassembles ESCRT-III and it allows the release of the new ILV inside MVB¹¹².

Recently has been observed that syndecan heparan sulfate proteoglycans are important for exosomes formation via ESCRT complex. Syndecan interacts with the adaptor protein syntenin, which makes a bridge between proteoglycan components and ESCRT complex, interacting with Alix protein, which is a protein associated with ESCRT-III complex¹²¹. There is a specific guide for EVs characterization (Figure 10). Exosomes in fact, possess proteins which participate together with ESCRT complex for the assembly of the vesicles such as the aforementioned syntenin, Alix, TSG101, and they also possess the tetraspanins such as CD63, CD9, CD81, scaffold membrane proteins, important for the recruitment of cargo proteins. To fully define the extracellular vesicles as exosomes, is necessary to detect at least three indispensable proteins which participate in their synthesis such as syntenin, Alix and CD63^{122–124}.

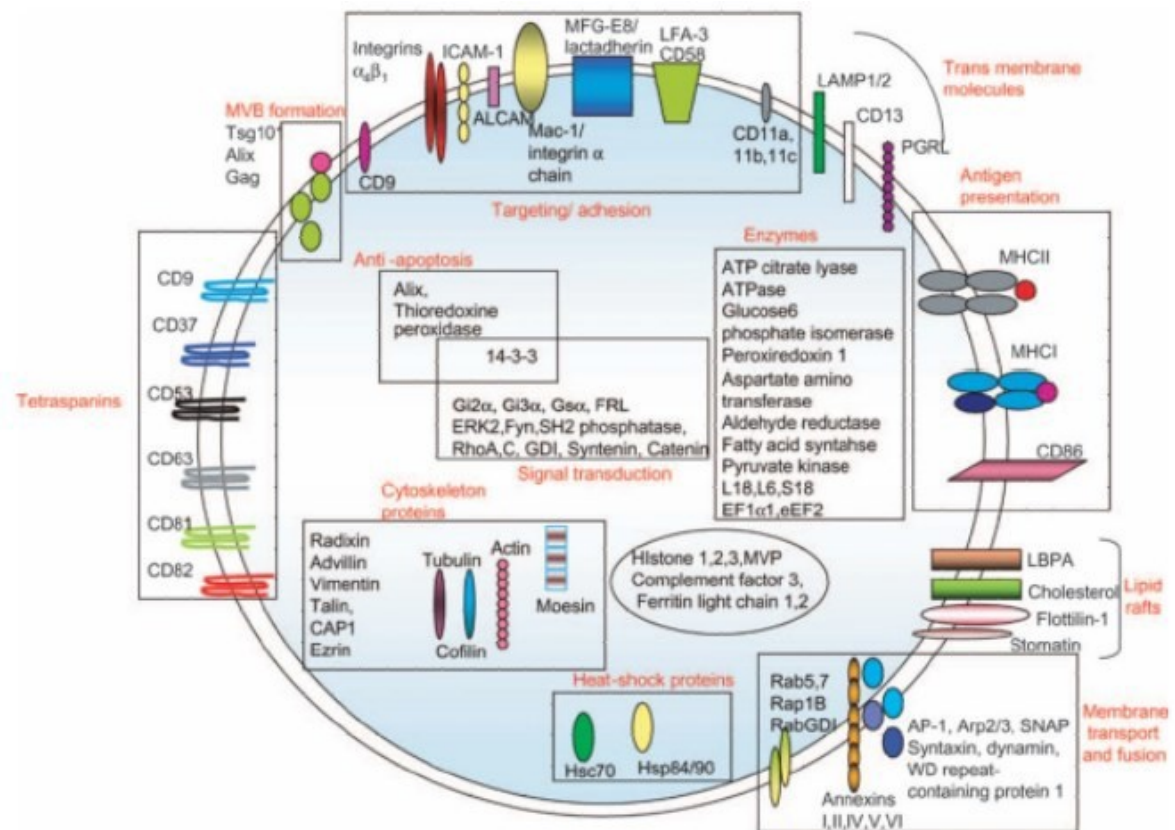


Figure 10: Exosomes protein constitution. Intravesicular and transmembrane proteins are illustrated.

Exosomes content

Exosomes can be directly received by the neighbouring cells or travel into bio-fluids such serum, saliva, blood, breast milk¹²⁵ and act very distantly¹¹⁰, distributing their molecular content. Exosomes contain lipids such as sphingomyelin, cholesterol, phosphatidylserine¹²⁵, proteins, small RNAs, and also *mitochondrial DNA* (mtDNA) and *fragmented genomic DNA* (gDNA)^{110,126}.

The majority of the protein content identified in exosomes until now seems to be necessary for the formation of the vesicles, but there are some evidences about the presence of oncoproteins in exosomes derived from tumor cells, or molecules that can modulate immune response of receiving cells, involved in tumor propagation, such as the receptor for tyrosine kinase MET and Hsp72^{127–129}. Further investigations about

exosomes protein contents will be helpful to understand exosome function in cellular communication.

As already mentioned, exosomes contain many RNA molecules such as mRNAs, *long non coding RNAs* (lncRNAs) and miRNAs. mRNAs loading into exosomes could depend on a specific sequence, “zipcode”-like, (CUGCC), which is present in the 3’UTR of exosomal mRNAs¹³⁰. Noteworthy, among RNA molecules present in exosomes, microRNAs are the most abundant¹¹⁰. Some ribonucleoproteins have an important role in the sorting of specific miRNAs into exosomes¹³¹, one example is the already described APE1 protein partner hnRNPA2B1, which is deputy for recognizing and loading miRNAs, having a specific EXO motif (GGAG) sequence⁵⁶. Also gDNA, no more longer than 10kb, has been found in exosome particles, even if it is impossible to exclude in this case contamination with apoptotic bodies and EVs membrane fragments, due to the ultra-centrifugation methods used for the exosomes extraction¹²⁶. Usually, gDNA can be released in the cytosol after DNA damage occurrence, and induces the activation of DNA sensor proteins which promote the beginning of senescence or apoptotic pathways¹³². The release of gDNA through exosomes, may prevent the activation of cytosol DNA sensor factor and may protect damaged cells from senescence mechanisms activation promoting cellular homeostasis. This mechanism would explain why cancer cells are much more prone to exosomes release¹³³.

Exosomes and cancer

It seems that under un-physiological conditions, especially under stress conditions such as hypoxia and cancer, the exosomes release is increased but, the specific mechanism of the regulation of this process is still unknown^{108,134,135}. As the healthy cells secreted less exosomes compared to the tumor cells, studying exosome functions at basal condition is very difficult, easier instead it is acquire information about exosomes contribution in tumor progression and metastasis¹²⁵, due to a greater concentration of exosomes released by tumor cells, such as ovarian, pancreatic, and

breast cancer^{125,136,137}. Through the analysis of circulating exosome content some markers specific for certain kind of tumors can be used for diagnosis, reinforcing the relevant role of these EVs.

There are many indications about the powerful action of exosomes to induce certain behaviours in receiving cells, especially through oncogenic miRNAs delivery¹¹⁰ and many are the microRNAs that have been individuated with a great potential in the tumor features propagation, because they are able to affect the whole transcriptome of the receiving cells¹²⁵. Some miRNAs may also be considered as good target for the diagnosis of a specific tumor and are also predictive biomarkers, because they are indicative of the stage of the disease. One example could be miR-21, which is highly expressed in serum of patient with oesophageal squamous carcinoma, and it is indicative of an advanced stage of the tumor¹³⁸. Another example is miR-141, which expression in serum of patients with prostate cancer is indicative of metastatic process establishment and for this reason it is considered a poor prognostic factor¹³⁹. Recent evidences suggest also that miRNAs derived from metastatic cells are able to induce a malignant transformation in receiving cells, demonstrating the important role of exosomal miRNAs in tumor propagation¹⁴⁰.

Exosomes and cancer therapy

Exosomes contribute to tumor spread, proliferation and metastasis. They are able to activate chemoresistance and radio-therapy resistance in the recipient cells¹⁴¹, and affect chemotherapy treatment efficacy, because they are responsible for exocytosis of chemotherapeutic drugs such as cisplatin and doxorubicin from tumor cells^{142,143}. These evidences suggest that exosomes could be considered as a good target for cancer treatment. Affecting exosome production and release in fact could be possible abolish oncogenic miRNAs transferring to hamper metastatic propagation¹⁴⁴. Future and deeper investigations about exosomes composition, cargo selection, and functions need to be done to comprehend this new emergent cell-cell conditioning system and its important relevance in cancer progression.

Aims of the study

Nowadays, new evidences are emerging about active secretion of APE1 by cancer cells and its involvement as a biomarker for different kind of tumors. It seems that extracellular APE1 is involved in regulation of apoptotic or inflammatory processes, even if no clear evidences about its biological impact in tumor biology has been elucidated, yet. Moreover, indication about extracellular APE1 and its contribution in chemoresistance have been recently provided. Our hypothesis is that APE1 might operate as a *damage associated molecular pattern* (DAMP) factor in tumor microenvironment, triggering the inflammatory response. Exosomes are released EVs that deliver proteins, RNA and DNA molecules. Their production and secretion is higher in tumor cells compared to the healthy ones, for this reason EVs become vehicles of tumor effector factors and significantly participate in the progression of the disease.

In this work we wanted to explore the extracellular APE1 role in the progression of HCC, by measuring the sAPE1 amount in sera of affected patients in comparison with healthy controls. We wanted also to study the sAPE1 secretion process and its biological contribution to tumor progression, focusing our attention on the activity of APE1 in triggering inflammation responses.

We wanted also to unveil the APE1 contribution in HCC tumor progression and chemoresistance, by investigating its role in the regulation of miRNA processing/decay. For this purpose, we carried out Nanostring analysis in JHH-6 APE1 silenced cells, to detect miRNAs, whose expression is affected by APE1 in HCC.

To understand the APE1 role in miRNA processing regulation, we wanted to characterize its interaction with the ribonucleoprotein hnRNPA2B1, which participates in RNA splicing, miRNA processing and miRNA EVs sorting, performing CoIP and PLA analyses. Further investigations need to be performed to analyse the hypothetic role of this protein complex in the circulating miRNAs world. Data

obtained clearly pointed to the relevance of studying the extracellular roles of this unusual DNA repair proteins for translational and personalized medicine.

Results:

Chapter 1

Serum APE1 (sAPE1) a prognostic biomarker in HCC

Serum APE1 is considered as a negative prognostic biomarker in NSCLC and bladder cancer^{94,96}. To understand if also in HCC sAPE1 could be considered as a prognostic biomarker, its detection in serum samples of 99 HCC, 50 cirrhotic and 100 healthy patients, was carried out, through the Human APEX1 ELISA kit, as already reported in⁹⁵. The case-control study was performed in patients referring to the Liver Center of the University Hospital of Trieste and the aetiology of HCC samples analysed, derived from alcohol or metabolic syndrome. Serum APE1 levels were obtained by using a standard linear regression curve fitting by NCSS 11 Statistical Software (2016). For the specificity of the test, 62.5 and 31.25 pg/ml of rAPE1 protein were spiked into blood donor's sera. It was used a curve-fitting model, built on OD vs sAPE1 concentration (pg/ml) for the evaluation of the two spiked samples (data not shown).

As reported in Figure 11, the levels of APE1 protein, obtained by ELISA and expressed as median (95% CI), are significantly higher in serum of HCC patients (median= 75.8 pg/ml), compared to the healthy donors (median= 10.8 pg/ml). Intermediate concentration values have been found for cirrhotic patients (median= 29.8 pg/ml), indicating that with the evolution of the disease a progressive increase of sAPE1 is observed. These experiments were executed in collaboration with Fondazione Fegato (FIF), Trieste, Italy.

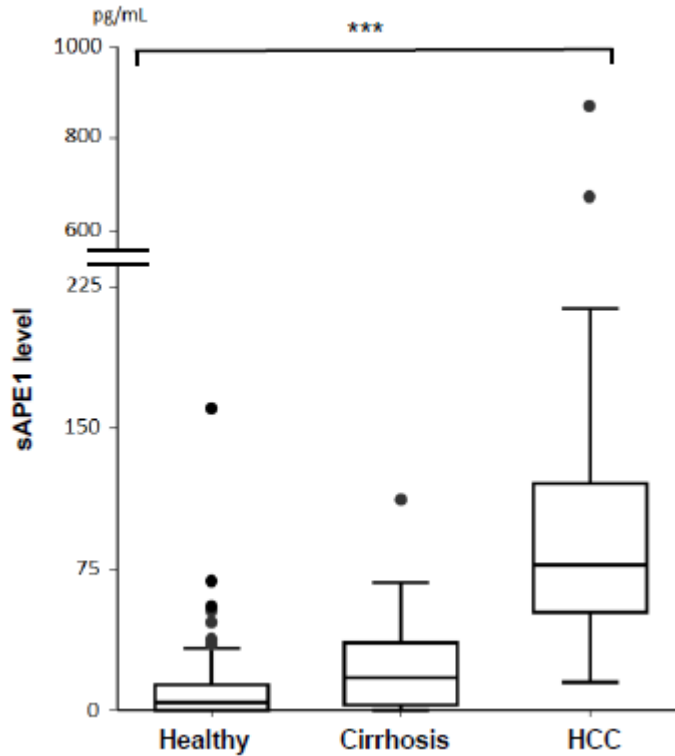


Figure 11: Serum APE1 protein levels detection in healthy, cirrhotic and HCC blood donors. ***P<0.001.

In order to evaluate if the observed trend was coherent to APE1 tissue expression in terms of mRNA and protein levels, qPCR and western blot analysis were performed. APE1 mRNA expression levels resulted increased in HCC tissue samples compared to the healthy control (CTRL), moreover intermediated mRNA levels were registered in *surrounding liver cirrhosis* (SLC) and peri-HCC tissues. Data were normalized for 18S RNA and ACTB expression levels (Figure 12). Western blot for APE1 protein levels were carried out analysing the protein content of a pool of HCC tissue sample lysates, compared with that one of SLC. We observed higher APE1 protein levels in HCC tissue compared to SLC. Moreover, two bands for APE1 protein, the first one of 37 kDa correspondent to the full length, and the second one shorter correspondent to the truncated APE1^{NA33} form, were detected (Figure 13, *left panel*). The densitometry analysis of APE1 immune-reactive bands normalized for actin in both HCC and SLC was reported in the histogram (Figure 13, *right panel*). These data demonstrated a correspondence between serum and tissue APE1 levels.

These observations were also confirmed through immunohistochemistry analysis in HCC, SLC and CTRL. Interestingly HCC tissue was characterized by having higher level of APE1, but also an altered cellular distribution of the protein (Figure 14). APE1 in fact, was localized non only in the nuclei of HCC cells, but also in the cytoplasm, while in SLC only an overexpression of the protein was observed, without showing any alteration of its distribution. Control cells instead, displayed normal protein expression levels and localization. These data indicated that in HCC tumor biology APE1 overexpression can be followed by its displacement. Unfortunately, we could not provide correlations between APE1 cellular dislocation and serum secretion.

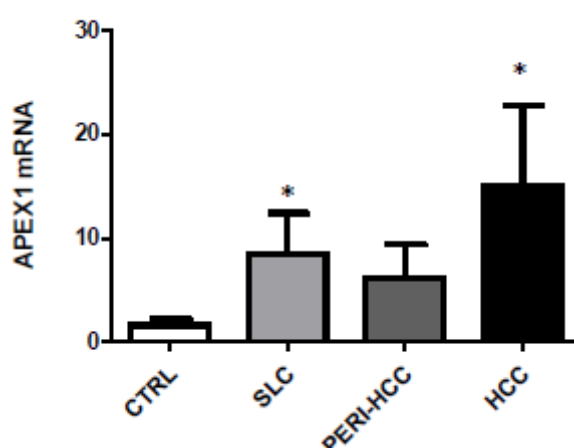


Figure 12: APE1 mRNA expression levels in HCC, peri-HCC, surrounding liver cirrhosis (SLC) and CTR tissues. Bar graph indicates mean and SEM.

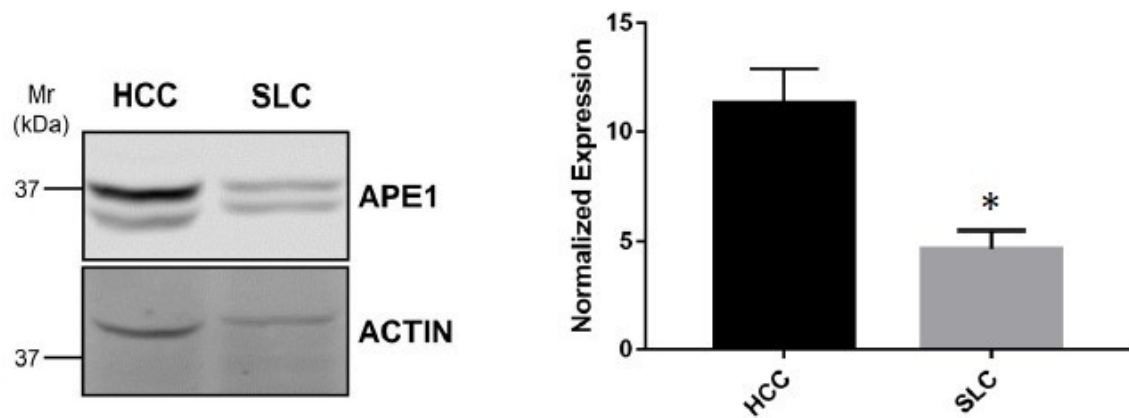


Figure 13: Western blot analysis carried out in lysates of SLC and HCC tissue samples. Actin was used as a loading control. Histogram shows the densitometric analysis of APE1 protein content normalised for actin. Bar graph indicates mean \pm SD of three independent experiment. *P<0.05.

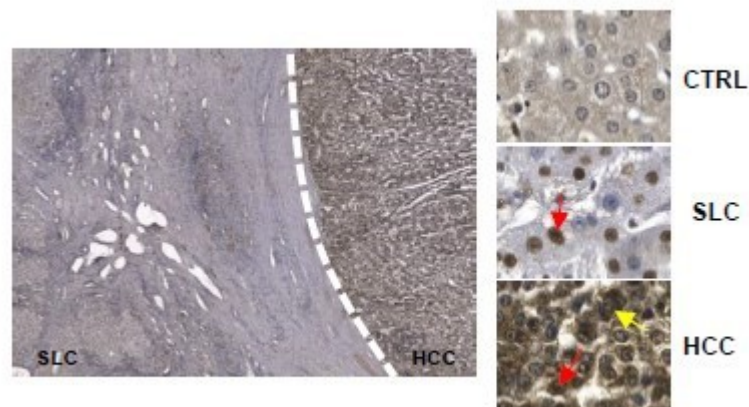
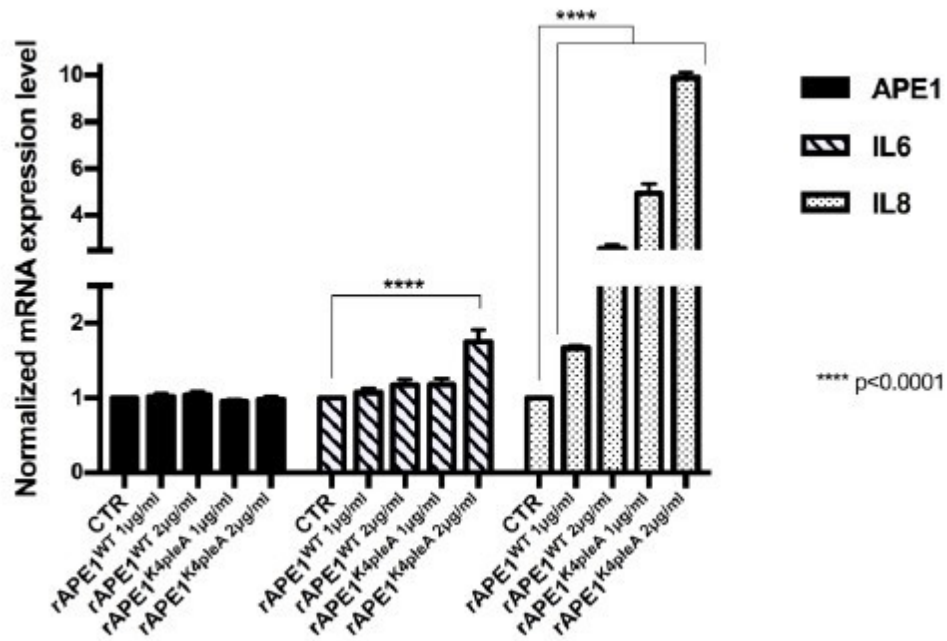


Figure 14: Immunohistochemistry carried out on SLC, HCC and CTRL tissues. Red arrows indicate nuclear APE1 localisation. Yellow arrow indicates cytosolic APE1 distribution.

In order to unveil serum APE1 biological role, we tested if exogenously added recombinant purified APE1 protein (rAPE), could trigger an inflammatory response activating interleukins expression, as already demonstrated for human monocytes cells⁹⁷. For this purpose, JHH-6 hepatocellular carcinoma cells were treated for 24

hours with “non-tagged” rAPE1^{WT} and also with rAPE1^{K4pleA}, an APE1 mutant form where lysine residues (K27, K31, K33 and K35) of the N-terminal domain are replaced by arginine, mimicking a constitutive acetylation status of the protein, that, as it already demonstrated, has a relevance in tumor proliferation¹⁰⁷. We proved that exogenously added rAPE1 was able to promote IL-6 and IL-8 mRNA expression and that the mutated form rAPE1^{K4pleA} induced a greater extent of activation compared to the rAPE1^{WT} (Figure 15A). TNF- α treatment performed for 3 hours at the concentration of 2000U/ml was performed as a positive control for IL-6 and IL-8 activation (Figure 15B). According to these data, serum APE1 could be defined as a prognostic biomarker in HCC and exogenous APE1 could participate to the HCC progression contributing in perpetuating the inflammatory status.

A



B

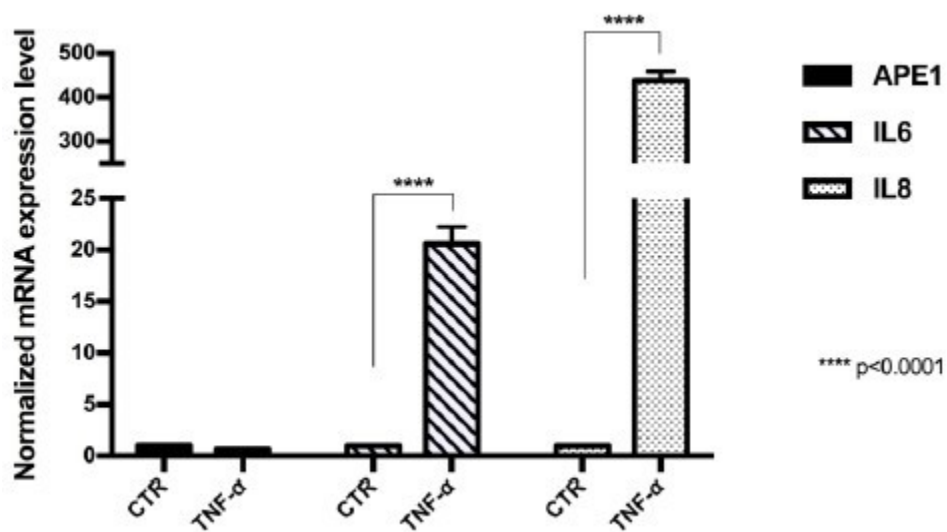


Figure 15: **A)** APE1, IL-6 and IL-8 expression levels in JHH-6 cell line treated for 24 hours with rAPE1^{WT} and rAPE1^{K4pleA} proteins at the concentration of 1/2µg/ml. Serum starved cells for 24 hours were used as a control. **B)** APE1, IL-6 and IL-8 mRNA expression levels of JHH-6 cells treated for 3 hours with TNF-α at the concentration of 2000U/ml. Untreated cells were used as a control (CTR). Data represent means ±SD of three independent experiments. Statistical analysis was achieved by applying Two-way ANOVA test. ****P<0.0001.

Chapter 2

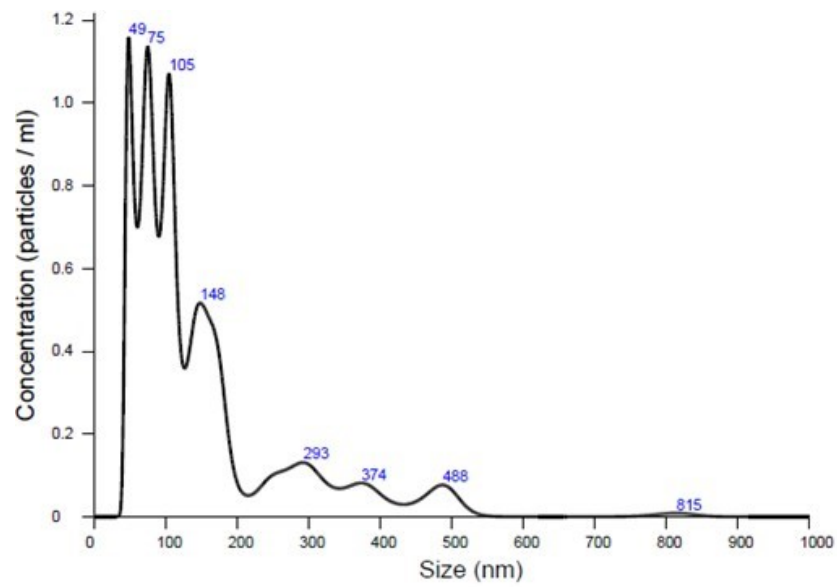
Study of extracellular APE1 role in tumor biology

Once it was demonstrated that sAPE1 could be considered as a biomarker in HCC, an analysis on the secretion mechanism of the protein, its function or effects were evaluated.

Extracellular vesicles characterization from JHH-6 cell line

In order to set up the conditions to analyze *extracellular vesicles* (EVs), we isolated them, by Total exosome isolation kit, from the media of JHH-6 hepatocellular carcinoma cell line and characterized the quality of the preparations (*see Material and Methods*). Particles were analysed by dynamic light scattering using the NanoSight instrument for *nanoparticle tracking analysis* (NTA). The distribution of the obtained vesicles and the measured range of size, that showed an average of 237nm with a mode of 149.5 nm, indicating the expected dimensions of small vesicles, were shown in (Figure 16A). Regarding the EVs shape and size characterization, vesicles obtained from serum depleted medium of JHH-6 cells were validated by TEM (Figure 16B). The image shows vesicles having a round shape with a mean diameter below 100 nm, corroborating the NTA analysis. Therefore, this characterization confirmed that the EVs preparations we used in our assays are compatible with exosomes.

A



B

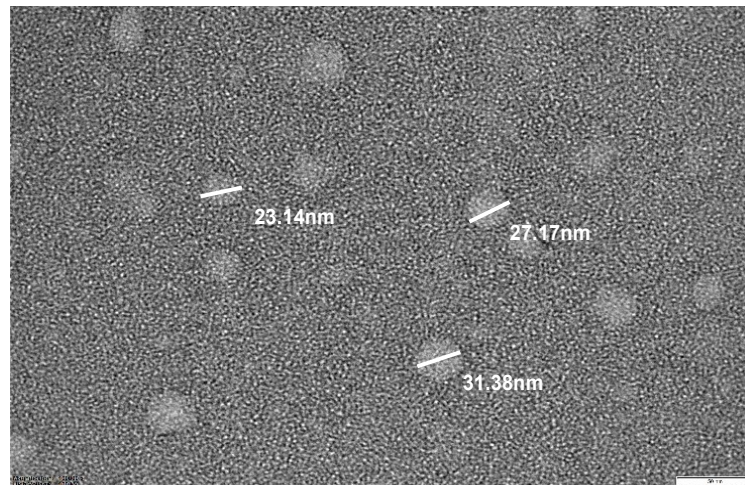


Figure 16: JHH-6 exosome vesicles characterization. **A)** NTA analysis of JHH-6 exosomes. The picture shows the quantification spectre of exosomes extracted from JHH-6. The prominent vesicles size range registered is from 50 to 150nm, correspondent to exosome range dimensions. **B)** TEM analysis of exosomes extracted from JHH-6 medium after 48 hours. The picture shows spheroid exosome particles. The diameter of exosome particles registered is below 100nm.

APE1 protein is present in EVs of different cell lines

Some recent preliminary evidences showed the presence of APE1 in the extracellular environment. However, limited information is available regarding the mechanism of this secretion as well as if it may be associated with EVs release⁹⁷. For these reasons, we were interested in understanding if APE1 could be secreted in EVs. To test this hypothesis, JHH-6 cells were kept in culture for 48h under serum starvation conditions and, later, EVs were extracted from the serum-free medium. The *EVs extract* (EXE) prepared, was analysed for the presence of APE1 protein. As positive control for proper EVs isolation, enriched in exosomes, Syntenin and Alix proteins were analysed. In addition, *Golgi apparatus protein* (GM130) was assayed as an EXE negative marker¹⁴⁵. Moreover, JHH-6 *whole cell extract* (WCE) was used as a reference control for protein expression. As shown in (Figure 17), JHH-6 EXE were positive for the presence of APE1 full length, indicated as (APE1 p37), but were also positive for the truncated form of 33kDa, indicated as APE1 p33.

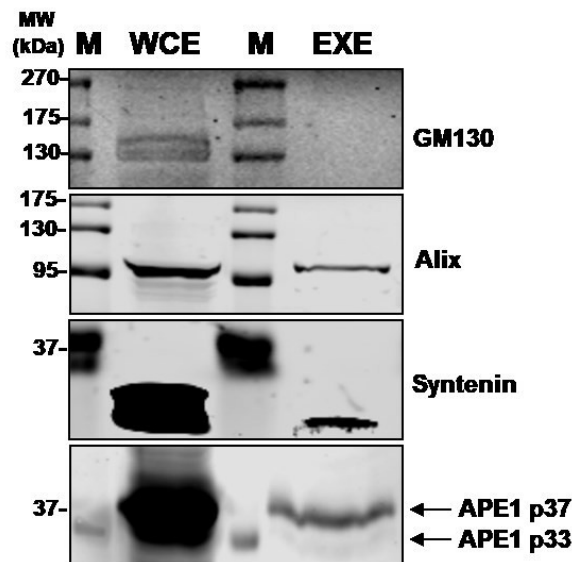


Figure 17: APE1 detection and quantification analysis in exosome extract. Western blot analysis performed in whole cell extracts (WCE) and exosome extract (EXE) of JHH-6 cells. APE1 detection was observed in JHH-6 EXE. WCE were used as a reference control for APE1 expression (*panel below*). Cellular and exosome markers were also tested for EXE characterization. Golgi apparatus protein GM130 was assayed as a EXE negative marker (*panel above*), Alix and Syntenin were assayed as a EXE positive markers (*middle panels*).

Notably, by using an antibody specific for the N-terminal part of APE1 we were able to demonstrate that this truncated form corresponded to the N Δ 33 form (Figure 18), which lost the first 33 amino acid residues as a consequence of proteolysis, already described in previous papers by us and others^{15,107}.

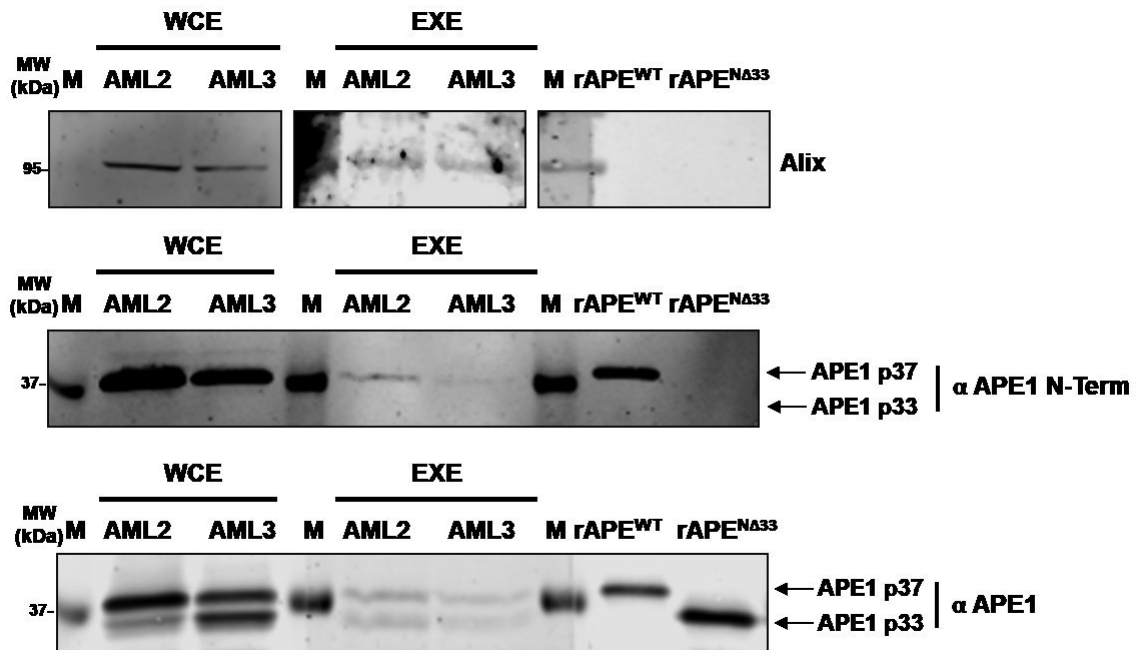


Figure 18: Western blot analysis of APE1 p37 and p33 forms in WCE and EXE of AML2 and AML3 cell lines. Alix detection was performed as a loading control (*panel above*). Two different APE1 antibodies were used. In the *middle panel* antibody against APE1 N-terminal region detects only full length APE1, the detection of both isoforms is observed using anti APE1 antibody (*panel below*).

We also tested the presence of other base-excision repair (BER) enzymes in exosomal fractions and we demonstrated the presence of XRCC1 protein. Interestingly, the absence of Pol δ , OGG1, and of the highly abundant intra-nuclear Pol β protein, was indicative of the fact that APE1 release is a specific process and is not associated with the release of BER proteins as a consequence of general cell disruption processes (Figure 19).

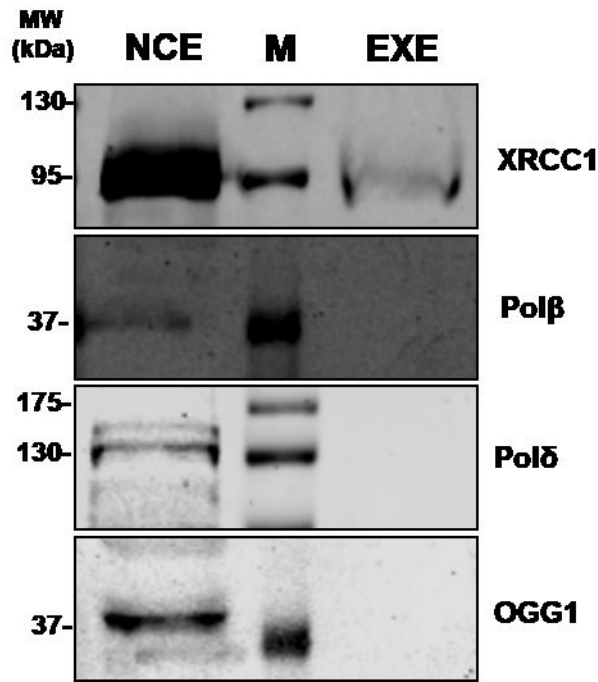


Figure 19: BER enzymes analysis in JHH-6 EXE. JHH-6 EXE were assessed by western blot for the detection of XRCC1, Polβ, Polδ and OGG1 BER enzymes. JHH-6 *nuclear cell extracts* (NCE) were also examined as reference control for proteins expression.

In order to prove that secretion of the p33 and p37 forms in EVs is a general feature of mammalian cells, we also performed EXE analysis in lymphocytes mouse isogenic cell lines, i.e. the CH12F3^{Δ++} and CH12F3^{ΔΔΔ} cell lines, expressing and or not APE1, respectively¹⁴⁶. The latter is an APE1-KO cell line, while the CH12F3^{Δ++} represented the isogenic control expressing the APE1 protein. Using these two cell lines, we demonstrated that APE1 was indeed only present in the EVs from the CH12F3^{Δ++} expressing cells (Figure 20). Moreover, these data suggested that the release of APE1 in EVs was not exclusively found from JHH6 cells. In order to demonstrate whether the presence of APE1 in exosomal vesicles was a general phenomenon of cancer cells from different origin, we used the A549, lung tumor cell line and the HCT116p53^{+/+} and HCT116p53^{-/-} colon carcinoma isogenic cell lines. We observed that APE1 presence in EVs of different tumor cell lines is a general phenomenon, being common to all tested cell lines. Interestingly, the amount of p33 form was variable between the different tested cell lines. These data clearly demonstrated that both p37 and p33 forms of APE1

protein may be released in EVs of different cancer cell lines and that, among the tested BER factors, APE1 is the only enzyme present in these secreted particles together with XRCC1.

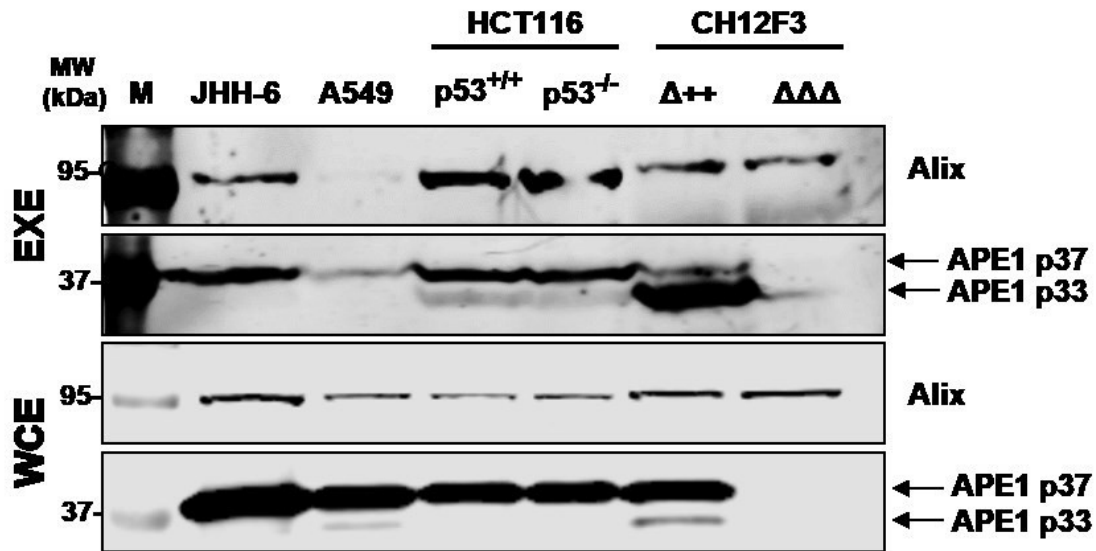


Figure 20: APE1 secretion through ESCRT is a general process that occurs in different cell lines: EXE from JHH-6, A549, HCT116 p53^{+/+}, HCT116 p53^{-/-} were analysed by western blot for the presence of APE1 protein. Alix detection was performed as a positive exosomal marker. WCE were also analysed as a reference control of APE1 expression.

Based on the observation of the consistent presence of the p33 APE1 form in EXE of cancer cells and on our previous characterization of this protein form in cancer cells from hematopoietic origin, i.e. Acute Myeloid Leukemia¹⁵, we tested the distribution of APE1 in EXE of these cancer cells. For these experiments, we used the OCI-AML3 (expressing mutated NPM1c⁺ protein) and the OCI-AML2 control cells¹⁴⁷. These two cell lines represent a suitable model for this analysis. In fact, OCI-AML2 cells show normal subcellular expression and nuclear distribution of APE1 protein and do not have any significant accumulation of APE1 p33 form. Interestingly, the OCI-AML3 cell line harbours a driver mutation of NPM1 protein, a known APE1 protein interacting partner¹⁴⁸ called NPM1c⁺, which causes APE1 cytoplasmic localisation and consequent

BER impairment¹⁵. In OCI-AML3 cells in fact, APE1 protein is re-localized within the cytoplasm where it is subjected to proteolytic degradation of the first 33 amino acids at the N-terminal sequence¹⁵. For this reasons, OCI-AML3 possesses significant levels of APE1 p33 form, as shown in Western blot analysis of WCE, (Figure 21, *left panel*). When examining APE1 p37 and p33 proteins content in EXE obtained from OCI-AML2 and OCI-AML3 cells, we surprisingly observed that both forms are indeed released by the two different cell lines, as shown in (Figure 21, *right panel*). In particular, in OCI-AML2 cells, the amount of total secreted APE1 (comprising both p37 and p33 APE1 forms) was higher than that secreted by OCI-AML3 cells. Interestingly, the ratio between p37 and p33 APE1 forms was comparable between EXE of both cell lines (Figure 21, *histogram below*). These evidences suggest that while OCI-AML2 cells, differently from the OCI-AML3 cells, did not show any truncated protein in WCE, as previously observed¹⁵, the truncated form was present in the EXE extracts of both cell lines at comparable levels. These data would denote that an additional proteolytic event, which is absent into the cytoplasm may occur in EVs of OCI-AML2 cells.

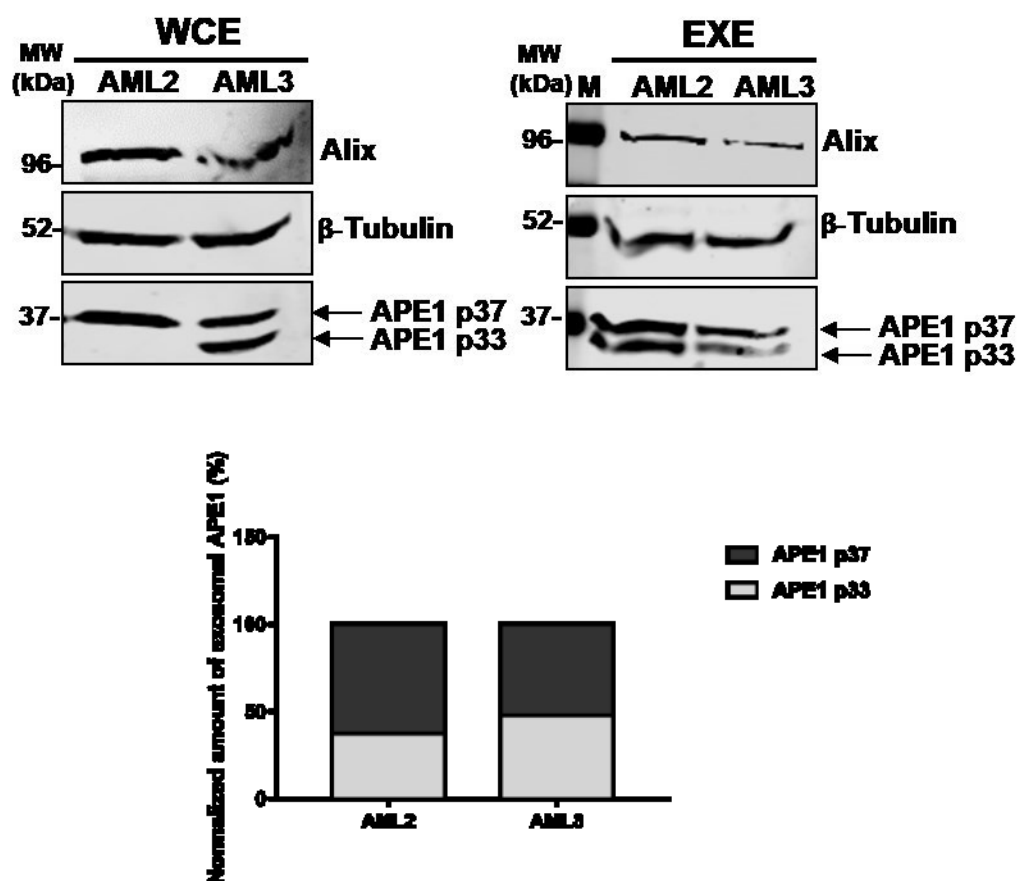
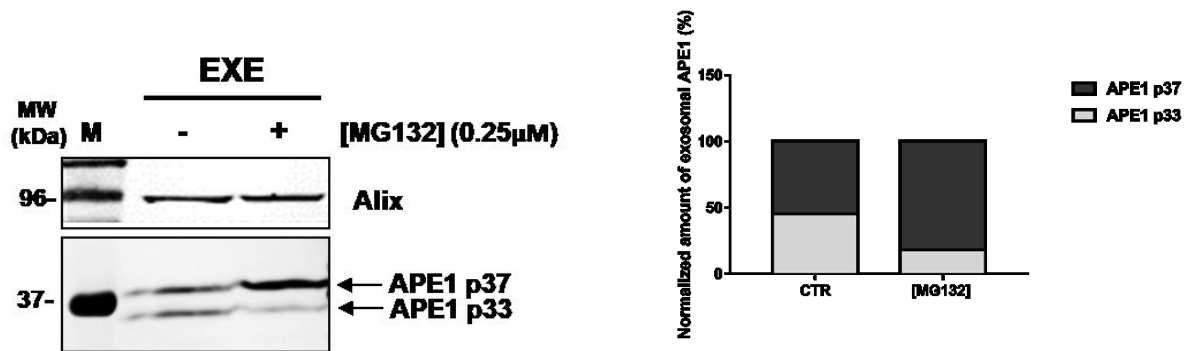


Figure 21: APE1 isoforms analysis in WCE and EXE derived from OCI-AML2 and OCI-AML3 cell lines. β -Tubulin and Alix detections were performed as loading controls. APE1 p37 and APE1 p33 are indicated by arrows. The histogram below shows the percentage of exosomal APE1 p37 and p33 isoforms. Data were obtained through densitometry analysis and were normalized for β -Tubulin and Alix.

Unpublished data from our Laboratory clearly demonstrated that the truncation of APE1-N-terminal region giving rise to the p33 form of the protein is, at least in part, contributed by cytoplasmic proteasome complex (Lirussi et al., in preparation). In order to evaluate whether the proteasomal pathway can be also involved in the observed accumulation of the p33 form in EVs, we blocked proteasomal degradation by the specific MG-132 inhibitor. The treatment was performed at the concentration of 0.25 μ M for 48 hours¹⁴⁹. EXE analysis (Figure 22A) clearly demonstrated a significant reduction of the only p33 form upon MG-132 treatment, as represented in the histogram (Figure 22A, *right panel*), demonstrating that the truncated form of APE1 accumulated in the EVs might be contributed, at least in part, by a proteasomal

degradation-pathway. Moreover, WCE were analysed and not significant difference of the amount of the two isoforms was registered in MG132 treated cells compared to control, probably because the low concentration used for treatment was not enough to appreciate significant APE1 intracellular isoforms pool variations (Figure 22B, *left panel*), for this reason I κ B- α accumulation was also tested as positive control for MG132 treatment (Figure 22B, *right panel*).

A



B

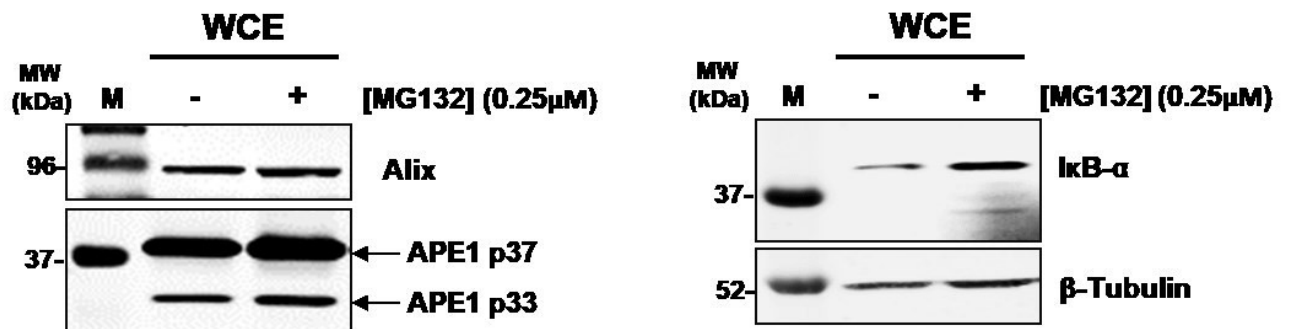


Figure 22: A) APE1 p37 and p33 detection in EXE of JHH-6 [MG132] treated cells (*left panels*). Alix detection was performed as a loading control. The histogram shows the percentage of exosomal APE1 p37 and p33 in JHH-6 CTR and MG132 treated samples (*right panel*). The percentages of APE1 p37 and p33, were obtained through densitometry analysis and have been normalised for Alix. B) APE1 p37 and p33 detection in WCE of JHH-6 [MG132] treated cells, Alix detection was performed as a loading control (*left panel*). I κ B- α detection in WCE as a positive control for MG132 treatment. β -Tubulin detection was carried out as a loading control (*right panel*).

Proteosomal components can be actively secreted in EVs¹⁵⁰. We therefore tested whether EVs isolated from JHH-6 cells could contribute to APE1 N-terminal cleavage. For this purpose, JHH-6 EXE (0.1µg) proteolytic activity was tested in rGST APE1^{WT} protein (0.2µg). The reaction was carried out for 15, 30 minutes, 1, 2, 4 hours at 37°C. rGST and rGST APE1^{WT} were used as control to check eventual protein degradation. After reaction the proteins were denatured loaded in 12% acrylamide/bis-acrylamide gel and resolved in SDS page. JHH-6 EXE exerts cleavage activity upon rGST APE1^{WT} protein in a time dependent manner (Figure 23) and seems that proteases are able to remove the GST tag to the rGST APE1^{WT} because the obtained products showed the p37 APE1 molecular weight.

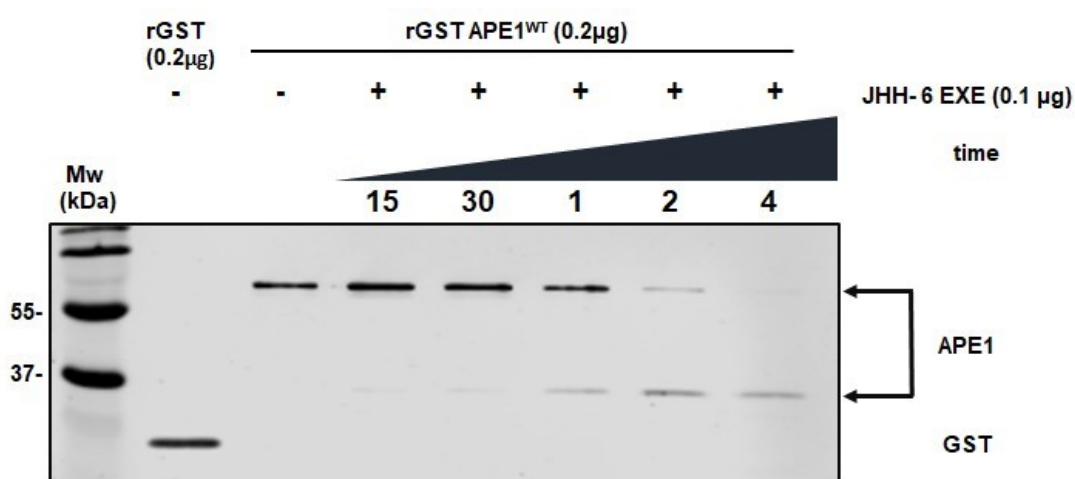


Figure 23: JHH-6 EXE proteolytic activity upon rGST APE1^{WT}. EXE (0.1µg) proteolytic activity was tested in rGST APE1^{WT} (0.2 µg). The reaction was performed at 37°C for 15, 30 minutes, 1, 2, 4 hours. rGST and rGST APE1^{WT} were used as control for protein degradation. The reaction was loaded in 12% acrylamide/bis-acrylamide gel and resolved in SDS page. Western blot analysis was later performed for APE1 and GST protein detection. The formation of APE1 cleaved product increases in a time dependent manner.

APE1 can be efficiently detected in NBI-isolated vesicles

In order to confirm the presence of APE1 in secreted EVs by quantitative approaches, we subjected the media of JHH-6 cells to nickel-based isolation (NBI) and detected the intra-vesicular APE1 using an *amplified luminescence proximity homogeneous assay*

(alpha)¹⁵¹. These experiments were executed thanks to the kind collaboration of CIBIO Trento. We used purified GST APE1^{WT} protein (Figure 24). We performed a quantification analysis by western blot, using known amount of recombinant APE1 protein as a reference and also a known amount of JHH-6 whole cell extract (WCE) as control for APE1 detection (Figure 25A). We titrated the recombinant protein as a reference substrate in the alpha assay using Glutathione-Donor beads and Protein G-Acceptor beads recognizing the anti-APE1 antibody. In this setting, we sensitively and specifically detected APE1-GST in the low nanomolar range compared with GST alone as further control (Figure 25B). In (Figure 25B), 100 nM of APE-GST represents the hook point. Subsequently, we isolated vesicles from JHH-6 by NBI, which prevents aggregation of the EVs in solution, and applied the alpha assay using a range of 10² to 10⁵ vesicles as determined by qNANO with a NP250 nanopore (the applied stretch gave a size window of approximately 80-800 nm). We only detected specific signals using EVs exposed to 90°C for 5 min before using them in the assay (Figure 25C), indicating that the APE1 is enclosed within vesicles. According to the standard curve obtained using the purified APE1-GST, we calculated the remarkable amount of 1.27 ng of protein every 10³ EVs measured in the range between 80 and 800 nm.

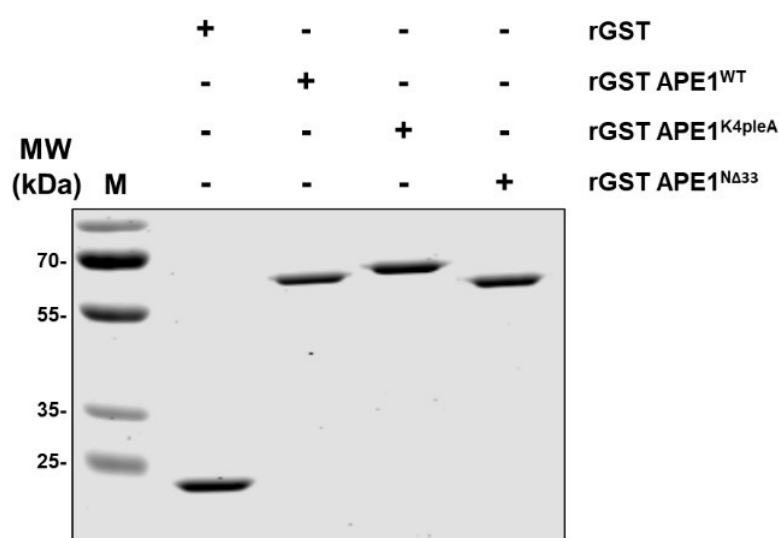
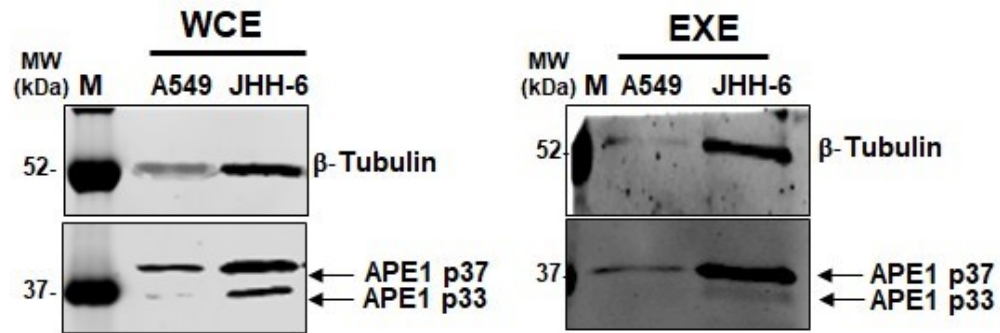
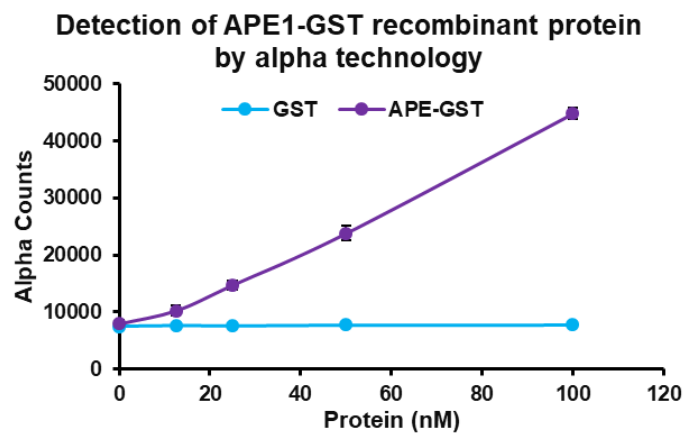


Figure 24: Coomassie staining of GST and GST APE1 recombinant proteins. (1.5µg loaded).

A



B



C

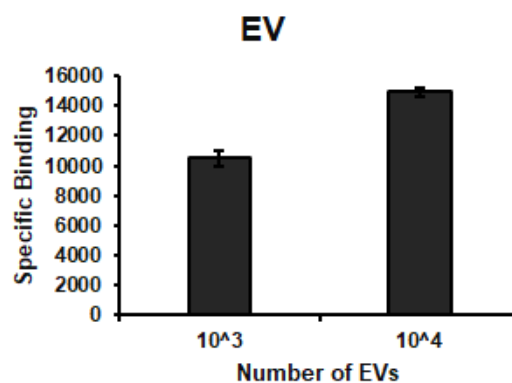
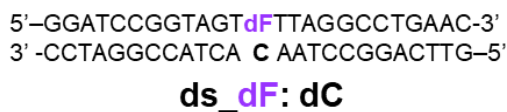


Figure 25: A) APE1 detection in A549 and JHH-6 EVs obtained by NBI. β -Tubulin detection was performed as a loading control. APE1_p37 and APE1_p33 are evident in both cell lines. **B)** setting of the reference substrate for the alpha assay through a titration curve of rGST APE^{WT} by alpha technology. rGST APE^{WT} detection resulted in low nanomolar range compared to rGST alone. **C)** Alpha assay executed for APE1 detection, performed on a range of 10^2 - 10^5 EVs derived from JHH-6 cells.

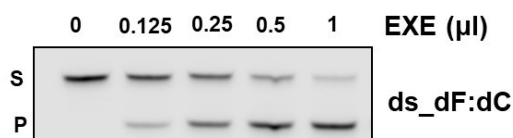
EVs APE1 protein is enzymatically active

We then tested whether APE1 was enzymatically active on different kind of DNA substrates²⁹. For this purpose, we used increasing amount of EXE to check its capability to exert a specific endonuclease activity. First of all, we checked exosomal APE1 activity on canonical *abasic deoxyribonucleotides in dsDNA* (ds_dF:dC) shown in (Figure 26A). Representative denaturing polyacrylamide gel (Figure 26B) showed the EXE endonuclease activity upon the described oligonucleotide. Substrate (S) and the relative product (P) of reaction are indicated. With this experiment, we were able to demonstrate that exosomal APE1 was competent to process a canonical substrate in a dose-dependent manner. Then, in order to check whether the enzymatic activity of EXE was exclusively ascribed to APE1, an endonuclease assay was performed after treating EXE with different doses of compound #3¹⁵², a specific inhibitor of APE1 endonuclease activity (Figure 26C). This experiment confirmed that in EXE the only endonuclease activity on abasic dsDNA present in exosomes is executed by APE1 protein.

A



B



C

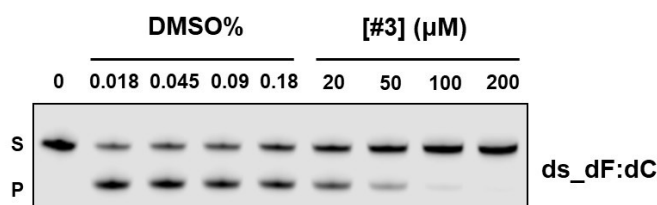
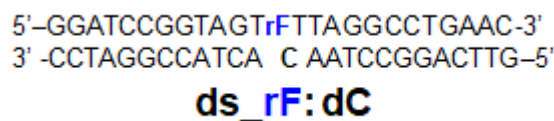


Figure 26: A) Schematic representation of double strand (ds) DNA 25-mer substrate (ds_dF:dC), generated by annealing of IRDye fluorophore labelled single strand (ss) oligonucleotide (5'-GGATCCGGTAGTGT^{dF}TTAGGCCTGAAC-3'), in which the 13th position G, indicated in light purple, is modified in deoxy-tetrahydrofuran (dF) with a ss_dC complementary oligonucleotide (5'-GTTCAGGCCTAACACTACCGGATCC-3'). Moreover, the 5' and 3' ends of each DNA strand are indicated. The name of the modified dsDNA oligonucleotide is indicated below the sequence. **B)** JHH-6 EXE-containing APE1 possesses endonuclease activity on the canonical abasic dsDNA substrate. Representative denaturing polyacrylamide gel of EXE incision on ds_dF:dC oligonucleotide. The volume of EXE used, expressed in μ l, is shown on the top of the figure. The reaction was performed for 15 minutes. **C)** Representative denaturing polyacrylamide gel showing the incision on ds_dF:dC executed by EXE (0.5 μ l), pre-treated for 15 minutes with different concentrations (μ M) of APE1 inhibitor #3. The reaction was performed for 15 minutes and different concentrations of DMSO (%) were used as control.

Then, we tested whether APE1 was able to process *abasic ribonucleotide embedded in dsDNA* (ds_rF:dC), shown in (Figure 27A) in a dose dependent manner, similarly to what we recently found for nuclear APE1²⁹. Enzymatic assays clearly showed that exosomal APE1 was indeed able to process this substrate, showing an activity even higher compared to that one observed for the ds_dF:dC (Figure 27B).

A



B

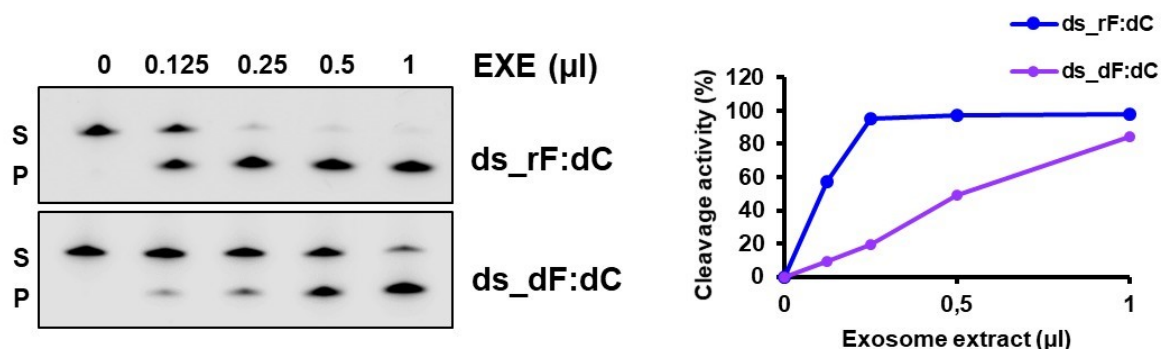


Figure 27: A) Schematic representation of double strand (ds) DNA 25-mer substrate (ds_rF:dC), generated by annealing of IRDye fluorophore labelled single strand (ss) oligonucleotide (5'-GGATCCGGTAGT**r**TTAGGCCTGAAC-3'), in which the 13th position G, indicated in blue, is modified in ribotetrahydrofuran (rF) with a ss_dC complementary oligonucleotide (5'-GTTTCAGGCCTAACACTACCGGATCC-3'). Moreover, the 5' and 3' ends of each DNA strand are indicated. The name of the modified dsDNA oligonucleotide is indicated below the sequence. **B)** JHH-6 EXE-containing APE1 possesses endonuclease activity on abasic ribonucleotides embedded in dsDNA. Representative denaturing polyacrylamide gel of EXE incision on ds_rF:dC oligonucleotide. The volume of EXE used, expressed in μl, is shown on the top of the figure. The reaction was performed for 15 minutes. ds_dF:dC oligonucleotide was used as positive control, (*lower panel*). Graph illustrating the comparison of EXE activity on ds_dF:dC and ds_rF:dC oligonucleotides. Data are expressed as mean + SD of three independent technical replicas, (*right*).

Then, we tested the EXE activity on a non-canonical substrate, containing an *oxidized ribonucleotide embedded in dsDNA* (ds_r8oxoG:dC), shown in (Figure 28A), as we recently proved²⁹. We observed that APE1 was able to process and generate a peculiar cutting pattern upon this dsDNA substrate. In fact, APE1 exerted not only a 5' endonuclease activity on ds_r8oxoG:dC, that gave rise to a 12nt long product, but also a 3' exonuclease activity, that gave rise to a 11nt shorter product, in agreement with

recent findings²⁹. As positive controls of incision on this substrate, we used rAPE1, to have a simultaneous evaluation of the expected products, and also *E. coli* rRNase HII, that possesses a stronger 5' endonuclease activity upon this substrate¹⁵³ (Figure 28B).

A



B

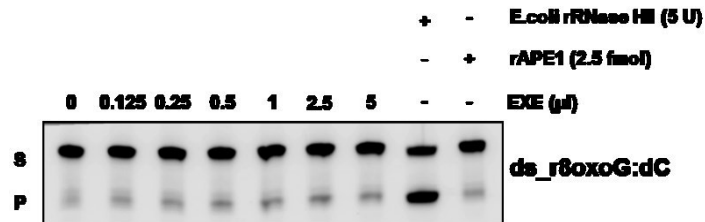


Figure 28: A) Schematic representation of double strand (ds) DNA 25-mer substrate (ds_r8oxoG:dC), generated by annealing of IRDye fluorophore labelled single strand (ss) oligonucleotide (5'-GGATCCGGTAGT**r8oxoG**TTAGGCCTGAAC-3'), in which the 13th position G, indicated in pink, is modified in oxidized ribo- guanosine (r8oxoG) with a ss_dC complementary oligonucleotide (5'-GTTTCAGGCCTAACACTACCGGATCC-3'). Moreover, the 5' and 3' ends of each DNA strand are indicated. The name of the modified dsDNA oligonucleotide is indicated below the sequence. **B)** JHH-6 EXE-containing APE1 possesses a weak endo- and exo- nuclease activity on oxidized ribo- G embedded in dsDNA. Representative denaturing polyacrylamide gel of EXE incision on ds_r8oxoG:dC oligonucleotide. The volume of EXE used, expressed in µl, is shown on the top of the figure. The EXE-containing APE1 activity was compared to the recombinant APE1 (rAPE1) activity on the same substrate at the indicated dose. The reaction was performed for 30 minutes.

Overall, these experiments proved that also in the EVs APE1 is able to fully perform its enzymatic activities on different canonical (abasic sites containing DNA) and non-canonical (r8oxoG containing DNA) substrates.

APE1 regulates steady-state levels of intracellular and EV-sorted RNA content

Given its intra-vesicular-secreted active form and its nucleic acid-binding activity, we exploited a quantitative approach to interrogate the abundance of RNA (detectable in the heterogeneous sub-micrometer-sized EVs) enclosed in vesicles released from CH12F3 cells expressing or not APE1 (CH12F3 Δ^{++} and CH12F3 $\Delta\Delta\Delta$, respectively) (Figure 29). We subjected the media exposed for 24 hours to these cells to NBI for EV isolation, then, after characterization of the prep by TRPS, we extracted and analyzed the total RNA from the same amount of vesicles. Albeit the EVs recovered from the two cell lines showed an equivalent size-distribution and abundance (Figure 30A), the RNA electrophoresis clearly showed that the presence of APE1 is responsible for a more than 3-fold enrichment (~45%) of transcripts spanning 30 to 4000 nt in length, with major peaks around 150-200 nt typically profiling the small/fragmented EV-RNA (Figure 30B). Interestingly, the profile of the total RNA isolated from the two cell lines showed a similar trend, in which the absence of APE1 caused a 30% reduction in the global abundance of transcripts (Figure 30C).

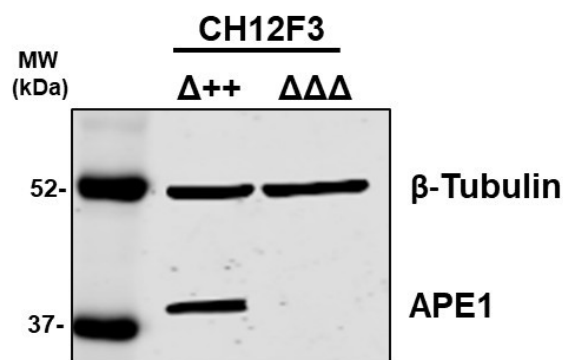
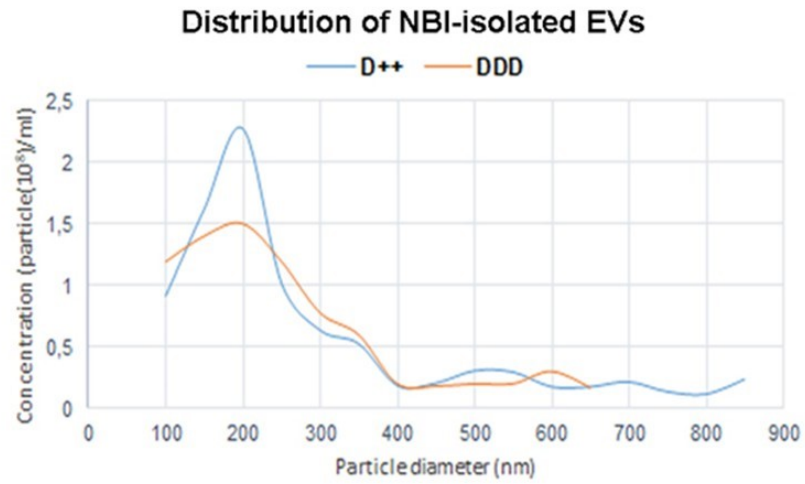
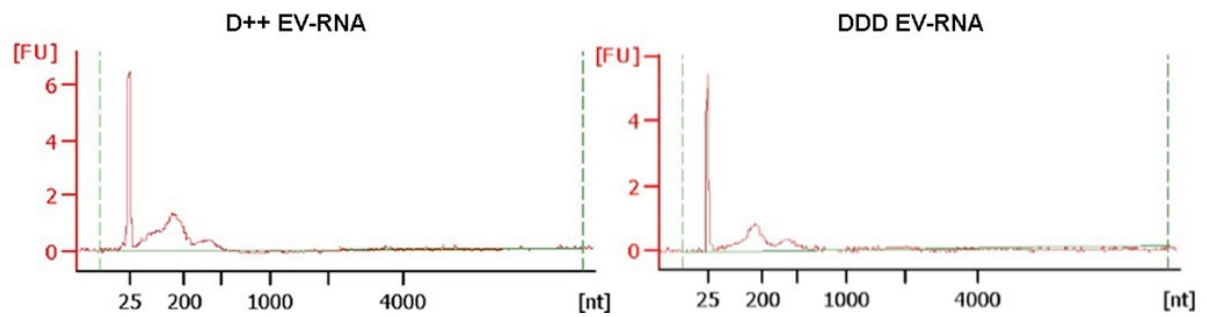


Figure 29: Western blot analysis for APE1 detection was carried out in murine positive for APE1 expression CH12F3 Δ^{++} cells, and in CH12F3 $\Delta\Delta\Delta$ KO for APE1 cells. Western blot for β -Tubulin was carried out as loading control.

A



B



C

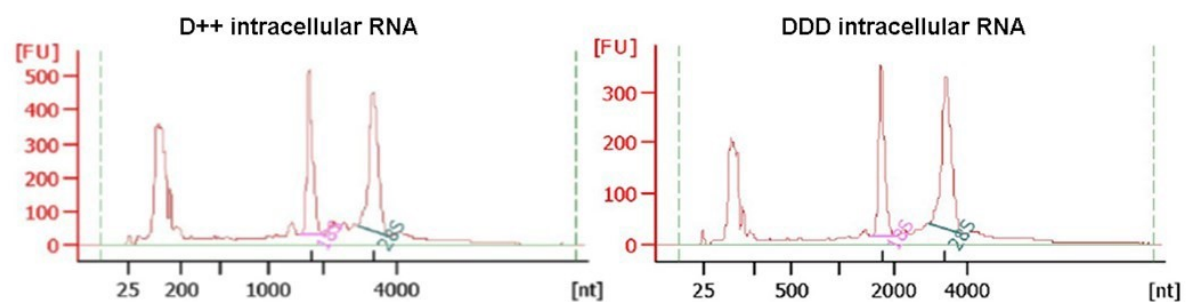
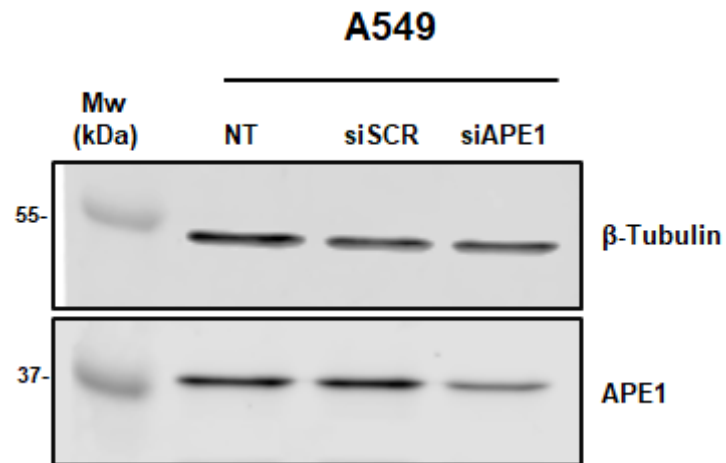


Figure 30: A) Analysis of CH12F3^{Δ++} and CH12F3^{ΔΔΔ} EVs distribution. The figure shows the concentration and the size-distribution spectre of EVs obtained from CH12F3^{Δ++} and CH12F3^{ΔΔΔ} media. B) Graphical representation of EVs RNA size distribution obtained from media exposed to CH12F3^{Δ++} and CH12F3^{ΔΔΔ} cells C) Graphical representation of CH12F3^{Δ++} and CH12F3^{ΔΔΔ} intracellular RNA size distribution.

Analogously, the EV-RNA profile obtained from A549 cell line transiently transfected for 72 hours with control (SCR) or APE1-targeting (siAPE) siRNAs (Figure 31A), showed a reduction of ~30% in the recovered RNA from EVs of APE1-silenced cells, while considering an average fluctuation of 6% in the SCR condition *versus* non-transfected cells (NT) (Figure 31B).

A



B

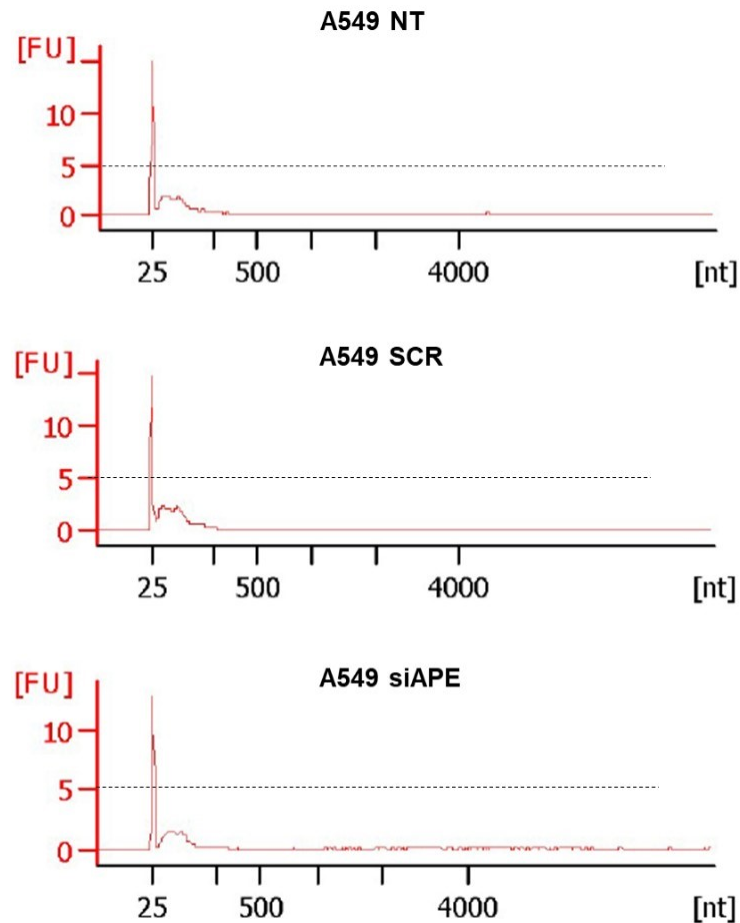
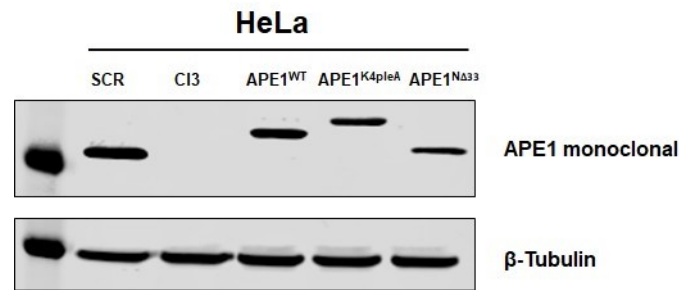


Figure 31: A) Western blot analysis for APE1 detection executed in A549 siAPE1 silenced for 72 hours and the respective SCR control. β - Tubulin detection was carried out as loading control. **B)** Graphical representation of EVs RNA size distribution obtained from media exposed to A549 not transfected cells (NT), A549 siSCR and A549 siAPE1 transfected cells.

Interestingly, a HeLa cell clone selected for a stable knock-down of APE1 (HeLa Cl3) (Figure 32A), consistently showing a reduction of near 50% in the EV-RNA in comparison to those from SCR cells, secreted EVs with a partial recover of RNA in case of concomitant expression of APE1^{WT} (15%). This partial rescue was not observed in case of transfection with mutated APE1^{K4pleA} or APE1^{NΔ33} APE-encoding plasmids (Figure 32B).

All of these data were obtained thanks to the kind collaboration with CIBIO of Trento.

A



B

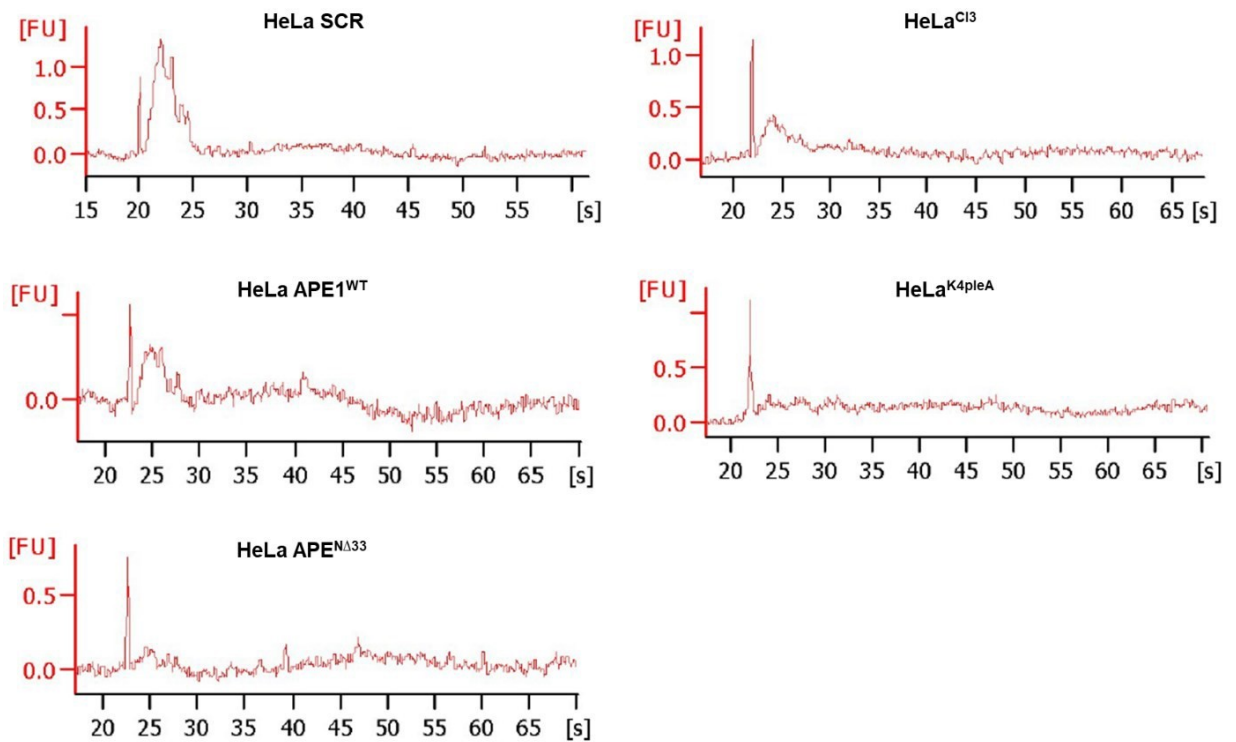


Figure 32: A) Western blot analysis for APE1 protein was carried out in HeLa inducible knock down cell lines. HeLa SCR indicates cell line which expresses endogenous APE1 protein levels. HeLa CI3 indicates cell line in which only downregulation of endogenous APE1 was carried out. The respective reconstituted APE1^{WT}, APE1^{K4pleA}, APE1^{NA33} clones are also indicated. Western blot for β-Tubulin was executed as loading control. **B)** Graphical representation of EVs RNA size distribution obtained from media exposed to HeLa SCR, CL3 and reconstituted WT, K4pleA and NA33 clones.

These analyses indicate that APE1 has a remarkable impact on the global intracellular RNA processing/stability and intravesicular RNA sorting, further influencing the metabolism of recipient cells.

Secretion of APE1 p33 form is stimulated by doxorubicin treatment in JHH-6 cell line and by CDDP treatment in A549 cells

To evaluate if APE1 release could be affected by induced genotoxic treatment, we evaluated APE1 secretion upon doxorubicin treatment. First, we determined the proper treatment conditions, represented by sub-lethal drug doses, in order to correlate the effect of the treatment on exosomal APE1 composition with the viability of JHH-6 cells. As shown in (Figure 33), a treatment with doxorubicin at the dose of 0.25 μM was considered ideal because of low toxicity at 24hours of treatment and a toxicity of 50% at 48 and 72 hours.

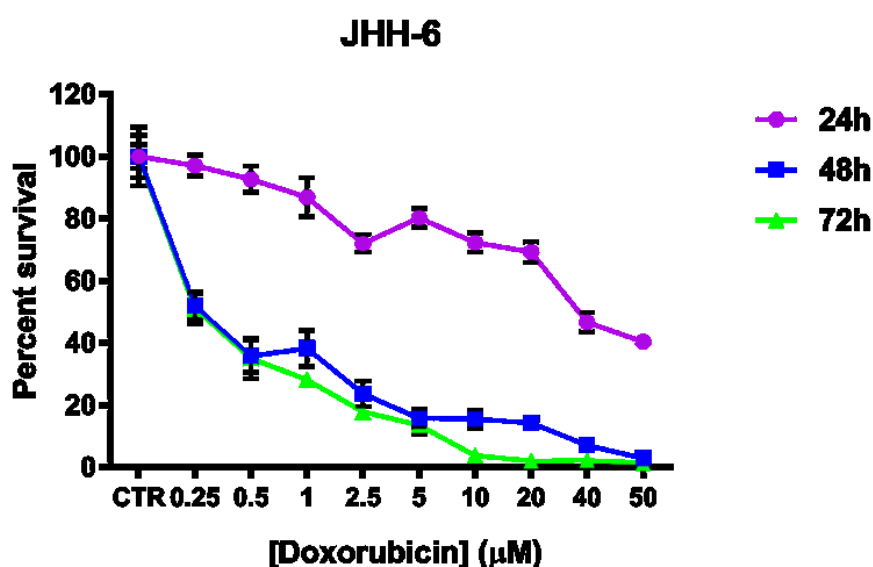


Figure 33: Analysis of Cell viability upon JHH-6 cell line after Doxorubicin treatment. MTS assay was performed upon JHH-6 cells after 24, 48, 72 hours of treatments with the indicated concentrations of Doxorubicin. The viability of untreated cells at the previously indicated time points was evaluated as a control. Data are expressed as mean \pm S.D.

Then, JHH-6 cells were treated for 24, 48, 72 hours with Doxorubicin at the concentration of 0.25 μ M and exosomes isolation was performed as indicated before. In parallel, the cell pellets of control- and Doxorubicin-treated cells were processed in order to evaluate the expression of APE1 and the other protein markers in WCE. Western blot analyses of WCE clearly demonstrated that Doxorubicin treatment did not affect neither the expression of APE1 nor that of Alix proteins. When analysing the content of APE1 in EXE as a function of time, we clearly observed a higher accumulation of APE1 total protein under Doxorubicin treatment condition compared to the untreated control. Interestingly, when we compared the expression of APE1, as a function of Doxorubicin treatment, we clearly noticed that the accumulation of the p33 form was significantly increased in Doxo-treated cells with respect to controls (Figure 34A), as quantified in the histograms (Figure 34B).

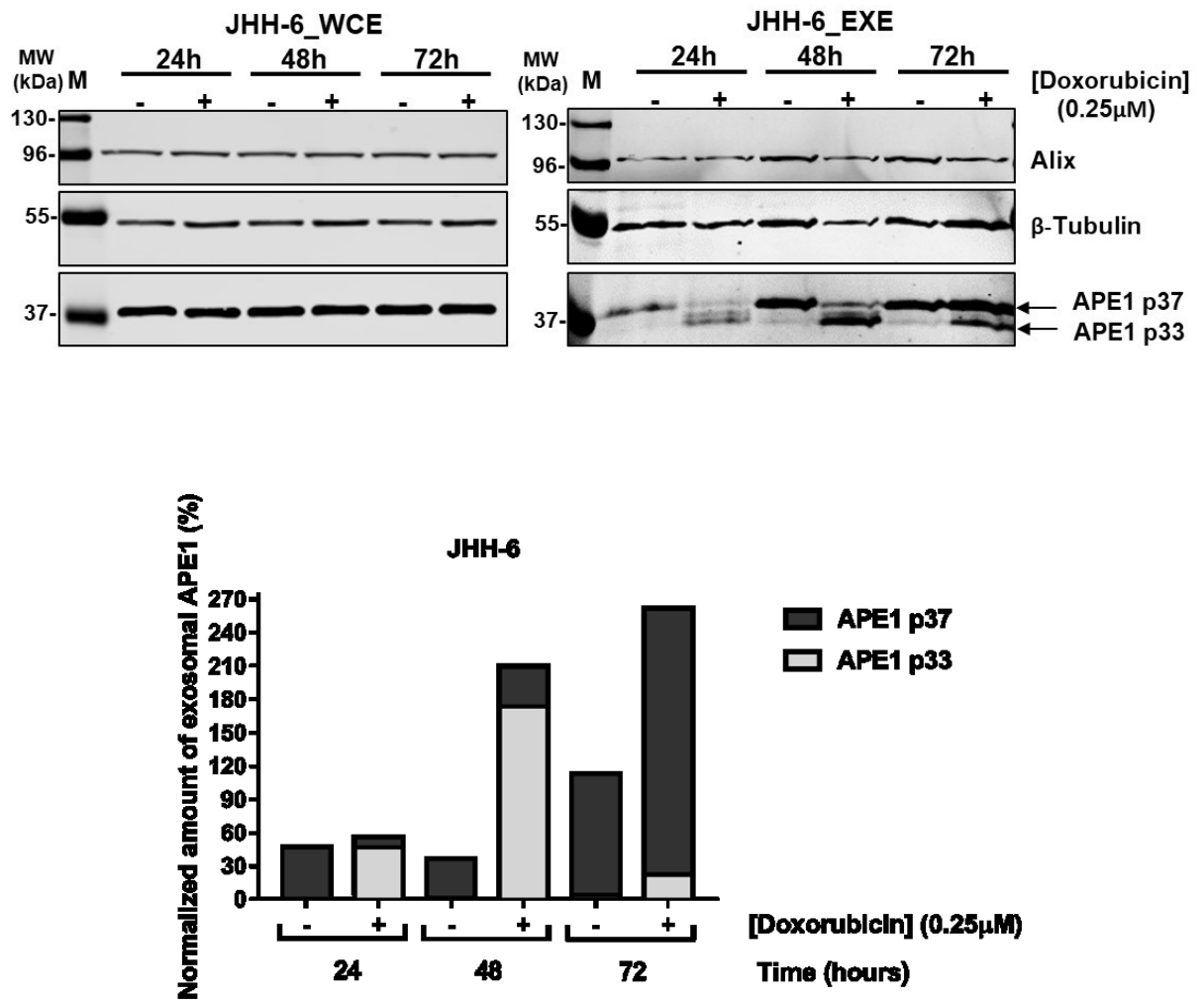


Figure 34: **A)** Analysis of APE1 content in JHH-6 WCE and EXE after 24, 48, 72 hours of Doxorubicin treatments. JHH-6 cells were treated with 0.25μM of doxorubicin for 24, 48 and 72 hours. Cells and media were collected and processed for the production respectively of WCE and EXE. WCE and EXE were also obtained from JHH-6 untreated cells at the three previously indicated time points. APE1 p37 and APE1 p33 isoforms were later analysed in WCE and EXE by western blot. Alix and β-Tubulin were detected as loading controls for both extracts. **B)** The accumulation of APE1 content in EVs, obtained from media of CTR and Doxorubicin treated cells and the percentage of the two APE1 fractions p33 and p37 in EXE is indicated in the histograms.

In order to check if this trend was only related to a specific effect of doxorubicin upon exosomal APE1 or it was common to other genotoxic treatments, JHH-6 cells were treated with Cisplatin (CDDP). According to the cell viability analysis (Figure 35), we chose a CDDP concentration of 6.25 μM because of low toxicity at 24hours of treatment and a toxicity of 50% at 48 and 72 hours, similarly to previous doxorubicin treatment. The treatment with CDDP at the concentration of 6.25 μM was performed for 24, 48,

72 hours and EXE were isolated as indicated before. As shown in (Figure 36A), also in EXE obtained from CDDP-treated JHH-6 cells, an accumulation of APE1 protein compared to the JHH-6 EXE of the untreated control was clearly apparent. In addition, we observed that, especially at 24 and 48 hours of CDDP-treatment, the relative amount of APE1 p33 form quantified was higher compared to that of the p37 form, as indicated in the histograms (Figure 36B).

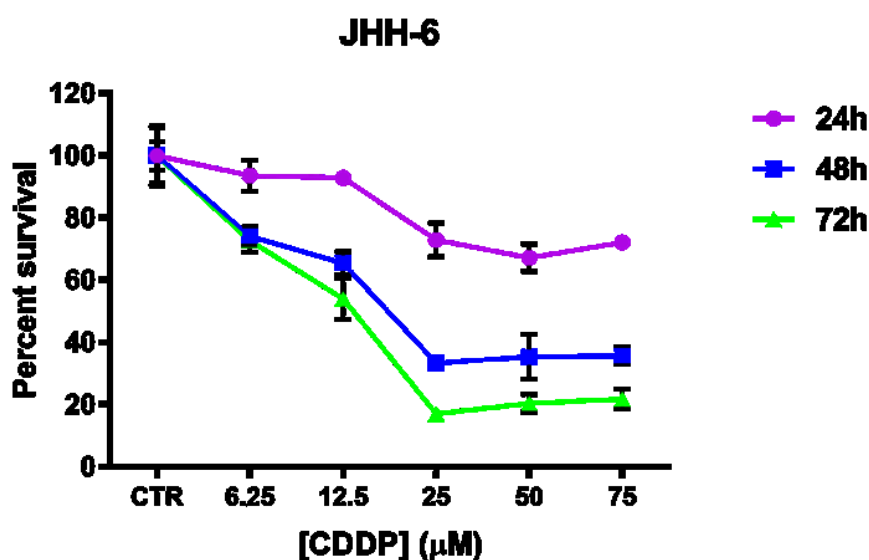


Figure 35: Analysis of cell viability upon JHH-6 cell line after CDDP treatment. MTS assay was performed upon JHH-6 cells after 24, 48, 72 hours of treatments with the indicated concentrations of CDDP. The viability of untreated cells at the previously indicated time points was evaluated as a control. Data are expressed as mean \pm S.D of three independent technical replicas.

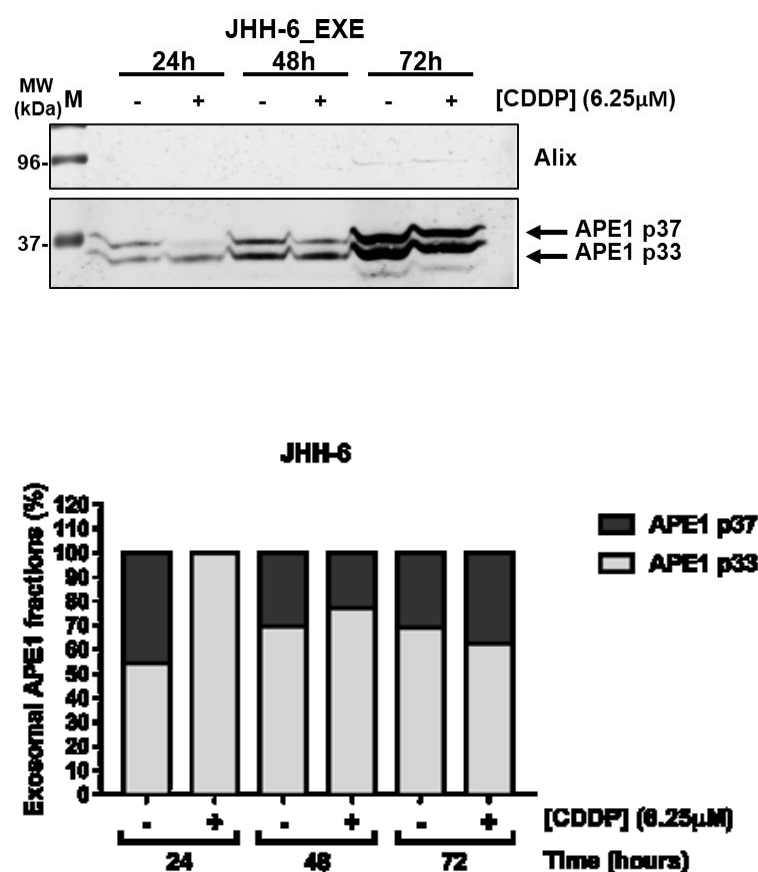


Figure 36: A) Analysis of APE1 content in JHH-6 WCE and EXE after 24, 48, 72 hours of CDDP treatments. JHH-6 cells were treated with 6.25μM of CDDP for 24, 48 and 72 hours. Cells and media were collected and processed for the production respectively of WCE and EXE. WCE and EXE were also obtained from JHH-6 cells untreated cells at the three previously indicated time points. APE1 p37 and APE1 p33 isoforms were later analysed in WCE and EXE by western blot. Alix was detected as loading control for both extracts. **B)** The percentage of exosomal APE1 fractions p33 and p37 in EXE, obtained from media of CTR and CDDP treated cells is indicated in the histograms below.

This result confirms that different genotoxic agents could promote an increase of APE1 exosomal release and also that genotoxic agents may promote the release of higher amount of APE1 p33 form compared to the p37 one, corroborating our hypothesis about the possible different functions absolved respectively by p33 and p37 forms in EXE released in the microenvironment of cancer cells. To check if the effect observed in JHH-6 cells was a general effect reproducible in different cell lines, we repeated the experiment of CDDP-treatment in A549 lung cancer cell line. Therefore, in agreement with the previous approach on JHH6 cells, we performed viability analysis on A549

cells treated with different doses of CDDP. Also for this cell line, we choose the concentration of 6.25 μM , as shown in (Figure 37), because CDDP-treatment at this concentration caused low toxicity at 24 hours and a toxicity of about 50% upon 48 and 72 hours of treatment, similarly to what we observed in the case of JHH-6 cells. Then, we performed EXE isolation from A549-conditioned media after 24, 48, 72 hours of CDDP-treatment, and we analysed the amount of APE1 p33 and p37 forms in EXE. As shown in (Figure 38A), similarly to JHH6 cells, we observed an accumulation of the total APE1 in EXE also in CDDP-treated A549 cells, and an increase of the relative amount of APE1 p33 form compared to the p37 full length protein (Figure 38B).

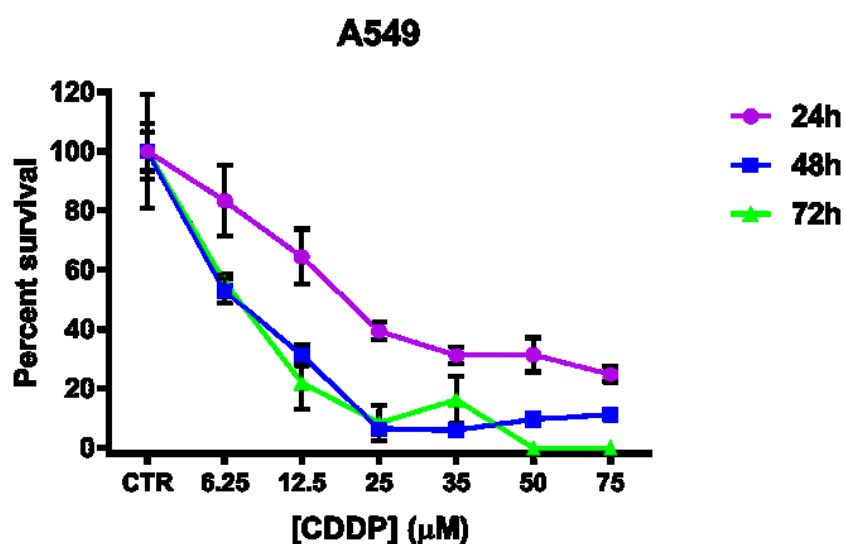


Figure 37: Analysis of cell viability upon A549 cell line after CDDP treatment. MTS assay was performed upon A549 cells after 24, 48, 72 hours of treatments with the indicated concentrations of CDDP. The viability of untreated cells at the previously indicated time points was evaluated as a control. Data are expressed as mean \pm S.D of three independent technical replicas.

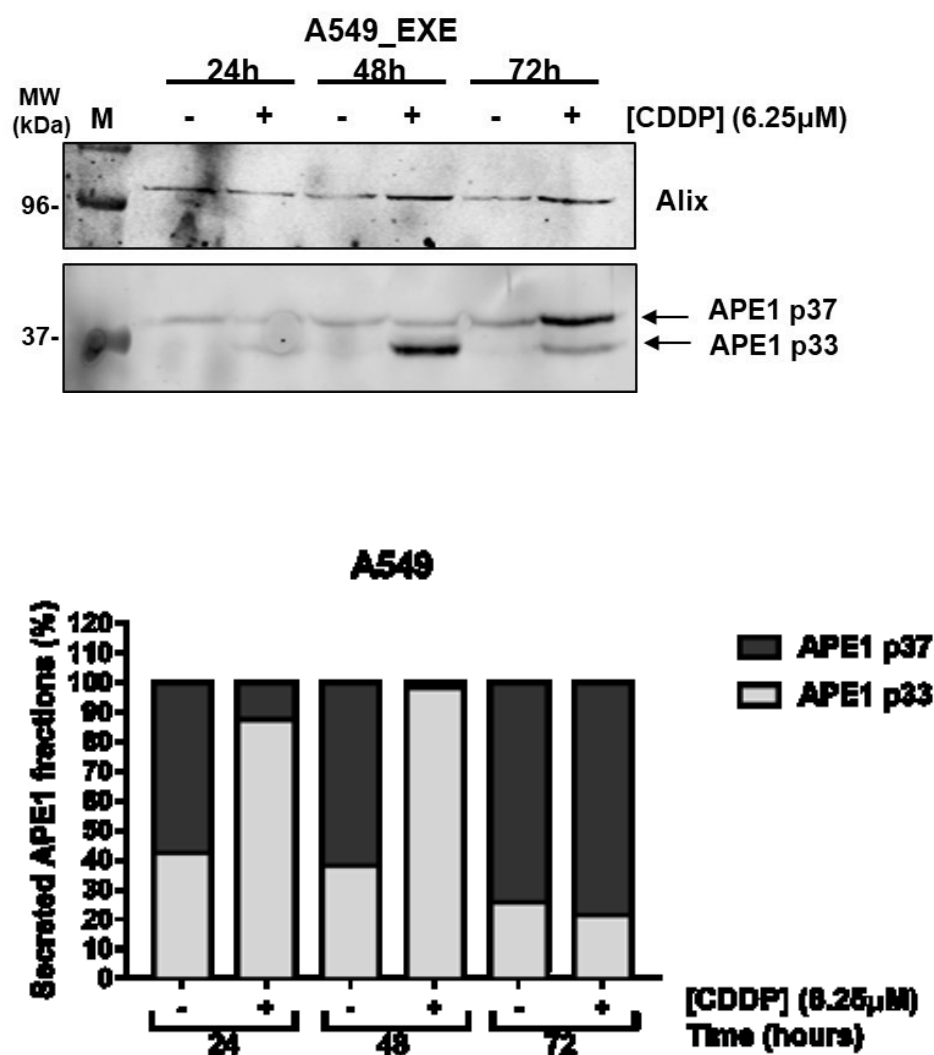


Figure 38: A) Analysis of APE1 content in A549 WCE and EXE after 24, 48, 72 hours of CDDP treatments. A549 cells were treated with 6.25μM of CDDP for 24, 48 and 72 hours. Cells and media were collected and processed for the production respectively of WCE and EXE. WCE and EXE were also obtained from A549 untreated cells at the three previously indicated time points. APE1_p37 and APE1_p33 isoforms were later analysed in WCE and EXE by western blot. Alix was detected as loading control for both extracts. **B)** The percentage of exosomal APE1 fractions p33 and p37 in EXE, obtained from media of CTR and CDDP treated cells, is indicated in the histograms below.

Altogether, these results confirmed that the increase of APE1 exosomal release upon genotoxic stress is a general process, observed in different cancer cell lines and upon different genotoxic stresses and that chemotherapeutic drugs induce an accumulation of APE1 p33 form compared to the p37 protein.

We also wanted to test if the proteolytic activity of EXE derived from JHH-6 genotoxic treated cells could show different cleavage efficiency profiles. For this purpose, EVs proteolytic activity onto 0.2µg of rMAT APE1^{WT} was evaluated using different amount of EVs (0.1, 0.5, 1 µg), derived from JHH-6 untreated and doxorubicin treated cells. A higher proteolytic activity mediated by EVs derived from doxorubicin treated cells was clearly observed, compared to that one mediated by EVs of untreated cells (Figure 39). We need to repeat the same experiment decreasing the time of reaction to better appreciate the differences. This experiment was performed using rMAT APE1^{WT}, another rAPE^{WT}, MAT tagged. In this experiment is possible to appreciate the different profile of proteolytic activity exerted by the two EVs samples upon the rAPE^{WT} (Figure 39).

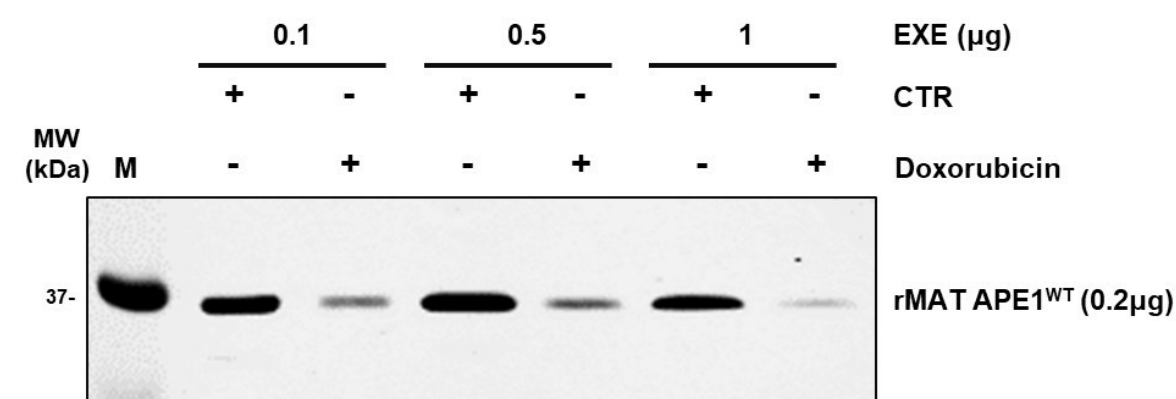


Figure 39: JHH-6 EXE derived from doxorubicin treated cells and untreated cells proteolytic activity upon rMAT APE1^{WT}. Different doses of EXE derived from JHH-6 doxorubicin treated cells and untreated cells were tested for their proteolytic activity upon rMAT APE1^{WT} (0.2 µg). The reaction was performed at 37°C for 4 hours. The reaction was loaded in 12% acrylamide/bis-acrylamide gel and resolved in SDS page. Western blot analysis was later performed for APE1 protein detection. The formation of APE1 cleaved product is higher in EXE derived from doxorubicin treated cells.

Soluble rAPE1 triggers SASPs factors expression

SASPs factors expression is emerging as important paracrine mechanisms to promote inter-cellular communication of DDR responses being involved in triggering cancer cell-senescence phenotypes⁹⁹. In order to evaluate a possible role for secreted soluble APE1 in cancer cells, we tested whether exogenous addition of recombinant purified APE1 may trigger SASPs factors expression in JHH-6 cell line (Figure 40 *panel above*)⁹⁷. Recombinant proteins used here were GST-tagged APE1 proteins expressed in *E. coli* and purified to the homogeneity by FPLC-chromatography^{11,154,155} (Figure 24). To this aim, in addition to the wild-type protein (rAPE1^{WT}) and the 33N-terminal deletion mutant (rAPE1^{Δ33}), we also used an acetylated-mimicking mutant on residues 27, 31, 32, 35 (rAPE1^{K4pleA}). In this mutant, the Lys residues have been replaced by Ala, (as described previously) and whose relevance in cancer have been recently demonstrated⁵⁶.

As a negative control, we used purified GST protein that constitutes the tag of each of the above mentioned proteins. As a positive control of IL-6 and IL-8 inductions, we treated the cells with rTNF- α (Figure 40 *panel below*). As previously described, cells were treated for 24 hours with two doses of recombinant purified proteins, and the expression of IL-6 and IL-8 genes was assayed by qPCR. As can be observed (Figure 40, *panel above*), while GST alone did not exert any major effect, treatment with soluble rAPE1 proteins induced an upregulation of both cytokines in the treated cells, showing a more pronounced effect on IL-8, rather than on IL-6, gene expression. Interestingly, treatments with either rAPE1^{Δ33} or the rAPE1^{K4pleA} proteins promoted a higher increase of both IL-6 and IL-8 compared to rAPE1^{WT}.

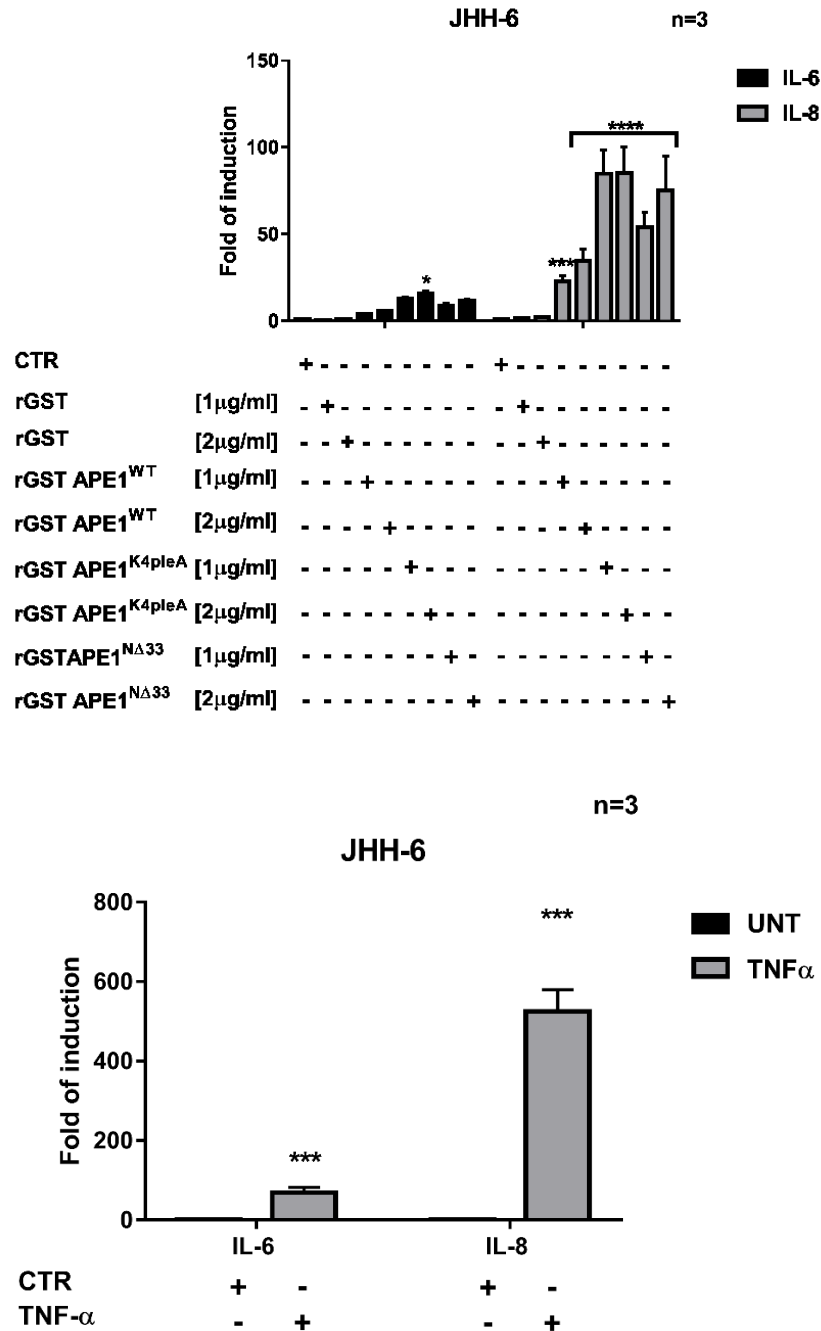


Figure 40: Exogenously added recombinant APE1_GST proteins are able to induce the mRNA expression of IL-6 and IL-8 genes: IL-6 and IL-8 mRNA expression levels analysis upon JHH-6 cells treated for 24 hours with 1μg/ml or 2μg/ml of rGST APE1 proteins. JHH-6 untreated cells and treated for 24 hours with 1μg/ml or 2μg/ml of rGST protein where used as a negative controls. After treatments, total RNAs were extracted, cDNAs were obtained and quantitative Real Time PCR was executed. Data show that while rGST APE1^{WT} is slightly able to induce IL-6 and IL-8 mRNA expression, the mutated forms rGST APE1^{K4pleA} and rGST APE1^{NΔ33} more efficiently have the capability to induce the activation of IL-6 and IL-8 mRNA expression (*panel above*). IL-6 and IL-8 mRNA expression analysis upon JHH-6 cells treated for 3 hours with TNF-α as a positive control for interleukins induction (*panel below*). Data represent means ±SD of three independent experiments. Statistical analysis was achieved by applying Two-way ANOVA test. ****P<0.0001.

In order to exclude that the observed stimulatory effect could be due to possible contaminants, deriving from the *E. coli* as hosting vector used to express recombinant APE1 proteins or from the use of the GST-tag, we also performed similar experiments, by testing the effect on IL-8 gene expression, using recombinant Flag-tagged APE1 proteins expressed in JHH-6 cells and immune-purified using an anti-Flag M2 affinity chromatography (*see materials and methods*). Also in this case, treatments of JHH-6 cells for 24h with 1µg/ml immune-purified Flag-APE1^{WT}, Flag-APE1^{K4pleA}, Flag-APE1^{NA33} proteins were performed. As negative control, immune-purified material of extract from JHH-6 transfected with pCMV5.1-empty vector was used. As shown in (Figure 41), the induction of IL-8 mRNA expression, even though to a lower extent than in the previous case, was confirmed by qPCR also performing the treatment with immune-purified APE1 proteins, corroborating the data previously obtained with APE1 recombinant proteins treatment.

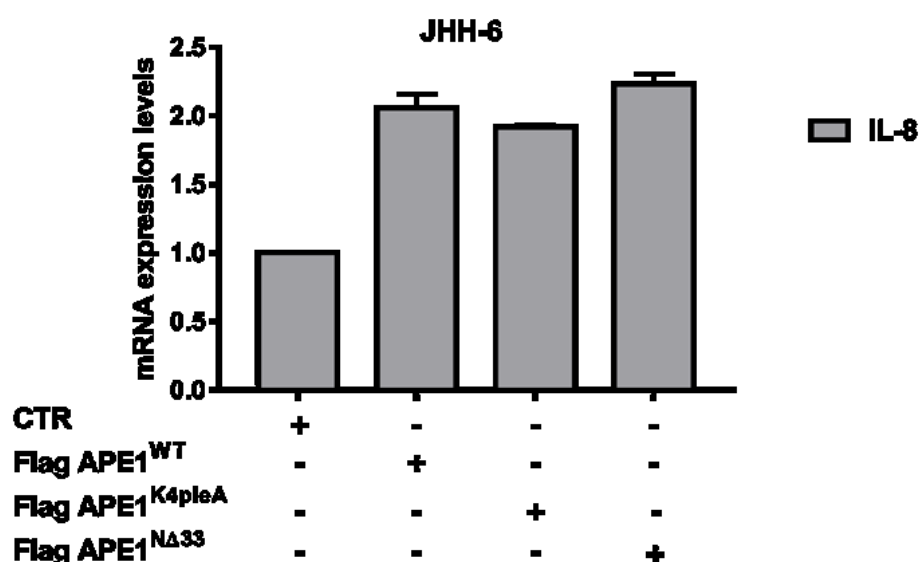


Figure 41: JHH-6 cells were treated for 24h with 1µg/ml of immune-purified Flag APE1^{WT}, Flag APE1^{K4pleA} and Flag APE1^{NA33} proteins. Treatment with 1µg/ml of immune-purified extracts derived from cells transfected with pCMV5.1_empty vector was executed as a negative control. After treatments, total RNAs were extracted, cDNAs were obtained and quantitative Real Time PCR was executed. Data show that immune-purified APE1 proteins are able to induce the mRNA expression of IL-8 gene.

In order to generalize our findings with a different cell model, we performed the same experiments described in (Figure 40) using the A549 cell line. Data shown in (Figure 42), clearly demonstrated that the stimulatory effect on endogenous IL-6 and IL-8 expression by treatment with the recombinant proteins was clearly obtained also in the A549 cell line, even to different extent relative to the JHH-6 cell model, with a more pronounced effect on IL-6 rather than IL-8. Altogether, these data suggest a role of secreted APE1 as a paracrine pro-inflammatory molecule, which may modulate the SASPs factors expression in cancer cells.

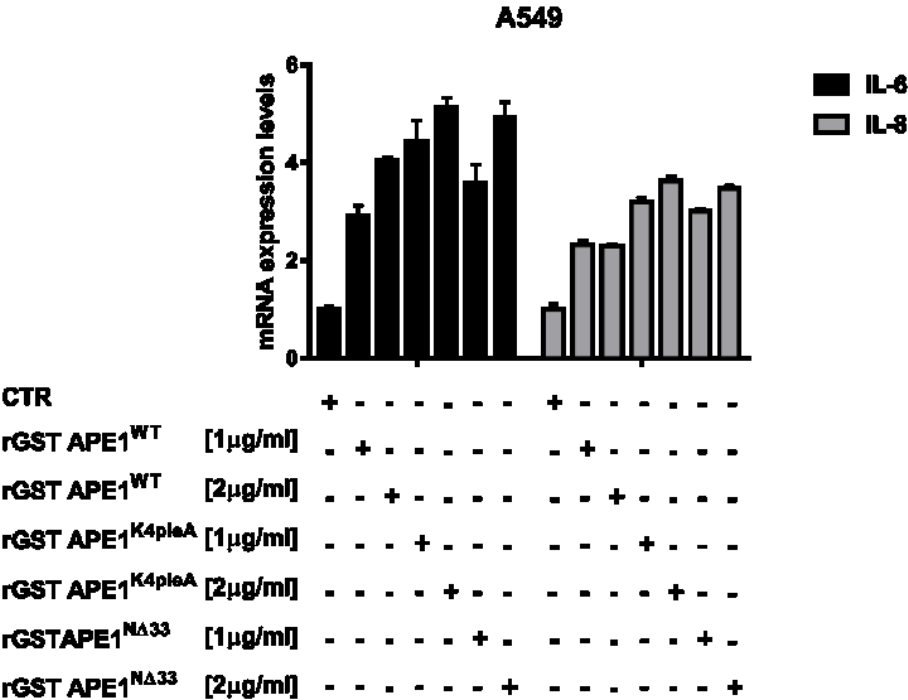
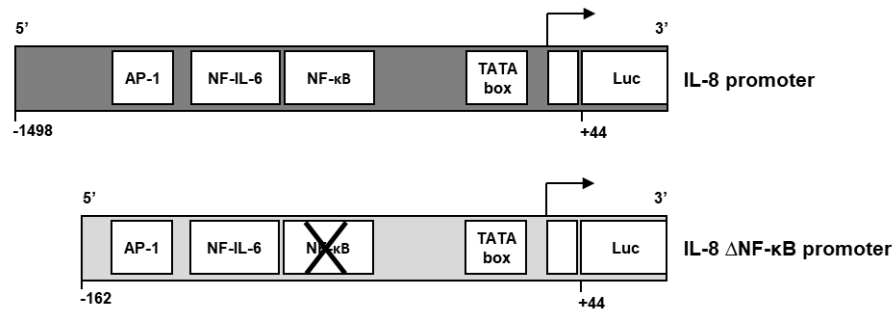


Figure 42: IL-6 and IL-8 mRNA expression levels analysis in A549 cells treated for 24h with rGST APE1 proteins. A549 untreated cells were used as control. After treatments, total RNAs were extracted, cDNAs were obtained and quantitative Real Time PCR was executed.

Soluble rAPE1 promotes the activation of IL-8 promoter through NF- κ B transcription factor

APE1 is known to be an activator of IL-8 expression through NF- κ B transcription factor activation^{12,98}. Thus, we tested whether the APE1 paracrine effect on IL-8 expression was due to a transcriptional activation process on IL-8 promoter. For this purpose, Luciferase Reporter assay was performed on JHH-6 cells, previously transfected with IL-8_promoter or IL-8_ Δ NF- κ B_promoter, the last one characterized by the deletion of NF- κ B binding sites, as already described in Cesaratto et al., 2013⁹⁸ (Figure 43A). It was evaluated the ability of exogenously added recombinant APE1 to promote the activation of IL-8 gene expression. JHH6 cells transfected with the indicated promoters, were treated for 24 hours with 1 μ g/ml of rGST-APE1^{WT}, rGST-APE1^{K4pleA} and rGST-APE1^{N Δ 33}. As a negative control, treatment with rGST alone was performed. As a positive control for IL-8 promoter activation, TNF- α treatment [2000U/ml] was executed. Then, Luciferase activity was measured. Data obtained, clearly showed that recombinant exogenously added APE1 protein was able to activate IL-8 promoter through NF- κ B pathway, being abolished in the IL-8 Δ NF- κ B promoter (Figure 43B). Interestingly, the activation of IL-8 promoter was more effective when treating the cells with GST-APE1^{K4pleA} or with GST-APE1^{N Δ 33} mutant forms, in agreement with the endogenous gene expression, data shown in (Figure 40A), while no activation of IL-8 promoter was induced when treating with the rGST protein alone (Figure 43B). As a positive control, activation of IL-8 promoter, mediated by TNF- α was also measured. These data clearly suggest that stimulation of IL-8 expression by exogenously added recombinant APE1 proteins requires a transcriptional activation process involving NF- κ B transcription factor.

A



B

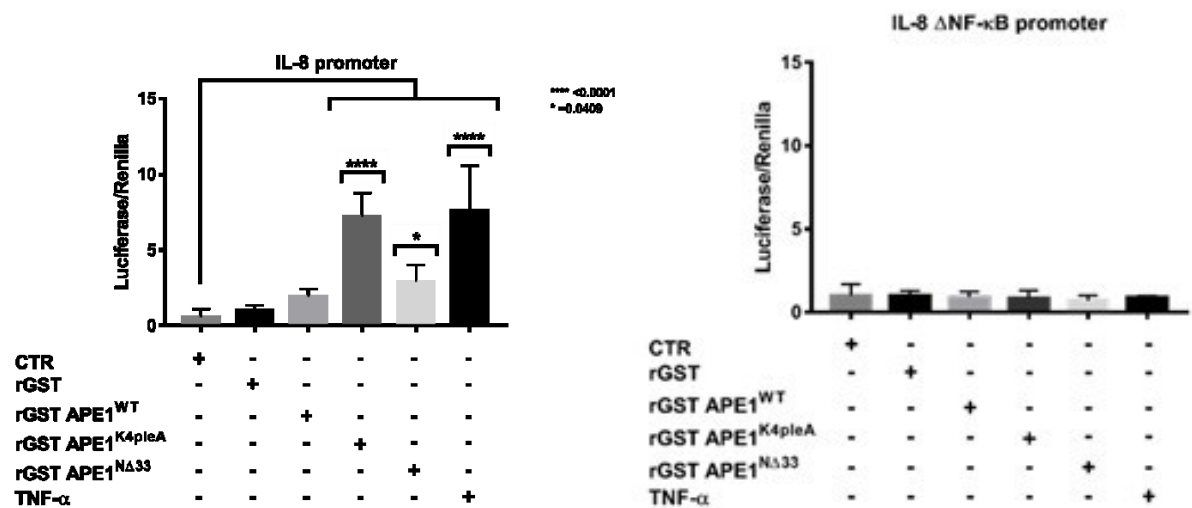


Figure 43: Exogenously added rGST APE1 proteins are able to promote the activation of the IL-8 promoter: **A)** Schematic representation of -1498/+44 hIL-8/Luc (IL-8 promoter) and -162/+44 hIL-8 Luc Δ NF- κ B (IL-8 Δ NF- κ B) promoters; **B)** Gene reporter assay upon JHH-6 respectively transfected with IL-8 and IL-8 Δ NF- κ B promoters. The day after transfection cells were treated for 24h with 1 μ g/ml rGST APE1 proteins in serum starvation and the activity of IL-8 and IL-8 Δ NF- κ B promoters was measured. As a negative control for the activation of the IL-8 promoter, a treatment for 24h with rGST protein at the concentration of 1 μ g/ml was performed. As a positive control a TNF- α treatment for 3 hours at the concentration of 2000U/ml was executed. Data represent means \pm SD of two independent experiments. Statistical analysis was achieved by applying Two-way ANOVA test. ****P<0.0001

Activation of IL-8 gene expression induced by soluble rAPE1 depends on ATM and on the APE1-redox function

It is known that NF- κ B activation is regulated during DDR by ATM¹⁵⁶. For this purpose, ATM inhibitor [KU60019] treatment for 24 hours (2 μ M) was performed coupled to reporter assay, as above¹⁵⁶. As shown in (Figure 44), ATM inhibitor treatment significantly affected the activation of IL-8 promoter mediated by exogenously added recombinant APE1 proteins. Moreover, since it is known that activation of NF- κ B could be exerted through a redox-based mechanism by endogenous APE1¹⁵⁷, we wanted to evaluate whether intracellular APE1 redox function was essential for the activation of IL-8 promoter via NF- κ B, as previously reported in Cesaratto et al., 2013⁹⁸, IL-8 promoter reporter assay was performed as above, in combination with the inhibition of the APE1 redox function through [E3330]¹⁵⁸. For this purpose, after 20 hours of treatment with recombinant GST APE1 proteins, E3330 treatment (125 μ M), (as reported in Cesaratto et al., 2013)⁹⁸ was performed together with rGST APE1 proteins for the remaining 4 hours. Inhibition of APE1 redox function blocked the induction of IL-8 promoter induced by exogenously added APE1 recombinant proteins. Overall, these data clearly demonstrate that ATM-signalling participates in the NF- κ B induction of IL-8 gene expression by exogenously added APE1 recombinant proteins and suggest that the redox function of APE1 is also involved.

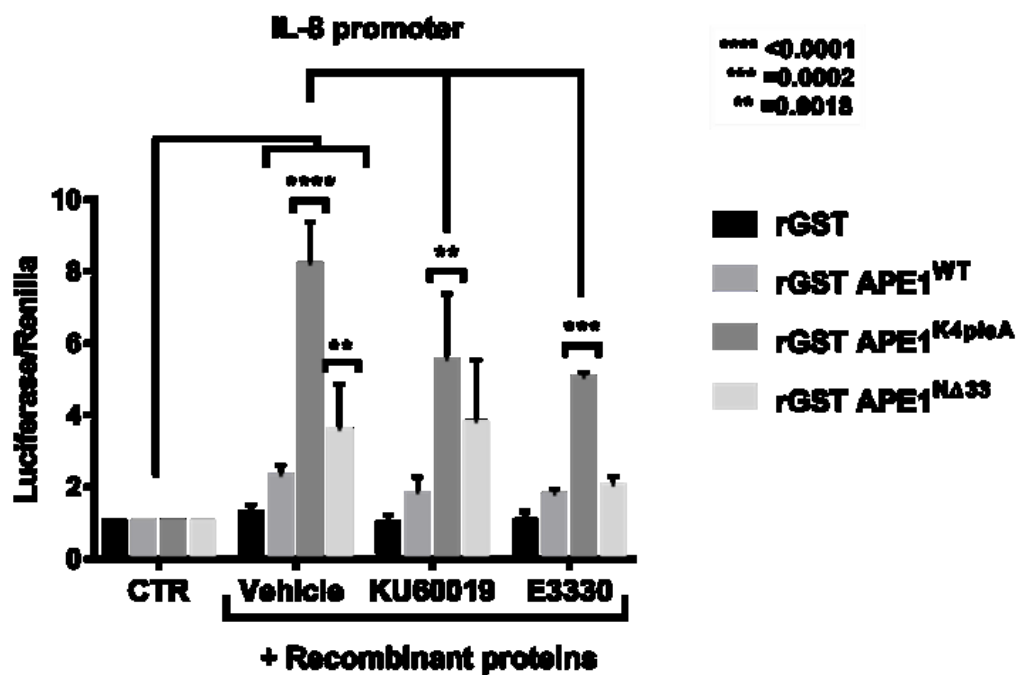


Figure 44: Gene reporter assay upon JHH-6 transfected with IL-8 promoter. The day after transfection cells were treated for 24h with 1μg/ml rGST APE1 proteins together with 2μM of the ATM inhibitor KU60019. Cells were also treated firstly for 20 hours with 1μg/ml rGST APE1 proteins followed by E3330 [125μM] in combination with rGST APE1 proteins for the remaining 4 hours. IL-8 promoter activity after the indicated treatments was measured.

Chapter 3

Characterization of APE1-hnRNPA2B1 interaction

In order to unveil non-canonical APE1 role in EVs and its contribution in the regulation of extracellular miRNA, we decide to validate the interaction between APE1 and hnRNPA2B1. hnRNPA2B1 is a ribonucleoprotein that exerts different functions such as participates in splicing events⁵³, takes part in RNA decay⁵⁵, interestingly regulates miRNAs processing⁶², and miRNA sorting in EVs⁵⁶. Because also APE1 participates in many of these processes and according to the recent indication, obtained through APE1 interactome analysis³, about the possible direct interaction between APE1 and hnRNPA2B1, we decide to properly validate the existence of this complex in JHH-6 cells. For this purpose, we first carried out a *Co-immunoprecipitation* (Co-IP) experiment (*see material and method*) in JHH-6 cells overexpressing Flag APE1^{WT}, while co-immunoprecipitation in JHH-6 transfected with an *empty vector* (Empty) was carried out as a negative control. The obtained IPs and the respective INPUTs, were resolved in SDS page and western blot using anti hnRNPA2B1 antibody was executed. In parallel western blot with anti Flag antibody was performed to check if the IPs had been opportunely normalized. To better characterize the interaction, and understand if is direct or if is mediated by nucleic acids, Co-IP were also performed in cell lysates treated with RNaseA or with DNaseI (*for treatment see material and methods*). As shown in (Figure 45), APE1 clearly interacts together with hnRNPA2B1 and this interaction is mediated by RNA, while DNaseI does not affect the interaction between these two proteins.

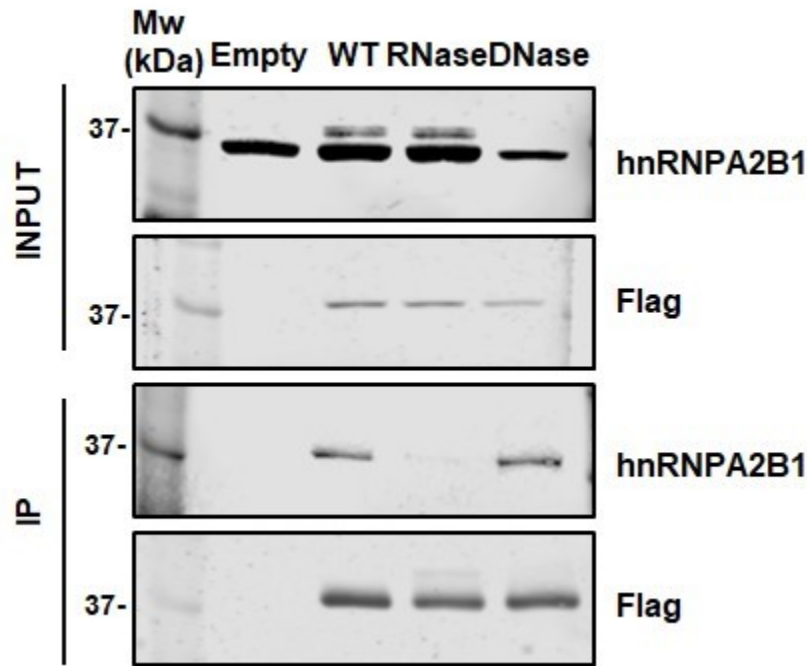


Figure 45: APE1-hnRNPA2B1 interaction analysis. Co-IP experiment carried out in JHH-6 cells overexpressing Flag APE1^{WT} and in JHH-6 cells transfected with an empty vector (Empty) as a negative control. INPUT and IP are indicated. Western blot was performed using anti hnRNPA2B1 antibody. Western blot using anti-Flag antibody was performed to check if the IP samples were opportunely normalized.

To prove the specificity of the interaction, it was performed a *Proximity ligation assay* (PLA) in JHH-6 knock down for APE1 protein. The knock down was obtained transfecting the cells with siRNA against APE1 (siAPE1) and a transfection with a *siRNA scramble* (siSCR) was performed in parallel as a control. PLA positive signal, indicative of the interaction between the two proteins, was represented by red spots present in siSCR condition (Figure 46) (*higher middle panel*), confirming the interaction observed before with Co-IP analysis. The PLA signal was missing in siAPE1 condition, proving the specificity of the signal. In the panels on the left are shown immunofluorescence carried out using APE1 antibody to observe APE1 cellular amount and distribution. In siAPE1 condition a weaker APE1 signal compared to the signal of siSCR is shown, indicating the downregulation of the protein. The merge of the two acquisition is shown on the right panels. A negative control, realized performing PLA in JHH-6 cells not incubated with anti hnRNPA2B1 antibody was also

realized and the relative APE1 cellular distribution and PLA signals were shown in the lower panels.

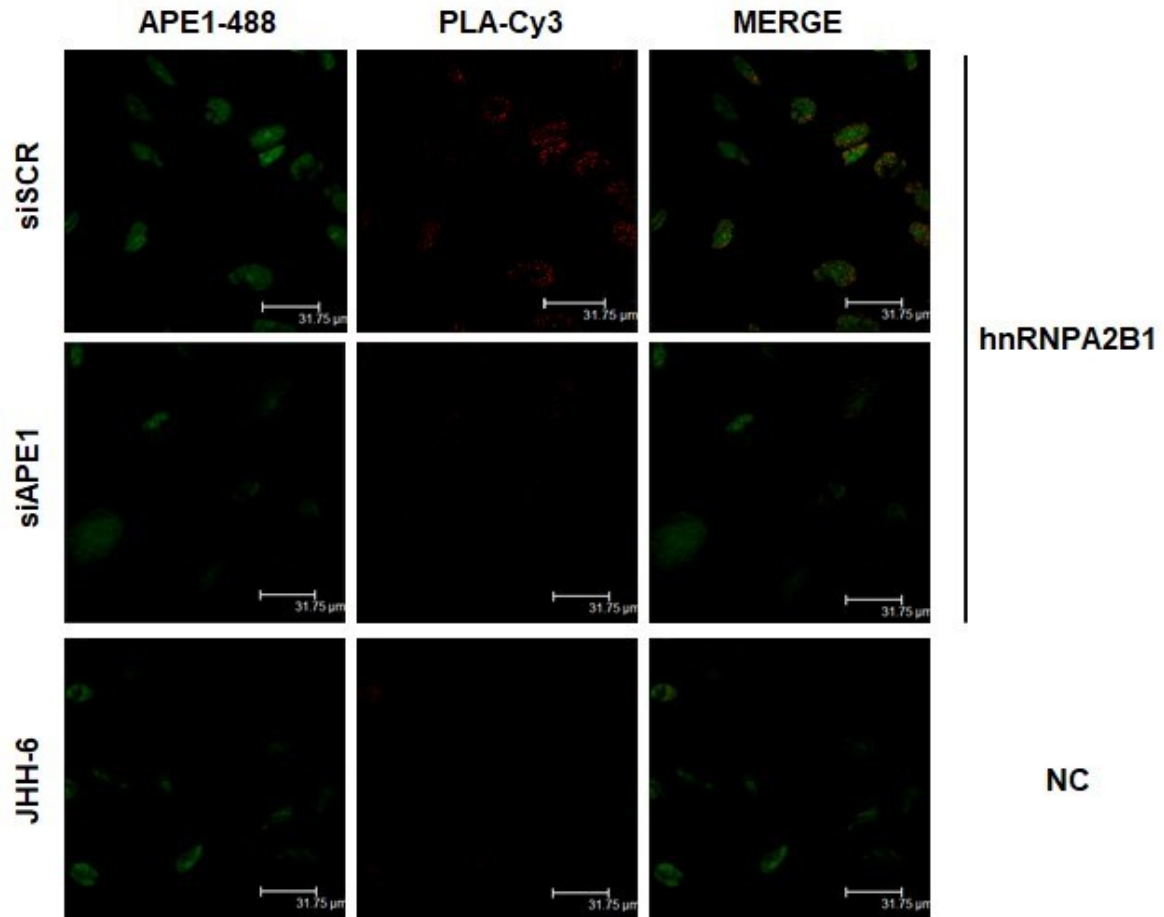


Figure 46: Validation of APE1-hnRNPA2B1 interaction. PLA was performed using anti APE1 and anti hnRNPA2B1 antibodies in JHH-6 cells silenced for APE1 protein (siAPE1), and JHH-6 silenced with siRNA scramble (siSCR) as a control. In the lower panels PLA was carried out in JHH-6 not-transfected cells omitting hnRNPA2B1 antibody, as a negative control.

To further evaluate the APE1 function involved in the interaction with hnRNPA2B1, CoIP experiments were carried out overexpressing the functional Flag APE1 mutants C65S, E96A and NΔ33. APE1^{C65S} is a mutant that displays a substitution of cysteine 65 with a serine residue, this mutation cause the removal of the thiol group involved in APE1 redox activity²², abolishing this function. APE1^{E96A} is a mutant which displays a substitution of glutamic acid with alanine residue, which impairs the endonuclease

activity of the protein³. APE1^{NΔ33} is the APE1 truncated form lacking of the first 33 amino-acids of the N-terminal region that are used to be involved in RNA-protein interaction and protein-protein interaction^{15,85}. Immunoprecipitation with empty vector and APE1^{WT} were carried out respectively for negative and positive control. The (Figure 47) shows that the interaction between APE1 and hnRNPA2B1 is not dependent by APE1 redox or endonuclease activity, the N-terminal region of the protein instead is clearly essential for maintaining this interaction.

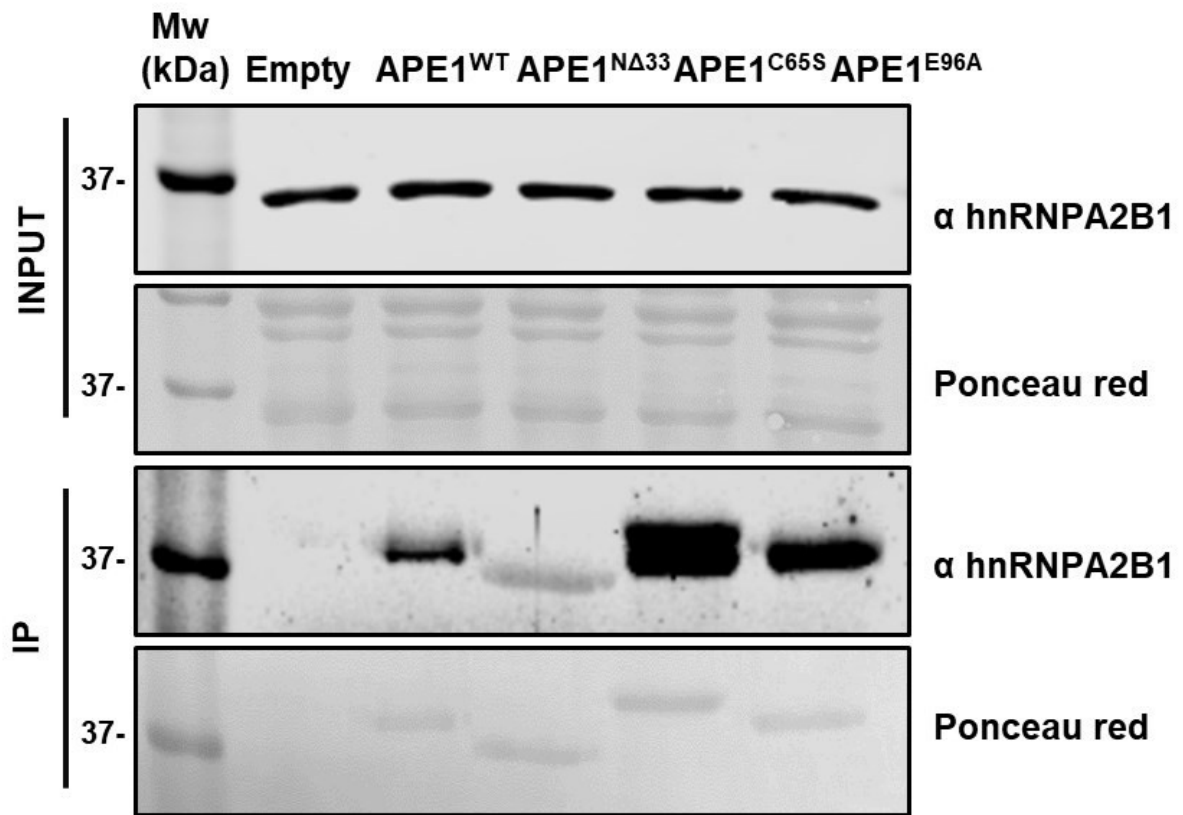


Figure 47: APE1-hnRNPA2B1 interaction analysis. Co-IP experiment carried out in JHH-6 cells overexpressing Flag APE1^{WT}, Flag APE1^{NΔ33}, Flag APE1^{C65S}, Flag APE1^{E96A} proteins and in JHH-6 cells transfected with an empty vector (Empty) as a negative control. INPUT and IP are indicated. Western blot was performed using anti hnRNPA2B1 antibody. Ponceau red staining was executed to evaluate if the IP samples were opportunely normalized.

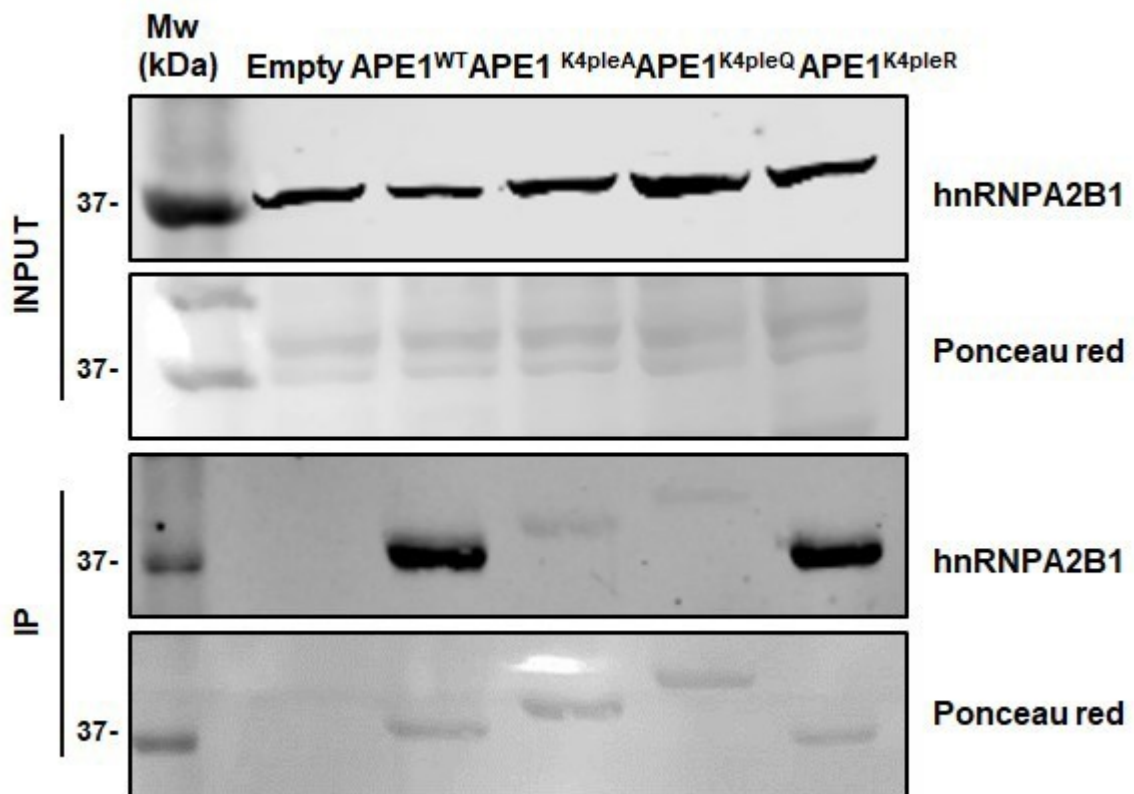


Figure 48 APE1-hnRNPA2B1 interaction analysis. Co-IP experiment carried out in JHH-6 cells overexpressing Flag APE1^{WT}, Flag APE1^{K4^{ple}A}, Flag APE1^{K4^{ple}Q}, Flag APE1^{K4^{ple}R}, proteins and in JHH-6 cells transfected with an empty vector (Empty) as a negative control. INPUT and IP are indicated. Western blot was performed using anti hnRNPA2B1 antibody. Ponceau red staining was executed to evaluate if the IP samples were opportunely normalized.

Once we demonstrated that APE1 interacts together with hnRNPA2B1 through its N-terminal domain and considering that usually APE1 interacts with several proteins through the lysine residues located to the same region¹¹, we wanted to evaluate if also this interaction occurred through the same mode. CoIP experiments were carried out overexpressing the lysine Flag APE1 mutants K4^{ple}A, K4^{ple}Q and K4^{ple}R. APE1^{K4^{ple}A}, is characterized by having the substitution of K27, K31, K32, K35 lysine residues with alanine. These substitutions neutralize the positive charges of lysines and simulates a constitutive acetylation status of the protein^{11,19}. APE1^{K4^{ple}Q}, is characterized by the substitution of the K27, K31, K32, K35 residues with glutamine. Also this mutant displays a constitutive acetylated APE1 form. APE1^{K4^{ple}R} instead is characterized by

having the substitution of the four K residues with arginine. This mutation confers a not-acetylatable status to APE1 protein¹⁵⁹. As shown in (Figure 48), APE1 lysine residues located at the N-terminal region of the protein are essential for the interaction with hnRNPA2B1 protein, and their acetylation status regulates this interaction.

Considering that APE1 and hnRNPA2B1 are both negative prognostic factor in several tumors^{1,60}, we wanted to check the correlation between these two factors in cancer. For this purpose, correlation analysis was performed consulting *The Cancer Genome Atlas* (TCGA) datasets. As shown in (Figure 49) there is a strong positive correlation between the expression levels of APE1 and hnRNPA2B1 in many tumors. The levels of correlation are reported in the (Table 1) below. This bioinformatics analysis supports the hypothesis that this complex could have an important role in tumor biology.

Due to the APE1 contribution in miRNA processing³ and to the hypothetic role of extracellular APE1 in EVs miRNA sorting, considering also that hnRNPA2B1 contributes in the same biological events, further investigation need to be executed to unveil if hnRNPA2B1 and APE1 contribute together in these processes.

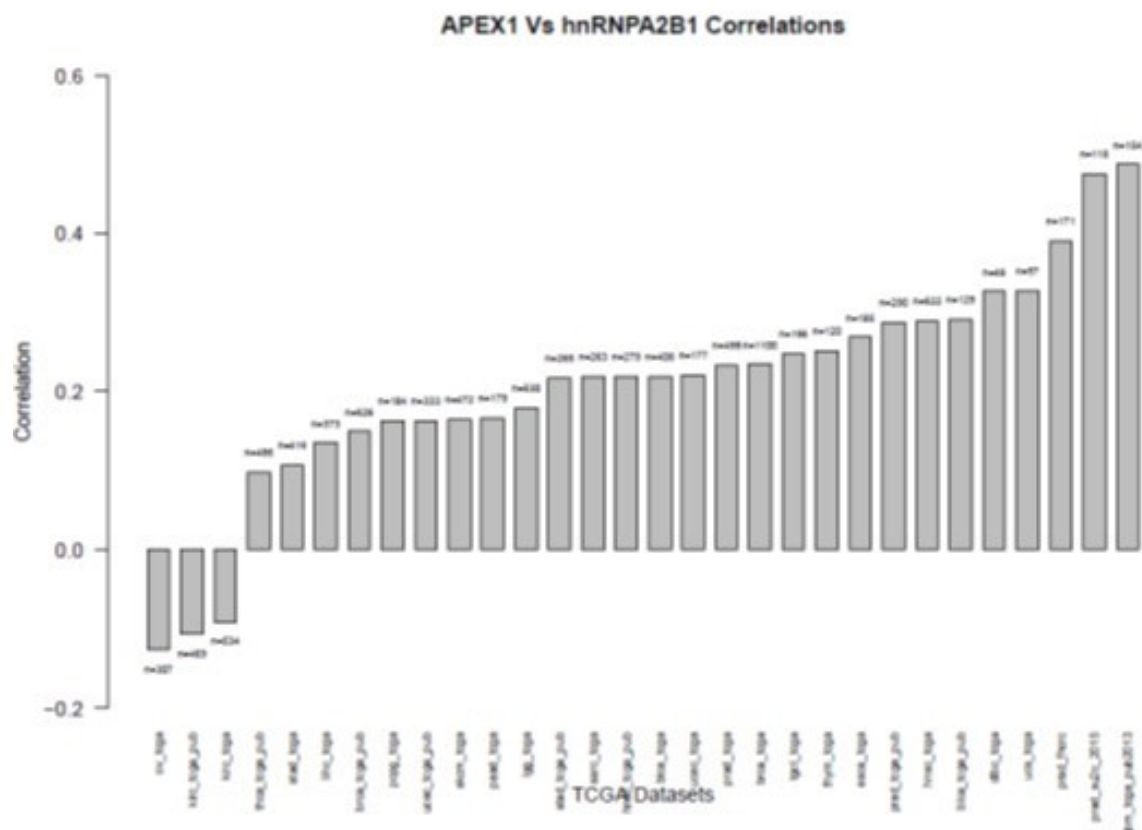


Figure 49: APE1 hnRNPA2B1 correlation analysis was performed consulting 30 TCGA datasets. In the graph is shown the trend of the correlation in the various cancer datasets analyzed.

Significant Datasets	Correlation
Glioblastoma (TCGA, Cell 2013)	0,487032084
Metastatic Prostate Cancer, SU2C/PCF Dream Team (Robinson et al., Cell 2015)	0,475666974
Prostate Adenocarcinoma (Fred Hutchinson CRC, Nat Med 2016)	0,390125045
Uterine Carcinosarcoma (TCGA, Provisional)	0,326633212
Lymphoid Neoplasm Diffuse Large B-cell Lymphoma (TCGA, Provisional)	0,326265497
Bladder Urothelial Carcinoma (TCGA, Nature 2014)	0,290703458
Head and Neck Squamous Cell Carcinoma (TCGA, Provisional)	0,28896331
Prostate Adenocarcinoma (TCGA, Cell 2015)	0,286795203
Esophageal Carcinoma (TCGA, Provisional)	0,268537272
Thymoma (TCGA, Provisional)	0,251154153
Testicular Germ Cell Cancer (TCGA, Provisional)	0,24792893
Breast Invasive Carcinoma (TCGA, Provisional)	0,234192521
Prostate Adenocarcinoma (TCGA, Provisional)	0,233716922
Uterine Corpus Endometrial Carcinoma (TCGA, Provisional)	0,220399784
Bladder Urothelial Carcinoma (TCGA, Provisional)	0,21957195
Head and Neck Squamous Cell Carcinoma (TCGA, Nature 2015)	0,219000459
Sarcoma (TCGA, Provisional)	0,218449279
Stomach Adenocarcinoma (TCGA, Nature 2014)	0,216512905
Brain Lower Grade Glioma (TCGA, Provisional)	0,179872684
Pancreatic Adenocarcinoma (TCGA, Provisional)	0,16705432
Skin Cutaneous Melanoma (TCGA, Provisional)	0,164285415
Uterine Corpus Endometrial Carcinoma (TCGA, Nature 2013)	0,163663624
Pheochromocytoma and Paraganglioma (TCGA, Provisional)	0,162541457
Breast Invasive Carcinoma (TCGA, Nature 2012)	0,149393589
Liver Hepatocellular Carcinoma (TCGA, Provisional)	0,135022492
Stomach Adenocarcinoma (TCGA, Provisional)	0,107192477
Papillary Thyroid Carcinoma (TCGA, Cell 2014)	0,097252965
Kidney Renal Clear Cell Carcinoma (TCGA, Provisional)	-0,090948703
Kidney Renal Clear Cell Carcinoma (TCGA, Nature 2013)	-0,106371848
Ovarian Serous Cystadenocarcinoma (TCGA, Provisional)	-0,126183969

Table 1: The chart shows all the analyzed TCGA data sets. Positive correlation data are indicated in green, negative correlation are indicated in red.

Chapter 4

Analysis of miRNA expression profiles in hepatocellular carcinoma cells APE1-depleted

APE1 participates in tumor progression regulating miRNA processing in cancer cells³. In order to explore APE1 contribution to miRNA processing/decay, based on our recent findings correlating APE1 protein expression levels to miRNA sorting in EVs, we wanted to identify miRNAs that a) participates in the progression of HCC, b) whose expression is affected by the APE1 protein, for comprehending APE1 role in HCC tumor biology and c) can have a prognostic value. For this purpose, Nanostring analysis in JHH-6 depleted for APE1 protein was carried out. APE1 depletion was realized through custom APE1 siRNA transfection (Figure 50). In parallel, siRNA transfection with a SCR pool (siSCR) was performed as a control (*see material and methods*). Once obtained these JHH-6 cells, miRNA extraction was executed and NanoString analysis was carried out to estimate *differentially expressed miRNAs* (DE-miRNAs) in HCC upon APE1 depletion. Through this analysis we could identify 7 DE-miRNAs (*see table 2*). Five of them are up-regulated and two are downregulated in APE1 depletion condition. We did not obtain a higher number of significantly DE-miRNAs because the silencing efficiency in this specific cell line was around 50%.

Using the database TarBase v7.0, queried through the DIANA-MirPath v.3 web-server, we defined the experimentally validated target genes for each identified miRNA. It was used DIANA-MirPath also to perform the functional enrichment analysis for Gene Ontology-Biological Process terms. Through this analysis, we obtained a Heat-map showing the significantly enriched functional terms associated with DE-miRNAs validated targets (Figure 51). We also represented the most informative enriched GO terms through a treemap, summarizing the output with REVIGO tool (Figure 52A). This kind of representation allow to identify the different biological pathways, whose regulation could be indirectly mediated by the identified DE-miRNAs. Many pathways are associated with biosynthesis, regulation and metabolism of RNA, as well

as the regulation of gene expression, reinforcing our previous collected evidences about APE1 participation in tumor biology through the regulation of these cellular processes.

To further study the interconnections between the identified pathways, we also performed a functional enrichment analysis using the KEGG database, summarizing the output with the KEGG-PathwayConnector web tool. From this analysis we obtained a network of the top 15 enriched KEGG functional terms associated with the validated DE-miRNAs (Figure 52B). 11 major clusters were defined, including Hippo pathway¹⁶⁰, Wnt signaling¹⁶¹, p53 pathway¹⁶² and FoxO. Interestingly the RNA transport pathway was also observed among the significantly enriched terms. These results strengthen APE1 contribution in controlling processes related to tumorigenesis, cancer cell proliferation and possibly to RNA sorting into EVs.

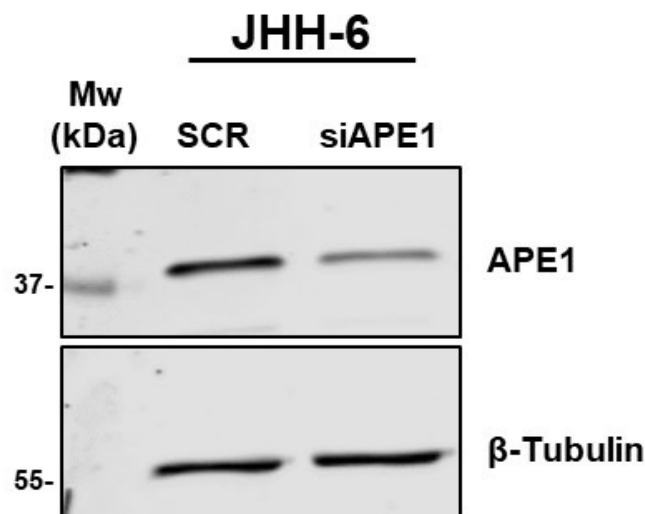


Figure 50: western blot analysis for APE1 detection executed in siAPE1 JHH-6 cells silenced for 48 hours and the respective SCR control. β- Tubulin detection was carried out as loading control.

DE miRNA	logFC	lr	pvalue	qvalue
hsa-miR-2117	3,09677127	10,27502848	0,001348428	0,071736365
hsa-miR-1973	2,496912937	11,82620768	0,000584028	0,042368593
hsa-miR-1246	2,488238926	101,3730911	0	0
hsa-miR-378e	1,255136703	43,25076396	4,82E-11	1,92E-08
hsa-miR-575	1,148905355	9,757444053	0,00178598	0,079178466
hsa-miR-99a-5p	-1,052832225	33,37004321	7,62E-09	2,03E-06
hsa-miR-33a-5p	-1,162374783	9,987186854	0,001576332	0,073994896

Table 2: DE miRNAs obtained by the Nanostring analysis carried out upon JHH-6 cells silenced for 48 hours with siAPE1 or siSCR as control. LogFC, lr, pvalue and qvalue for each DE miRNA are indicated.

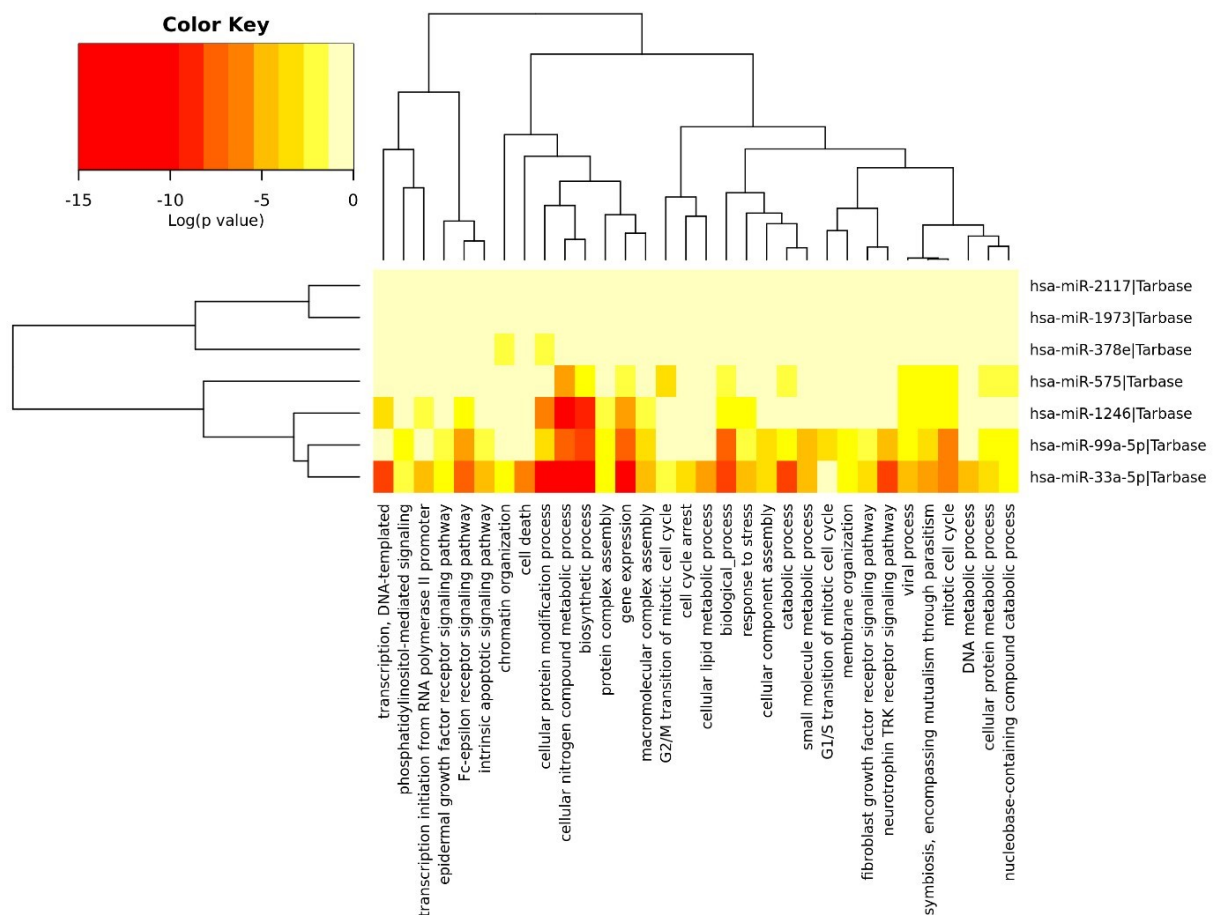
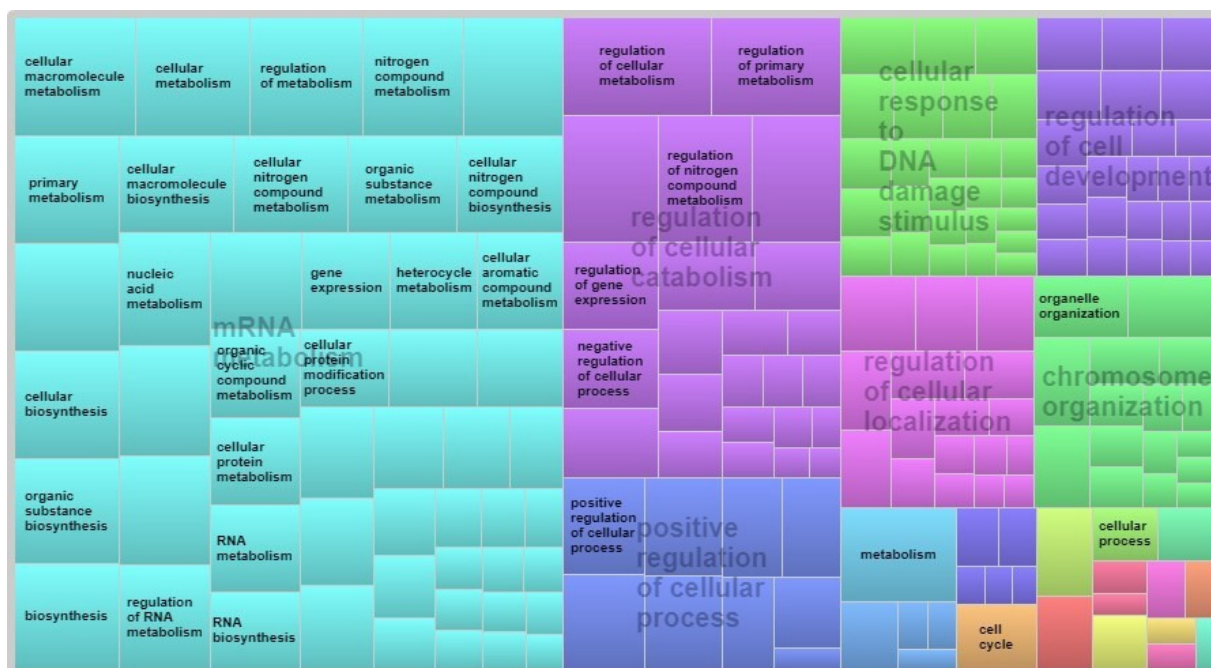


Figure 51: Functional enrichment analysis of DE-miRNAs validated targets. Heatmap showing the significantly enriched functional terms (adj pvalue≤0.05) associated with DE-miRNAs validated targets, according to DIANA-MirPath (GO – Biological Process). Enriched terms and miRNAs are clustered, based on the log (adjpvalue).

A



B



Figure 52: Functional enrichment analysis of DE-miRNAs validated targets. A) Gorilla/REVIGO TreeMap representation summarizing the most informative enriched GO terms ($p\text{value} \leq 0.001$). B) Network of the top 15 enriched KEGG functional terms ($p\text{value} \leq 0.05$) associated with DE-miRNAs validated targets, according to the KEGG-PathwayConnector web tool.

Conclusions

Cancer cells are able to counteract cell death through the activation of DDR in response to chemotherapeutic treatment, by triggering chemoresistance phenomena and maintaining their proliferative rate^{163,164}. BER enzymes, that are mainly involved in DDR but are also able to induce the regulation of gene expression, are considered as a good target for cancer treatment^{26,165}. Chemoresistance process causes a modulation of immune response¹⁶⁶. Many secreted factors, which act in autocrine and paracrine manner, are also able to modulate inflammatory response in tumor microenvironment¹⁶⁵ and the study of tumor microenvironment appears to become relevant for comprehending the mechanisms activated by cancer cells in order to support tumor maintenance and proliferation. *Damage associated molecular patterns* (DAMP), are secreted factors, which contribute in tumor progression. Some DNA repair protein are also DAMP factors, and when secreted, they may act as chemokines and cytokines, contributing in cell signalling and inflammation. APE1 is a multifunctional protein that participates in DNA repair and in the regulation of gene expression. Elevated levels of APE1 protein in sera of different tumors like bladder and NSCLC have been registered, and extracellular APE1 contribution in promoting chemoresistance, by affecting cell sensitivity to chemotherapy it was proved^{95,96}, suggesting that APE1 could be considered as a prognostic biomarker in cancer. Moreover, it seems that APE1 extracellular release could be mediated by acetylation upon N-terminal region of the protein¹⁰⁰, but no clear evidences about the extracellular APE1 biological function have been elucidated, yet. A recent work, in fact, suggested that extracellular APE1 could be involved in triggering apoptosis in TNBC cells through its binding to RAGE receptors¹⁰⁰. Other evidences claim that extracellular APE1 can control TNF- α induced inflammatory response, modulating the activation status of TNFR receptor through its redox activity¹⁶⁷, other data instead sustain that exogenous APE1 can participate in the early phases of inflammation process, inducing the activation of IL-6 gene expression through NF- κ B⁹⁷. For all of these reasons it is possible to hypothesize that APE1 could act as a novel unsuspected DAMP factor.

In the present thesis, the extracellular role of APE1 and its relevance in HCC tumor progression was analysed. It was proved that APE1 is present in HCC serum samples and that serum APE1 levels parallel the cellular protein amounts in tumor tissues. APE1 paracrine function was characterized, demonstrating that exogenously added APE1 and its mutant forms APE1^{K4pleA} and APE1^{NΔ33} may trigger endogenous IL-6 and IL-8 expression in a paracrine way, using both rGST APE1 from *E. coli* and IP-purified proteins from HeLa cells. In particular, we observed that rAPE1^{K4pleA} and rAPE1^{NΔ33} were more efficient in inducing IL-6 and IL-8 expression than rAPE1^{WT}. IL-6 and IL-8 are SASP factors but also important players in triggering immune-response in cancer microenvironment. Considering these data, we can hypothesize that APE1 may contribute to HCC tumor maintenance and progression possibly through the activation of cytokines that support cells senescence and also tumor cell invasiveness through triggering the inflammatory response.

APE1 protein lacks of the classical secretory signal in its sequence even if its secretion was observed in different works^{105,106}. We were able to demonstrate that APE1 is released by means of EVs, and that is the only BER enzyme that takes part to EVs protein composition, together with the scaffold protein XRCC1, that possibly contributes in stabilizing a complex between APE1 and nucleic acids. We found, in fact, that APE1 is enzymatically active in EVs, because is able to exert its endonuclease activity upon 8oxoy-riboG and also in abasic ribo- embedded in DNA. APE1 EVs secretion process is a general mechanism carried out by all tumor cell lines we analysed, and its accumulation in EVs is increased upon different genotoxic stresses, specifically doxorubicin and cisplatin. Moreover, we found that APE1 truncated form increases in EVs upon oxidative stresses.

Few publications elucidate how EVs could contain different kind of proteases, some of them are exposed to EVs membrane and contribute to the remodeling of extracellular matrix promoting tumor invasiveness and sustaining inflammation processes^{150,168}. We observed that APE1 can undergo proteolytic cleavage inside EVs

and that proteases activity increased under genotoxic stress conditions, but we still need to properly identify the protease(s) responsible for APE1 cleavage and also to characterize APE1 function in EVs according to its nature. It could be speculated that the full length protein function is related to the RNA/DNA processing on the encapsulated nucleic acid, while the paracrine function could be exerted by both full length and APE1^{NA33} forms, according to the evidences that we collected regarding rAPE1 role in the activation of IL-8 promoter. These data demonstrated that the IL-8 gene expression is promoted by a transcriptional regulatory mechanism, exerted by exogenous APE1 through its redox function. We think in fact that extracellular APE1 could act in a paracrine manner modulating the activity of not yet identified receptors exposed by the recipient cells, which are responsible for the activation of signaling cascades, that culminate with the IL-8 gene transcription initiation. The inhibition of APE1 redox function in fact, represses the activation of IL-8 promoter. The proposed mechanism is similar to that one exerted by the DAMP factor *High mobility group box 1* (HMGB1) protein^{169,170}. HMGB1 is an early DDR factor which rapidly accumulates in loci where oxidative stress occurs¹⁷¹. It is also like a sort of BER cofactor because is able to stimulate BER enzyme activities such as the APE1 endonuclease and also FEN1 flap cleavage activity¹⁶⁹ when DNA damage occurs. Studies demonstrated that HMGB1 cellular localization is altered by oxidative stress, which causes the translocation and later the secretion of the protein. HMGB1 cysteine residues are important for the regulation of its extracellular biological activity. In particular, three are the cysteine residues involved in its reversible regulation Cys23, Cys45 and Cys106. When all the cysteine residues are in the thiol state, HMGB1 exerts its chemotactic activity, forming a complex with CXCL12, which binds CXCR4 to trigger the process. In an intermediate oxidation status, a disulphide bond between Cys23 and Cys45 residues occurs and the protein becomes able to interact with MD-2 and TLR4, acquiring the pro-inflammatory cytokine behaviour. In the condition in which all the cysteine residues are oxidised into sulfonates HMGB1 is not able to act as chemokine or cytokine. Moreover, other post-translational modifications are indispensable for switching

HMGB1 protein functions and also for promoting its secretion. Acetylation occurring in the NLS sequence of the protein makes for instance HMGB1 able to promote inflammation and when it is hyper-acetylated, the protein can shuttle from nucleus to cytoplasm, where it can be later secreted and participate in inflammation and immunity response¹⁷².

As a secreted factor, HMGB1 is enrolled to act as a pro-inflammatory molecule^{173,174}. The evidences about the role of secreted HMGB1 in tumor progression, are presently contradictory. Some studies, in fact, demonstrated that its secretion is promoted by chemotherapeutic treatment, and its function is related to the stimulation of chemokine CXCL11, taking part to antitumor immune response^{166,175}. Conversely, other evidences suggested that secreted HMGB1 could have a role in supporting cancer progression, as demonstrated for *oesophageal squamous cell carcinoma* (ESCC)¹⁶⁵. These indications suggest that some DNA repair proteins, like HMGB1 can be also molecules that acting as autocrine or paracrine factors could have an important role in supporting cancer progression, and in the activation of inflammatory status in tumor microenvironment. It is conceivable that APE1 could act similarly to HMGB1, because of a similar redox domain that is responsible for the modulation of APE1 function.

APE1 participates in the processing of some oncogenic miRNAs under genotoxic stress³. In this thesis, it was proved that the protein significantly contributes to the regulation of miRNAs expression/processing and to their sorting into EVs, considering that EVs from APE1 murine KO cells (CH12F3) and also from HeLa and A549 APE1 depleted cells, displayed a strongly reduced content of miRNAs. Moreover, the intracellular levels of mature miRNAs are lower in APE1 KO cell lines suggesting that APE1 could have a strong impact also in miRNAs production.

For better comprehending APE1 contribution in this field, a preliminary characterization of APE1-hnRNPA2B1 interaction was performed. hnRNPA2B1 is an APE1 protein partner identified through the interactome analysis and resulted

interesting to study for its implications in miRNA processing and also in EVs miRNA sorting^{3,56,62}.

It was proved that this interaction occurs through APE1 N-terminal region and that is mediated by RNA. Furthermore, APE1 N-terminal acetylation impairs this interaction. It will be interesting, in the future, to characterize the role of this complex. We hypothesized that these two proteins could be involved, together, in the regulation of extracellular miRNAs, starting from their expression/processing up to their sorting.

In order to understand the APE1 role in the regulation of miRNAs processing in HCC, a Nanostring analysis in JHH-6 depleted for the protein was performed. Unfortunately, due to the low efficiency of silencing, in this specific cell line, we could not provide many DE-miRNAs, but we could notice that the identified ones participate in the regulation of important cellular pathways such as Wnt, FoxO and p53. Surprisingly, we also noticed that some of them are implicated in the regulation of proteoglycan synthesis in cancer, sphingolipids biosynthesis and RNA transport. All of these processes are possibly related to EVs formation and sorting of macromolecules, strengthening the concept of APE1 involvement in biogenesis and transport of miRNA in EVs.

In the future, further investigation will be necessary to characterize these phenomena. In the meantime, a representative model illustrating the hypothetical extracellular APE1 role as DAMP factor and its implication in the regulation/sorting of miRNAs in tumor biology is shown (Figure 53).

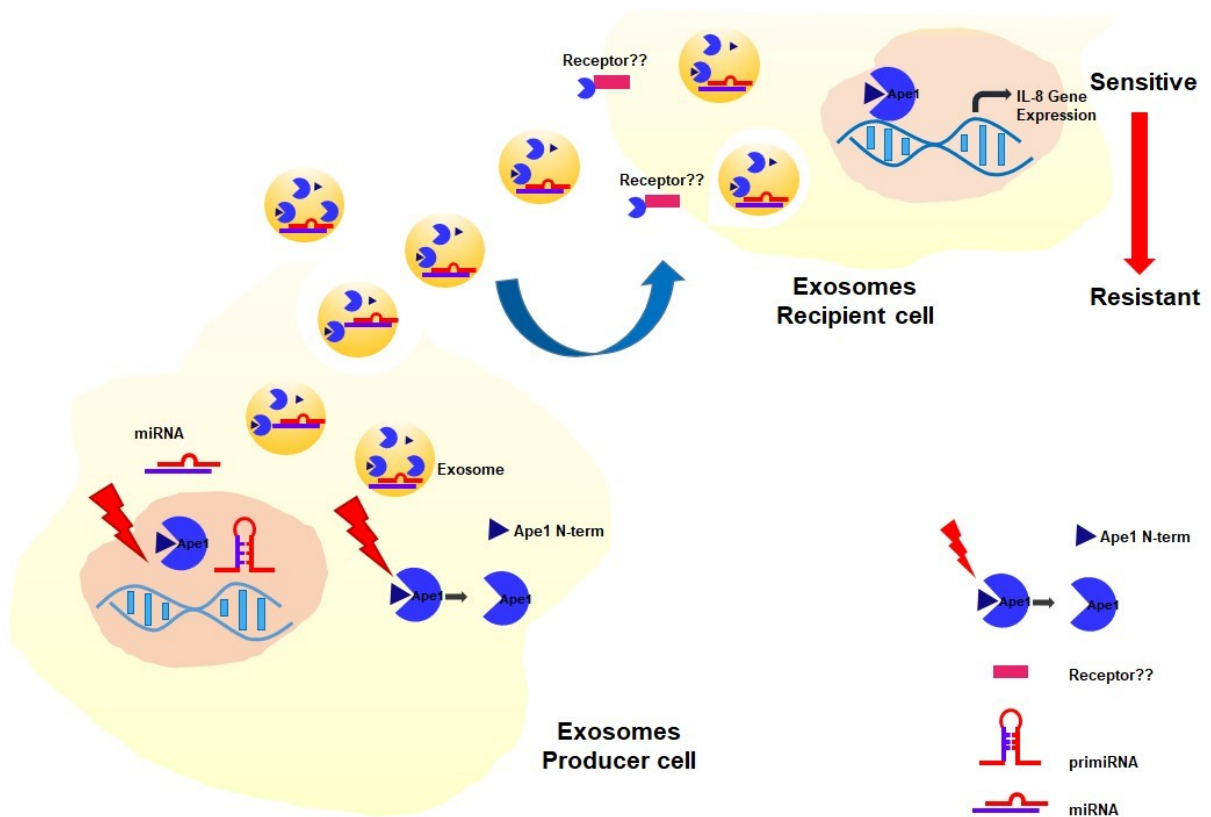


Figure 53: Representative model of APE1 as miRNA expression/processing/sorting regulator and as DAMP factor, which promotes tumor progression, modulating gene expression of recipient cancer cells.

Future perspectives

Some major aspects that came out from the work of this Thesis need further specific studies.

We observed that exogenously added rAPE1 can act as a DAMP factor, because it is able to induce IL-6 and IL-8 mRNA expression in the receiving cells. We also demonstrated APE1 secretion through EVs. Further investigations will be carried out to shed light on the hypothesis of these two different secretion mechanisms, involving or not vesicular bodies, and their contribution in tumor biology.

Moreover, we need to characterize the molecular mechanism by which APE1 may act in a paracrine manner, inducing the inflammatory response in the receiving cells. For this purpose, we will try to understand if the mechanism could occur *via* any not yet identified receptor and if the APE1 redox domain could be involved in this process, as it was demonstrated for HMGB1 protein. For this purpose, treatment using rAPE1 redox mutants will be performed.

It was proved that APE1 can undergo proteolytic cleavage inside EVs, therefore we need to identify the protease(s) responsible for this event, to understand APE1 function in EVs according to its nature.

To comprehend the APE1 role in controlling miRNAs processing and sorting, Nanostring analyses will be performed in HeLa inducible APE1 knock down cells and in HeLa SCR as a control, in order to identify those EXE miRNAs regulated by APE1. Moreover, further investigation about the function of the complex hnRNPA2B1-APE1 in EVs will be done.

Material and methods:

Cell culture and treatments

JHH-6, an undifferentiated HCC cell line, was grown in William's medium E (Sigma-Aldrich), supplemented with 10% fetal bovine serum, 100 U/ml penicillin, 100 µg/ml streptomycin (Euroclone, Milan, Italy). A549, human epithelial lung cell line, was grown in RPMI 1640 supplemented with 10% fetal bovine serum, 100 U/ml penicillin, 100 µg/ml streptomycin (Euroclone, Milan, Italy). Hct116 ^{+/p53} and Hct116 ^{-/-p53}, human epithelial colon cancer cell lines, were grown in Dulbecco's Modified medium (DMEM) supplemented with 10% fetal bovine serum, 100 U/ml penicillin, 100 µg/ml streptomycin (Euroclone, Milan, Italy). Acute myeloid leukemia cell lines OCI-AML2, and OCI-AML3, the last one characterized by having a mutation on the third helix of the C-Term domain (h3 mutA and H3 mutE) of NPM1 protein⁸⁵, were grown in α -MEM with ribonucleosides, 20% fetal bovine serum, 100 U/ml penicillin, 100 µg/ml streptomycin (Euroclone, Milan, Italy). CH12F3^{Δ++}, murine B cell line, biallelic for Ape1 gene, and CH12F3^{ΔΔΔ} murine B cell line, allelic null for Ape1, were grown in RPMI 1640 medium supplemented with 10% fetal bovine serum, Non Essential Aminoacids, 1mM Sodium Pyruvate, 100 U/ml penicillin, 100 µg/ml streptomycin (Euroclone, Milan, Italy). HeLa inducible cell clones expressing ectopic Flag APE1 proteins were grown in Dulbecco's modified Eagle's medium as indicated in ^{65,176}.

Viability assay

JHH-6 or A549 were seeded at the density of 4×10^3 cells in 96well plates. The day after seeding, cells were treated for 24, 48 and 72 hours with the following genotoxic agents: Doxorubicin hydrochloride (Sigma Aldrich, Milan Italy), dissolved in UltraPure™ DNase/RNase-Free Distilled Water (Invitrogen™, Thermo Fisher Scientific, Waltham, Massachusetts, United States) or with cis-Diammineplatinum(II) dichloride (CDDP), (Sigma Aldrich, Milan Italy), dissolved in dimethylformamide (DMF), at the indicated concentrations (*see results section*). The cellular viability was assayed by using CellTiter

96® AQueous One Solution Cell Proliferation Assay (Promega, Milan, Italy). Absorbance at 490nm, indicative of cellular metabolic activity, was measured with EnSpire 2300 Multilabel reader, (Perkin Elmer, Waltham, Massachusetts United States). Each treatment was performed in three biological replicas, and for every single experiment a four technical replicas were executed. Each absorbance value registered was standardized with the absorbance value obtained from wells containing only medium.

Extracellular vesicles (EVs) isolation

Exosomes were isolated from medium supplemented with 10% Fetal Bovine Serum, exosome-depleted (ThermoFisher Scientific, Waltham, Massachusetts United States), 100 U/ml penicillin, 100 µg/ml streptomycin (Euroclone, Milan, Italy), using Total exosome Isolation kit (Thermo Fisher Scientific Waltham, Massachusetts United States), according to the manufacturer instructions. Polydisperse EVs in the range of 80-800 nm were obtained by nickel-based isolation (NBI)¹⁵¹. Briefly, nickel-charged beads were added to the media to capture EVs during 30 min incubation at RT in shaking, Then EVs from recovered beads were eluted using a pH 7.4 elution buffer containing EDTA and sodium citrate as chelating agents.

Exosome quantification and characterization

Exosomes range size analysis and quantification was assayed performing the nanoparticle tracking analysis (NTA) with the Nano-Sight instrument, version NTA 3.2 Dev Build 3.2.16. Exosomes vesicles were characterized by transmission electron microscopy (TEM). EVs isolated by NBI were characterized by Tunable Resistive Pulse Sensing (TRPS) technology, using qNANO instrument (iZON Science) and NP250

nanopores. Stretch conditions and quality of acquisitions were assessed based on CPC200 calibration beads (iZON Science).

Exosome extracts preparation (EXE)

Once the EVs have been obtained, laemmly buffer (SDS 2%, Glycerol 10%, Tris-HCl pH 6.8 0.5M, β -mercaptoethanol 3.5%, bromophenol blue) was added to shatter the vesicles and to denature their protein content. The samples were later boiled for 5 minutes at 95°C and kept on ice until use.

Whole cell extracts preparation (WCE)

Cells were harvested, centrifuged at 1200 rpm for 3 minutes, washed with PBS, and resuspended with lysis buffer (50mM Tris HCl pH 7.5, 150mM NaCl, 1mM EDTA pH 8.0, 1% Triton X-100). After 20 minutes of incubation on ice, the lysate was centrifuged at 13000rpm to remove debris and the whole cell extract was recuperated and kept at -80°C.

Nuclear cell extracts preparation (NCE)

Cells were washed twice with PBS, harvested in PBS complemented with DTT 0.1mM and PMSF 0.5mM and centrifuged at 1000rpm for 10 minutes at 4°C. The cell pellet was later resuspended with T1 solution (HEPES pH 7.9, 10mM, KCl 10mM, MgCl₂ 0.1mM, EDTA pH 8.0, 0.1mM) and centrifuged at 2400 rpm for 10 minutes at 4°C. The supernatant, consisting of cytosolic proteins, was harvested and kept on ice. Nuclear pellet was resuspended in T1 solution, centrifuged at 2400 rpm for 10 minutes at 4°C for pelleting nuclei again. The supernatant was discarded and nuclear pellet was properly resuspended with T2 solution (HEPES pH 7.9, 20mM, NaCl 420mM, MgCl₂

1.5mM, EDTA pH 8.0, 0.1mM, Glycerol 5%). After 30 minutes of incubation, the sample was centrifuged at 12000rpm for 20 minutes at 4°C and the supernatant containing nuclear proteins was harvested and kept on ice. Both cytosolic and nuclear extracts were later quantified and used for protein analysis.

Western blot analysis

Protein extracts were suitably quantified with Bradford solution (Bio-rad, California, United States), according to the manufacturer's instructions, resolved in 10%/12% gel SureCast™ Acrylamide Solution (40%) (Invitrogen, California, United States) and transferred in nitrocellulose membrane, (Amersham, United Kingdom). Western blot analyses were executed using the listed primary antibodies: anti APE1 antibody (13B8E5C2, Novus), anti β -tubulin antibody (T0198, Sigma-Aldrich), anti DNA Polymerase beta antibody (ab26343, Abcam), Anti-DNA Polymerase delta (ab10362 Abcam), anti OGG1 antibody, supplied by Radicella, anti Alix Antibody (1A12) (SC-53540, Santa Cruz), anti GM130 Antibody (B-10) (SC-55591, Santa Cruz), anti Syntenin antibody (EPR8102) (ab133267, Abcam), anti GST antibody (ab19256, Abcam), anti Flag M2 antibody (F1804, Sigma Aldrich). After incubation with primary antibodies, membranes were washed three times with PBS-0.1% Tween-20, (Sigma Aldrich, Milan, Italy), incubated for 1 hour at room temperature with the appropriate IRDye800/IRDye600 labelled secondary antibodies (diluted to 1:2000). The acquisition of the images and the quantifications analyses were achieved using Odyssey CLx Infrared Imaging system (LI-COR GmbH, Germany).

Comassie brilliant blue staining

Comassie brilliant blue staining was performed for the following GST recombinant proteins: rGST, rGST APE1^{WT}, rGST APE1^{k4pleA}, rGST APE1^{NA33}. 1.5µg of each

recombinant protein was loaded in a 10% polyacrylamide gel and SDS PAGE was executed. Later Comassie staining was made for 15 minutes and finally the gel was incubated for 30 minutes in destaining solution. The acquisition of the image was achieved using Odyssey CLx Infrared Imaging system (LI-COR GmbH, Germany).

Cell transfection and immuno-purified protein production

Immuno-purified proteins APE1^{WT-flag}, APE1^{K4pleA-flag}, APE1^{NΔ33-flag} were obtained as indicated below. On day one 3×10^6 JHH-6 were seeded in 10cm dish, the day after they were transfected with 6μg of pCMV5.1_hAPE1^{WT-flag}, pCMV5.1_hAPE1^{K4pleA-flag}, pCMV5.1_hAPE1^{NΔ33-flag}, pCMV5.1_empty vectors with Lipofectamine 2000 reagent (Invitrogen, California, Unites States), according to the manufacturer's instructions. On day three, immunoprecipitation was carried out using FLAG[®] magnetic affinity resin and the elution for competition was made with Flag peptide, (both supplied by Sigma Aldrich, Milan Italy). The immunoprecipitation was performed as indicated below. Later, the obtained immune-purified proteins were directly used to treat JHH-6 for 24h at the concentration of 1μg/ml.

Co-immunoprecipitation

On day one 3×10^6 JHH-6 cells were seeded in 10 cm dish and the day after were transfected with pCMV5.1_hAPE1 constructs, using Lipofectamine 2000 reagent (Invitrogen, California United States), according to the manufacturer's instructions. The following day, cells were washed twice with PBS, and 800μl of lysis buffer (Tris HCl pH 7.4, 50mM, NaCl 150mM, EDTA 1mM, Triton 1%, protease inhibitor, PMSF, NaF, Na₃VO₄) was directly added to the dish. The lysis was performed in shaker at 4°C for 20 minutes. Later cells were scraped, lysates were harvested and centrifuged at 12000g for 10 minutes at 4°C. Supernatants were collected and 50μl of lysate for each

condition were kept as INPUT and quantified with Bradford solution. In parallel 30µl of FLAG® magnetic affinity resin, (Sigma Aldrich, Milan, Italy), for each experimental condition was centrifuged at 8000g for 1 minutes at 4°C to remove the storage liquid. Later resin was washed three times with TBS solution (Tris HCl pH 7.4, 50mM, NaCl 150mM) at 8000g for 1 minute at 4°C and an incubation of the lysate with resin for 3 hours on the rocker at 4°C was performed. After incubation, the resin was centrifuged at 8000g for 1 minute, washed three times with TBS and later the elution was performed adding to the resin 3µl of peptide FLAG, (Sigma Aldrich, Milan, Italy), resuspended in 50µl of TBS complemented with protease inhibitors. The elution was performed on the rocker for 30 minutes at 4°C. Subsequently the resin was centrifuged and the immuno-precipitated extract (IP) was collected. A comassie staining loading just 3µl of IP in a 10% polyacrylamide gel was executed in a way to normalize the different IPs.

The treatment with RNaseA (Sigma Aldrich, Milan Italy) were performed at the concentration of 100µg/ml for 30 minutes at 37°C. For treatments with DNaseI RNase free (Thermo Fisher Scientific Massachusetts, United States), lysates were prepared using the following lysis buffer: DNaseI Reaction buffer, protease inhibitor, NaCl 25mM, TritonX-100 1%. Once lysates were ready, DNase I was added to the lysate and the treatment was performed for 30 minutes at 37°C. The inactivation of DNaseI was executed simply adding DTT 1mM to the lysate. No heat inactivation was made to avoid protein degradation.

siRNA transfection

2.5*10⁶ JHH-6 cells were seeded in 10 cm dishes. The day after, cells were transfected with 600 pmol of custom hAPE1 siRNA (*see hAPE1 siRNA sequence below*). Non-targeting siRNA pool (siSCR) transfection was in parallel performed as a control. Both siRNAs were supplied by GE Healthcare Dharmacon, (Colorado, Unites States). The

transfection was executed with DharmaFECT transfection reagent (Thermo Fisher Scientific, Massachusetts, United States), according to the manufacturer's instructions. After 6 hours of transfections, fresh medium was added to the complexes for reducing cytotoxicity. The day after transfection cells were washed twice with PBS, fresh media was added and after 48 hours from transfection cells were collected, washed twice with PBS, centrifuged and later miRNAs extraction was performed using miRNeasy Mini Kit (QIAGEN, Hilden, Germany), according to the manufacturer's instructions.

Custom hAPE1 siRNA sequence:

Sense: 5' U.A.C.U.C.C.A.G.U.C.G.U.A.C.C.A.G.A.C.C.U.U.U 3'

Antisense: 5' A.G.G.U.C.U.G.G.U.A.C.G.A.C.U.G.G.A.G.U.A.U.U 3'

siSCR used is a pool of selected siRNAs, for this reason no sequences were provided by GE Healthcare Dharmacon.

Gene expression analysis

For the analysis of gene expression profiles, cells were collected and total RNAs were extracted with NucleoSpin® RNA, (Macherey Nagel, Germany), according to the manufacturer's instructions. The obtained RNA was later retro-transcribed using SensiFAST™ cDNA Synthesis Kit, (Bioline, Ohio, United States), and cDNA were tested for IL-6 and IL-8 gene expression. The housekeeping genes GAPDH, HPRT, 18S RNA and ACTB were used for normalization. qRT-PCR was executed using SensiFAST™ SYBR® No-ROX Kit, (Bioline, Ohio, United States), according to the manufacturer's instruction. Reaction were run on CFX96 Real-Time System, (Bio-Rad, California, United States), applying the following cycling parameters: denaturation at 95° C for 10 seconds and annealing/extension at 60° C for 30 seconds repeated for 40

times. The analysis was executed performing three biological replicas. Data were resolved applying $\Delta\Delta\text{Ct}$ method.

Primer list	Forward primer	Reverse primer
GAPDH	5'-TCTCTGCTCCTCCTGTTTC-3'	5'-GCCCAATACGACCAAATCC-3'
HPRT	5'-AGACTTTGCTTTCCTTGGTCAGG-3'	5'-GTCTGGCTTATATCCAACACTTCG-3'
18S RNA	5'-TAACCCGTTGAACCCCATTC-3'	5'-CCATCCAATCGGTAGTAGCG-3'
ACTB	5'-CGCCGCCAGCTCACCATG-3'	5'-CACGATGGAGGGGAAGACGG-3'
APE1	5'-CTGCCTGGACTCTCTCATCAATAC-3'	5'-CCTCATCGCCTATGCCGTAAG-3'
IL-6	5'-CAAAGATGTAGCCGC-3'	5'-GTTCAAGTTGTTTTC-3'
IL-8	5'-CTGGCCGTGGCTCTCTTG-3'	5'-CCTTGGCAAACTGCACCTT-3'

Description of modified DNA and RNA substrates used in this study

The 25-mer oligonucleotide containing a deoxy- and a ribo- tetrahydrofuran, called ss_dF and ss_rF respectively, and its reverse complementary sequence, ss_dC, were synthesized from Metabion International AG (Steinkirchen, Germany), purified through RP-HPLC, checked in Mass Check and re-suspended in RNase- and DNase-free water. Then, the modified oligonucleotides were labelled with either IRDye800 and IRDye700 fluorophores, respectively. Synthesis of oligonucleotide containing an internal ribose 8-oxo-guanosine (r8oxoG) and an IRDye700 fluorophore at 5' end was in-house carried out as explained in Malfatti et al., 2017²⁹.

All oligonucleotides used in the present study were re-suspended in RNase- and DNase- free water at 100 μM . In order to favorite the double strand annealing, 100 pmol of each oligonucleotide was annealed with an excess of 150 pmol of its complementary DNA oligonucleotide in 10 mM TrisHCl pH 7.4 and 10 mM MgCl_2 , heated at 95°C and cooling down over night in the dark.

Modified oligonucleotides

ss_dF 5'-GGATCCGGTAGT**dF**TTAGGCCTGAAC-3'

ss_rF 5'-GGATCCGGTAGT**rF**TTAGGCCTGAAC-3'

ss_r8oxoG 5'-GGATCCGGTAGT**r8oxoG**TTAGGCCTGAAC-3'

Complementary oligonucleotide

ss_dC 5'-GTTCAAGGCCTAACACTACCGGATCC-3'

Ribonucleotides are in red and bolded, and the deoxyribonucleotides are in blue and bolded.

Recombinant proteins

Human recombinant GST APE1 proteins (rGST APE1) were produced as explained in Fantini *et al.*,¹¹ and in Erzberger and Wilson¹⁷⁷. *E. coli* RNase HIII and RNase A from bovine pancreas were respectively purchased from New England BioLabs® Inc (Milan, Italy) and from Sigma Aldrich (Milan, Italy).

Serum APE1 quantification

Serum APE1 protein level was determined using Human APEX1 ELISA kit (Cusabio, Houston, USA). The detection of the optical density (OD) at 450nm, with a correction set at 540 nm, was executed with EnSpire microplate reader (Perkin Elmer, Waltham, USA). sAPE1 levels were later calculated through a standard linear regression curve fitting by NCSS 11 Statistical software (2016) (NCSS, LLC Kaysville, USA).

Amplified luminescent proximity homogeneous assay (alpha)

Glutathione-Donor beads (Perkin Elmer, #6765300) and Protein G-Acceptor beads (Perkin Elmer, #AL102C) were used in saturation binding experiments to detect and quantify the secreted, recombinant APE1 protein. Briefly, a mix of Donor and Acceptor beads, at final concentration of 10 mg/ml each, was added to 3 nM of APE1 antibody (13B8E5C2, Novus) pre-incubated with increasing concentration of rGST APE1 or rGST to reach hooking point. In case of EV experiments, aliquots of vesicles were denatured or not at 90°C for 5 min and equilibrated at RT before adding the alpha mix of beads plus antibody. All the reactions were performed in 20 µl as final volume in 384-Optiplates (Perkin Elmer, Massachusetts, United States) and incubated for 1 hour at RT before acquiring the results with an Enspire Plate Reader (Perkin Elmer, Massachusetts, United States). Curves were analyzed by GraphPad Prism software v.5.

Enzymatic activity assays

To measure enzymatic activity of EXE on different modified DNA substrates (25 nM), each reaction was prepared following different volumes of the extract, expressed in µl, as specified in the legend of each panel. Reactions were performed in a buffer containing 20 mM Tris-HCl, 25 mM KCl, 4 mM MgCl₂, 0.1% BSA, 0.01% Tween20, pH 7.4 for the indicated time at 37°C. Final volume for each reaction was 10 µl. At the end of all reactions, samples were blocked with a stop solution, containing 99.5% v/v Formamide (Sigma Aldrich, Milan, Italy) supplemented with 10X Orange Loading Dye (LI-COR Biosciences, Milan, Italy) and heated at 95°C for 5 minutes. Then, all samples were loaded onto a 7 M denaturing 20% polyacrylamide gel in TBE buffer pH 8.0 and run at 4°C at 300V for 1 hour. Later, the gel was of the non-incised substrate (S) and the incision product (P) bands were quantified using Image Studio software (LI-COR GmbH, Germany).

Study of IL-8 promoter activity

1*10⁴ JHH-6 cells were seeded in 96well plate. 24 hours after seeding, cells were transfected with 200ng of IL-8_promoter or IL-8_ΔNf-κB_promoter, together with 4ng pRL-CMV Renilla Luciferase construct, using Lipofectamine 2000 reagent (Invitrogen, California, United States), as indicated from the manufacturer's instructions. The day after transfection, cells were treated for 24 hours in medium without serum, with 1μg/ml GST APE1 recombinant proteins and the activity of the IL-8 or IL-8_ ΔNf-κB promoters was assayed by Dual-Glo Luciferase Assay System, (Promega, Madison, Wisconsin, United States), according to the manufacturer's instructions. As a positive control for the induction of the IL-8 promoter activity, a treatment in serum starvation for 3 hours with 2000U/ml of TNF-α (Peprotech Inc., New Jersey, United States) was performed, as already reported in Cesaratto et al., 2013⁹⁸.

The ATM inhibitor KU60019 (Sigma Aldrich, Milan, Italy) was dissolved in DMSO and treatments for 24 hours at the concentration of 2μM were performed as shown in Ivanov, Oncotarget 2019¹⁵⁶.

The redox APE1 inhibitor E3330 (Sigma Aldrich, Milan, Italy) was dissolved in DMSO and treatments at the concentration of 175μM for 4 hours were performed as indicated in Cesaratto et al., 2013⁹⁸

Extracellular vesicle proteolytic activity

Extracellular vesicles suspension was diluted in a solution with PBS-Triton X-100 (Sigma Aldrich, Milan, Italy) at the final concentration of 0.1% and quantified with Bradford solution (Bio-rad California, United States). Different concentrations of extracellular vesicles (0.1, 0.5, 1μg) were incubated with 200ng of GST APE1^{WT}, GST APE1^{K4pleA} or rMAT APE1^{WT} recombinant proteins and the reactions were performed at 37°C for 4 hours. The reactions were stopped adding Laemmly sample buffer 4x

(SDS, Glycerol, Tris-HCl 0.5M pH 6.8, β -mercaptoethanol, Bromophenol blue) and denaturing the samples for 5 minutes at 95°C. Each reaction was later loaded in 10% polyacrylamide gel, SDS PAGE was made and in conclusion Western blot was executed.

Proximity ligation assay

For the experiment 2×10^4 JHH-6 cells were seeded on top of slides disposed inside a 12-well plate. The following day cells were fixed for 20 minutes with 4% paraformaldehyde in PBS, and permeabilized for 5 minutes with 0.25% Triton X-100 in PBS. After permeabilization, blocking for 1 hour with FBS 10% in PBS was performed. Later an incubation for 3 hours at 37°C with anti APE1 primary antibody (13B8E5C2, Novus), diluted 1 to 22 was executed. After incubation with anti APE1 antibody, an O/N incubation at 4°C with hnRNPA2B1 antibody (PA5-34939, Thermo Fisher Scientific, Massachusetts, United States) diluted 1 to 500 was made. The following day in situ Proximity Ligation assay technology (Duolink Sigma Aldrich, Milan Italy) was performed according to the manufacturer's instructions. Images were acquired with Leica TCS SP laser-scanning confocal microscope (Leica Microsystems).

miRNA targets functional enrichment analysis

DE-miRNAs human validated targets were retrieved through the DIANA-MirPath v.3 web-server¹⁷⁸. Functional enrichment analysis was performed querying the Gene Ontology – Biological Process databases ($p \leq 0.05$), applying the “genes union” and “pathways union” methods. To reduce output redundancy and provide an easier visualization of the results, a graphical representation of raw data was obtained using GOrilla/REVIGO^{179,180} (default settings) and KEGG-PathwayConnector¹⁸¹ (Select score

to sort: Adjusted pvalue; Select sort order: Ascending Order; Select number of EnrichR pathways to analyse: 10).

Statistical Analyses

Statistical analyses were achieved performing Two-way ANOVA test using GraphPad Prism7 data analysis program. $P < 0.05$ was considered statistically significant.

Bibliography

1. Tell, G., Fantini, D. & Quadrifoglio, F. Understanding different functions of mammalian AP endonuclease (APE1) as a promising tool for cancer treatment. *Cell. Mol. Life Sci. CMLS* **67**, 3589–3608 (2010).
2. Tell, G. & Demple, B. Base excision DNA repair and cancer. *Oncotarget* **6**, 584–585 (2015).
3. Antoniali, G. *et al.* Mammalian APE1 controls miRNA processing and its interactome is linked to cancer RNA metabolism. *Nat. Commun.* **8**, 797 (2017).
4. Dyrkheeva, N. S., Lebedeva, N. A. & Lavrik, O. I. AP Endonuclease 1 as a Key Enzyme in Repair of Apurinic/Apyrimidinic Sites. *Biochem. Biokhimiia* **81**, 951–967 (2016).
5. Fung, H., Bennett, R. A. & Demple, B. Key role of a downstream specificity protein 1 site in cell cycle-regulated transcription of the AP endonuclease gene APE1/APEX in NIH3T3 cells. *J. Biol. Chem.* **276**, 42011–42017 (2001).
6. Ramana, C. V., Boldogh, I., Izumi, T. & Mitra, S. Activation of apurinic/apyrimidinic endonuclease in human cells by reactive oxygen species and its correlation with their adaptive response to genotoxicity of free radicals. *Proc. Natl. Acad. Sci. U. S. A.* **95**, 5061–5066 (1998).

7. Kuninger, D. T., Izumi, T., Papaconstantinou, J. & Mitra, S. Human AP-endonuclease 1 and hnRNP-L interact with a nCaRE-like repressor element in the AP-endonuclease 1 promoter. *Nucleic Acids Res.* **30**, 823–829 (2002).
8. Zaky, A. *et al.* Regulation of the human AP-endonuclease (APE1/Ref-1) expression by the tumor suppressor p53 in response to DNA damage. *Nucleic Acids Res.* **36**, 1555–1566 (2008).
9. Gorman, M. A. *et al.* The crystal structure of the human DNA repair endonuclease HAP1 suggests the recognition of extra-helical deoxyribose at DNA abasic sites. *EMBO J.* **16**, 6548–6558 (1997).
10. Baldwin, M. R. & O'Brien, P. J. Defining the functional footprint for recognition and repair of deaminated DNA. *Nucleic Acids Res.* **40**, 11638–11647 (2012).
11. Fantini, D. *et al.* Critical lysine residues within the overlooked N-terminal domain of human APE1 regulate its biological functions. *Nucleic Acids Res.* **38**, 8239–8256 (2010).
12. Tell, G., Quadrifoglio, F., Tiribelli, C. & Kelley, M. R. The many functions of APE1/Ref-1: not only a DNA repair enzyme. *Antioxid. Redox Signal.* **11**, 601–620 (2009).
13. Georgiadis, M. M. *et al.* Evolution of the redox function in mammalian apurinic/apyrimidinic endonuclease. *Mutat. Res.* **643**, 54–63 (2008).
14. Vidal, A. E., Boiteux, S., Hickson, I. D. & Radicella, J. P. XRCC1 coordinates the initial and late stages of DNA abasic site repair through protein-protein interactions. *EMBO J.* **20**, 6530–6539 (2001).

15. Vascotto, C. *et al.* Functional regulation of the apurinic/apyrimidinic endonuclease 1 by nucleophosmin: impact on tumor biology. *Oncogene* **34**, 3482 (2015).
16. Fantini, D. *et al.* APE1/Ref-1 regulates PTEN expression mediated by Egr-1. *Free Radic. Res.* **42**, 20–29 (2008).
17. Busso, C. S., Iwakuma, T. & Izumi, T. Ubiquitination of mammalian AP endonuclease (APE1) regulated by the p53-MDM2 signaling pathway. *Oncogene* **28**, 1616–1625 (2009).
18. Busso, C. S., Lake, M. W. & Izumi, T. Posttranslational modification of mammalian AP endonuclease (APE1). *Cell. Mol. Life Sci. CMLS* **67**, 3609–3620 (2010).
19. Lirussi, L. *et al.* Nucleolar accumulation of APE1 depends on charged lysine residues that undergo acetylation upon genotoxic stress and modulate its BER activity in cells. *Mol. Biol. Cell* **23**, 4079–4096 (2012).
20. Roychoudhury, S. *et al.* Human Apurinic/Apyrimidinic Endonuclease (APE1) Is Acetylated at DNA Damage Sites in Chromatin, and Acetylation Modulates Its DNA Repair Activity. *Mol. Cell. Biol.* **37**, (2017).
21. Fan, Z. *et al.* Cleaving the oxidative repair protein Ape1 enhances cell death mediated by granzyme A. *Nat. Immunol.* **4**, 145–153 (2003).
22. Luo, M. *et al.* Characterization of the redox activity and disulfide bond formation in apurinic/apyrimidinic endonuclease. *Biochemistry* **51**, 695–705 (2012).

23. Su, D. *et al.* Interactions of apurinic/apyrimidinic endonuclease with a redox inhibitor: evidence for an alternate conformation of the enzyme. *Biochemistry* **50**, 82–92 (2011).
24. Shah, F. *et al.* Exploiting the Ref-1-APE1 node in cancer signaling and other diseases: from bench to clinic. *NPJ Precis. Oncol.* **1**, (2017).
25. Nyland, R. L., Luo, M., Kelley, M. R. & Borch, R. F. Design and synthesis of novel quinone inhibitors targeted to the redox function of apurinic/apyrimidinic endonuclease 1/redox enhancing factor-1 (Ape1/ref-1). *J. Med. Chem.* **53**, 1200–1210 (2010).
26. Antoniali, G., Malfatti, M. C. & Tell, G. Unveiling the non-repair face of the Base Excision Repair pathway in RNA processing: A missing link between DNA repair and gene expression? *DNA Repair* **56**, 65–74 (2017).
27. Prasad, R. *et al.* A review of recent experiments on step-to-step ‘hand-off’ of the DNA intermediates in mammalian base excision repair pathways. *Mol. Biol. (Mosk.)* **45**, 586–600 (2011).
28. Akbari, M., Morevati, M., Croteau, D. & Bohr, V. A. The role of DNA base excision repair in brain homeostasis and disease. *DNA Repair* **32**, 172–179 (2015).
29. Malfatti, M. C. *et al.* Abasic and oxidized ribonucleotides embedded in DNA are processed by human APE1 and not by RNase H2. *Nucleic Acids Res.* **45**, 11193–11212 (2017).

30. Gros, L., Ishchenko, A. A., Ide, H., Elder, R. H. & Saparbaev, M. K. The major human AP endonuclease (Ape1) is involved in the nucleotide incision repair pathway. *Nucleic Acids Res.* **32**, 73–81 (2004).
31. Tell, G., Damante, G., Caldwell, D. & Kelley, M. R. The intracellular localization of APE1/Ref-1: more than a passive phenomenon? *Antioxid. Redox Signal.* **7**, 367–384 (2005).
32. Li, M. & Wilson, D. M. Human apurinic/apyrimidinic endonuclease 1. *Antioxid. Redox Signal.* **20**, 678–707 (2014).
33. Kelley, M. R., Georgiadis, M. M. & Fishel, M. L. APE1/Ref-1 role in redox signaling: translational applications of targeting the redox function of the DNA repair/redox protein APE1/Ref-1. *Curr. Mol. Pharmacol.* **5**, 36–53 (2012).
34. Kaur, G., Cholia, R. P., Mantha, A. K. & Kumar, R. DNA repair and redox activities and inhibitors of apurinic/apyrimidinic endonuclease 1/redox effector factor 1 (APE1/Ref-1): a comparative analysis and their scope and limitations toward anticancer drug development. *J. Med. Chem.* **57**, 10241–10256 (2014).
35. Chen, G. *et al.* Maternal diabetes modulates dental epithelial stem cells proliferation and self-renewal in offspring through apurinic/apyrimidinic endonuclease 1-mediated DNA methylation. *Sci. Rep.* **7**, 40762 (2017).
36. Antoniali, G. *et al.* SIRT1 gene expression upon genotoxic damage is regulated by APE1 through nCaRE-promoter elements. *Mol. Biol. Cell* **25**, 532–547 (2014).

37. McHaffie, G. S. & Ralston, S. H. Origin of a negative calcium response element in an ALU-repeat: implications for regulation of gene expression by extracellular calcium. *Bone* **17**, 11–14 (1995).
38. Izumi, T., Henner, W. D. & Mitra, S. Negative regulation of the major human AP-endonuclease, a multifunctional protein. *Biochemistry* **35**, 14679–14683 (1996).
39. Fuchs, S., Philippe, J., Corvol, P. & Pinet, F. Implication of Ref-1 in the repression of renin gene transcription by intracellular calcium. *J. Hypertens.* **21**, 327–335 (2003).
40. Bhattacharyya, A. *et al.* Acetylation of apurinic/apyrimidinic endonuclease-1 regulates *Helicobacter pylori*-mediated gastric epithelial cell apoptosis. *Gastroenterology* **136**, 2258–2269 (2009).
41. Fleming, A. M., Ding, Y. & Burrows, C. J. Oxidative DNA damage is epigenetic by regulating gene transcription via base excision repair. *Proc. Natl. Acad. Sci. U. S. A.* **114**, 2604–2609 (2017).
42. Li, M., Dai, N., Wang, D. & Zhong, Z. Distinct APE1 Activities Affect the Regulation of VEGF Transcription Under Hypoxic Conditions. *Comput. Struct. Biotechnol. J.* **17**, 324–332 (2019).
43. Ayyildiz, D. *et al.* Architecture of The Human Ape1 Interactome Defines Novel Cancers Signatures. *Sci. Rep.* **10**, 28 (2020).
44. Kim, W.-C., King, D. & Lee, C. H. RNA-cleaving properties of human apurinic/apyrimidinic endonuclease 1 (APE1). *Int. J. Biochem. Mol. Biol.* **1**, 12–25 (2010).

45. Chohan, M., Mackedenski, S., Li, W.-M. & Lee, C. H. Human apurinic/apyrimidinic endonuclease 1 (APE1) has 3' RNA phosphatase and 3' exoribonuclease activities. *J. Mol. Biol.* **427**, 298–311 (2015).
46. Barnes, T. *et al.* Identification of Apurinic/apyrimidinic endonuclease 1 (APE1) as the endoribonuclease that cleaves c-myc mRNA. *Nucleic Acids Res.* **37**, 3946–3958 (2009).
47. Lin, S. & Gregory, R. I. MicroRNA biogenesis pathways in cancer. *Nat. Rev. Cancer* **15**, 321–333 (2015).
48. Carthew, R. W. & Sontheimer, E. J. Origins and Mechanisms of miRNAs and siRNAs. *Cell* **136**, 642–655 (2009).
49. Shan, X., Tashiro, H. & Lin, C. G. The identification and characterization of oxidized RNAs in Alzheimer's disease. *J. Neurosci. Off. J. Soc. Neurosci.* **23**, 4913–4921 (2003).
50. Wang, J.-X. *et al.* Oxidative Modification of miR-184 Enables It to Target Bcl-xL and Bcl-w. *Mol. Cell* **59**, 50–61 (2015).
51. He, Y. & Smith, R. Nuclear functions of heterogeneous nuclear ribonucleoproteins A/B. *Cell. Mol. Life Sci. CMLS* **66**, 1239–1256 (2009).
52. Siomi, H. & Dreyfuss, G. A nuclear localization domain in the hnRNP A1 protein. *J. Cell Biol.* **129**, 551–560 (1995).
53. Martinez, F. J. *et al.* Protein-RNA Networks Regulated by Normal and ALS-Associated Mutant HNRNPA2B1 in the Nervous System. *Neuron* **92**, 780–795 (2016).

54. Huelga, S. C. *et al.* Integrative genome-wide analysis reveals cooperative regulation of alternative splicing by hnRNP proteins. *Cell Rep.* **1**, 167–178 (2012).
55. Geissler, R. *et al.* A widespread sequence-specific mRNA decay pathway mediated by hnRNPs A1 and A2/B1. *Genes Dev.* **30**, 1070–1085 (2016).
56. Villarroya-Beltri, C. *et al.* Sumoylated hnRNPA2B1 controls the sorting of miRNAs into exosomes through binding to specific motifs. *Nat. Commun.* **4**, 2980 (2013).
57. Correa, B. R. *et al.* Functional genomics analyses of RNA-binding proteins reveal the splicing regulator SNRPB as an oncogenic candidate in glioblastoma. *Genome Biol.* **17**, 125 (2016).
58. Kim, H. J. *et al.* Mutations in prion-like domains in hnRNPA2B1 and hnRNPA1 cause multisystem proteinopathy and ALS. *Nature* **495**, 467–473 (2013).
59. Fielding, P., Turnbull, L., Prime, W., Walshaw, M. & Field, J. K. Heterogeneous nuclear ribonucleoprotein A2/B1 up-regulation in bronchial lavage specimens: a clinical marker of early lung cancer detection. *Clin. Cancer Res. Off. J. Am. Assoc. Cancer Res.* **5**, 4048–4052 (1999).
60. Hu, Y. *et al.* Splicing factor hnRNPA2B1 contributes to tumorigenic potential of breast cancer cells through STAT3 and ERK1/2 signaling pathway. *Tumour Biol. J. Int. Soc. Oncodevelopmental Biol. Med.* **39**, 1010428317694318 (2017).
61. Hung, C.-Y. *et al.* Nm23-H1-stabilized hnRNPA2/B1 promotes internal ribosomal entry site (IRES)-mediated translation of Sp1 in the lung cancer progression. *Sci. Rep.* **7**, 9166 (2017).

62. Alarcón, C. R. *et al.* HNRNPA2B1 Is a Mediator of m(6)A-Dependent Nuclear RNA Processing Events. *Cell* **162**, 1299–1308 (2015).
63. Tchurikov, N. A. *et al.* DNA double-strand breaks coupled with PARP1 and HNRNPA2B1 binding sites flank coordinately expressed domains in human chromosomes. *PLoS Genet.* **9**, e1003429 (2013).
64. Tchurikov, N. A. *et al.* Hot spots of DNA double-strand breaks and genomic contacts of human rDNA units are involved in epigenetic regulation. *J. Mol. Cell Biol.* **7**, 366–382 (2015).
65. Vascotto, C. *et al.* APE1/Ref-1 interacts with NPM1 within nucleoli and plays a role in the rRNA quality control process. *Mol. Cell. Biol.* **29**, 1834–1854 (2009).
66. Antoniali, G., Lirussi, L., Poletto, M. & Tell, G. Emerging roles of the nucleolus in regulating the DNA damage response: the noncanonical DNA repair enzyme APE1/Ref-1 as a paradigmatic example. *Antioxid. Redox Signal.* **20**, 621–639 (2014).
67. Koh, K. D., Balachander, S., Hesselberth, J. R. & Storici, F. Ribose-seq: global mapping of ribonucleotides embedded in genomic DNA. *Nat. Methods* **12**, 251–257, 3 p following 257 (2015).
68. Crespan, E. *et al.* Impact of ribonucleotide incorporation by DNA polymerases β and λ on oxidative base excision repair. *Nat. Commun.* **7**, 10805 (2016).
69. Randerath, K. *et al.* Formation of ribonucleotides in DNA modified by oxidative damage in vitro and in vivo. Characterization by ^{32}P -postlabeling. *Mutat. Res.* **275**, 355–366 (1992).

70. Chiu, H.-C. *et al.* RNA intrusions change DNA elastic properties and structure. *Nanoscale* **6**, 10009–10017 (2014).
71. Cerritelli, S. M. & Crouch, R. J. The Balancing Act of Ribonucleotides in DNA. *Trends Biochem. Sci.* **41**, 434–445 (2016).
72. Thakur, S., Dhiman, M., Tell, G. & Mantha, A. K. A review on protein-protein interaction network of APE1/Ref-1 and its associated biological functions. *Cell Biochem. Funct.* **33**, 101–112 (2015).
73. Londero, A. P. *et al.* Expression and prognostic significance of APE1/Ref-1 and NPM1 proteins in high-grade ovarian serous cancer. *Am. J. Clin. Pathol.* **141**, 404–414 (2014).
74. Bobola, M. S. *et al.* Apurinic/apyrimidinic endonuclease is inversely associated with response to radiotherapy in pediatric ependymoma. *Int. J. Cancer* **129**, 2370–2379 (2011).
75. Di Maso, V. *et al.* Transcriptional Up-Regulation of APE1/Ref-1 in Hepatic Tumor: Role in Hepatocytes Resistance to Oxidative Stress and Apoptosis. *PloS One* **10**, e0143289 (2015).
76. Puglisi, F. *et al.* Prognostic significance of Ape1/ref-1 subcellular localization in non-small cell lung carcinomas. *Anticancer Res.* **21**, 4041–4049 (2001).
77. Kelley, M. R. *et al.* Elevated and altered expression of the multifunctional DNA base excision repair and redox enzyme Ape1/ref-1 in prostate cancer. *Clin. Cancer Res. Off. J. Am. Assoc. Cancer Res.* **7**, 824–830 (2001).

78. Schindl, M. *et al.* DNA repair-redox enzyme apurinic endonuclease in cervical cancer: evaluation of redox control of HIF-1alpha and prognostic significance. *Int. J. Oncol.* **19**, 799–802 (2001).
79. Fan, X. *et al.* The expression profile and prognostic value of APE/Ref-1 and NPM1 in high-grade serous ovarian adenocarcinoma. *APMIS Acta Pathol. Microbiol. Immunol. Scand.* **125**, 857–862 (2017).
80. Juhnke, M. *et al.* Apurinic/apyrimidinic endonuclease 1 (APE1/Ref-1) overexpression is an independent prognostic marker in prostate cancer without TMPRSS2:ERG fusion. *Mol. Carcinog.* **56**, 2135–2145 (2017).
81. Evans, A. R., Limp-Foster, M. & Kelley, M. R. Going APE over ref-1. *Mutat. Res.* **461**, 83–108 (2000).
82. Prakash, A. & Doubl  , S. Base Excision Repair in the Mitochondria. *J. Cell. Biochem.* **116**, 1490–1499 (2015).
83. Park, M. S. *et al.* Cytoplasmic localization and redox cysteine residue of APE1/Ref-1 are associated with its anti-inflammatory activity in cultured endothelial cells. *Mol. Cells* **36**, 439–445 (2013).
84. Di Maso, V. *et al.* Subcellular localization of APE1/Ref-1 in human hepatocellular carcinoma: possible prognostic significance. *Mol. Med. Camb. Mass* **13**, 89–96 (2007).
85. Scognamiglio, P. L. *et al.* Destabilisation, aggregation, toxicity and cytosolic mislocalisation of nucleophosmin regions associated with acute myeloid leukemia. *Oncotarget* **7**, 59129–59143 (2016).

86. Siegel, R. L., Miller, K. D. & Jemal, A. Cancer statistics, 2017. *CA. Cancer J. Clin.* **67**, 7–30 (2017).
87. Koduru, S. V. *et al.* Non-coding RNAs in Various Stages of Liver Disease Leading to Hepatocellular Carcinoma: Differential Expression of miRNAs, piRNAs, lncRNAs, circRNAs, and sno/mt-RNAs. *Sci. Rep.* **8**, 7967 (2018).
88. Farazi, P. A. & DePinho, R. A. Hepatocellular carcinoma pathogenesis: from genes to environment. *Nat. Rev. Cancer* **6**, 674–687 (2006).
89. Zhang, Y.-C., Xu, Z., Zhang, T.-F. & Wang, Y.-L. Circulating microRNAs as diagnostic and prognostic tools for hepatocellular carcinoma. *World J. Gastroenterol.* **21**, 9853–9862 (2015).
90. Zhe, Y. *et al.* Extracellular HSP70-peptide complexes promote the proliferation of hepatocellular carcinoma cells via TLR2/4/JNK1/2MAPK pathway. *Tumour Biol. J. Int. Soc. Oncodevelopmental Biol. Med.* **37**, 13951–13959 (2016).
91. Pascut, D. *et al.* A comparative characterization of the circulating miRNome in whole blood and serum of HCC patients. *Sci. Rep.* **9**, 8265 (2019).
92. Chattopadhyay, R. *et al.* Regulatory role of human AP-endonuclease (APE1/Ref-1) in YB-1-mediated activation of the multidrug resistance gene MDR1. *Mol. Cell. Biol.* **28**, 7066–7080 (2008).
93. Katsumata, Y. *et al.* Identification of three new autoantibodies associated with systemic lupus erythematosus using two proteomic approaches. *Mol. Cell. Proteomics MCP* **10**, M110.005330 (2011).

94. Dai, N. *et al.* Serum APE1 autoantibodies: a novel potential tumor marker and predictor of chemotherapeutic efficacy in non-small cell lung cancer. *PloS One* **8**, e58001 (2013).
95. Zhang, S. *et al.* Serum APE1 as a predictive marker for platinum-based chemotherapy of non-small cell lung cancer patients. *Oncotarget* **7**, 77482–77494 (2016).
96. Shin, J. H. *et al.* APE1/Ref-1 as a Serological Biomarker for the Detection of Bladder Cancer. *Cancer Res. Treat. Off. J. Korean Cancer Assoc.* **47**, 823–833 (2015).
97. Nath, S. *et al.* The extracellular role of DNA damage repair protein APE1 in regulation of IL-6 expression. *Cell. Signal.* **39**, 18–31 (2017).
98. Cesaratto, L. *et al.* Specific inhibition of the redox activity of ape1/ref-1 by e3330 blocks tn α -induced activation of IL-8 production in liver cancer cell lines. *PloS One* **8**, e70909 (2013).
99. Coppé, J.-P., Desprez, P.-Y., Krtolica, A. & Campisi, J. The senescence-associated secretory phenotype: the dark side of tumor suppression. *Annu. Rev. Pathol.* **5**, 99–118 (2010).
100. Lee, Y. R., Kim, K. M., Jeon, B. H. & Choi, S. Extracellularly secreted APE1/Ref-1 triggers apoptosis in triple-negative breast cancer cells via RAGE binding, which is mediated through acetylation. *Oncotarget* **6**, 23383–23398 (2015).
101. Bendtsen, J. D., Jensen, L. J., Blom, N., Von Heijne, G. & Brunak, S. Feature-based prediction of non-classical and leaderless protein secretion. *Protein Eng. Des. Sel. PEDS* **17**, 349–356 (2004).

102. Qu, J., Liu, G.-H., Huang, B. & Chen, C. Nitric oxide controls nuclear export of APE1/Ref-1 through S-nitrosation of cysteines 93 and 310. *Nucleic Acids Res.* **35**, 2522–2532 (2007).
103. Bhakat, K. K., Izumi, T., Yang, S.-H., Hazra, T. K. & Mitra, S. Role of acetylated human AP-endonuclease (APE1/Ref-1) in regulation of the parathyroid hormone gene. *EMBO J.* **22**, 6299–6309 (2003).
104. Bonaldi, T. *et al.* Monocytic cells hyperacetylate chromatin protein HMGB1 to redirect it towards secretion. *EMBO J.* **22**, 5551–5560 (2003).
105. Choi, S. *et al.* Histone deacetylases inhibitor trichostatin A modulates the extracellular release of APE1/Ref-1. *Biochem. Biophys. Res. Commun.* **435**, 403–407 (2013).
106. Park, M. S. *et al.* Identification of plasma APE1/Ref-1 in lipopolysaccharide-induced endotoxemic rats: implication of serological biomarker for an endotoxemia. *Biochem. Biophys. Res. Commun.* **435**, 621–626 (2013).
107. Bhakat, K. K. *et al.* Regulation of limited N-terminal proteolysis of APE1 in tumor via acetylation and its role in cell proliferation. *Oncotarget* **7**, 22590–22604 (2016).
108. Console, L., Scalise, M. & Indiveri, C. Exosomes in inflammation and role as biomarkers. *Clin. Chim. Acta Int. J. Clin. Chem.* **488**, 165–171 (2019).
109. Hannafon, B. N. *et al.* Metastasis-associated protein 1 (MTA1) is transferred by exosomes and contributes to the regulation of hypoxia and estrogen signaling in breast cancer cells. *Cell Commun. Signal. CCS* **17**, 13 (2019).

110. Bebelman, M. P., Smit, M. J., Pegtel, D. M. & Baglio, S. R. Biogenesis and function of extracellular vesicles in cancer. *Pharmacol. Ther.* **188**, 1–11 (2018).
111. Trajkovic, K. *et al.* Ceramide Triggers Budding of Exosome Vesicles into Multivesicular Endosomes. *Science* **319**, 1244–1247 (2008).
112. Henne, W. M., Buchkovich, N. J. & Emr, S. D. The ESCRT pathway. *Dev. Cell* **21**, 77–91 (2011).
113. Christ, L., Raiborg, C., Wenzel, E. M., Campsteijn, C. & Stenmark, H. Cellular Functions and Molecular Mechanisms of the ESCRT Membrane-Scission Machinery. *Trends Biochem. Sci.* **42**, 42–56 (2017).
114. Raiborg, C. & Stenmark, H. The ESCRT machinery in endosomal sorting of ubiquitylated membrane proteins. *Nature* **458**, 445–452 (2009).
115. Schöneberg, J., Lee, I.-H., Iwasa, J. H. & Hurley, J. H. Reverse-topology membrane scission by the ESCRT proteins. *Nat. Rev. Mol. Cell Biol.* **18**, 5–17 (2017).
116. Hsu, C. *et al.* Regulation of exosome secretion by Rab35 and its GTPase-activating proteins TBC1D10A-C. *J. Cell Biol.* **189**, 223–232 (2010).
117. Hoshino, D. *et al.* Exosome Secretion Is Enhanced by Invadopodia and Drives Invasive Behavior. *Cell Rep.* **5**, 1159–1168 (2013).
118. Peinado, H. *et al.* Pre-metastatic niches: organ-specific homes for metastases. *Nat. Rev. Cancer* **17**, 302–317 (2017).
119. Hong, W. & Lev, S. Tethering the assembly of SNARE complexes. *Trends Cell Biol.* **24**, 35–43 (2014).

120. Sudhof, T. C. & Rothman, J. E. Membrane Fusion: Grappling with SNARE and SM Proteins. *Science* **323**, 474–477 (2009).
121. Baietti, M. F. *et al.* Syndecan-syntenin-ALIX regulates the biogenesis of exosomes. *Nat. Cell Biol.* **14**, 677–685 (2012).
122. Bhome, R. *et al.* Exosomal microRNAs (exomiRs): Small molecules with a big role in cancer. *Cancer Lett.* **420**, 228–235 (2018).
123. Lötvall, J. *et al.* Minimal experimental requirements for definition of extracellular vesicles and their functions: a position statement from the International Society for Extracellular Vesicles. *J. Extracell. Vesicles* **3**, 26913 (2014).
124. Malla, R. R., Pandrangi, S., Kumari, S., Gavara, M. M. & Badana, A. K. Exosomal tetraspanins as regulators of cancer progression and metastasis and novel diagnostic markers. *Asia Pac. J. Clin. Oncol.* **14**, 383–391 (2018).
125. Kalluri, R. The biology and function of exosomes in cancer. *J. Clin. Invest.* **126**, 1208–1215 (2016).
126. Kahlert, C. *et al.* Identification of double-stranded genomic DNA spanning all chromosomes with mutated KRAS and p53 DNA in the serum exosomes of patients with pancreatic cancer. *J. Biol. Chem.* **289**, 3869–3875 (2014).
127. Chalmin, F. *et al.* Membrane-associated Hsp72 from tumor-derived exosomes mediates STAT3-dependent immunosuppressive function of mouse and human myeloid-derived suppressor cells. *J. Clin. Invest.* **120**, 457–471 (2010).

128. Clayton, A., Mitchell, J. P., Court, J., Mason, M. D. & Tabi, Z. Human tumor-derived exosomes selectively impair lymphocyte responses to interleukin-2. *Cancer Res.* **67**, 7458–7466 (2007).
129. Peinado, H. *et al.* Melanoma exosomes educate bone marrow progenitor cells toward a pro-metastatic phenotype through MET. *Nat. Med.* **18**, 883–891 (2012).
130. Bolukbasi, M. F. *et al.* miR-1289 and ‘Zipcode’-like Sequence Enrich mRNAs in Microvesicles. *Mol. Ther. Nucleic Acids* **1**, e10 (2012).
131. Lu, P. *et al.* MEX3C interacts with adaptor-related protein complex 2 and involves in miR-451a exosomal sorting. *PLOS ONE* **12**, e0185992 (2017).
132. Lan, Y. Y., Londoño, D., Bouley, R., Rooney, M. S. & Hacohen, N. Dnase2a deficiency uncovers lysosomal clearance of damaged nuclear DNA via autophagy. *Cell Rep.* **9**, 180–192 (2014).
133. Takahashi, A. *et al.* Exosomes maintain cellular homeostasis by excreting harmful DNA from cells. *Nat. Commun.* **8**, 15287 (2017).
134. Verweij, F. J. *et al.* Quantifying exosome secretion from single cells reveals a modulatory role for GPCR signaling. *J. Cell Biol.* **217**, 1129–1142 (2018).
135. Dorayappan, K. D. P. *et al.* Hypoxia-induced exosomes contribute to a more aggressive and chemoresistant ovarian cancer phenotype: a novel mechanism linking STAT3/Rab proteins. *Oncogene* **37**, 3806–3821 (2018).
136. Melo, S. A. *et al.* Glypican-1 identifies cancer exosomes and detects early pancreatic cancer. *Nature* **523**, 177–182 (2015).

137. Taylor, D. D. & Gerzel-Taylor, C. MicroRNA signatures of tumor-derived exosomes as diagnostic biomarkers of ovarian cancer. *Gynecol. Oncol.* **110**, 13–21 (2008).
138. Tanaka, Y. *et al.* Clinical impact of serum exosomal microRNA-21 as a clinical biomarker in human esophageal squamous cell carcinoma: Exosomal MicroRNA-21 Expression in ESCC. *Cancer* **119**, 1159–1167 (2013).
139. Li, Z. *et al.* Exosomal microRNA-141 is upregulated in the serum of prostate cancer patients. *OncoTargets Ther.* **9**, 139–148 (2016).
140. Kia, V., Mortazavi, Y., Paryan, M., Biglari, A. & Mohammadi-Yeganeh, S. Exosomal miRNAs from highly metastatic cells can induce metastasis in non-metastatic cells. *Life Sci.* **220**, 162–168 (2019).
141. Boelens, M. C. *et al.* Exosome transfer from stromal to breast cancer cells regulates therapy resistance pathways. *Cell* **159**, 499–513 (2014).
142. Yin, J. *et al.* Secretion of annexin A3 from ovarian cancer cells and its association with platinum resistance in ovarian cancer patients. *J. Cell. Mol. Med.* **16**, 337–348 (2012).
143. Federici, C. *et al.* Exosome release and low pH belong to a framework of resistance of human melanoma cells to cisplatin. *PloS One* **9**, e88193 (2014).
144. Kosaka, N. *et al.* Neutral sphingomyelinase 2 (nSMase2)-dependent exosomal transfer of angiogenic microRNAs regulate cancer cell metastasis. *J. Biol. Chem.* **288**, 10849–10859 (2013).

145. Kalimuthu, S. *et al.* A New Approach for Loading Anticancer Drugs Into Mesenchymal Stem Cell-Derived Exosome Mimetics for Cancer Therapy. *Front. Pharmacol.* **9**, 1116 (2018).
146. Masani, S., Han, L. & Yu, K. Apurinic/apyrimidinic endonuclease 1 is the essential nuclease during immunoglobulin class switch recombination. *Mol. Cell. Biol.* **33**, 1468–1473 (2013).
147. Falini, B., Nicoletti, I., Martelli, M. F. & Mecucci, C. Acute myeloid leukemia carrying cytoplasmic/mutated nucleophosmin (NPMc+ AML): biologic and clinical features. *Blood* **109**, 874–885 (2007).
148. Poletto, M. *et al.* Inhibitors of the apurinic/apyrimidinic endonuclease 1 (APE1)/nucleophosmin (NPM1) interaction that display anti-tumor properties. *Mol. Carcinog.* **55**, 688–704 (2016).
149. Sun, F. *et al.* Proteasome Inhibitor MG132 Enhances Cisplatin-Induced Apoptosis in Osteosarcoma Cells and Inhibits Tumor Growth. *Oncol. Res. Featur. Preclin. Clin. Cancer Ther.* **26**, 655–664 (2018).
150. Sanderson, R. D., Bandari, S. K. & Vlodavsky, I. Proteases and glycosidases on the surface of exosomes: Newly discovered mechanisms for extracellular remodeling. *Matrix Biol. J. Int. Soc. Matrix Biol.* **75–76**, 160–169 (2019).
151. Notarangelo, M. *et al.* Ultrasensitive detection of cancer biomarkers by nickel-based isolation of polydisperse extracellular vesicles from blood. *EBioMedicine* **43**, 114–126 (2019).

152. Rai, G. *et al.* Synthesis, biological evaluation, and structure-activity relationships of a novel class of apurinic/aprimidinic endonuclease 1 inhibitors. *J. Med. Chem.* **55**, 3101–3112 (2012).
153. Malfatti, M. C. *et al.* Unlike the *Escherichia coli* counterpart, archaeal RNase HII cannot process ribose monophosphate abasic sites and oxidized ribonucleotides embedded in DNA. *J. Biol. Chem.* **294**, 13061–13072 (2019).
154. Salzano, A. M. *et al.* Differential proteomic analysis of nuclear extracts from thyroid cell lines. *J. Chromatogr. B Analyt. Technol. Biomed. Life. Sci.* **833**, 41–50 (2006).
155. Burra, S. *et al.* Human AP-endonuclease (Ape1) activity on telomeric G4 structures is modulated by acetylatable lysine residues in the N-terminal sequence. *DNA Repair* **73**, 129–143 (2019).
156. Ivanov, V. N., Wu, J., Wang, T. J. C. & Hei, T. K. Inhibition of ATM kinase upregulates levels of cell death induced by cannabidiol and γ -irradiation in human glioblastoma cells. *Oncotarget* **10**, 825–846 (2019).
157. Nishi, T. *et al.* Spatial redox regulation of a critical cysteine residue of NF-kappa B in vivo. *J. Biol. Chem.* **277**, 44548–44556 (2002).
158. Shimizu, N. *et al.* High-performance affinity beads for identifying drug receptors. *Nat. Biotechnol.* **18**, 877–881 (2000).
159. Lirussi, L. *et al.* APE1 polymorphic variants cause persistent genomic stress and affect cancer cell proliferation. *Oncotarget* **7**, 26293–26306 (2016).

160. Zygulska, A. L., Krzemieniecki, K. & Pierzchalski, P. Hippo pathway - brief overview of its relevance in cancer. *J. Physiol. Pharmacol. Off. J. Pol. Physiol. Soc.* **68**, 311–335 (2017).
161. Anastas, J. N. & Moon, R. T. WNT signalling pathways as therapeutic targets in cancer. *Nat. Rev. Cancer* **13**, 11–26 (2013).
162. Hientz, K., Mohr, A., Bhakta-Guha, D. & Efferth, T. The role of p53 in cancer drug resistance and targeted chemotherapy. *Oncotarget* **8**, 8921–8946 (2017).
163. Sarkaria, J. N. *et al.* Mechanisms of chemoresistance to alkylating agents in malignant glioma. *Clin. Cancer Res. Off. J. Am. Assoc. Cancer Res.* **14**, 2900–2908 (2008).
164. Visnes, T. *et al.* Targeting BER enzymes in cancer therapy. *DNA Repair* **71**, 118–126 (2018).
165. Li, B. *et al.* Tumor-derived exosomal HMGB1 promotes esophageal squamous cell carcinoma progression through inducing PD1+ TAM expansion. *Oncogenesis* **8**, 17 (2019).
166. Gao, Q. *et al.* Cancer-cell-secreted CXCL11 promoted CD8+ T cells infiltration through docetaxel-induced-release of HMGB1 in NSCLC. *J. Immunother. Cancer* **7**, 42 (2019).
167. Park, M. S. *et al.* Secreted APE1/Ref-1 inhibits TNF- α -stimulated endothelial inflammation via thiol-disulfide exchange in TNF receptor. *Sci. Rep.* **6**, 23015 (2016).
168. Shimoda, M. & Khokha, R. Proteolytic factors in exosomes. *Proteomics* **13**, 1624–1636 (2013).

169. Liu, Y., Prasad, R. & Wilson, S. H. HMGB1: roles in base excision repair and related function. *Biochim. Biophys. Acta* **1799**, 119–130 (2010).
170. Paudel, Y. N. *et al.* Enlightening the role of high mobility group box 1 (HMGB1) in inflammation: Updates on receptor signalling. *Eur. J. Pharmacol.* **858**, 172487 (2019).
171. Tang, D., Kang, R., Zeh, H. J. & Lotze, M. T. High-mobility group box 1, oxidative stress, and disease. *Antioxid. Redox Signal.* **14**, 1315–1335 (2011).
172. Yang, H., Antoine, D. J., Andersson, U. & Tracey, K. J. The many faces of HMGB1: molecular structure-functional activity in inflammation, apoptosis, and chemotaxis. *J. Leukoc. Biol.* **93**, 865–873 (2013).
173. Sheller-Miller, S., Urrabaz-Garza, R., Saade, G. & Menon, R. Damage-Associated molecular pattern markers HMGB1 and cell-Free fetal telomere fragments in oxidative-Stressed amnion epithelial cell-Derived exosomes. *J. Reprod. Immunol.* **123**, 3–11 (2017).
174. Yu, Y., Tang, D. & Kang, R. Oxidative stress-mediated HMGB1 biology. *Front. Physiol.* **6**, 93 (2015).
175. Buoncervello, M. *et al.* Apicidin and docetaxel combination treatment drives CTCFL expression and HMGB1 release acting as potential antitumor immune response inducers in metastatic breast cancer cells. *Neoplasia N. Y. N* **14**, 855–867 (2012).
176. Vascotto, C. *et al.* Genome-wide analysis and proteomic studies reveal APE1/Ref-1 multifunctional role in mammalian cells. *Proteomics* **9**, 1058–1074 (2009).

177. Erzberger, J. P. & Wilson, D. M. The role of Mg²⁺ and specific amino acid residues in the catalytic reaction of the major human abasic endonuclease: new insights from EDTA-resistant incision of acyclic abasic site analogs and site-directed mutagenesis. *J. Mol. Biol.* **290**, 447–457 (1999).
178. Vlachos, I. S. *et al.* DIANA-miRPath v3.0: deciphering microRNA function with experimental support. *Nucleic Acids Res.* **43**, W460-466 (2015).
179. Supek, F., Bošnjak, M., Škunca, N. & Šmuc, T. REVIGO summarizes and visualizes long lists of gene ontology terms. *PloS One* **6**, e21800 (2011).
180. Eden, E., Navon, R., Steinfeld, I., Lipson, D. & Yakhini, Z. GOrilla: a tool for discovery and visualization of enriched GO terms in ranked gene lists. *BMC Bioinformatics* **10**, 48 (2009).
181. Minadakis, G., Zachariou, M., Oulas, A. & Spyrou, G. M. PathwayConnector: finding complementary pathways to enhance functional analysis. *Bioinforma. Oxf. Engl.* **35**, 889–891 (2019).

Abbreviations

AGO	Argonaute
alpha	amplified luminescence proximity homogeneous assay
AML	Acute myeloid leukemia
APE1/Ref1	Apurinic/Apyrimidinic endonuclease 1/redox factor1
AS	Alternative splicing
BER	Base Excision Repair pathway
CDDP	cis-Diamineplatinum(II) dichloride
Cys	cysteine
DAMP	damage associated molecular pattern
DAO	D-amino acid oxidase
DDR	DNA damage response
DE-miRNA	differentially expressed miRNA
DGCR8	DiGeorge critical region 8
dNTPs	deoxyribonucleotide triphosphate
dNTPs	deoxyribonucleotide triphosphate
dsDNA	double strand DNA
ds_dF:dC	abasic deoxyribonucleotides in dsDNA
ds_r8oxoG:dC	oxidized ribonucleotide embedded in dsDNA
ds_rF:dC	abasic ribonucleotide embedded in dsDNA
DSB	Double Strand Breaks
EMT	Epithelial to mesenchymal transition
ESCC	Oesophageal squamous cell carcinoma
ESCRT	Endosomal Sorting Complex Required for Transport
EVs	extracellular vesicles
EXE	EVs extract
FEN1	Flap endonuclease 1 (FEN1)

gDNA	fragmented genomic DNA
GM130	Golgi apparatus protein
HAT	p300 histone acetyl transferase
HBV	chronic hepatitis B
HCC	Hepatocellular carcinoma
HCV	Chronic hepatitis C
HDAC	histone deacetylases
HGDN	High grade dysplastic nodule
HMGB1	High mobility group-1 protein
hnRNPL	Heterogeneous nuclear ribonucleoprotein L
HRE	Hypoxic response element
ILVs	Intraluminal vesicles
KO	Knock out
LGDN	Low-grade dysplastic nodules
Lig I	Ligase I
Lig III	DNA ligase III
lnRNA	long non coding RNA
LP BER	Long Patch Base Excision Repair
m⁶A	N ⁶ -methiladenosine
miRNA	microRNA
MSP	multisystem proteinopathy
mtDNA	mitochondrial DNA
MVBs	multivesicular bodies
NASH	non-alcoholic steatohepatitis
nCaRE	Negative calcium Responsive Elements
NCE	Nuclear cell extracts
NIR	Nucleotide incision repair pathway
NLS	Nuclear localization signal

NPM1	Nucleophosmin 1
NSCLC	Not small cell lung cancer
nSMase2	neutral sphingomyelinase 2
NTA	nanoparticle tracking analysis
PARP1	Poly ADP Ribose Polymerase 1
PCNA	Proliferating cell nuclear antigen
PLA	Proximity ligation assay
Pol II	RNA Polymerase II
Pol δ	Polymerase δ
Pol ϵ	Polymerase ϵ
PTH	Parathyroid hormone
PTMs	Post translational modification
Rac1	Rac Family Small GTPase1
RAGE	Receptor for advanced glycation end product
rAPE1^{K4pleA}	recombinant APE1 ^{K4pleA} protein
rAPE1^{NA33}	recombinant APE1 ^{NA33} protein
rAPE1^{WT}	recombinant APE1 ^{WT} protein
RGG	arginine/glycine-rich
rGST APE1^{K4pleA}	recombinant GST APE1 ^{K4pleA} protein
rGST APE1^{NA33}	recombinant GST APE1 ^{NA33} protein
rGST APE1^{WT}	recombinant GST APE1 ^{WT} protein
rGST	recombinant GST
RISC	RNA induced silencing complex
rMAT APE1^{WT}	recombinant MAT APE1 ^{WT} protein
rNMPs	ribonucleotides monosphate
rNTPs	ribonucleotides triphosphate
SASP	Senescence-associated secretory phenotype
SET	endoplasmic reticulum-associated complex

SLC	surrounding liver cirrhosis
SN BER	Single Nucleotide Base Excision Repair
SNARE receptor	Soluble N-ethylmaleimide-sensitive component attachment protein
TFs	Transcription factors
TNBC	Triple negative breast cancer cells
TRX	Thioredoxin
TSA	Trichostatin A
TSS	Transcription start site
WCE	Whole cell extract
XPO-5	Exportin-5 protein
XRCC1	X-ray repair cross complementing 1

List of Publications:

Serum AP-endonuclease 1 (sAPE1) as novel biomarker for hepatocellular carcinoma

Devis Pascut^{1,*}, Caecilia Hapsari Ceriapuri Sukowati^{1,2,*}, Giulia Antoniali², Giovanna Mangiapane², Silvia Burra², Luca Giovanni Mascaretti⁴, Matteo Rossano Buonocore³, Lory Saveria Crocè^{3,5,1}, Claudio Tiribelli¹ and Gianluca Tell²

¹Liver Research Center, Fondazione Italiana Fegato, ONLUS, AREA Science Park, Basovizza, Trieste, Italy

²Laboratory of Molecular Biology and DNA Repair, Department of Medicine (DAME), University of Udine, Udine, Italy

³Department of Medical Sciences, University of Trieste, Trieste, Italy

⁴Transfusion Medicine Department, Azienda Sanitaria Universitaria Integrata di Trieste (ASUITS), Trieste, Italy

⁵Clinica Patologia Fegato, Azienda Sanitaria Universitaria Integrata di Trieste (ASUITS), Trieste, Italy

*These authors contributed equally to this work

Correspondence to: Gianluca Tell, **email:** gianluca.tell@uniud.it
Claudio Tiribelli, **email:** ctliver@fegato.it

Keywords: APE1; hepatocellular carcinoma; diagnosis; biomarker; DNA repair

Received: November 12, 2018

Accepted: December 27, 2018

Published: January 08, 2019

Copyright: Pascut et al. This is an open-access article distributed under the terms of the Creative Commons Attribution License 3.0 (CC BY 3.0), which permits unrestricted use, distribution, and reproduction in any medium, provided the original author and source are credited.

ABSTRACT

Late diagnosis for Hepatocellular Carcinoma (HCC) remains one of the leading causes for the high mortality rate. The apurinic/apyrimidinic endonuclease 1 (APE1), an essential member of the base excision DNA repair (BER) pathway, contributes to cell response to oxidative stress and has other non-repair activities. In this study, we evaluate the role of serum APE1 (sAPE1) as a new diagnostic biomarker and we investigate the biological role for extracellular APE1 in HCC. sAPE1 level was quantified in 99 HCC patients, 50 non-HCC cirrhotic and 100 healthy controls. The expression level was significantly high in HCC (75.8 [67.3–87.9] pg/mL) compared to cirrhosis (29.8 [18.3–36.5] pg/mL) and controls (10.8 [7.5–13.2] pg/mL) ($p < 0.001$). The sAPE1 level corresponded with its protein expression in HCC tissue. sAPE1 had high diagnostic accuracy to differentiate HCC from cirrhotic (AUC = 0.87, sensitivity 88%, specificity 71%, cut-off of 36.3 pg/mL) and healthy subjects (AUC 0.98, sensibility 98% and specificity 83%, cut-off of 19.0 pg/mL). Recombinant APE1, exogenously added to JHH6 cells, significantly promotes IL-6 and IL-8 expression, suggesting a role of sAPE1 as a paracrine pro-inflammatory molecule, which may modulate the inflammatory status in cancer microenvironment. We described herein, for the first time to our knowledge, that sAPE1 might be considered as a promising diagnostic biomarker for HCC.

INTRODUCTION

Hepatocellular carcinoma (HCC) ranks sixth as the most frequent cancer worldwide [1] with more than 800,000 new cases diagnosed every year. The late diagnosis still remains one of the leading causes for the high mortality rate [1]. The recent molecular characterization of the disease [2] provided new insights into the cellular networks involved in hepatocarcinogenesis becoming a source of potential new therapeutic targets as well as new biomarker to use in a clinical setting.

DNA repair pathways play a significant role in the cellular and organismal response to environmental exposure by maintaining the genome integrity and thus helping to prevent the onset of disease, aging phenotypes, and cancer development. Tumor cells can develop drug resistance *via* repair mechanisms that counteract the DNA damage from chemotherapy or radiation therapy, and DNA repair enzymes are emerging targets for novel anticancer strategies [3, 4].

The base excision DNA repair (BER) pathway handles simple alkylation and oxidative lesions arising

from both endogenous and exogenous sources, including cancer therapy agents [5]. The essential BER enzyme, the apurinic/apyrimidinic endonuclease 1 (APE1), contributes to the regulation of oxidative stress responses and has other non-repair activities, such as regulating the expression of chemoresistance genes through direct and indirect mechanisms [6, 7]. By using APE1 knock-down models, we and others have demonstrated the pleiotropic ability of this protein to regulate the expression of hundreds of genes, involved in different biological processes, which are associated with cancer cell proliferation, invasion and drug resistance [8–11]. Interestingly, accumulating evidences indicate that APE1 may control gene expression via unsuspected functions in RNA metabolism [5, 12, 13] including miRNA expression [10], thus enhancing APE1 critical functions in tumor progression.

Well-known features linking APE1 and tumor development are its over-expression in many tumors and the correlation with the onset of chemoresistance in HCC and Non-Small Cell Lung Cancer (NSCLC), as well as neurologic, ovarian and breast tumors [11, 14]. Notably, its inhibition or down-regulation sensitizes cancer cells to DNA-damaging chemotherapeutic drugs and ionizing radiation [15]. Interestingly, a recent pioneering study found that plasmatic APE1 may represent a biomarker for predicting prognosis and therapeutic efficacy in NSCLC [16]. In fact, the chemotherapy-naïve serum APE1 level, which correlates with its tissue level, is inversely associated with progression-free survival of platinum-containing doublet chemotherapy; whereas post-treatment serum APE1 level is inversely associated with overall survival [16]. Interestingly, increasing evidences support the finding that extracellular APE1 secretion is a common feature of cancer cells, while the biological meaning remains to be elucidated but could be associated to triggering the inflammatory response of cancer microenvironment [17–19].

Despite several findings that associated APE1 to chemo- and radio resistance in tumors [16], marginal information exists in HCC. From our previous studies performed in cancer tissue biopsies, we defined a prognostic role for APE1 expression in HCC [20, 21]; however, nobody still evaluated the expression of APE1 in serum (sAPE1) of HCC patients.

Considering all these observations, we checked whether sAPE1 may serve as a biomarker for HCC. This work was undertaken to answer this issue and could represent a further step in biomarker discovery associated to patient's prognosis, helpful to ameliorate therapy efficacy. Also, we show here that extracellular APE1 may contribute to triggering a pro-inflammatory state being able to promote IL-8 expression in a hepatic cancer cell line. Our novel findings open new perspectives in HCC biomarker discovery as well as APE1 functional role in cancer development.

RESULTS

Baseline characteristics

The demographic features of the groups are shown in Table 1. The participants were predominantly male (78%, 62%, and 71%) with a median age of 72, 67, and 56 years, respectively ($p < 0.001$). The etiology of chronic liver disease was alcohol abuse and/or metabolic in the majority of HCC and cirrhotic patients (55% and 40%, respectively), while viral hepatitis was in 23% and 16%.

As of cirrhosis severity, most of the patients were CTP score A for 74% and 80%, whereas it was B or C in 23% and 20% for HCC and cirrhosis group, respectively. No significant difference was noticed between the two groups. In HCC group BCLC 0, A, B, C/D scores were recorded in 7%, 59%, 26%, and 7% of patients, respectively.

Regarding the prognosis scores, GRETCH score was intermediate in most patients (68%), low in 15%, and high in only 1%. CLIP score distribution appears to be more homogeneous, with a score 0 in 27% of the patients, score 1 in 32%, score 2 in 16%, and score 3/4 in 9%. As regards ITA.LI.CA Prognostic, score 2 was in 44%, score 3 in 21%, score 4 in 12%, and score >5 in 7%.

ECOG score was 0 in the vast majority of HCC patients (85%), score 1 in 7%, and score 2/3 in 5% of the study group. No statistical differences exist among all groups.

In HCC group, tumor mass, number of lesions, and the level of alpha-fetoprotein (AFP) were recorded. With respect to tumor mass and number of lesions, 15% subjects showed a single nodule smaller or equal to 2 cm in diameter, 47% had either a single nodule ranging 2 to 5 cm, or 2–3 nodules up to 3 cm each, while 37% had single nodule larger than 5 cm in diameter or multifocal. As for AFP level, 53% had AFP level lower than 20 ng/mL, 13% between 20 ng/mL and 400 ng/mL, and 12% with AFP level above 400 ng/mL.

Serum APE1 level significantly distinguishes HCC from cirrhotic patients and healthy subjects

The level of sAPE1 was measured by ELISA and expressed as median (95% CI), as previously described [16]. As a validation of the specificity of the ELISA assays used, we included a pool of blood donors' sera spiked with different concentrations of recombinant purified APE1 protein (data not shown).

The highest concentration of sAPE1 was found in HCC, with median concentration of 75.8 (67.3–87.9) pg/mL with a minimum and maximum value of 15.2 and 881.4 pg/mL, respectively, and it was significantly higher ($p < 0.001$) compared to median concentration in either cirrhosis (29.8; 18.3–36.5 pg/mL) or healthy blood donors of (10.8; 7.5–13.2) (Figure 1A). sAPE1 was undetectable in 36 (36%) of healthy and in 10 (20%) of cirrhotic samples. A significant difference was observed also in cirrhosis compared to healthy control ($p < 0.001$).

Table 1: Demographic characteristics of the study populations

	HCC	Cirrhosis	Healthy	P value
Patients characteristics				
Age (mean, 95%CI)	71 (68.8–72.1)	66 (63.6–68.3)	56 (55.1–56.6)	<0.001
Sex (M/F)	77/22	31/19	71/29	ns
Etiology				ns
Alcohol metabolic	54	20		
Alcohol metabolic viral	18	17		
Viral	23	8		
Other*	4	5		
Disease scores				
CTP A/B/C	73/20/3	40/7/3		ns
BCLC 0/A/B/C–D	7/58/26/6			
ECOG 0/1/2–3	84/7/5			
GRETCH Low/Intermediate/High	15/67/1			
CLIP 0/1/2/3–4	27/32/16/9			
ITA.LI.CA Prognostic 2/3/4/5–8	44/21/12/7			
Tumor parameters				
Number of lesions				
Single <2 cm	15			
Single or 3 <3 cm	46			
Large-single or multi	37			
Alpha fetoprotein				
<20 ng/mL	52			
20–400 ng/mL	13			
>400 ng/mL	12			

*autoimmune, hemochromatosis, cryptogenic, usually in combination with other.

Circulating sAPE1 as diagnostic biomarker for HCC

When considering the diagnostic value of sAPE1, the area under the curve (AUC) of the receiver operator characteristic (ROC) curve was 0.87 (0.78–0.92) (Figure 1B). Using a cut-off of 36.3 pg/mL, sAPE1 can distinguish HCC patients from cirrhotic subjects with sensitivity and specificity of 88% and 71%, respectively. When considering the predictive value of sAPE1 in distinguishing HCC patients from healthy subjects, the AUC score improves to 0.98 (0.96–0.99) (Figure 1C). At a cut-off determined at 19.0 pg/mL, the sensibility and specificity increased to 98% and 83%, respectively.

sAPE1 level in HCC is associated with viral infection but not with other clinical parameters

sAPE1 levels were significantly higher when comparing HCC-related viral infection to other non-viral etiologies ($p < 0.001$). In patients with either viral hepatitis C or B infection, the median sAPE1 was 98.8 (85.4–141.1).

However, highest sAPE1 level was observed in patients with multiple etiologies (viral, metabolic, and alcohol) with median concentration of 132.37 (84.3–208.2).

The association of sAPE1 level and clinical and pathological characteristics of HCC patients was shown in Table 2. With respect to HCC staging and prognostic scores, there was a significant correlation between sAPE1 and GRETCH score, but not with any other HCC scores. No correlation with other clinical parameters, such as AFP, transaminases, transferrin, albumin, and insulin was observed.

APE1 expression is higher in HCC compared to its surrounding and normal tissue

In order to determine whether high sAPE1 levels found in HCC tumor samples correlate with an overall overexpression of APE1 both at protein and mRNA levels, Western blot analysis and qPCR were performed in non-tumor and tumor tissue of liver cancer. APE1 mRNA expression was analyzed in 59 tissues from 24 HCC patients, and 4 normal liver (CTRL). As shown in

Figure 2A, an increase of APE1 mRNA was observed in HCC as compared either to the SLC and peri-HCC or also to normal liver (CTRL). When the mRNA expression was compared in paired samples of HCC to its corresponding SLC and peri-HCC, the ratio of mRNA up-regulation between HCC/SLC and HCC/peri-HCC was 4.9 ± 6.9 and 5.8 ± 11.3 -fold, respectively.

APE1 protein levels were quantified in tissues from patients with high sAPE1 levels. Analysis were performed either within single patients (Figure 2B and Supplementary Figure 1) and pooled samples (Figure

2C). APE1 protein expression levels were determined by densitometric scanning of the immunoreactive bands and normalized against actin loading control. Besides the full-length protein band, a truncated form of the protein was detectable (Figure 2C), corresponding to a proteolytic form called NΔ33 (Supplementary Figure 2) [22]. A significant increase of APE1 total protein was observed in tumor samples, particularly in the full-length form (Figure 2C).

These results were confirmed by immunohistochemistry staining (Figure 2D), where APE1 protein resulted highly expressed in the HCC nodule compared to its paired SLC,

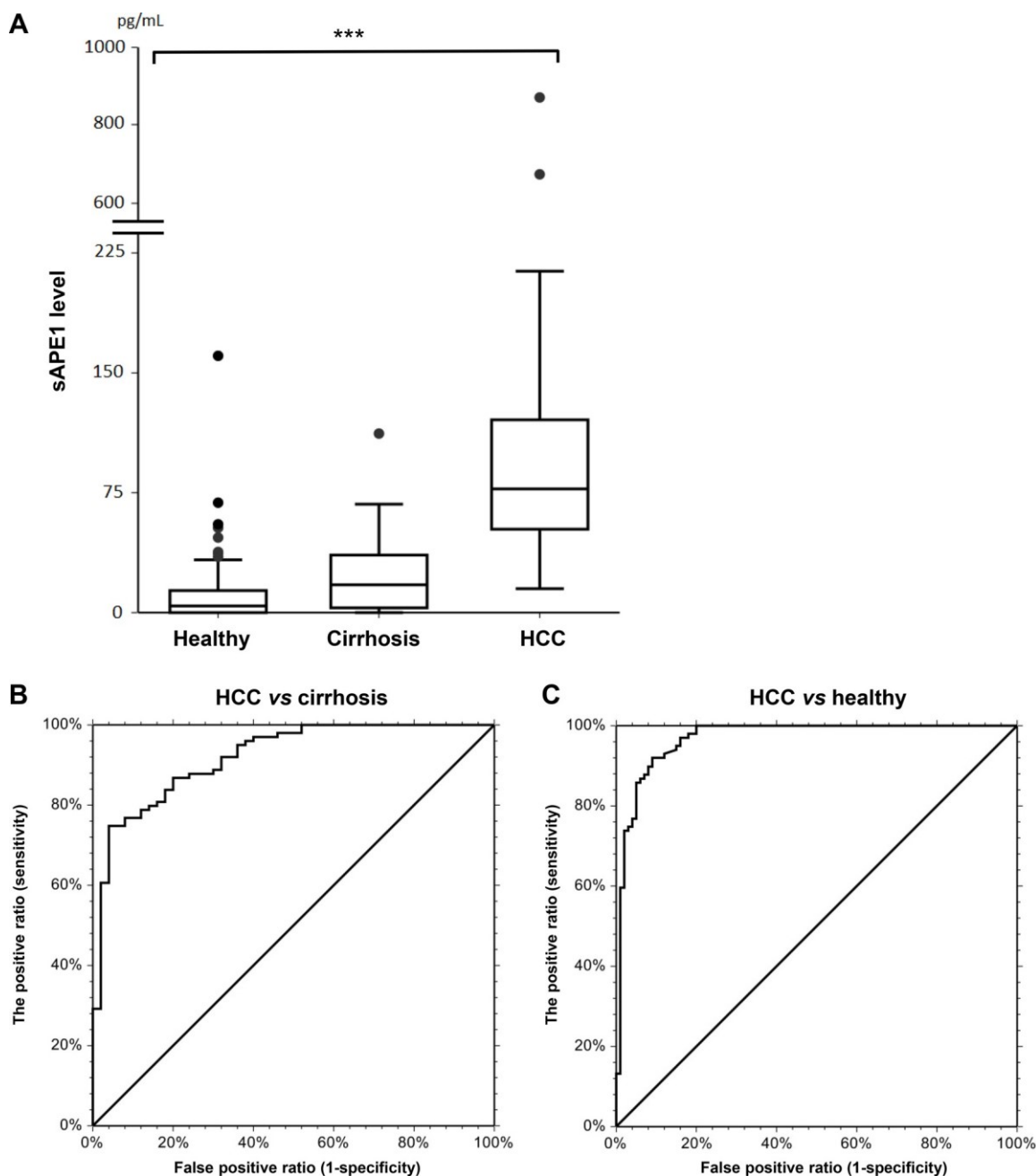


Figure 1: sAPE1 level in circulation. (A) circulating sAPE levels in healthy blood donors, cirrhosis and HCC groups. *** $P < 0.001$ among groups. (B) ROC curve for HCC diagnostic from cirrhosis with AUC score of 0.87 (0.78–0.92, 95%CI) with 36.3 pg/mL as a cut-off. (C) ROC curve for HCC diagnostic from healthy blood donors with AUC score of 0.98 (0.96–0.99, 95%CI) with 19.0 pg/mL as a cut-off.

Table 2: sAPE1 level and its association with clinical and pathological characteristics of the HCC group

sAPE1 (pg/mL)			
	Count	Median (95% CI)	<i>p</i> value
Age			ns
<72	52	74.2 (60.5–96.4)	
>72	47	78.8 (66.2–103.7)	
Sex			ns
Male	77	73.9 (63.2–87.2)	
Female	22	97.1 (65.0–122.9)	
Etiology			<0.001
Alcohol metabolic	54	62.6 (48.6–73.9)	
Alcohol metabolic viral	18	132.37 (84.3–208.2)	
Viral	23	98.8 (85.4–141.1)	
Other*	4	63.2	
CTP			ns
A	73	78.8 (65.0–96.4)	
B/C	23	70.76 (44.5–128.6)	
BCLC			ns
0-A	65	77.3 (60.5–96.4)	
B-C-D	32	74.5 (48.6–101.3)	
GRETCH			<0.05
Low	15	60.5 (33.0–101.3)	
Intermediate-high	68	83.2 (68.1–91.1)	
CLIP			ns
0–1	59	78.7 (67.3–97.7)	
2–3–4	25	71.6 (56.1–114.7)	
ITA.LI.CA prognostic			ns
2	44	87.1 (69.7–107.8)	
3	21	74.6 (56.1–108.7)	
4	12	53.5 (32.3–159.2)	
5–8	7	71.6 (40.3–138.3)	
Number of lesions			ns
Single <2 cm	15	86.9 (43.8–120.4)	
Single or 3 <3 cm	46	74.6 (60.5–117.9)	
Large-single or multi	37	74.5 (61.2–89.5)	
AFP			ns
<20 ng/mL	52	76.7 (65–87.2)	
20–400 ng/mL	13	138.3 (37.1–179.9)	
>400 ng/mL	12	80.5 (43.8–122.9)	

while it was not noticed in normal liver. In SLC, the positivity of APE1 was mostly noticed in the nucleus, while in HCC tissues, both strong nuclear and cytoplasmic expressions were detected. To check whether the sAPE1 might be correlated

with its expression in HCC nodule, the level of sAPE1 and hepatic APE1 protein were compared within the same patients. As shown in Figure 2E, the high sAPE1 expression corresponded with that found in HCC nodules.

Recombinant exogenously added APE1 protein promotes the expression of IL-6 and IL-8 genes in JHH-6 cell line

In order to evaluate a possible role for secreted APE1 in HCC, we tested whether exogenous addition of recombinant purified APE1 (rAPE1) may trigger a pro-inflammatory status in JHH-6 HCC cell line, as recently

demonstrated in human monocytes cell lines [19]. In addition to the wild-type protein (rAPE1^{WT}), we used an acetylated-mimicking mutant on residues 27, 31, 32, 35 (rAPE1^{K4pleA}), in which Lys residues have been replaced by Ala, as described before [23, 24] and whose relevance in cancer have been recently demonstrated [22] (Supplementary Figure 3). As previously described, cells were treated for 24 hours with two doses of recombinant

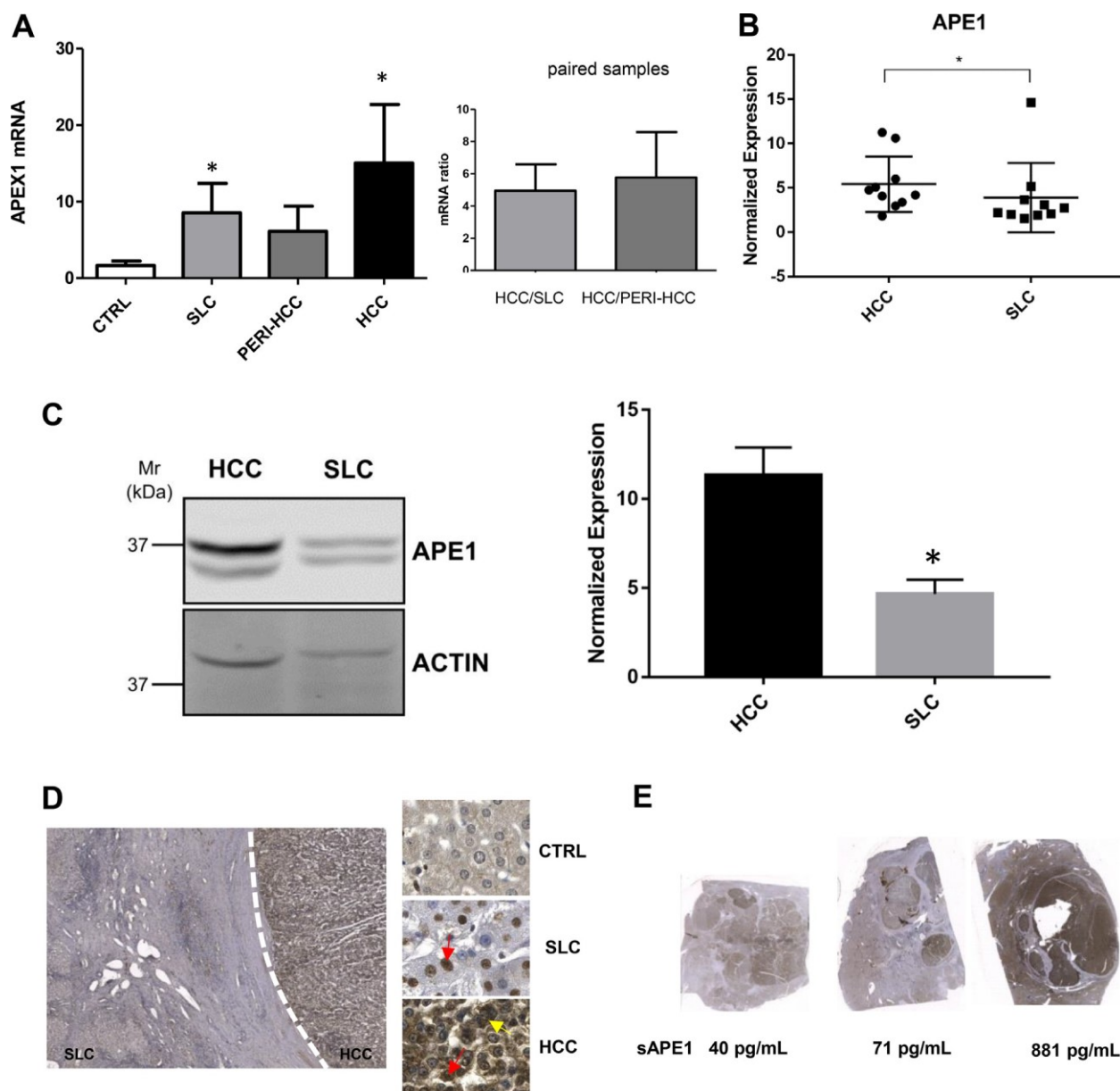


Figure 2: APE1 expression in HCC tissues. (A) qPCR of tumor (HCC), peri-HCC, and surrounding liver cirrhosis (SLC), and normal liver (CTRL) (left panel). Ratio between HCC and SLC and HCC and peri-HCC within the same patients (right panel). APE1 mRNA quantification was normalized to two reference genes 18sRNA and Actin. Bar graphs indicate mean and SEM. (B) APE1 protein quantification in HCC and SLC tissue lysates from HCC cancer patients. Graphs indicate the different distributions of the fold of protein expression for each sample as the ratio between APE1 and actin. (see Supplementary Figure 1). * $P < 0.05$. (C) Western blot analysis of HCC and SLC tissue lysates patients performed on pooled samples from HCC cancer. Actin was used as loading control and for the relative normalization. A representative image of western blot analysis is shown. Data represent the means of \pm SD of three independent experiments. * $P < 0.05$. (D) Immunohistochemistry of HCC, SLC, and normal (CTRL) tissue. Red and yellow arrows indicate nuclear and cytoplasmic positivity, respectively. (E) Scan of HCC nodules and its corresponding sAPE1 from 3 patients representing for each low, median, and high sAPE1.

purified proteins, and the expression of IL-6 and IL-8 genes was assayed by qPCR. APE1 recombinant proteins induced an upregulation of both cytokines in treated cells; the rAPE1^{K4pleA} promoted a higher increase of IL-6/IL-8 compared to rAPE1^{WT} (Figure 3A). The cells responsiveness to a proinflammatory stimulation was verified by treating cells with rTNF- α (Figure 3B). This stimulatory activity of rAPE1 was also confirmed, even to different extents, in other cancer cell lines, such as: A549 from lung cancer, confirming the generality of this phenomenon that requires further additional careful characterization. However, we checked the stimulatory activity by rAPE1 using also GST-tagged rAPE1 as well as recombinant Glutathione -S-Transferase (a bacterial protein) alone obtained from the same *E. coli* strain. Data obtained (not shown) clearly demonstrated that, while GST-APE1 exerts the same stimulatory activity of rAPE1, the GST alone did not produce any effect on IL-6/-8 induction, eliminating the possibility of IL-6/-8 induction by any contaminating LPS or other proteins. These data suggest a role of sAPE1 as a paracrine pro-inflammatory molecule, which may modulate the inflammatory status in cancer microenvironment. However, in clinical samples there were not significant correlation between sAPE1 with both IL-6 and IL-8 levels in sera and in tissues (Supplementary Figures 4 and 5).

DISCUSSION

In the present study, we found that sAPE1 protein, an essential DNA repair enzyme in the BER pathway, could be a promising diagnostic biomarker for HCC patients. Interestingly, this previously reported nuclear protein has been recently detected in the serum of patients of coronary artery disease [25] and bladder cancer patients where its level correlated with the level measured in cancer tissue [26]. More recently, this unexpected finding was confirmed in the plasma of both lipopolysaccharides-induced endotoxemic rats [27] and in NSCLC human patients [16], opening new perspectives in understanding the many functions of this unusual DNA repair protein in different conditions associated to oxidative stress and cancer development. We report that the sAPE1 levels correlate with its level in HCC tissue, in line with previous findings in non-small cell lung cancer [16].

The secretion of this protein seems to be a regulated phenomenon, depending on acetylation occurring on specific Lysine residues [17]. The biological relevance of secreted APE1 is still a matter of debate. It has been demonstrated that acetylated-APE1 may trigger apoptosis in TNBC cells by binding to the receptor for advanced glycation end products (RAGE) [28]. Other recent data demonstrated that the redox-function of APE1 may contribute to the control of the inflammatory response by inhibiting the TNF- α -induced endothelial inflammation via thiol-disulfide exchange in TNFR [18]. Moreover,

very recently, a role for extracellular APE1 in the control of early stages of inflammation processes has been proposed [19]. Treatment of human THP-1 and RAW264.7 monocytes with rAPE1 increased the expression and secretion of the pro-inflammatory cytokine IL-6, through the involvement of NF- κ B transcriptional activation, eliciting an autocrine/paracrine cellular response in a functional feedforward loop between APE1 and IL-6 regulation. However, detailed information regarding the mechanism responsible of APE1 release is still controversial, though it seems plausible that it might occur through extracellular vesicles formation via endosomal sorting complex [19].

Therefore, as a mainly nuclear protein, the source of sAPE1, whether it be from normal or cancer cells, is currently unknown and it is the focus of ongoing investigations. In our present study, we show a direct correlation between serum and tissue APE1 levels in the cohort we analyzed. We already described that the cytoplasmic expression of the protein in HCC patients correlates with poor prognosis, but we could not provide a significant biological role for cytoplasmic APE1 in HCC [20]. APE1 is a non-canonical secretory protein lacking a classic secretory signal based on protein sequence analysis. Intriguingly, several reports showed that APE1 is secreted under specific stimuli, such as those provided by Trichostatin-A [17] and LPS [19, 27]. According to these studies, secretion of APE1 was associated with its cytoplasmic translocation; however, in the present study, we failed to find a positive correlation between sAPE1 and its cytoplasmic distribution in HCC. Future work is warranted to inspect the secretory pathway of APE1 and its biological relevance. We believe that a passive release of sAPE1 by a necrotic process is unlikely, as its level does not correlate with any of the markers of liver damage analyzed. Moreover, cultured JHH-6 liver cancer cell lines do actively secrete APE1 in the culture media (data not shown) supporting the hypothesis that sAPE1 derives from an active secretion process involving, for instance, an exosomal pathway. Work is ongoing in our lab along this line to test this hypothesis.

Regarding the biological relevance of APE1 secretion, we found that recombinant exogenously added rAPE1 is able to promote IL-6/8 gene expression in JHH-6 HCC cell line. Two of the major pro-inflammatory cytokines secreted by senescent cells, IL-6 and IL-8, may function either to reinforce senescence [29] or to promote tumor invasiveness [30]. Thereafter, regulation of the inflammatory environment may have a critical role in determining the fate of both senescent and proliferating tumor cells. Based on the evidence that exogenous rAPE1 may trigger expression of both IL-6/8 cytokines, we may hypothesize that secreted APE1 may act as a paracrine molecule in regulating tumor microenvironment cell decision fates. These findings provide new insight into the underlying the clinical and biological relevance of

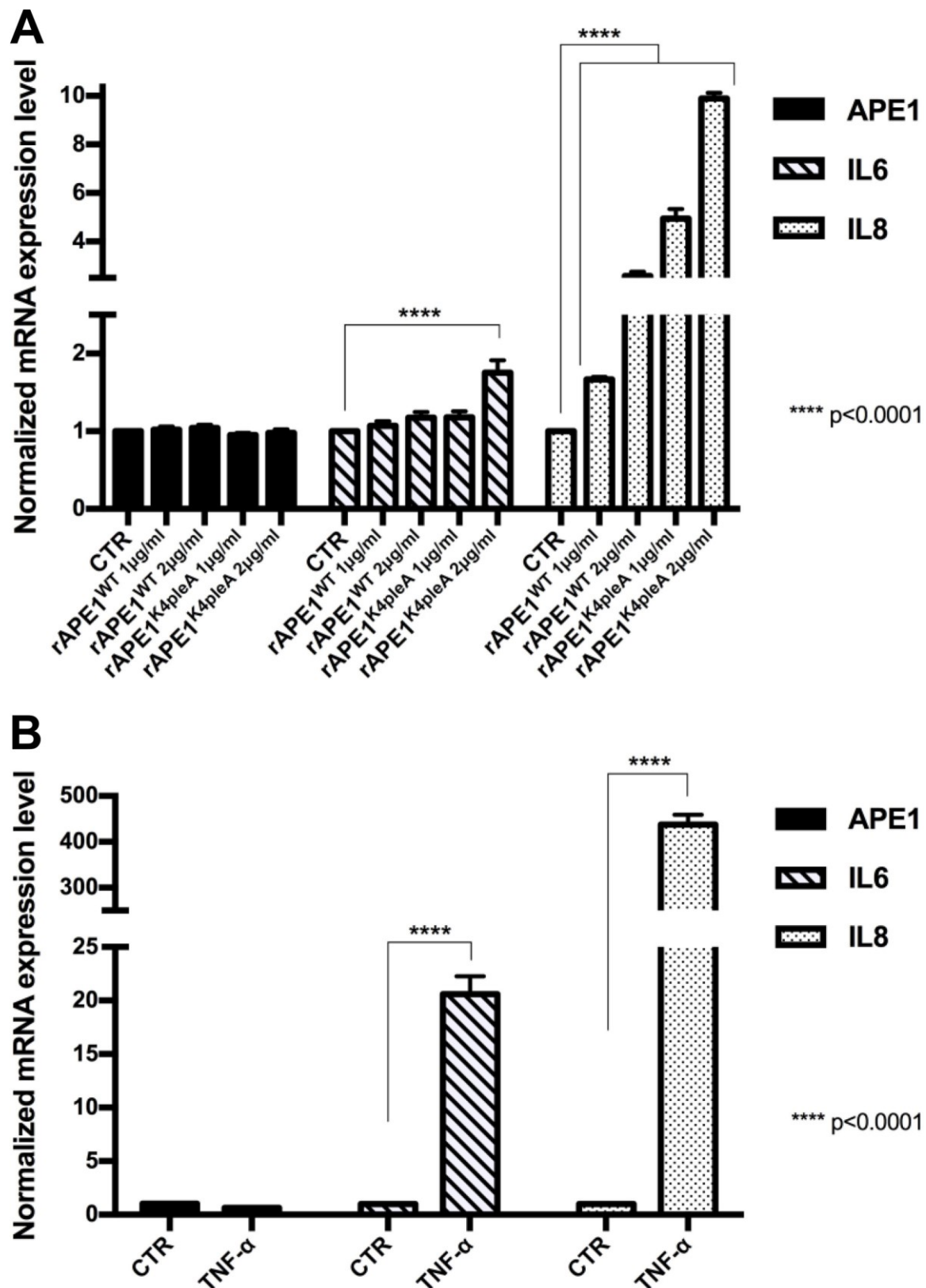


Figure 3: Recombinant APE1 promotes IL-6 and IL-8 mRNA expression in JHH-6 HCC cell line. (A) JHH-6 cells were treated for 24 h in serum free medium with recombinant rAPE1^{WT} and rAPE1^{K4pleA} proteins (1–2 µg/ml concentration). 24 h serum free medium JHH-6 cells were used as a control (CTR). Performed qPCR analyses show that rAPE1^{K4pleA} recombinant protein promotes an induction of IL-6 and IL-8 mRNA expression levels. (B) IL-6 and IL-8 induction in JHH-6 TNF-α treated cells. JHH-6 cells were treated for 3 h in serum free medium with TNF-α (2000 U/ml concentration). Performed qPCR analyses show the induction of IL-6 and IL-8 mRNA expression mediated by TNF-α. Statistical analyses were achieved by using Two-way ANOVA test.

circulating sAPE1, however, future work is needed to address these issues, which may have a strong relevance in the clinics of HCC prognosis and therapy.

MATERIALS AND METHODS

Patients

This case-control study was conducted in patients referring to the Liver Center of the University Hospital of Trieste, Italy. Fasting blood samples were collected in three groups: 99 consecutive patients observed between 2008 and 2018 whose HCC was diagnosed according to the EASL criteria [31]; 50 consecutive patients with cirrhosis confirmed by imaging, elastography, blood tests, and/or histological evaluation, without echographic evidence of HCC observed between April and June 2018; 100 consecutive healthy blood donors recruited in 2018 at the Transfusion Clinic.

Cirrhosis and HCC groups were further defined according to Child-Turcotte-Pugh score (CTP) and etiology (i.e. viral, alcoholic, metabolic, and other uncommon etiologies). For HCC group, classifications of Barcelona Clinic Liver Cancer (BCLC) [31], Eastern Cooperative Oncology Group (ECOG) [32], GReTCH d'Etude et de Traitement du Carcinoma Hépatocellulaire (GRETCH) [33], Cancer of Liver Italian Program (CLIP) [34], and the Italian Liver Cancer (ITA.LI.CA) [35] prognostic were defined. HCC samples were collected at the time of diagnosis, before any oncological treatment.

Exclusion criteria for all groups were age lower than 18 years old, pregnancy, and other malignancies. All the patients provided written informed consent and patient anonymity has been preserved. Investigation was conducted according to the principles expressed in the Declaration of Helsinki. The study was approved by the regional ethical committee (Comitato Etico Regionale Unico del Friuli Venezia Giulia, Prot. No. 2018 Os-008-ASUITS, CINECA no. 2225).

Serum samples collection and sAPE1 quantification

Serum samples were collected in Vacuette® tubes, centrifuged at 3500 rpm for 10 min and stored at -80°C until use. Hemolyzed samples were discarded from the analysis. Hemoglobin in serum was assessed with Beckman Coulter®DU®730 spectrophotometer using the Harboe Direct method [36] with Allen correction [37]. The considered cut-off for serum was 0.040 g/L. sAPE1 levels were determined using Human APEX1 ELISA kit (Cusabio, Houston, USA). The optical density (OD) was detected with an EnSpire microplate reader (PerkinElmer, Waltham, USA), at a wavelength of 450 nm with a correction set at 540 nm. sAPE1 levels (pg/mL) were then calculated by using a standard linear regression curve fitting by NCSS 11 Statistical Software (2016) (NCSS,

LLC, Kaysville, USA). To determine the specificity of the test we spiked into blood donors' serum 62.5 and 31.25 pg/mL of rAPEX1. We use the curve-fitting model built on OD vs sAPE1 concentration (pg/mL) to estimate the concentration of the two spiked samples (data not shown).

HCC tissues collection and hepatic APE1 mRNA and protein expression

Fresh hepatic tissues were collected from HCC patients undergoing liver resection without any prior treatments. Samples consisted of HCC nodule, peri-HCC and surrounding liver cirrhosis (SLC). Tissues were quickly snap-frozen and stored in -80°C.

Real time PCR

Total RNA was extracted using TriReagent (Sigma-Aldrich) and reversed transcribed using the iScript cDNA synthesis Kit (Bio-Rad Laboratories, Hercules, USA) according to the manufactures' protocols. Reactions were run on IQ5 PCR detection system (Bio-Rad).

Western blot

Lysates were resolved on 12% SDS-PAGE, transferred onto nitrocellulose membranes (Amersham™ Protran™, GE Healthcare) and probed with antibodies for APE1 (NB 100-116, Novus Biologicals, USA) (1:1000), APE1 N-terminal 1-14 aa specific goat polyclonal Antibody (NB100-897, Novus Biologicals) (1:2000) and actin (A2066, Sigma-Aldrich) (1:2000) as internal control. The IR-Dye labelled secondary antibodies (anti-rabbit IgG IRDye 680 and anti-mouse IgG IRDye 800) were used. Detection and quantification was performed with the Odyssey CLx Infrared imaging system (LI-COR GmbH, Germany). The membranes were scanned in two different channels using an Odyssey IR imager; protein bands were quantified using Odyssey software (Image Studio 5.0) and the relative signal was calculated.

Immunohistochemistry

Paraffined hepatic slices were de-paraffinized with xylene and rehydrated with gradual concentration of ethanol. Tissues were incubated with APE1 antibody (NB100-101, Novus Biologicals, USA) followed by incubation with primary universal antibody enhancer and HRP polymer (Thermo Fisher Scientific, Cheshire, UK). The complex was visualized with the DBA peroxidase substrate kit (Vector Laboratories, UK) and nucleus was stained with hematoxylin. Slides were scanned by using Zenit G Sight 2.0 (A.Menarini Diagnostics, Italy) and images were generated using two microscopical systems Leica DM2000 (Leica, Wetzlar, Germany) and Zenit G Sight 2.0.

Cell culture and treatments

JHH-6, an undifferentiated HCC cell line, were grown in William's medium E (Sigma–Aldrich), supplemented with 10% fetal bovine serum, 100 U/ml penicillin, 100 µg/ml streptomycin (Euroclone, Milan, Italy). A total of 1.5×10^5 JHH-6 cells were seeded in six-well plate for 24 h. For rAPE1 treatment, cells were treated for 24 h with rAPE1^{WT} or rAPE1^{K4plcA} with concentrations 1 µg/mL and 2 µg/mL in serum-free medium. While for TNF-α treatment, cells were treated with recombinant human TNF-α (Peprotech Inc., Rocky Hill, NJ) in serum-free medium using the same condition reported in [38].

Total RNA was extracted from JHH-6 treated cells using NucleoSpin® RNA kit (Machery Nagel, Düren, Germany) according to the manufacturer's instructions and reverse transcribed using SensiFAST cDNA Synthesis Kit (Bioline GmbH, Luckenwalde, Germany). qRT-PCR was performed with CFX96 Real-Time System, using SensiFAST™ SYBR® No-ROX Kit (Bioline GmbH, Luckenwalde, Germany). APEX, IL6 and IL8 mRNA expressions were normalized to GAPDH and HPRT expression. The primers used were included in Supplementary Table 1.

Recombinant APE1 protein expression and FPLC purification

Expression and purification of rAPE1 proteins from *E. coli* were performed as previously described [24, 39]. Briefly, *E. coli* BL21(DE3) cells were transformed with the construct pGex2T-APE1, coding for the glutathione S-transferase (GST)-APE1 full-length protein and for the APE1 acetylated mutant (K27A, K31A, K32A, K35A) and induced for 4 hours with 1.0 mM IPTG (Sigma–Aldrich) and collected upon centrifugation. The pellet was lysed and sonicated in the presence of protease inhibitor 2.1 mg/mL and Lysozyme 0.3 mg/mL. Samples were centrifuged at 23000 g for 20 minutes at 4°C, the supernatants were filtered and FPLC purified.

GST-tagged proteins were purified through a GSTrap column (GE Healthcare) and they were eluted in an increasing range of GSH concentration following the manufacturer's instructions. The proteins were incubated with Factor X (Amersham) to remove the tag and separated from the enzyme through a benzamidine column (GE Healthcare). A cation exchange purification was performed. The fractions were pooled together and stored in buffer containing 25 mM Tris pH 7.5, 100 mM NaCl, 1 mM DTT, and 10% glycerol.

Statistical analysis

Serum APE1 differences in a pairwise comparison were calculated by Mann–Whitney U. Differences among groups were calculated by Kruskal–Wallis test in one way ANOVA, with Bonferroni correction. The receiver operating characteristic (ROC) curves were plotted to estimate the

diagnostic value of sAPE1. Analyses were performed by using NCSS 11 Software (2016) (NCSS, LLC. Kaysville, Utah, USA, <https://www.ncss.com/software/ncss/>).

Abbreviations

AFP, Alpha-fetoprotein; APE1, Apurinic/apyrimidinic endonuclease 1; AUC, Area under the curve; BCLC, Barcelona Clinic Liver Cancer; BER, Base excision DNA repair; CLIP, Cancer of Liver Italian Program; CTP score, Child-Turcotte-Pugh score; CTRL, Control; DDR, DNA damage responses; ECOG, Eastern Cooperative Oncology Group; GRETCH, Groupe d'Etude et de Traitement du Carcinoma Hépatocellulaire; HCC, Hepatocellular Carcinoma; ITA.LI.CA, Italian Liver Cancer; NSCLC, Non-Small Cell Lung Cancer; OD, Optical density; rAPE1, recombinant apurinic/apyrimidinic endonuclease 1; rAPE1^{K4plcA}, acetylated-mimicking mutant recombinant APE1 on residues 27, 31, 32, 35; rAPE1^{WT}, recombinant wild-type APE1 protein; ROC curves, receiver operating characteristic curves; sAPE1, Serum apurinic/apyrimidinic endonuclease 1; SLC, surrounding liver cirrhosis.

Author contributions

DP, CT and GT designed the study. LSC and MRB enrolled the patients, collected the samples and elaborated the clinical database. LGM enrolled blood donors and collected the blood samples. DP performed the ELISA and the statistical analysis, CS performed the IHC on the human samples and performed RNA and protein extractions from tissues. GA, GM, and SB performed the *in vitro* experiments, Western blot and qRT-PCRs. DP, CS, GA, GM, SB, MRB, LSC and GT analyzed the data and participate in the discussion of the results. DP, CS, LSC, CT, and GT wrote the manuscript. All authors contributed to the manuscript revision.

ACKNOWLEDGMENTS

The authors thank the Tell and Tiribelli laboratories for constructive feedbacks during the development of this work. The authors also thank prof. F Zanconati, dr. D Bonazza, and C Bottin (UCO Anatomia ed Istologia Patologica, Azienda Sanitaria Universitaria Integrata di Trieste ASUITS) and dr. P Tarchi (UCO Clinica Chirurgica, ASUITS) for samples collection.

Ethics approval and consent to participate

All the patients provided written informed consent and patient anonymity has been preserved. Investigation was conducted according to the principles expressed in the Declaration of Helsinki. The study was approved by the regional ethical committee (Comitato Etico Regionale

CONFLICTS OF INTEREST

Authors declare no conflicts of interest.

FUNDING

This work was supported by a grant from Associazione Italiana per la Ricerca sul Cancro (AIRC) (IG19862) to GT and by an intramural grant of Fondazione Italiana Fegato to DP and CS.

REFERENCES

- Bray F, Ferlay J, Soerjomataram I, Siegel RL, Torre LA, Jemal A. Global cancer statistics 2018: GLOBOCAN estimates of incidence and mortality worldwide for 36 cancers in 185 countries. *CA Cancer J Clin*. 2018; 68:394–424. <https://doi.org/10.3322/caac.21492>.
- Ally A, Balasundaram M, Carlsen R, Chuah E, Clarke A, Dhalla N, Holt RA, Jones SJ, Lee D, Ma Y, Marra MA, Mayo M, Moore RA, et al, and Cancer Genome Atlas Research Network. Electronic address: wheeler@bcm.edu, Cancer Genome Atlas Research Network. Comprehensive and Integrative Genomic Characterization of Hepatocellular Carcinoma. *Cell*. 2017; 169:1327–1341.e23. <https://doi.org/10.1016/j.cell.2017.05.046>.
- Hein N, Hannan KM, George AJ, Sanij E, Hannan RD. The nucleolus: an emerging target for cancer therapy. *Trends Mol Med*. 2013; 19:643–54. <https://doi.org/10.1016/j.molmed.2013.07.005>.
- Hanahan D, Weinberg RA. Hallmarks of cancer: the next generation. *Cell*. 2011; 144:646–74. <https://doi.org/10.1016/j.cell.2011.02.013>.
- Jobert L, Nilsen H. Regulatory mechanisms of RNA function: emerging roles of DNA repair enzymes. *Cell Mol Life Sci*. 2014; 71:2451–65. <https://doi.org/10.1007/s00018-014-1562-y>.
- Antoniali G, Lirussi L, D'Ambrosio C, Dal Piaz F, Vascotto C, Casarano E, Marasco D, Scaloni A, Fogolari F, Tell G. SIRT1 gene expression upon genotoxic damage is regulated by APE1 through nCaRE-promoter elements. *Mol Biol Cell*. 2014; 25:532–47. <https://doi.org/10.1091/mbc.e13-05-0286>.
- Antoniali G, Malfatti MC, Tell G. Unveiling the non-repair face of the Base Excision Repair pathway in RNA processing: A missing link between DNA repair and gene expression? *DNA Repair (Amst)*. 2017; 56:65–74. <https://doi.org/10.1016/j.dnarep.2017.06.008>.
- Vascotto C, Cesaratto L, Zeef LA, Deganuto M, D'Ambrosio C, Scaloni A, Romanello M, Damante G, Tagliatela G, Delneri D, Kelley MR, Mitra S, Quadrifoglio F, Tell G. Genome-wide analysis and proteomic studies reveal APE1/Ref-1 multifunctional role in mammalian cells. *Proteomics*. 2009; 9:1058–74. <https://doi.org/10.1002/pmic.200800638>.
- Dai N, Zhong ZY, Cun YP, Qing Y, Chen C, Jiang P, Li MX, Wang D. Alteration of the microRNA expression profile in human osteosarcoma cells transfected with APE1 siRNA. *Neoplasma*. 2013; 60:384–94. https://doi.org/10.4149/neo_2013_050.
- Antoniali G, Serra F, Lirussi L, Tanaka M, D'Ambrosio C, Zhang S, Radovic S, Dalla E, Ciani Y, Scaloni A, Li M, Piazza S, Tell G. Mammalian APE1 controls miRNA processing and its interactome is linked to cancer RNA metabolism. *Nat Commun*. 2017; 8:797. <https://doi.org/10.1038/s41467-017-00842-8>.
- Tell G, Fantini D, Quadrifoglio F. Understanding different functions of mammalian AP endonuclease (APE1) as a promising tool for cancer treatment. *Cell Mol Life Sci*. 2010; 67:3589–608. <https://doi.org/10.1007/s00018-010-0486-4>.
- Antoniali G, Lirussi L, Poletto M, Tell G. Emerging roles of the nucleolus in regulating the DNA damage response: the noncanonical DNA repair enzyme APE1/Ref-1 as a paradigmatic example. *Antioxid Redox Signal*. 2014; 20:621–39. <https://doi.org/10.1089/ars.2013.5491>.
- Vohhodina J, Harkin DP, Savage KI. Dual roles of DNA repair enzymes in RNA biology/post-transcriptional control. *Wiley Interdiscip Rev RNA*. 2016; 7:604–19. <https://doi.org/10.1002/wrna.1353>.
- Tell G, Demple B. Base excision DNA repair and cancer. *Oncotarget*. 2015; 6:584–85. <https://doi.org/10.18632/oncotarget.2705>.
- Tell G, Wilson DM 3rd, Lee CH. Intrusion of a DNA repair protein in the RNome world: is this the beginning of a new era? *Mol Cell Biol*. 2010; 30:366–71. <https://doi.org/10.1128/MCB.01174-09>.
- Zhang S, He L, Dai N, Guan W, Shan J, Yang X, Zhong Z, Qing Y, Jin F, Chen C, Yang Y, Wang H, Baugh L, et al. Serum APE1 as a predictive marker for platinum-based chemotherapy of non-small cell lung cancer patients. *Oncotarget*. 2016; 7:77482–94. <https://doi.org/10.18632/oncotarget.13030>.
- Choi S, Lee YR, Park MS, Joo HK, Cho EJ, Kim HS, Kim CS, Park JB, Irani K, Jeon BH. Histone deacetylases inhibitor trichostatin A modulates the extracellular release of APE1/Ref-1. *Biochem Biophys Res Commun*. 2013; 435:403–07. <https://doi.org/10.1016/j.bbrc.2013.04.101>.
- Park MS, Choi S, Lee YR, Joo HK, Kang G, Kim CS, Kim SJ, Lee SD, Jeon BH. Secreted APE1/Ref-1 inhibits TNF- α -stimulated endothelial inflammation via thiol-disulfide exchange in TNF receptor. *Sci Rep*. 2016; 6:23015. <https://doi.org/10.1038/srep23015>.
- Nath S, Roychoudhury S, Kling MJ, Song H, Biswas P, Shukla A, Band H, Joshi S, Bhakat KK. The extracellular role of DNA damage repair protein APE1 in regulation of IL-6 expression. *Cell Signal*. 2017; 39:18–31. <https://doi.org/10.1016/j.cellsig.2017.07.019>.

20. Di Maso V, Avellini C, Crocè LS, Rosso N, Quadrifoglio F, Cesaratto L, Codarin E, Bedogni G, Beltrami CA, Tell G, Tiribelli C. Subcellular localization of APE1/Ref-1 in human hepatocellular carcinoma: possible prognostic significance. *Mol Med*. 2007; 13:89–96.
21. Di Maso V, Mediavilla MG, Vascotto C, Lupo F, Baccarani U, Avellini C, Tell G, Tiribelli C, Crocè LS. Transcriptional Up-Regulation of APE1/Ref-1 in Hepatic Tumor: Role in Hepatocytes Resistance to Oxidative Stress and Apoptosis. *PLoS One*. 2015; 10:e0143289. <https://doi.org/10.1371/journal.pone.0143289>.
22. Bhakat KK, Sengupta S, Adeniyi VF, Roychoudhury S, Nath S, Bellot LJ, Feng D, Mantha AK, Sinha M, Qiu S, Luxon BA. Regulation of limited N-terminal proteolysis of APE1 in tumor via acetylation and its role in cell proliferation. *Oncotarget*. 2016; 7:22590–604. <https://doi.org/10.18632/oncotarget.8026>.
23. Lirussi L, Antoniali G, Vascotto C, D'Ambrosio C, Poletto M, Romanello M, Marasco D, Leone M, Quadrifoglio F, Bhakat KK, Scaloni A, Tell G. Nucleolar accumulation of APE1 depends on charged lysine residues that undergo acetylation upon genotoxic stress and modulate its BER activity in cells. *Mol Biol Cell*. 2012; 23:4079–96. <https://doi.org/10.1091/mbc.e12-04-0299>.
24. Fantini D, Vascotto C, Marasco D, D'Ambrosio C, Romanello M, Vitagliano L, Pedone C, Poletto M, Cesaratto L, Quadrifoglio F, Scaloni A, Radicella JP, Tell G. Critical lysine residues within the overlooked N-terminal domain of human APE1 regulate its biological functions. *Nucleic Acids Res*. 2010; 38:8239–56. <https://doi.org/10.1093/nar/gkq691>.
25. Jin SA, Seo HJ, Kim SK, Lee YR, Choi S, Ahn KT, Kim JH, Park JH, Lee JH, Choi SW, Seong IW, Jeon BH, Jeong JO. Elevation of the Serum Apurinic/Apyrimidinic Endonuclease 1/Redox Factor-1 in Coronary Artery Disease. *Korean Circ J*. 2015; 45:364–71. <https://doi.org/10.4070/kcj.2015.45.5.364>.
26. Shin JH, Choi S, Lee YR, Park MS, Na YG, Irani K, Lee SD, Park JB, Kim JM, Lim JS, Jeon BH. APE1/Ref-1 as a Serological Biomarker for the Detection of Bladder Cancer. *Cancer Res Treat*. 2015; 47:823–33. <https://doi.org/10.4143/crt.2014.074>.
27. Park MS, Lee YR, Choi S, Joo HK, Cho EJ, Kim CS, Park JB, Jo EK, Jeon BH. Identification of plasma APE1/Ref-1 in lipopolysaccharide-induced endotoxemic rats: implication of serological biomarker for an endotoxemia. *Biochem Biophys Res Commun*. 2013; 435:621–26. <https://doi.org/10.1016/j.bbrc.2013.05.030>.
28. Lee YR, Kim KM, Jeon BH, Choi S. Extracellularly secreted APE1/Ref-1 triggers apoptosis in triple-negative breast cancer cells via RAGE binding, which is mediated through acetylation. *Oncotarget*. 2015; 6:23383–98. <https://doi.org/10.18632/oncotarget.4345>.
29. Kuilman T, Michaloglou C, Vredeveld LC, Douma S, van Doorn R, Desmet CJ, Aarden LA, Mooi WJ, Peeper DS. Oncogene-induced senescence relayed by an interleukin-dependent inflammatory network. *Cell*. 2008; 133:1019–31. <https://doi.org/10.1016/j.cell.2008.03.039>.
30. Coppé JP, Desprez PY, Krtolica A, Campisi J. The senescence-associated secretory phenotype: the dark side of tumor suppression. *Annu Rev Pathol*. 2010; 5:99–118. <https://doi.org/10.1146/annurev-pathol-121808-102144>.
31. European Association For The Study Of The Liver; European Organisation For Research And Treatment Of Cancer. EASL-EORTC clinical practice guidelines: management of hepatocellular carcinoma. *J Hepatol*. 2012; 56:908–43. <https://doi.org/10.1016/j.jhep.2011.12.001>.
32. Oken MM, Creech RH, Tormey DC, Horton J, Davis TE, McFadden ET, Carbone PP. Toxicity and response criteria of the Eastern Cooperative Oncology Group. *Am J Clin Oncol*. 1982; 5:649–55. <https://doi.org/10.1097/00000421-198212000-00014>.
33. Chevret S, Trinchet JC, Mathieu D, Rached AA, Beaugrand M, Chastang C. A new prognostic classification for predicting survival in patients with hepatocellular carcinoma. Groupe d'Etude et de Traitement du Carcinome Hépatocellulaire. *J Hepatol*. 1999; 31:133–41. [https://doi.org/10.1016/S0168-8278\(99\)80173-1](https://doi.org/10.1016/S0168-8278(99)80173-1).
34. A new prognostic system for hepatocellular carcinoma: a retrospective study of 435 patients: the Cancer of the Liver Italian Program (CLIP) investigators. *Hepatology*. 1998; 28:751–5. <https://doi.org/10.1002/hep.510280322>.
35. Farinati F, Vitale A, Spolverato G, Pawlik TM, Huo TL, Lee YH, Frigo AC, Giacomini A, Giannini EG, Ciccarese F, Piscaglia F, Rapaccini GL, Di Marco M, et al, and I.T.A. LI.CA study group. Development and Validation of a New Prognostic System for Patients with Hepatocellular Carcinoma. *PLoS Med*. 2016; 13:e1002006. <https://doi.org/10.1371/journal.pmed.1002006>.
36. Harboe M. A method for determination of hemoglobin in plasma by near-ultraviolet spectrophotometry. *Scand J Clin Lab Invest*. 1959; 11:66–70. <https://doi.org/10.3109/00365515909060410>.
37. Noe DA, Weedn V, Bell WR. Direct spectrophotometry of serum hemoglobin: an Allen correction compared with a three-wavelength polychromatic analysis. *Clin Chem*. 1984; 30:627–30.
38. Cesaratto L, Codarin E, Vascotto C, Leonardi A, Kelley MR, Tiribelli C, Tell G. Specific inhibition of the redox activity of ape1/ref-1 by e3330 blocks tnfr-α-induced activation of IL-8 production in liver cancer cell lines. *PLoS One*. 2013; 8:e70909. <https://doi.org/10.1371/journal.pone.0070909>.
39. Vascotto C, Fantini D, Romanello M, Cesaratto L, Deganuto M, Leonardi A, Radicella JP, Kelley MR, D'Ambrosio C, Scaloni A, Quadrifoglio F, Tell G. APE1/Ref-1 interacts with NPM1 within nucleoli and plays a role in the rRNA quality control process. *Mol Cell Biol*. 2009; 29:1834–54. <https://doi.org/10.1128/MCB.01337-08>.

Review

New perspectives in cancer biology from a study of canonical and non-canonical functions of base excision repair proteins with a focus on early steps

Matilde Clarissa Malfatti, Giulia Antoniali, Marta Codrich, Silvia Burra, Giovanna Mangiapane, Emiliano Dalla and Gianluca Tell*,[✉]

Laboratory of Molecular Biology and DNA repair, Department of Medicine (DAME), University of Udine, Piazzale M. Kolbe 4, 33100 Udine, Italy

*To whom correspondence should be addressed. Tel: +39 0432 494311; Fax: +39 0432 494301; Email: gianluca.tell@uniud.it

Received 16 May 2019; Editorial decision 29 November 2019; Accepted 5 December 2019.

Abstract

Alterations of DNA repair enzymes and consequential triggering of aberrant DNA damage response (DDR) pathways are thought to play a pivotal role in genomic instabilities associated with cancer development, and are further thought to be important predictive biomarkers for therapy using the synthetic lethality paradigm. However, novel unpredicted perspectives are emerging from the identification of several non-canonical roles of DNA repair enzymes, particularly in gene expression regulation, by different molecular mechanisms, such as (i) non-coding RNA regulation of tumour suppressors, (ii) epigenetic and transcriptional regulation of genes involved in genotoxic responses and (iii) paracrine effects of secreted DNA repair enzymes triggering the cell senescence phenotype. The base excision repair (BER) pathway, canonically involved in the repair of non-distorting DNA lesions generated by oxidative stress, ionising radiation, alkylation damage and spontaneous or enzymatic deamination of nucleotide bases, represents a paradigm for the multifaceted roles of complex DDR in human cells. This review will focus on what is known about the canonical and non-canonical functions of BER enzymes related to cancer development, highlighting novel opportunities to understand the biology of cancer and representing future perspectives for designing new anticancer strategies. We will specifically focus on APE1 as an example of a pleiotropic and multifunctional BER protein.

Introduction

Tumour cells can develop drug resistance via repair mechanisms that counteract the DNA damage induced by chemo- and radiotherapies. DNA repair enzymes are therefore possible targets for promising and novel anticancer strategies (1,2), in which specific DNA repair inhibitors are combined with DNA-damaging agents to improve current anticancer therapies. In parallel, some cancer cells show a reduced repertoire of DNA damage responses (DDRs), which provide other therapeutic possibilities, relying on the synthetic lethality paradigm. Indeed, many polymorphic variants of DDR enzymes have been described in the whole population, but their causal link

with genome instability, associated with tumour development, is still controversial. Emerging evidence in tumour biology has shown that RNA processing pathways participate in DDR, and that defects in these regulatory connections are associated with genomic instability in cancers (3,4). Indeed, many DNA repair proteins interact with proteins involved in RNA metabolism, non-coding RNA (ncRNA) processing and gene transcriptional regulation (5), indicating a substantial role of the deriving interactome network in determining their non-canonical functions, thus impacting gene expression in tumour cells. Moreover, recent studies have shown several interactions among DDR components and microRNAs (miRNAs) and, notably, a dysregulation of the miRNA biogenesis process has been linked

to cancer development (2). Importantly, the molecular mechanisms of miRNA processing and/or decay during genotoxic stress are still largely unknown, but it is possible that enzymes of the DNA repair pathways may be protagonists. We have recently reported that enzymes of the base excision DNA repair (BER) pathway play a crucial role in these molecular processes (6,7). Due to its function in the maintenance of genome stability under conditions of oxidative stress as well as exposure to DNA damaging agents used in chemotherapy, and its central involvement in transcriptional regulatory circuits, the BER pathway represents an unexpected and intriguing opportunity to identify novel cancer biomarkers and design new anticancer strategies. These findings prompted us to study the role of BER proteins in a different way, to understand their real contribution to the onset of cancer. These findings will help us to better understand the role of these enzymes from benchtop to bedside using a powerful translational perspective. This review will focus on what is known of the canonical (canonical DNA repair of DNA damage) and non-canonical functions (transcriptional, immunological, or repair of RNA-decay/processing) of BER enzymes, to link these functions with the biology of cancer.

Focus on the canonical roles of the BER pathway in DNA repair and telomere maintenance

Exposure to endogenous (i.e. mitochondrial respiration and inflammatory processes) or exogenous (i.e. ionising radiation, chemotherapy treatment by alkylating agents and antimetabolites) damaging effectors including deaminating agents, triggers an accumulation of non-bulky single base lesions on both nuclear and mitochondrial DNA (8,9), which can be efficiently repaired by the BER pathway. Thus, this pathway, which is largely conserved from *Bacteria* to *Eukaria*, preserves genomic integrity (10). The first enzymatic step in the BER pathway involves lesion-specific DNA glycosylase activity. In mammalian cells, each of the 11 existing *N*-glycosylase proteins differs from the others in its mechanism of action, substrate specificity and excision kinetics (11–13). Generally, the recognition of specific damaged bases occurs through a flipping out mechanism followed by a sophisticated process involving excision of the damaged base (14), thus leaving an abasic (AP) site. DNA glycosylases are classified into mono- and bifunctional glycosylases on the basis of the type of recognised damaged site and on the mechanism of action. Monofunctional DNA glycosylases, e.g. uracil DNA glycosylases (UDG), including the mitochondrial uracil *N*-glycosylase (UNG1), nuclear UNG2 and a single strand selective monofunctional uracil DNA glycosylase (SMUG1), process uracil, thymine and alkylated bases, to cleave the C1-*N*-glycosidic bond, leaving an AP site and liberating a nucleobase. Bifunctional glycosylases, including the 8-oxo-7,8-dihydroguanine DNA glycosylase (OGG1), NTH1 and the Nei-like DNA glycosylase (NEIL) family, cleave oxidative lesions and display, in addition to their glycosylase activity, an extra AP-lyase activity (15). As already demonstrated by Hill *et al.* (16) and by our recent work (7), OGG1 activity is stimulated by the presence of APE1 endonuclease, an enzyme that acts following OGG1 during the BER pathway. After the recognition of damage, bifunctional glycosylases use an amine nucleophile, such as a lysine side chain, to cleave the *N*-glycosidic bond, generating a Schiff base (imine) intermediate (17). Subsequently, through their AP-lyase activity, they cleave the DNA phosphodiester backbone on the 3' side of the lesion, through a β -elimination resulting in a single-strand break. Moreover, some of them perform a second cleavage on the

DNA phosphodiester backbone on the 5' side of the lesion through a δ -elimination process (18). Although the importance of the BER pathway has been clearly demonstrated using BER gene knock-out models, resulting in embryonic or early postnatal lethality (19), it has been reported that a high variety of glycosylases in mammalian cells causes a significant redundancy in their damage selectivity, which would explain why a single knock-out of one of the multiple DNA glycosylases is not always lethal (14).

After the hydrolysis of the *N*-glycosidic bond by DNA glycosylases, the newly generated AP site must be processed by a specific apurinic/apyrimidinic endonuclease (20). Furthermore, a spontaneous depurination of DNA also occurs very frequently. It has been estimated that, considering only spontaneous hydrolysis of the *N*-glycosidic bond, up to 10 000 abasic sites are formed per day/cell in higher eukaryotes (21,22). Unrepaired abasic sites are mutagenic and lethal for the cell, so it is clear that their repair is imperative (23). In this context, the apurinic/apyrimidinic endonuclease 1 (APE1) is the only enzyme having a role in DNA repair (24,25). Embryonic lethality as a consequence of the deletion of the *ape1* gene highlights the importance of APE1, which is not only restricted to the BER pathway, but is also related to all its physiological cellular functions (26). APE1 is a monomeric protein, structured in a α/β -sandwich globular fold coupled to a 48-amino acid, unstructured part in the N-terminal portion (27). Through its C-terminal globular region (residues 61–318), mainly responsible for endonuclease activity (28), APE1 specifies the presence of abasic sites among any normal nucleoside, principally distorting the DNA backbone with an 35°-angled extrahelical distortion (29). When the APE1–DNA complex is formed, an additional rearrangement is needed to allow the efficient execution of the hydrolytic reaction. The presence of Mg²⁺ (or Mn²⁺) ions, positioned in the active site of APE1 and principally coordinated by the E96 residue, is necessary to promote this rearrangement and to allow for cleavage of the AP site (30). The excision of the phosphodiester bond, at the 5' side of the AP-site, also requires a water molecule acting as a nucleophile (31). The active site of the endonuclease is defined by several residues including His-309, Glu-96, Asp-283, Thr-265, Tyr-171, Asn-68, Asp-210, Asp-70 and Asn-212, which are mostly involved in hydrogen bonding (31–33). Through this pocket site, APE1 is also active on damaged single-stranded DNA (ssDNA), suggesting a possible role in transcription, replication and/or recombination (34). Furthermore, *in vitro* studies have demonstrated the capability of APE1 to act as a 3' DNA phosphatase and 3'→5' DNA exonuclease on mismatched deoxyribonucleotides located at the 3'-end of nicked or gapped DNA (35–37). Recently, great importance has also been ascribed to the APE1 N-terminal region (1–127 residues), which is responsible for protein–protein interactions, RNA interactions (residues 1–33) and redox-dependent activities (38). Among all the well-known interactions of APE1 (39), nucleophosmin (NPM1) is a paradigmatic example of how APE1 functions may be modulated by protein interacting partners, thus impacting tumour biology (40). As demonstrated in acute myeloid leukemia (AML), cells expressing a nuclear deficient form of the NPM1 protein (i.e. NPM1c+) have an altered APE1–NPM1 functional interaction with consequential BER impairment (40,41). This finding supports the hypothesis that an alteration of APE1 interactions may be causally involved in cancer development and chemoresistance. Moreover, the N-terminal region of APE1 is also subjected to different post-translational modifications (PTMs) (42). Although its functional relevance is still controversial, the most well-known PTM of APE1 is the cleavage of the first 33 amino acids. This truncated protein lacks the nuclear localisation

signal sequence, leading to the accumulation of protein within the cytoplasmic compartment, and impairing the ability of the protein to interact with its canonical protein partners, including NPM1. Moreover, it has been clearly shown how the removal of the first 33 amino acids does not affect the APE1 binding affinity for the abasic site, but, in contrast, increases the enzymatic catalysis when compared with the full-length protein (38,43,44). Up to now, the protease responsible for the cleavage is still unknown, even though it has been suggested that a Granzyme-like factor could play a role (45). Beyond the N-terminal cleavage, a well-known *in vitro* and *in vivo* PTM of APE1 is represented by acetylation. Different lysine residues, including the lysine 27–35 (K27–K35) cluster could be subjected to acetylation (46). In acetylated (acAPE1), the positive charge of the N-tail of APE1 is neutralised, triggering a conformational change of the whole protein. Thus, acAPE1 is more prone to associate with chromatin, and less prone to interact with NPM1. A decrease of the APE1–NPM1 interaction, as a consequence of APE1 acetylation, determines inhibition of the APE1 accumulation within nucleoli (44,47) and an enhancement of its AP endonuclease activity due to an increase of the speed of product release upon cleavage (38,46,48). The observed effects of the PTMs occurring on the N-tail of APE1 highlight how the N-terminal region may indirectly influence the BER activity of APE1. Currently, the acetylation of APE1 is the main PTM of APE1 detected *in vivo*, as described in the subsequent paragraphs.

Upon AP cleavage promoted by APE1, a single-strand break bearing a free hydroxyl (OH) group at the 3' end and a deoxyribose phosphate (dRP) at the 5' end is generated. In this phase, BER could follow two alternative sub-pathways. In the classical mechanism, also called 'short patch' (SP-BER), polymerase β (Pol β) replaces the single missing nucleotide, adding the correct one at the 3' end of the nick. Then, DNA ligase I (Lig I) or a XRCC1–Lig III complex, complete the repair (49). Another sub-pathway of BER exists, called 'long patch' (LP-BER), in which Pol β , coordinated with polymerase δ (Pol δ), polymerase ϵ (Pol ϵ), and the sliding clamp proliferating cell nuclear antigen, synthesise a 2–12 nucleotides strand. The remaining flap is excised by flap endonuclease 1 (FEN1), while the nick is sealed by Lig I (50). Due to its elevated complexity, including the high number of BER factors involved as generated DNA intermediates, different hypothesis have been proposed to explain how the BER pathway steps may proceed in a coordinated way. Specifically, in the 'passing the baton' mechanism proposed by Tainer *et al.* (33), a coordination among all the BER factors in the passage of the DNA intermediates (BER baton) has been suggested. This model would explain how the cell works to preserve cellular stability, and protect it from the presence of potentially mutagenic DNA intermediates (51). In contrast, in the "BERosome" model, proposed in different studies (52,53), a fine regulation exists among all BER enzymes to coordinate every step of DNA repair. This coordination depends on several PTMs that regulate protein–protein interactions, including pathway cascade signaling, cellular localisation, conformational changes and protein stability (52,54). In this scenario, several other proteins, including p53 and NPM1, act as BER modulators (55,56). The efficiency of BER is also due to the coordinated use of additional scaffold proteins. Among them, the poly (ADP-ribose) polymerase 1 assumes an important role in the regulation of BER enzymes. Recent reports have shown the AP lyase activity of poly(ADP-ribose) polymerase 1 (PARP1) (57), and the stimulating activity of PARP1 on APE1 endonuclease activity (58).

Since knock-out of DNA glycosylases does not increase sensitivity to oxidative stress or ionising radiations (59–61), the existence of a

backup mechanism acting on damaged bases, typically recognised by BER proteins, has been suggested. In this context, a pathway known as nucleotide incision repair (NIR), acts directly on the 5' side of the oxidised base by the direct action of APE1, thus ensuring the correct removal of the oxidised bases (62–67), which bypasses the action of glycosylases (Figure 1). The 3' OH terminals, thus generated, are processed by FEN1 (68,69) and DNA polymerases. Several studies have reported this non-canonical APE1 activity operating in NIR, pointing to substrates that are efficiently processed, which include 5,6-dihydro-2'-deoxyuridine (DHU), 5,6-dihydrothymidine, 5-hydroxy-2'-deoxyuridine (62,70), 5-hydroxy-2'-deoxycytidine (5OHc) (62,66,70) and alpha-2'-deoxynucleosides (α dA, α dT and α dC) (62,71). Notably, the majority of these damages are generated as a consequence of DNA exposure to ionising radiation (72–75). APE1 NIR activity is stimulated under significantly different experimental conditions, in terms of salts, pH and structural requirements (62), compared with the classical BER activity. Notably, although the N-terminal region of APE1 is indirectly involved in the regulation of BER endonuclease activity, it is essential for the NIR process (62). Timofeyeva *et al.* (63) have reported how the lysine residue at position 98 (K98) significantly contributes to the 5' phosphodiester bond hydrolysis of the DNA substrate, but not to the dissociation of the enzyme from the product complex. Furthermore, an amino acid substitution of K98 influences the NIR activity more than the BER activity, demonstrating how the catalytic site active in BER and NIR is the same, although different conformations of APE1 are responsible for the incision of unrelated lesions such as AP sites and DHU, which are substrates of BER and NIR, respectively (63).

A good and well-characterised example of canonical activity of BER in the maintenance of genomic stability is represented by its activity at telomeres. Telomeres are composed of a repetitive non-coding DNA sequence that avoids the loss of genetic information, as the DNA polymerase is generally able to replicate the template DNA until its end, but only on the leading strand (76). In humans, the telomeric sequence is represented by repetitive "TTAGGG" hexameric blocks (77). Human telomeres are bound by the shelterin complex, which is composed of several protein partners that ensure stability and protection to the chromosome ends (78). The shelterin complex also functions to guarantee the acquisition and maintenance of G4 folding (79). This secondary structure is preserved by the establishment of Hoogsteen hydrogen bonds between the G4 guanines (80). Because guanine is the base with the lowest redox potential, telomeres are hotspots for oxidative modifications with the consequential generation of 8-oxo-2'-deoxyguanosine (8-oxo-dG) (81), efficiently handled by the BER pathway to be removed and replaced. G4-8-oxo-dG sites are specifically recognised by the NEIL1 and NEIL3 glycosylases (82), which are able to cleave the oxidised base, leaving an abasic site that is then nicked by APE1 (83) (Figure 1). It has been shown that NEIL1 and NEIL3 process 8-oxo-dG located in G4 structures formed in the promoter region of VEGF and *c-Myc* (83). Regarding 8-oxo-dG generated in G4 structures at telomeric regions, only NEIL3 seems to be able to efficiently cleave it and subsequently recruits the LP-BER machinery to favor repair (84). Moreover, NEIL3 also interacts with the TRF1 shelterin complex, and seems to play an essential role in coordinating the repair of oxidation damages, as demonstrated by telomere dysfunction observed in the absence of this glycosylase (84). Wallace *et al.* hypothesised the possible involvement of NEIL glycosylases in both telomere maintenance and gene regulation (84). The abasic site generated by glycosylase is later handled by APE1 endonuclease, which is able to bind and process different types of G4, through the involvement of its acetylated lysine residues (i.e. K27–35 cluster) (48)

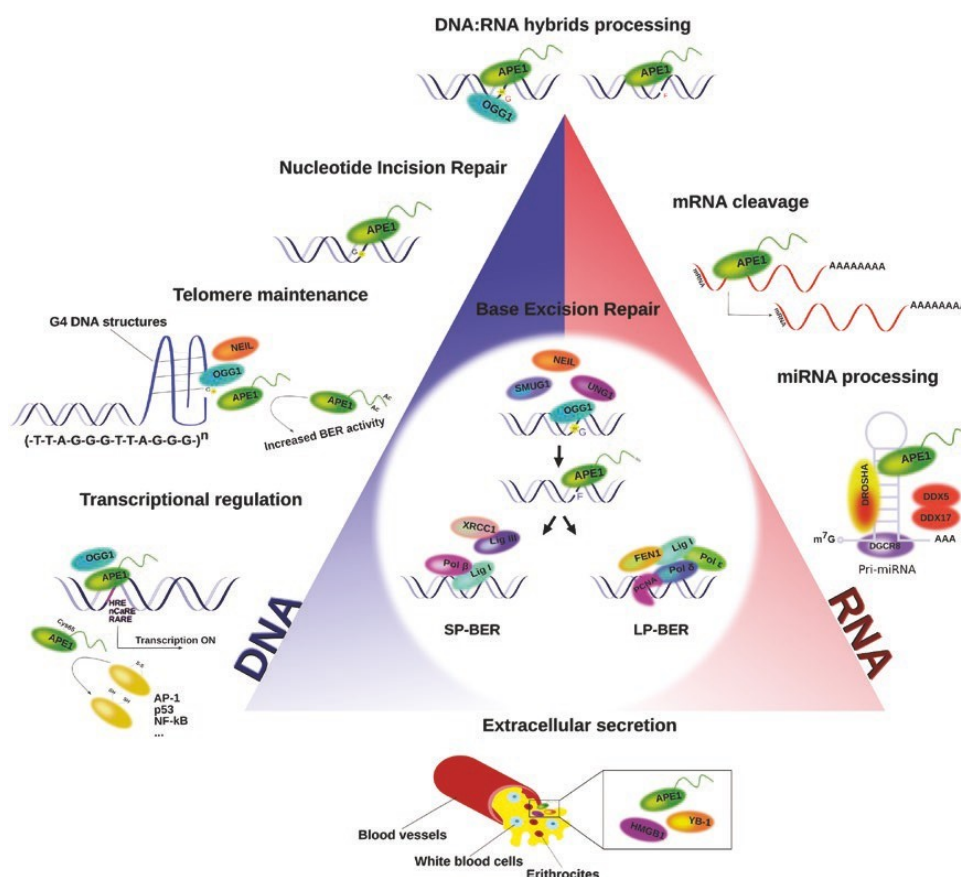


Figure 1. BER pathway and the 'Deathly Allows'. Representational cartoon of canonical and non-canonical functions of enzymes belonging to the BER pathway. In the middle, canonical BER is represented as starting by the action of several glycosylases on non-bulky lesions (8-oxo-dG). When the abasic site (F) is generated, APE1 cleaves it, generating a single-strand break that can be processed by a short- (SP-BER) and long- (LP-BER) patch. Several BER enzymes are also involved in other important cellular pathways regarding DNA processing (left blue side), including a NIR pathway, telomere maintenance and transcriptional regulation. Recently, new discoveries regarding a role of BER enzymes in RNA processing (right red side) are emerging, including mRNA and miRNA processing and/or decay. Moreover, BER enzymes are also involved in the processing of DNA:RNA hybrids, including 8-oxo-G and ribose monophosphate abasic site embedded in DNA (top). Finally, their extracellular secretion has been also recently hypothesised (bottom). See the text for further information. Figure available in colour online.

(Figure 1). The localisation of the abasic site in the quadruplex and the electrostatic interactions that mediate the contact of nucleic acids with APE1 then influence its activity on the lesion (48). The N-terminal region of APE1, and more specifically the lysine residues located in this region, are important for the regulation of the endonuclease activity on G4-containing abasic sites (56). Specifically, APE1 mutants, which mimic the acetylation of lysine residues, display increased endonuclease activity *in vitro*. The acetylation may therefore represent a dynamic mechanism to fine tune the activity of the protein at telomeric sites (48) (Figure 1). Cells depleted in APE1 showed reduced telomere length and the knock-out of APE1, in postnatal mice, resulted in compromised development and growth, and increased senescence (85). APE1 can also interact with the TRF2 and POT1 sheltering proteins, and its presence at telomeric sites is important in stabilising these regions (86). Moreover, the depletion of APE1 results in telomere dysfunction and segregation defects in cells that employ alternative lengthening of telomere pathways or telomerase re-expression to elongate telomeres (86). These results suggest an interdependence between the BER machinery and telomere homeostasis.

Non-canonical roles of the BER pathway in the immunological response

The BER pathway, besides being the main mechanism for coping with DNA lesions described above, plays an essential role in the

immunological response. It has been clearly shown that BER enzymes regulate the genomic rearrangement that induces the antigen-stimulated somatic hypermutation (SHM) process, responsible for the diversification of the variable genomic regions of the heavy and light chains of immunoglobulins, and plays a central function in the process of class switch recombination (CSR) responsible for diversification of the heavy chain constant region (87). These two antibody maturation mechanisms are dependent on the activation-induced cytidine deaminase (AID), which converts cytosine to uracil in the variable (V) and switch (S) regions of the immunoglobulin gene. APE1, through its AP-endonuclease activity, is responsible for the introduction of DNA nicks when AID-dependent deaminated cytosine is removed by the glycosylase, UNG2-dependent BER. Despite several uracil glycosylases being present in mammals, APE1 is the only AP-endonuclease, although a weak endonuclease activity has been recently identified for APE2 (88–90). Besides APE1 and UNG2, all the other BER enzymes have been found to participate in the uracil removal process (91). Their role in SHM and CSR strongly depends on crosstalk between each protein partner, and is finely tuned by the expression levels of each partner and by specific regulated posttranslational modifications, such as phosphorylation of Ser38 in the AID protein (92,93). In particular, while APE1 endonuclease activity is important for CSR, it has been shown to be dispensable for SHM- and AID-induced DNA breaks. In fact, APE1 does not contribute to DNA cleavage through processing of AP sites, but

rather, it may function as a DNA end-processing enzyme to facilitate the joining of broken ends during CSR (94,95). APE1 endonuclease activity is likely to remove 3'-tyrosyl residues from the DNA end after topoisomerase 1 (Top1) cleavage and Top1-cc degradation, which is essential to efficient recombination of broken S regions. Additionally, S regions are subjected to a high rate of transcription driven by cytokine-inducible promoters, which regulate the CSR process. Moreover, because APE1 is dispensable for AID activity, understanding the mechanism by which AID is targeted to its substrates is of great interest, given the potentially deleterious consequences of AID's mutagenic activity (96). While the endonuclease activity of APE1 in the CSR process is well-established, its contribution as a transcriptional coactivator has been only hypothesised. In fact, the remaining CSR activity observed in APE1-endonuclease activity deficient cells (88) could be explained by the ability of APE1 to stimulate the DNA-binding activity of several transcription factors, including nuclear factor kappa B (NF- κ B) and a few others, involved in inflammation and immunological responses (6,97,98). Very recently, using different APE1 inhibitors and APE1 DNA-repair and redox-defective mutants, we provided more evidence in support of this hypothesis, demonstrating that APE1 redox function also plays an important role in regulating CSR through the IL-6 signaling pathway and proper IgA expression (99).

The role of the BER pathway in transcriptional regulation

A growing list of BER proteins, that were initially thought to exclusively function in DNA repair, are emerging as important in transcription (100). It is perhaps not surprising that these two processes are often coupled, when considering the mutagenic potential of the transcriptional process. DNA lesion repair, in transcriptionally active genes, must be kept under strict control to maintain transcriptional fidelity and genome stability. However, it does not simply involve a preferential repair of the transcribed DNA strand but, as suggested by several findings, a more physically and functionally intertwined crosstalk between the two processes must exist. Importantly, recent studies have generated a substantial body of evidence pointing to a direct function of DNA repair enzymes as coactivators of transcription.

APE1 represents a paradigmatic example of a DNA repair enzyme with a peculiar function as a transcriptional regulator. Indeed, APE1 plays a role in the regulation of expression of human genes in response to oxidative stress conditions by stimulating the DNA binding activity of several transcription factors, such as nuclear factor kappa B (NF- κ B), Egr-1, Hif-1 α , Nrf1 and STAT3, thus influencing the onset of inflammatory and metastatic processes (97) (Figure 1). Recently, a direct role of APE1 has also been characterised in the transcription of sirtuin 1 (*SIRT1*) gene, by binding to negative calcium responsive element (nCaRE) sequences present on its promoter demonstrating that BER-mediated DNA repair promotes the initiation of transcription of the *SIRT1* gene upon oxidative DNA damage (98) (Figure 1). Paradoxically, it has been shown that programmed DNA single or double strand breaks, with concomitant activation of the DNA damage response, can induce transcription at gene promoters (101,102). Conventionally, DNA modifications (especially oxidation) are widely thought to be harmful for cell stability (103). The only described exceptions, relative to DNA modifications with important regulatory roles, are 5-methylcytosine and uracil, which are enzymatically generated in DNA under controlled conditions to fulfil crucial regulatory

functions as epigenetic marks, or to be involved in antibody diversification (104). The existence of modifications with potential regulatory functions on other bases remains to be investigated. Oxidative DNA modification, as a consequence of the exposure to reactive oxygen species, is very frequent and guanine is the most susceptible targeted base, with 8-oxo-dG as the most common product (105). The distribution of 8-oxo-dG sites is not random throughout the genome, but occurs more frequently at the promoter region of active genes, thus contributing to transcriptional regulation (106). If not repaired, 8-oxo-dG is moderately mutagenic, causing a G to T transversion mutation that is thought to be responsible for initiating and driving carcinogenesis and neurodegenerative diseases, such as Alzheimer's and Parkinson's diseases (107–109). Recent evidence has highlighted how the repair of 8-oxo-dG by OGG1 is involved in the regulation of transcription, through the action of specific transcription factors, and also in signal transduction. Numerous reports have reported an interplay between DNA repair of 8-oxo-dG and transcription activation, mostly when this modification is found in promoter regions (98,101,110). These studies proposed that the 8-oxo-dG BER-mediated repair may serve as a modulator for transcription efficiency, supporting a growing body of evidence regarding the role of 8-oxo-dG as an epigenetic-like DNA modification (102,111). The long-standing view has been that 8-oxo-dG is mutagenic and can negatively impact cellular processes such as transcription. When 8-oxo-dG is present in the template strand, it can slightly inhibit the advancement of RNA polymerase II (112), and the initiation of 8-oxo-dG repair may cause polymerases to stop (113); furthermore, the presence of 8-oxo-dG in transcription binding sites can negatively affect the transcription factor binding activity (114–116). For all these reasons, it is thought that 8-oxo-dG may act as a negative signal for transcription. However, there are a few notable findings showing that 8-oxo-dG, when recognised by OGG1, provides a platform for the coordination of the initial steps of the BER pathway repair coupled with the assembly of the transcriptional machinery to prompt the expression of redox-regulated genes. In particular, the presence of 8-oxo-dG in promoters can increase gene transcription via the BER pathway; these are well-documented cases of the BCL2 apoptosis regulator (B-cell lymphoma 2) (117), SIRT1 (98), vascular endothelial growth factor (VEGF) (118,119) and tumour necrosis factor-alpha (TNF α) (110) gene expression. We previously proposed that BER-mediated repair of an oxidised guanines at nCaRE sequences is a key event for SIRT1 transcription (98). We hypothesised that the nick, introduced by APE1 during DNA repair, might favor local topological relaxation, facilitating the recruitment of RNA polymerase for gene transcriptional activation. A similar mechanism of transcriptional activation was described later by Pastukh *et al.* (118), in the context of the VEGF gene, and by Boldogh *et al.*, who demonstrated OGG1 recruitment and upregulation of proinflammatory genes upon TNF α -induced oxidation of G in NF- κ B consensus sequences (110,120). Of note, this reported role of 8-oxo-dG and OGG1 in the activation of inflammatory genes could explain the documented immune deficiencies observed in OGG1^{-/-} mice (121,122). Furthermore, using 8-oxo-dG site-specifically synthesised reporters of the VEGF regulatory sequence, Burrows and co-workers have further characterised the mechanism of coupling BER and transcriptional activation. In particular, they suggested that the presence of 8-oxo-dG in DNA could provide a gene for up/down regulation depending on the strand context. Specifically, they demonstrated that the activation of VEGF transcription depended on the oxidation of Gs present in the guanine-rich potential G-quadruplex (G4)-forming sequence (PSQ). Their

model proposed that when 8-oxo-dG is present in the coding strand of the VEGF PSQ promoter, the produced AP site favors the prolonged stalling of APE1, leading to its inability to cleave in the G4 context but allowing the recruitment of the transcriptional activating machinery for gene induction. In contrast, the presence of 8-oxo-dG on the template strand activates the transcription-coupled nucleotide excision repair pathway, which attenuates transcription (101,119). Very recently, the same group reported a similar mechanism of action for the G-rich potential Z-DNA forming sequences (PZS) (123). This concept has also been shown for other promoters such as that of the endonuclease III-like protein 1 (NTHL1) (101), RAD17 (124), proliferating cell nuclear antigen (PCNA) (125) and NEIL3 (126), which expanded the generalisation of this model mechanism and emphasised the importance of G4-fold oxidation as a critical driver for gene activation. Secondary structures are key elements in the regulation of transcription, because the frequency of potential G4 forming sequences within gene promoters is 1.8-fold higher if compared with other randomly considered regions (127). In addition, the GC-content positively correlates with transcriptional activity of genes (128), further supporting the possibility that oxidation of G and BER activities have the potential to trigger gene expression. However, the selective induction of 8-oxo-dG in promoter sequences, described in the abovementioned studies, appears difficult to explain as a consequence of general oxidative stress. Perillo *et al.* (117) suggested an intriguing hypothesis involving a possible alternative explanation for the generation of oxidised bases localised in promoter regions. They showed that lysine specific histone demethylase (LSD1) accounted for the generation of 8-oxo-dG in the estrogen-responsive promoter region of the *bcl-2* gene. By an oxidative process that releases H_2O_2 , LSD1 promotes the demethylation of histone H3 at lysine 9, which, in turn, modifies the surrounding DNA and determines the recruitment of OGG1 and topoisomerase IIb to remove damaged DNA bases (129). Finally, another mechanism postulates a specific role for the excision of 8-oxo-dG. Boldogh *et al.* (130) showed that a stoichiometric complex of OGG1 with its excised substrate modification had a high binding affinity for small GTPases, such as Ras, Rac1 and Rho, and that this binding acted as a guanine exchange factor (GEF), consequently activating downstream cellular signaling. Together, these interesting results highlight an intertwined role between DNA repair and gene transcription, which is a phenomenon gaining more interest. Furthermore, coupling BER with transcriptional activation leads to the hypothesis that oxidative modification of G to 8-oxo-dG may have regulatory and possibly epigenetic-like features in cells. G4-forming sequences can especially sense oxidative stress and lead to repression or enhancement of transcription. However, whether 8-oxo-dG is an epigenetic modification is not clear and needs further discussion. Typically, epigenetic marks comprise DNA methylation, histone modification and nucleosome localisation, all of which are products of the activity of specific enzymes that modulate the access of transcription machinery. Conversely, DNA oxidation is efficiently repaired by BER and therefore has never been considered epigenetic, especially because it lacks the heritability from mother to daughter as established for the epigenetic definition. Furthermore, the toxic aspect of 8-oxo-dG cannot be ignored. Therefore, further studies are needed to establish whether this modification can be considered helpful, by facilitating gene expression, or as a process leading to mutagenic potential. It can probably be argued that deviations from the proper response to oxidative stress may be due to the impaired action of BER at oxidised guanines, which in turn might be the etiological link of 8-oxo-dG to several pathologies. This consideration also opens new scenarios to

pharmacologically modulate OGG1 and APE1 activity to prevent degenerative diseases associated with oxidative stress, which can be derived by an inaccurate action of the two proteins at oxidised guanines.

The roles of the BER pathway in RNA processing

In the past few years, a clear picture of the involvement of DNA repair enzymes in specific aspects of RNA metabolism has emerged. In particular, a large cohort of BER enzymes has been implicated in RNA processes, especially linked with quality control towards damaged (i.e. abasic and oxidised) RNA molecules (131–133). BER enzymes typically cope with oxidative modifications occurring on DNA, but increasing evidence has suggested the involvement of the BER pathway as the mechanism of surveillance needed to remove damaged RNA molecules to ensure cell viability (133). Currently, an unequivocal description of how cells may deal with oxidised RNA is still missing. Notably, no known enzyme seems to be devoted to the recognition and removal of abasic or oxidised RNA. However, a quality control mechanism should exist to protect from the negative consequences of unrepaired RNA damage, which could lead to an impairment of protein synthesis and noncoding RNA expression, with deleterious effects on the fate of cells. Therefore, a productive crosstalk between DNA repair enzymes and proteins associated with the RNA processing machinery seems more than reasonable. In this context, among the BER components, APE1 has been the particular focus of attention. Increasing evidence has reinforced the view, suggested by our studies of a role of APE1 as a ‘cleansing’ factor for damaged oxidised/abasic RNA, and possibly highlighted its unsuspected function in RNA metabolism, thus affecting gene expression (5,133,134) (Figure 1). Initially, the potential involvement of APE1 in RNA biology was mainly based on *in vitro* findings. In particular, we and others reported that APE1 bound structured RNA molecules (135), cleaved abasic single-stranded RNA (ssRNA), and was involved in RNA-decay, with 3'-RNA phosphatase and 3'-exoribonuclease activities (136). In parallel studies, as the interactome of APE1 has been shown, APE1 interaction with components of the RNA metabolism machinery definitively proved the significance of APE1's role in RNA metabolism *in vivo* (6,39). Proteomic analyses from our studies showed that the APE1 interactome was mostly comprised of proteins involved in ribosome assembly, regulation of mRNA stability (e.g. HNRNPK, YB-1, NPM1 and PABPC1), RNA splicing (e.g. PRPF19, SNRPB and SRPK1) and ribonucleoprotein complex biogenesis (e.g. RPL11, DDX6 and RPS14) (6). In support of these observations, we recently also showed that APE1 may represent a new hub in RNA-processing, including effects on ncRNAs such as miRNAs (6) (Figure 1). This is consistent with recent studies showing that the cellular response to damage requires not only protein-coding genes, but also a subset of ncRNAs (14,137,138). In fact, activation of DNA damage induces the expression of multiple kinds of ncRNAs, such as miRNAs and the recently discovered DROSHA- and Dicer-dependent RNA, the DSB-induced small RNAs and the long intragenic non-coding RNAs (lncRNAs), which contribute to the fine tuning of damage repair to ensure DNA integrity (4). Numerous studies reported that ncRNAs, in particular miRNAs, were able to regulate the DDR by acting on several sensors of damage (e.g. γ -H2AX), as well as on crucial signal transducers (e.g. ATM, ATR and DNA-PKcs.) and effectors (CHK1, p53 and p21) (137). However, a bidirectional regulatory pathway exists between ncRNAs and DDR factors. It has been postulated that

few DDR proteins modulate miRNA post-transcriptional processing by regulating the essential steps of their processing and maturation (6,137). Remarkably, in this context, we recently showed a role for APE1 in pri-miRNA processing and stability via association with the DROSHA-processing complex during genotoxic stress. We showed that APE1 endonuclease activity was required for the processing of miR-221/222 in regulating the expression of the tumour suppressor phosphatase and tensin homolog (PTEN). These results highlight how APE1 regulates gene expression through its direct binding and/or processing of specific miRNAs contributing to cancer progression (6). It is still unknown whether this mechanism is also involved in chemoresistance in cancer. The majority of studies on ncRNAs in the DNA damage field have so far focused on the role of miRNAs, although a role for lncRNAs has also been reported. They have been described to be induced upon DNA damage and associated with ribonucleoproteins and proteins in chromatin by acting in various ways, including as signals, as decoys, or as scaffolds for these protein complexes leading to the regulation of DDR genes (137,139). At present, nothing is known about a possible interaction between lncRNAs and BER enzymes; however, because the expression of lncRNAs has emerged as a new topic in DNA damage, this relationship cannot be excluded. Preliminary results from our laboratory identified few lncRNAs bound by APE1, which might function together with APE1 in DNA repair and safeguarding genome integrity (G. Antoniali *et al.*, in preparation). In accordance with a new role for APE1 in RNA described so far, depletion of this protein in tumour cells leads to nucleolar defects (140), accumulation of oxidised RNA species as well as pri-miRNAs (6,56), alteration of miRNAs expression, impaired protein synthesis and reduced cell growth (56). All these findings, together with the cytoplasmic accumulation of APE1 in several tumour cell types (141), support a major function of APE1 in RNA-processing/decay. Taking into account these observations, the importance of a better understanding of the role played by the BER enzymes in RNA-related processes becomes essential, especially when considering that some pathologies, including neurological disorders and cancer, are associated with deficiencies to both RNA processing and DNA repair (142). Furthermore, these insights might also explain the complexity that underlies BER involvement in the onset of chemoresistance. In conclusion, further studies unveiling the regulatory mechanisms coordinating the interplay between BER activity and RNA processing will be necessary to understand the complexity of DNA repair programs and, finally, these notions can definitively facilitate the development of new anticancer agents.

The BER pathway as a new player in RNA:DNA hybrid processing

RNA:DNA hybrids physiologically occur during DNA replication and transcription, telomere elongation, retroviral infection and retro-element mobilisation (143). In eukaryotic cells, RNA:DNA structures are classified in: (i) a configuration in which ssRNA is paired to ssDNA; (ii) a R-loop structure, in which a single DNA strand, belonging to the duplex DNA molecule, is hybridised with ssRNA and finally (iii) an incorporation of a single, or more, ribonucleotide(s) (rNMPs) in genomic DNA (144). Although RNA:DNA hybrids are needed for the successful ending of cellular processes, their persistent presence can induce harmful consequences to genome integrity causing replication fork arrest with replication-transcription collision and chromosomal breakage repair (145,146). For these reasons, a family of endoribonucleases, called RNase H, process the RNA:DNA hybrids to restore regular genomic stability.

Currently, in-depth studies regarding the incorporation of rNMPs within the DNA have been reported (147). This particular RNA:DNA hybrid structure is one of the most common types of DNA damage because of its high frequency and abundance in the genome of both prokaryotes and eukaryotes (148–151). Different methodologies are under development for the detection of ribonucleotides incorporated in DNA (152–155), but the development of different sophisticated high-throughput sequencing-based approaches (156), including ribose-seq (149,157), hydrolytic end-sequencing (HydEn-seq) (158), polymerase usage sequencing (PU-seq) (159), embedded ribose-sequencing (emRibo-seq) (160) and (trimethylsilyl)diazomethane derivatisation followed by liquid chromatography–tandem mass spectrometry (154) analyses have facilitated the discovery of distributions and abundances of rNMPs in genomic DNA. Remarkably, a widespread but nonrandom distribution of rNMPs presenting several hotspots and a preference for rCMPs and rGMPs has been discovered (149). The high frequency (>100 million in mammalian cells) of rNMPs included in the nascent DNA molecule found during each replication cycle and DNA repair could have different origins. An imbalance of the rNTPs:dNTPs ratio, generally in favour of rNTPs in normal conditions (149,161), and an imprecise discriminating capacity of DNA polymerases, which can erroneously incorporate rNTPs rather than dNTPs, are two aspects playing a role in these mechanisms (162–166). Moreover, RNA primers, synthesised to allow DNA lagging strand replication (167), could be considered an additional cause of the presence of rNMPs in DNA. Indeed, if RNA primers are not correctly removed, isolated rNMP(s) can be included among consecutive Okazaki fragments, which could then permanently persist within genomic DNA (168). The biological relevance of rNMP incorporation in genomic DNA is emerging from a growing body of recent scientific studies. Whatever the cause of the rNMP(s) incorporation, the additional 2'-OH group on one or more rNMP(s) alters DNA elasticity and structure in a sequence-dependent manner, destabilising the DNA backbone, increasing the susceptibility to DNA hydrolysis, and finally causing strand cleavage and/or mutability (148,169–174). The genomic DNA stability, perturbed by the rNMP(s) presence, is preserved by the combined action of several enzymes orchestrated in a unique pathway called ribonucleotide excision repair (RER) (160). One of the most important RER enzymes is RNase H2 (175), an endonuclease involved in the cleavage of the phosphodiester bond at the 5' side of a single, or more allocated in series, rNMP(s) embedded in DNA. Similar to BER, FEN1 incises the 3' side of the partially excised rNMP to definitely release it from the genomic DNA, leaving a nick that will be finally repaired by Pol δ , Pol ϵ and Lig I enzymes (175,176). The missing processing of rNMPs embedded in DNA results in embryonic lethality in mice (160,177), as a consequence of activation of a p53-dependent damage response (178), cell cycle arrest and blockage of DNA replication (179,180). Moreover, it has been documented how mutations in each of the three RNase H2 subunits are correlated with the onset of the Aicardi Goutières syndrome (AGS), an inflammatory disorder (181,182) whose effects are mainly associated with increased levels of rNMP(s) incorporated in genomic DNA, that partially stimulates the activation of the innate immune response by IFN γ signaling and DDR (160,180,183,184). Notably, a recent work performed on mice, expressing different types of AGS-mutated RNase H2, has demonstrated the existence of a threshold in rNMPs levels during embryonic development. When the level is moderate, an activation of the cGAS–Sting DNA sensing innate immune response leading to perinatal lethality was observed. When a high abundance of rNMPs exceeded the threshold, the subsequent activation of p53-dependent DNA

damage caused early embryonic lethality (185). Importantly, a relationship between RNase H2 and rNMPs incorporation with cancer is emerging. Screening of a cohort of patients with gastric cancers has recently revealed an association between the onset of gastric cancer and mutations in gene coding for the subunit B of RNase H2 (186). In parallel, a recent study has shown that RNase H2 can be also considered as a colorectal tumour suppressor gene (187). Furthermore, loss of RNase H2, in the murine epidermis, results in spontaneous DNA damage and development of squamous cell carcinoma (188). In light of this, it becomes clear how additional investigations are needed for clarifying the association between mutated RNase H2 and/or rNMP(s) DNA-incorporated and pathology. Although the deleterious effects of rNMP(s) incorporations in DNA are well-known, a new hypothesis has been suggested involving a putative helpful role for rNMP(s). Specifically, it has been shown that more rNMPs, consecutively incorporated in yeast genomic DNA, may mark the nascent DNA strand, initiating programmed mating-type switching (189). Furthermore, a recent study reported how the erroneous ability of polymerase μ (Pol μ) to discriminate rNMPs during the NHEJ pathway (190–192) could be detrimental, as well as advantageous, for the cell. Indeed, by inserting rNMPs with a higher base fidelity compared with dNMPs (192), Pol μ might stimulate Lig IV in promoting initiation of the NHEJ mechanism (193). In parallel, another interesting observation has linked the activity of RNase H2 with the mis-match repair (MMR) pathway (164,194). The rNMP cleavage mediated by RNase H2 works as a signal for MMR enzymes, which are then stimulated to process the mismatched sites located in the surroundings. Finally, although the results show that rNMP in DNA induced a decrease of DNA polymerases processivity (195), the choice of which rNMP is embedded in the template strand can influence the DNA synthesis (195–197). A still unanswered question is whether alternative DNA repair systems, other than the RER pathway, may remove rNMPs embedded in DNA (147,198,199). Until now, topoisomerase I (Top1) is the only enzyme able to cleave rNMPs embedded in DNA, when the RER pathway is not working. Top1 is an essential enzyme thought to resolve DNA supercoils generated during replication and transcription (200,201). It has been shown that Top1, cleaving at the 5'-side of rNMPs (199,202) and generating 5'-OH and 3'-cyclic 2'-3' phosphate as DNA termini, is able to compensate for RNase H2 deficiency, although it causes high levels of DNA mutations (199,203). Later, the cleavage is followed by nick processing by Srs2-Exo1 (204,205). A recent analysis of yeast has identified a role of Apn2 (homologous to human APE1) in restoring the genome integrity perturbed by the Top1-catalysed rNMPs cleavage by resolving 3'-end blocks generated by Top1 (206). Recently, Zimmermann *et al.* (207) have shown how the cleavage of rNMPs by Top1 results in the formation of PARP-trapping lesions that impede DNA replication. In contrast, studies performed on the MMR and the nucleotide excision repair (NER) pathways have shown the inefficiency of these pathways in the processing of this particular lesion (199,208). The NER pathway generally excises bulky and non-bulky DNA base adducts (209). Because rNMP incorporation distorts the DNA backbone, NER enzymes could be good candidates in repairing this type of damage. Data obtained from *Bacteria* showed an involvement of NER factors in the removal of rNMPs in the DNA (210,211), in contrast to what is observed for human NER factors, which are not involved in rNMP repair (208). Evidence about this difference has not improved, but may suggest that NER factors might have lost this function during evolution. In contrast, data collected *in vitro* have shown that the MMR mechanism can target mismatches with

rNMPs both in *Escherichia coli* and *Saccharomyces cerevisiae* genomic DNA (197). Increasing knowledge in this field represents an important goal in the DNA repair and in the pathogenesis associated with this type of damage. For this reason, we improved the study of DNA repair mechanisms acting on rNMPs embedded in DNA, under conditions in which RER is functionally inactive. In our laboratory, while studying a putative role of BER in the removal of rNMPs embedded in the DNA, we discovered that BER was not active on this type of lesion (7). In this context, several published reports have hypothesised that, among the many millions of rNMPs that are introduced into the mammalian genome per cell cycle (198), damaged rNMPs (such as the ribose monophosphate abasic site and oxidation) can also be incorporated into DNA. In fact, RNA molecules, as well as rNMPs present in the nucleotide pool, are also susceptible to oxidative insults (108,212). Although not fully explored, the generation of hydroxyl radicals from oxidative stress could be the cause of the conversion of the deoxyribose sugar into ribose *in vitro* and *in vivo* (212). This can happen both in the cellular nucleotide pool and directly into the DNA. Additional data are needed to support this hypothesis. Moreover, a significant generation of abasic sites has been demonstrated upon RNA oxidation and alkylation (23). For these reasons, whereas the role of the RNase H2-initiated RER mechanism of DNA repair in recognising and cleaving rNMPs embedded in DNA is well-established (178,198), little is known regarding the possible involvement of the RER pathway, or other DNA repair pathways, in the removal of damaged rNMPs. Again, a role of the BER pathway was addressed in our laboratory. For its abilities, BER may represent one of the best candidates to work on modified rNMP(s) during DNA repair. Although APE1, in contrast to RNase H2, does not work on rGMP embedded in DNA (7), it has nevertheless been demonstrated to cleave the ribose monophosphate abasic site incorporated in the DNA (Figure 1). In contrast with expectations, RNase H2 does not work on this damaged base, confirming an APE1-exclusive function. Additionally, we focused on the 8-oxo-guanosine (8-oxo-G)-modified base. First, we found an inability of human RNase H2 in recognising and cleaving this modified rNMP embedded in DNA. We then studied the BER pathway, in which one of the most known bifunctional glycosylases, active in processing the 8-oxo-dG and FapyG DNA lesions, is OGG1 (213,214). Although OGG1 also interacts with undamaged G, it is specific enough to discriminate and not to process it (215). In our recent report (7), we found that OGG1 was able to recognise and bind the 8-oxo-G embedded in DNA, as efficiently as its canonical substrate (8-oxo-dG) (Figure 1). Moreover, when co-incubated with APE1, it showed no glycosylase activity, being unable to process the 8-oxo-G and to generate a substrate suitable for APE1. Notably, we discovered and characterised the NIR activity of APE1 on the 8-oxo-G substrate. APE1, although weakly, was able to cleave 8-oxo-G using experimental conditions specific for NIR. Furthermore, as observed during canonical NIR activity, APE1 works as an 3'-exonuclease on the newly generated 3'-OH terminus (Figure 1). We recently improved our knowledge in this topic by discovering that, although human and *Archeal* RNase H2/II proteins are not able to process the 8-oxo-G or the ribose monophosphate abasic sites embedded in DNA, they were able to bind these damaged bases. In contrast, we found that *E. coli* RNase HII possessed a high enzymatic activity on both the 8-oxo-G and ribose monophosphate abasic containing substrates, suggesting a loss of function during phylogenetic evolution (216). Recently, it has been found that rNMP(s) is also incorporated by DNA polymerase γ in mitochondrial DNA (mtDNA), in heavy as well as light strand DNA.

Increased levels of embedded ribonucleotides, affecting mtDNA stability and impairing new rounds of mtDNA replication, may contribute to new pathogenic mechanisms (217–220). A recent work conducted on yeast has demonstrated that a repair mechanism for rNMPs mis-incorporated is lacking (221). Further studies are needed regarding the consequences of rNMP incorporation in mtDNA and its repair processing.

BER enzyme signatures in cancer

Because of the involvement of the BER pathway in cancer and because of evidence regarding BER factor secretion (see paragraph below), extensive efforts have been directed to evaluate the prognostic and predictive tumour biomarker potential of BER enzymes (222) (Figure 2). Several studies described the alterations of the APE1 genetic sequence, expression and distribution in several tumours (223). In different types of solid tumours, an increased APE1 expression is associated with lower survival rates and, at the same time, an aberrant nuclear and cytoplasmic localisation of APE1 is a sign of poor outcome (224). A study performed on a cohort of patients with gallbladder cancer showed that high expression of APE1 protein was positively correlated with tumour stage and positive

lymph node status; in contrast, no association with tumour differentiation and metastatic condition was detected (225). It should be noted that not only the protein level, but also the subcellular localisation of APE1 was altered. APE1 displayed a nucleo-cytoplasmic localisation, especially in patients in which a higher level of protein was detected (225). Regarding hepatocellular carcinoma (HCC), an upregulation of APE1 occurred at the transcriptional level, which was linked with the progression of the disease (226). Moreover, further studies showed an enhanced APE1 protein expression in tumour tissue compared with healthy controls (227). Immunostaining analysis revealed elevated levels of APE1 in pancreatic adenocarcinoma tissue (228), and also in prostate, esophageal, gastric, salivary gland carcinomas (229–232) and non-small-cell lung cancers (233). In all cases, this feature correlated with a lower survival of patients (231–233). Furthermore, in tumour tissues derived from ovarian cancer, several studies highlighted an altered overexpression and localisation of APE1 (234,235). However, in different cohorts of ovarian cancer, there were conflicting studies regarding the correlation between the subcellular localisation of APE1 and cancer outcomes (223). In colorectal cancer (CRC), increased APE1 levels and cytoplasmic localisation in tumour tissue and colon cancer stem cells have been observed (236,237); furthermore, the APE1 overexpression

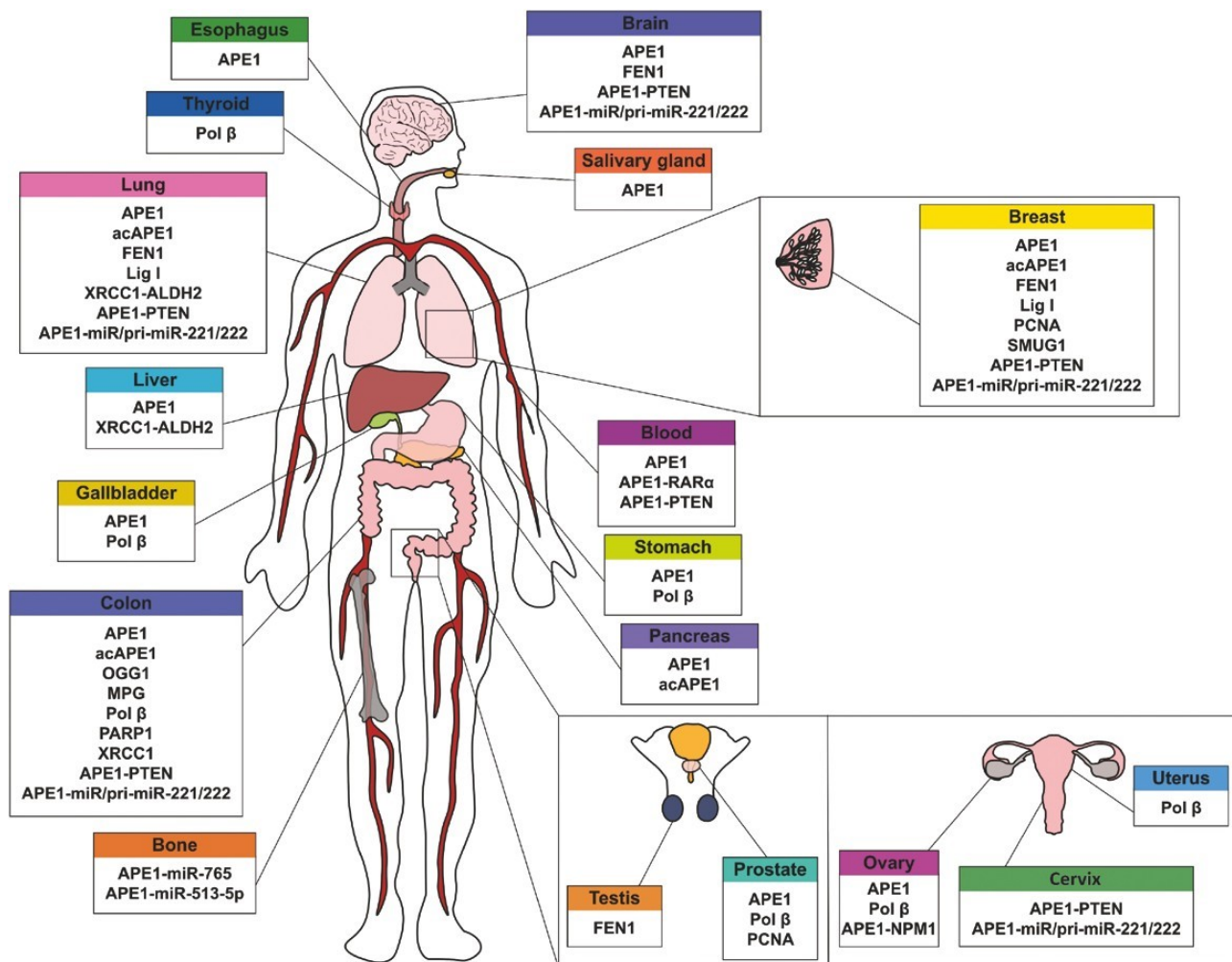


Figure 2. Overview of the most common BER-related alterations and relevance as potential molecular biomarkers in cancer. Symbolic illustrations of organs are shown, in which the main alterations of BER enzymes or BER-related alterations are listed into the connected colored boxes. See the text for further information. Figure available in colour online.

in liver metastasis has been correlated with poor prognoses (238). Concerning breast cancer, conflicting data are available. Some analyses reported that APE1 expression was higher in patients with triple negative breast cancer (TNBC), which was associated with tumour size (239), while another study reported that a decreased APE1 level was linked to aggressive histological features and triple negative phenotypes (240). Similarly, loss of APE1 expression and poor prognoses were found in glioma compared with normal brain tissue (241); however, an increase in the APE1 protein was observed in post-treatment glioblastoma tumours (242). Along with the expression level of APE1, its acetylated status has also been considered because it modulates APE1 activity. In particular, elevated levels of acAPE1 in colon, lung and pancreatic cancer tissues, leading to an increased AP-endonuclease activity, have suggested the occurrence of a compensatory mechanism in response to genotoxic stress induced by chemotherapy to maintain tumour cell proliferation capacity (243). Decreased APE1 acetylation status was associated with TNBC (244), demonstrating how PTMs occurring on APE1 is related to cancer development (244). Finally, a transcriptome analysis revealed an increased expression of APE1 and other genes of its interactome in the lymphocyte T cells of childhood acute lymphoblastic leukemia (245). Notably, correlation analyses were performed to link the overexpression of APE1 and the levels of its interacting proteins. For example, a cytoplasmic overexpression of APE1 and of its interacting protein, NPM1, were found in different studies, such as in a cohort of patients with ovarian cancer (246) with serous ovarian adenocarcinomas (247), indicating an association with lymph node metastasis, chemoresistance and an overall poor prognosis. Another positive correlation was observed between retinoic acid nuclear receptor (RAR α) and APE1 in patients with multiple myeloma (248). Indeed, the binding of RAR α to its DNA response elements (RARE) is dependent on the redox function of APE1 (249). However, an inverse association has been found between APE1 and the tumour suppressor, PTEN, in glioblastoma, colorectal, breast, cervical and non-small cell lung cancers (6). Notably, high levels of PTEN and low levels of APE1 mRNA expression were associated with better prognoses in human melanomas (250). Furthermore, not only proteins but also miRNAs have been shown to be correlated with APE1 in tumours. Indeed, a negative correlation was found between miR-765 and APE1 expression in osteosarcoma patients. Specifically, a higher expression of miR-765 was associated with decreased APE1 and good survival in response to cisplatin treatment (251). In addition, the downregulation of miR-513-5p was found in patients with osteosarcoma. The decreased level of miR-513-5p has been correlated with APE1 overexpression and radioresistance (252). Finally, an inverse correlation between APE1 and miR/priR-miR-221/222 expression was found in a cohort of human cancer specimens, such as glioblastoma, colorectal, breast, cervical and non-small cell lung cancers (6). In this context, the possibility to create a screening panel of the biomarker interactomes, involved in tumour development, should be carefully evaluated.

The expressions of other BER enzymes have been evaluated in the literature as potential biomarkers. For instance, OGG1 is estimated to be a prognostic biomarker of CRC patients survival; and low levels of OGG1 mRNA in marginal colon tissue were associated with longer survival in CRC patients following therapeutic surgery (253). Furthermore, low mRNA and protein levels of SMUG1 were associated with adverse clinic-pathological features in breast cancer patients (254). Regarding CRC, an overexpression of *N*-methylpurine DNA glycosylase (MPG), OGG1, APE1, Pol β , PARP1 and XRCC1 was also shown to be linked with poor pathological outcomes

(222,255); only the overexpression of MPG and Pol β , and not of XRCC1, were positively correlated with higher rates of tumour proliferation when each individual CRC case was taken into account (222). Moreover, an increased expression of Pol β was also observed in gastric, uterine, prostate, ovarian and thyroid carcinomas (256). Limited to Pol β , overexpression was also consistently associated with tumour stage of gallbladder cancer (225). Furthermore, a cancer-related isoform of PCNA has been specifically detected in prostate and breast cancer (257,258). Moreover, a positive correlation between the upregulation of FEN1 and aggressiveness in breast cancer patients has been observed (259). FEN1 has been also found overexpressed in testis, lung and brain tumours (260). In the case of XRCC1, its overexpression, in lung and liver-cancer patients, was associated with low expression of aldehyde dehydrogenase 2 (ALDH2), resulting in a poor prognostic value, suggesting that an efficient DNA repair mechanism is required in the presence of high aldehyde metabolism (261). Finally, an increased expression of Lig I has been reported in breast and lung tumour tissues (262).

Very importantly, along with the levels of the proteins, it is also fundamental to evaluate their activity, as biomarkers. The possibility to measure the DNA repair capacity (DRC) could provide a method to predict the outcome of a particular disease. For instance, 5-fluorouracil (5-FU) is the main chemotherapeutic drug used against solid tumours. The BER pathway is involved in the DNA repair process in response to 5-FU lesions, thus, removing 5-FU and uracil metabolites from the DNA (263). A prospective study demonstrated the association between DRC of BER in response to 5-FU and patient survival in a cohort affected by CRC. In the study, the overall survival was correlated with high activity of BER in non-malignant adjacent mucosa and low BER in tumour tissue in patients with TNM Stages II and III, together with good therapy response (264). Interestingly, APE1 enzymatic activity was also higher in gallbladder tumour patients than in chronic cholecystitis patients (225). Taking into account these results, Chaim *et al.* (265) developed a fluorescent-based multiplex flow-cytometric host cell reactivation assay, based on the transfection of reporter plasmids in primary T lymphocytes, that allowed measurement of the activity of BER enzymes, such as different glycosylases (OGG1, MPG, MUTYH and UNG) and APE1. The possibility to measure the activity of OGG1 and MPG through a DNA glycosylase-mediated cleavage of molecular beacons was demonstrated by Hu *et al.* (266).

BER polymorphisms and cancer

The identification of single-nucleotide polymorphisms (SNPs) in DNA repair genes has become increasingly important since they can determine a different DNA repair capacity and consequently generate higher frequency of mutations (267). Therefore, SNPs can be associated with a high susceptibility to cancer and with chemotherapy and radiotherapy resistance (268). Different SNPs involved in carcinogenesis have been identified in the main DNA repair pathways, such as BER, NER, MMR and double-strand breaks repair (DSBR) (267,269,270). For all these reasons, DNA repair pathway polymorphisms are of interest as predictive factors in the clinic. Here, we report the most frequent functional polymorphisms that have recently been published concerning the BER pathway enzymes (see Wallace *et al.* (14) for the complete list of polymorphisms).

Several evidences have been reported regarding the main BER DNA glycosylases, such as OGG1, NEIL3 and mutY DNA glycosylase (MUTYH). Several studies have been reported regarding the most studied OGG1 polymorphic variant: Ser326Cys (rs1052133). Up to

now, data regarding OGG1 Ser326Cys polymorphism and cancer has been conflicting, probably due to the susceptibility of the different populations and the different types of tumours that have been studied. Earlier evidence suggested that OGG1 Ser326Cys polymorphism did not increase the risk of developing lung cancer (271). Nevertheless, conflicting data of OGG1 Ser326Cys polymorphism was present for CRC (272,273) and breast cancer (274,275). However, a more recent study has shown how OGG1 Ser326Cys heterozygous genotype (Ser/Cys) is associated with a decrease of bladder cancer risk in a cohort of a Belarusian population (276). In a follow-up study, the same research group demonstrated how this polymorphism could affect cancer-related genes and the methylation status in patients diagnosed with bladder cancer. Indeed, the frequency of the oncogenic phosphatidylinositol 3-kinase (PIK3CA) mutations was reduced in smokers of heterozygous genotype (Ser/Cys) and minor allele (Cys) carriers. On the contrary, the same polymorphism correlated with an increased frequency of mutations in the RAS loci and affected the levels of runt-related transcription factor 3 (RUNX3) and ISL LIM homeobox 1 (ISL1) methylation (277). In addition, it has been shown that OGG1 Ser326Cys homozygous genotype (Cys/Cys) represents a risk factor for childhood leukaemia (278). An explanation is that the Cys/Cys genotype is associated with lower OGG1 activity, which translates to an increased AML relapse (279). Concerning polymorphisms involving other glycosylases, NEIL3 Pro117Arg (rs7689099) has been suggested for its relevance in susceptibility, survival and therapy outcome in patients with CRC from the Czech Republic and Austrian cohorts (280). Finally, MUTYH polymorphism Gln324His (rs3219489) (Gln/His and His/His) was associated with increased CRC risk in a Polish population (281) and Gln324His (His/His) was linked to a higher lung cancer risk in a Japanese population (271).

Concerning the endonuclease APE1, the most frequent polymorphism is Asp148Glu (rs3136820), covering about 46% of the population (14). Again, conflicting data are present in the literature regarding bladder, breast, colorectal and lung cancer (14,270). Furthermore, a recent meta-analysis has not shown any association between the Asp148Glu polymorphism and prostate cancer; however, in the same study, when a hospital-based population was considered, the presence of Asp148Glu dominant variants (Glu/Glu and Asp/Glu) was proposed as a risk factor to develop prostate cancer (282). In addition, in a recent study, APE1 Asp148Glu was not considered as a risk factor for HCC in an Egyptian population (283). These discrepancies probably are attributable to the fact that the Asp148Glu variant exhibits normal endonuclease activity (284). However, increasing incidence of AP sites has been observed in leukocytes derived from breast cancer patients compared to controls, thus increasing the risk of cancer (285). Finally, a meta-analysis has suggested that the APE1 polymorphism rs1760944 T > G could have a protective role in cancer development among Asians (286).

Few data are available regarding the association between PARP1, Pol β , FEN1 polymorphisms and tumours. Liu *et al.* (270) have reported the latest data regarding these BER enzyme polymorphisms and the risk of CRC.

Different studies concerning XRCC1 polymorphisms and the susceptibility to cancer have been reported. In a Caucasian population, the risk of gliomas was associated with both the homozygous variants of XRCC1 Gln399Gln and XRCC3 Met241Met (287). Another variant of XRCC1, Arg194Trp, was shown to be a risk factor for CRC in a Chinese and Kashmiri population with heterozygous (Arg/Trp) and homozygous variants (Trp/Trp) (288,289). The same polymorphism was considered a susceptibility factor for HCV-related

hepatocellular carcinoma progression in an Egyptian population; however, no association was found when Arg280His or Arg399Gln genotypes were taken into account (283). In a Chinese cohort, the polymorphism located at the promoter of XRCC1 (XRCC1 rs3213245 C genotype) was associated with a decreased risk of cervical cancer, due to a transcriptional overexpression of XRCC1, as a consequence of the enhanced binding of the Sp1-Knox-20 complex to the promoter region. Moreover, a decreased expression of XRCC1 has been observed in carriers of the XRCC1 rs3213245 T genotype, increasing the risk of cancer (290). BER polymorphism can affect the methylation status of some tumour suppressor genes, as previously mentioned. For instance, focusing on XRCC1, in a study which considered a cohort of patients with bladder cancer, the XRCC1 Arg399Gln (rs25487) heterozygous (Arg/Gln) genotype increased the frequency of p16 and TIMP3 methylation (277).

Extracellular secretion of BER proteins: novel insights in cancer biology

It has been widely reported how, in cancer cells, the activation of the BER pathway, in response to the chemotherapy treatment, promotes a resistant phenotype (291). Through the activation of repair mechanisms, in fact, stressed cancer cells can escape from cell death and maintain their ability to grow (292). This is the reason why BER enzymes are considered a good target for developing novel anti-cancer therapies. The chemoresistance phenomenon is not only connected with the activation of repair pathways in cancer cells, but also with the multifunctional role of the BER enzymes, particularly associated with the regulation of gene expression (133,293). Another interesting aspect supporting the chemoresistance occurrence is the capability of drug treatments to induce a modulation of the immune responses (294). Some secreted factors are also responsible for the modulation of immune responses, acting in the extracellular tumour microenvironment, to affect the metabolism of the accepting cancer cells (293). This property suggests a new scenario regarding the dynamic molecular mechanisms that are activated by the secreted factors that influence the behavior of the surrounding cancer cells. Specifically, it would be interesting to study some BER or BER-related proteins regarding their possible roles as damage associated molecular patterns (DAMP) proteins in tumour progression, such as the secreted protein high mobility group box 1 (HMGB1) (Figure 1). HMGB1 is a nuclear DNA repair protein that acts as a chromatin remodeling factor and as a transcriptional regulator, but it is also an extracellular protein, that can act as a chemokine and cytokine, having a role in cell signaling and inflammation (295,296). As a DNA repair protein, its accumulation is concomitant with oxidative DNA damage and, for this reason, it has been defined as an early DDR factor (297). It is also considered as a BER co-factor, because it is able to affect the activities of BER enzymes. HMGB1 stimulates APE1 endonuclease activity on AP sites, and promotes long-patch BER, through the stimulation of FEN1 flap cleavage activity (295). It is known that oxidative stress is responsible for HMGB1 translocation, release and activity (298). These secreted proteins therefore have a pro-inflammatory role (299). Indeed, HMGB1 secretion is induced upon chemotherapeutic treatment, and due to its capability to stimulate the chemokine CXCL11, it contributes to the antitumour immune response (294,300). In contrast, current data elucidate how this secreted protein is also connected to cancer development, due to its role in the progression of esophageal squamous cell carcinoma (ESCC) (293). These data suggest the importance of activated paracrine signaling in the tumour microenvironment for cancer evolution

and progression. Interestingly, other proteins whose role was initially thought to be restricted only to the nuclear compartment and with the maintenance of DNA structure and with the regulation of gene expression, have been recently demonstrated to play a role in paracrine signaling. Even if these proteins lack the leader sequence that promotes the canonical secretion through the endoplasmic reticulum and Golgi apparatus (301), their secretion is clearly documented. As secreted factors, the function of these proteins seems to be related to cytokines activity. One example is YB-1, an additional APE1-interacting protein, whose role as an extracellular mitogen was described in mesangial and monocyte cells after inflammatory challenges (302) (Figure 1). There are also consistent data about the secretion of the APE1 enzyme, whose elevated intracellular protein levels in cancer are linked to poor prognosis (141). APE1 confers resistance to chemotherapy or radiotherapy treatments in different kind of tumours like gliomas, breast cancer, HCC, thyroid cancer and osteosarcoma (226,303–305). Recent findings concerning APE1 cytoplasmic relocation and poor prognostic correlation in HCC cells led to new investigations about the multiple functions of this BER enzyme and to its emergent role in cancer progression relative to its own localisation (141,226). Studies regarding its possible secretion were reported since 2004, when it was predicted that APE1 was also a non-classically secreted protein (306). Its extracellular secretion was later revealed in the plasma of endotoxemic rats (307), and in the same year, the regulation of APE1 secretion occurring through PTMs and inducing its extracellular release was characterised. It seems, in fact, that the acetylation of residues K6/K7 in the APE1 N-terminal region promotes its secretion (308). APE1 acetylation as a post-translational modification promoting its extracellular release,

was also verified in TNBC, in which APE1 secretion and its action as an autocrine and paracrine factor seems to promote the apoptosis of cancer cells (309). Reports regarding APE1 functions as a secreted protein were also observed in monocytes, where an APE1 extracellular role under inflammatory conditions and its capability to promote the production and secretion of IL-6 were proven (310). We recently demonstrated a role of extracellular APE1 in HCC (311), finding a positive correlation between serum and tissue APE1 amounts in the HCC cohort analysed. These data prompted us to consider serum APE1 as a new diagnostic biomarker in HCC. We also showed that the exogenous APE1 protein was able to induce IL-6 and IL-8 expression in the JHH-6 HCC cell line, suggesting its role as a paracrine pro-inflammatory factor. Hence, these findings suggested that exogenous APE1 was able to modulate the inflammatory status of the tumour microenvironment, showing its possible role in cellular senescence and in tumour invasiveness (310–312). We believe that further characterisation of the roles of secreted BER proteins is required for an understanding of their role in tumour biology.

Cancer organoids as a novel approach to translate BER proteins in personalised medicine

Human cell lines and *in vivo* animal models have been largely used to characterise the biochemical functions and the biological relevance of BER proteins, and are a well-known model in cancer translational research. However, a better knowledge of the adult stem cells in combination with three-dimensional (3D) cultures has allowed the establishment of organoids as an advanced model

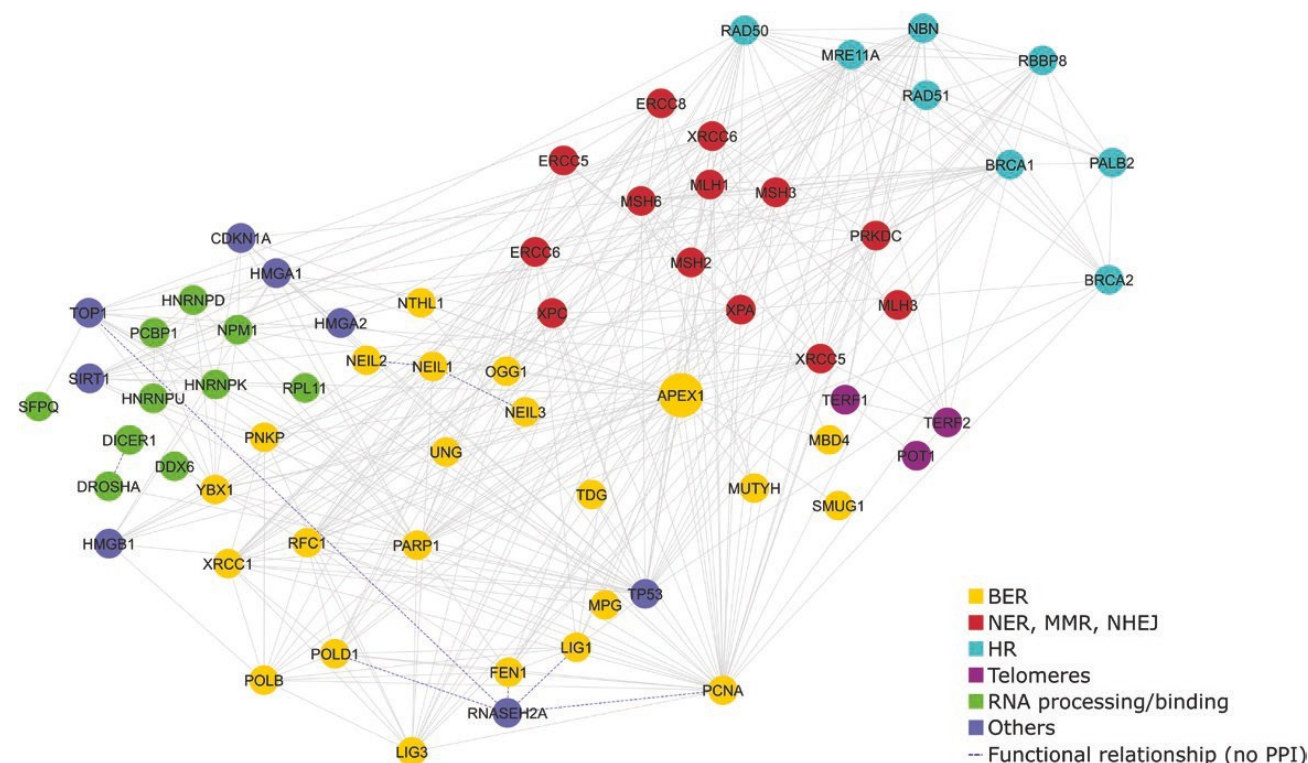


Figure 3. Protein–protein interaction network of proteins involved in DNA repair/stability and in RNA processing. Data, obtained from the InWeb_InBioMap platform (no network expansion, confidence score cut-off = 0.156 [recommended value]; (322)), shows the direct (solid lines) and indirect (dashed lines) interactions existing between BER (yellow nodes), nucleotide excision repair/DNA mismatch repair/non-homologous end joining (NER, MMR, NHEJ, red nodes), homologous recombination (HR, cyan nodes), telomeres (purple nodes) and RNA processing/binding (green nodes) proteins, as well as a few others (blue nodes) with heterogeneous molecular functions. Figure available in colour online.

system [313,314]. Organoids consist of a novel 3D technology, which allows the establishment of long-term stem cell-based cultures. Organoids represent a valuable tool to study the biology of stem cells and to evaluate their contribution to tissue homeostasis. Organoids have numerous valuable applications and may be used to improve our knowledge about several disease pathways [315,316], especially in cancer biology. Due to the intriguing mechanisms characterising tumour aetiology, different studies have focused on personalised precision treatments for cancer. By using patient-derived tumour organoids (PDOs), studies have tried to understand and reproduce the disease complexity and heterogeneity, for developing patient-specific therapies [317], because organoids reflect the key-features of the original patient's tissue [316]. Different types of analyses involving normal and tumour PDOs have been performed, such as genome, transcriptome [318] and proteome analyses [317], but DNA repair mechanisms have not been extensively studied. Based on previous studies, normal organoids could be engineered to study DNA repair enzymes deficiencies and evaluate mutational signatures in cancer. To date, few studies regarding BER enzymes and PDOs have been published. In a recent study, human normal intestinal organoids were engineered with the CRISPR-Cas9 genome editing system to delete key DNA repair genes, such as the MMR gene *MLH1* and the BER gene *NTHL1* [319]. This approach proved that *MLH1* knock-out organoids reflected mismatch repair-deficiency found in CRC; moreover, the lack of *NTHL1* was a predisposition to the development of a range of cancers, such as colorectal and breast cancer [319]. Furthermore, the opportunity to perform drug-screening assays on PDOs is very appealing, considering that chemoresistance can occur in patients [320]. Indeed, we recently tested the APE1 endonuclease inhibitor (Compound #3) on CRC PDOs, carrying a wild-type, and a stop-gain or missense mutant TP53, highlighting that the effectiveness of the inhibitor was dependent on the presence of wild-type or gained-of-function mutant p53 and independent of the null-mutant p53 [321]. Therefore, we strongly believe that the use of these 3D-cell models should be carefully considered in translating BER biochemistry into personalised medicine.

Conclusions

Forty years after the first characterisation of the BER glycosylases, integration of this pathway (Figure 3, yellow nodes) within the DDR (Figure 3, red and cyan nodes) has been somewhat elucidated. The recent discovery of a functional role of this highly conserved pathway in genomic stability, gene expression regulation and RNA processing/decay (Figure 3, purple, blue and green nodes) lays the foundations for the starting point of a new challenging field of research. These achievements will significantly contribute to our understanding of the complexity of BER and the DDR, in general. Moreover, these findings will help add further elements to the comprehension of the role of BER in human physiology and pathology, possibly opening new unpredicted therapeutic perspectives. Many issues still remain to be addressed and are prompting researchers to continue their efforts to understand the crosstalk between DNA damage and gene expression regulation. This can be considered as a fundamental process responsible for the adaptive cellular mechanisms to genotoxic damage, and is a concern regarding several possible mechanisms of cancer chemoresistance.

In the last 40 years, we have learned much regarding BER biochemistry and biology. However, a number of questions still remain to be elucidated.

- Should we reinterpret the overall biological function of DDR and its role in cancer based on the data about the relevance of the non-canonical functions of DDR and BER proteins?
- Several BER and other DDR enzymes are catalytically active on different modified RNA substrates. Should we ascribe to them an important role in RNA decay or in the editing mechanisms?
- Might the unique ability of BER DNA glycosylases to recognise even subtle chemical modifications of nucleobases serve to distinguish between normal and aberrant RNA molecules?
- Is there a concerted action between DNA glycosylases, APE1 and the downstream enzymes involved in decay/repair of damaged RNA molecules?
- Can the effects of BER enzymes, both on mRNA and ncRNA, alter the protein translational machinery, thus, contributing to chemoresistance through post-transcriptional regulation of gene expression?
- Is the role of some DNA repair proteins in secreted exosomal particles due to their canonical or non-canonical functions?

In 2009, thanks to the use of unbiased proteomics and genomics strategies, we were able to propose the novel concept of non-canonical functions of APE1 in RNA metabolism. We strongly believe that an integrated view of the canonical roles of BER proteins in DNA repair and in RNA functions will lead to new important and unexpected discoveries in the future.

Funding

This work was supported by grants from the Associazione Italiana per la Ricerca sul Cancro (IG14038) and the European Union, European Regional Development Fund and Interreg V-A Italia-Austria 2014-2020 ITAT1096-P (Program PRECANMED ITAT1009 CUP G22F16000890006) to G.T.

Acknowledgements

The authors thank all the members of the GT lab for constructive feedback during the development of this work.

Conflict of interest statement: None declared.

References

1. Hein, N., Hannan, K. M., George, A. J., Sanij, E. and Hannan, R. D. (2013) The nucleolus: an emerging target for cancer therapy. *Trends Mol. Med.*, 19, 643–654.
2. Hanahan, D. and Weinberg, R. A. (2011) Hallmarks of cancer: the next generation. *Cell*, 144, 646–674.
3. Wickramasinghe, V. O. and Venkitaraman, A. R. (2016) RNA processing and genome stability: cause and consequence. *Mol. Cell*, 61, 496–505.
4. Michelini, F., Jaliha, A. P., Francia, S., et al. (2018) From “cellular” RNA to “smart” RNA: multiple roles of RNA in genome stability and beyond. *Chem. Rev.*, 118, 4365–4403.
5. Antoniali, G., Lirussi, L., Poletto, M. and Tell, G. (2014) Emerging roles of the nucleolus in regulating the DNA damage response: the noncanonical DNA repair enzyme APE1/Ref-1 as a paradigmatic example. *Antioxid. Redox Signal.*, 20, 621–639.
6. Antoniali, G., Serra, F., Lirussi, L., et al. (2017) Mammalian APE1 controls miRNA processing and its interactome is linked to cancer RNA metabolism. *Nat. Commun.*, 8, 797.
7. Malfatti, M. C., Balachander, S., Antoniali, G., et al. (2017) Abasic and oxidized ribonucleotides embedded in DNA are processed by human APE1 and not by RNase H2. *Nucleic Acids Res.*, 45, 11193–11212.
8. Dianov, G. L., Souza-Pinto, N., Nyaga, S. G., Thybo, T., Stevnsner, T. and Bohr, V. A. (2001) Base excision repair in nuclear and mitochondrial DNA. *Prog. Nucleic Acid Res. Mol. Biol.*, 68, 285–297.

9. Krokan, H. E. and Bjørås, M. (2013) Base excision repair. *Cold Spring Harb. Perspect. Biol.*, 5, a012583.
10. Markkanen, E. (2017) Not breathing is not an option: how to deal with oxidative DNA damage. *DNA Repair (Amst.)*, 59, 82–105.
11. Sidorenko, V. S., Nevinsky, G. A. and Zharkov, D. O. (2007) Mechanism of interaction between human 8-oxoguanine-DNA glycosylase and AP endonuclease. *DNA Repair (Amst.)*, 6, 317–328.
12. Sidorenko, V. S. and Zharkov, D. O. (2008) Role of base excision repair DNA glycosylases in hereditary and infectious human diseases. *Mol. Biol.*, 42, 794–805.
13. Takao, M., Zhang, Q. M., Yonei, S. and Yasui, A. (1999) Differential subcellular localization of human MutY homolog (hMYH) and the functional activity of adenine:8-oxoguanine DNA glycosylase. *Nucleic Acids Res.*, 27, 3638–3644.
14. Wallace, S. S., Murphy, D. L. and Sweasy, J. B. (2012) Base excision repair and cancer. *Cancer Lett.*, 327, 73–89.
15. Svilar, D., Goellner, E. M., Almeida, K. H. and Sobol, R. W. (2011) Base excision repair and lesion-dependent subpathways for repair of oxidative DNA damage. *Antioxid. Redox Signal.*, 14, 2491–2507.
16. Hill, J. W., Hazra, T. K., Izumi, T. and Mitra, S. (2001) Stimulation of human 8-oxoguanine-DNA glycosylase by AP-endonuclease: potential coordination of the initial steps in base excision repair. *Nucleic Acids Res.*, 29, 430–438.
17. Prakash, A., Doublé, S. and Wallace, S. S. (2012) The Fpg/Nei family of DNA glycosylases: substrates, structures, and search for damage. *Prog. Mol. Biol. Transl. Sci.*, 110, 71–91.
18. Bailly, V. and Verly, W. G. (1988) Possible roles of beta-elimination and delta-elimination reactions in the repair of DNA containing AP (apurinic/apryrimidinic) sites in mammalian cells. *Biochem. J.*, 253, 553–559.
19. Iyama, T. and Wilson, D. M., III. (2013) DNA repair mechanisms in dividing and non-dividing cells. *DNA Repair (Amst.)*, 12, 620–636.
20. Bauer, N. C., Corbett, A. H. and Doetsch, P. W. (2015) The current state of eukaryotic DNA base damage and repair. *Nucleic Acids Res.*, 43, 10083–10101.
21. Dianov, G. L. and Hübscher, U. (2013) Mammalian base excision repair: the forgotten archangel. *Nucleic Acids Res.*, 41, 3483–3490.
22. Lindahl, T. (1993) Instability and decay of the primary structure of DNA. *Nature*, 362, 709–715.
23. Loeb, L. A. and Preston, B. D. (1986) Mutagenesis by apurinic/apryrimidinic sites. *Annu. Rev. Genet.*, 20, 201–230.
24. Demple, B., Herman, T. and Chen, D. S. (1991) Cloning and expression of APE, the cDNA encoding the major human apurinic endonuclease: definition of a family of DNA repair enzymes. *Proc. Natl. Acad. Sci. U. S. A.*, 88, 11450–11454.
25. Hadi, M. Z., Ginalska, K., Nguyen, L. H. and Wilson, D. M., III. (2002) Determinants in nuclease specificity of Ape1 and Ape2, human homologues of *Escherichia coli* exonuclease III. *J. Mol. Biol.*, 316, 853–866.
26. Meira, L. B., Devaraj, S., Kisby, G. E., Burns, D. K., Daniel, R. L., Hammer, R. E., Grundy, S., Jialal, I. and Friedberg, E. C. (2001) Heterozygosity for the mouse Apex gene results in phenotypes associated with oxidative stress. *Cancer Res.*, 61, 5552–5557.
27. Gorman, M. A., Morera, S., Rothwell, D. G., de La Fortelle, E., Mol, C. D., Tainer, J. A., Hickson, I. D. and Freemont, P. S. (1997) The crystal structure of the human DNA repair endonuclease HAP1 suggests the recognition of extra-helical deoxyribose at DNA abasic sites. *EMBO J.*, 16, 6548–6558.
28. Tell, G., Quadrifoglio, F., Tiribelli, C. and Kelley, M. R. (2009) The many functions of APE1/Ref-1: not only a DNA repair enzyme. *Antioxid. Redox Signal.*, 11, 601–620.
29. Whitaker, A. M. and Freudenthal, B. D. (2018) APE1: a skilled nucleic acid surgeon. *DNA Repair (Amst.)*, 71, 93–100.
30. Erzberger, J. P. and Wilson, D. M., III. (1999) The role of Mg²⁺ and specific amino acid residues in the catalytic reaction of the major human abasic endonuclease: new insights from EDTA-resistant incision of acyclic abasic site analogs and site-directed mutagenesis. *J. Mol. Biol.*, 290, 447–457.
31. Freudenthal, B. D., Beard, W. A., Cuneo, M. J., Dyrkheeva, N. S. and Wilson, S. H. (2015) Capturing snapshots of APE1 processing DNA damage. *Nat. Struct. Mol. Biol.*, 22, 924–931.
32. Beernink, P. T., Segelke, B. W., Hadi, M. Z., Erzberger, J. P., Wilson, D. M., III and Rupp, B. (2001) Two divalent metal ions in the active site of a new crystal form of human apurinic/apryrimidinic endonuclease, Ape1: implications for the catalytic mechanism. *J. Mol. Biol.*, 307, 1023–1034.
33. Mol, C. D., Izumi, T., Mitra, S. and Tainer, J. A. (2000) DNA-bound structures and mutants reveal abasic DNA binding by APE1 and DNA repair coordination [corrected]. *Nature*, 403, 451–456.
34. Marenstein, D. R., Wilson, D. M., III and Teebor, G. W. (2004) Human AP endonuclease (APE1) demonstrates endonucleolytic activity against AP sites in single-stranded DNA. *DNA Repair (Amst.)*, 3, 527–533.
35. Chou, K. M. and Cheng, Y. C. (2003) The exonuclease activity of human apurinic/apryrimidinic endonuclease (APE1). Biochemical properties and inhibition by the natural dinucleotide Gp4G. *J. Biol. Chem.*, 278, 18289–18296.
36. Wilson, D. M., 3rd. (2003) Properties of and substrate determinants for the exonuclease activity of human apurinic endonuclease Ape1. *J. Mol. Biol.*, 330, 1027–1037.
37. Izumi, T., Brown, D. B., Naidu, C. V., Bhakat, K. K., Macinnes, M. A., Saito, H., Chen, D. J. and Mitra, S. (2005) Two essential but distinct functions of the mammalian abasic endonuclease. *Proc. Natl. Acad. Sci. U. S. A.*, 102, 5739–5743.
38. Fantini, D., Vascotto, C., Marasco, D., et al. (2010) Critical lysine residues within the overlooked N-terminal domain of human APE1 regulate its biological functions. *Nucleic Acids Res.*, 38, 8239–8256.
39. Vascotto, C., Cesaratto, L., Zeef, L. A., et al. (2009) Genome-wide analysis and proteomic studies reveal APE1/Ref-1 multifunctional role in mammalian cells. *Proteomics*, 9, 1058–1074.
40. Vascotto, C., Lirussi, L., Poletto, M., et al. (2014) Functional regulation of the apurinic/apryrimidinic endonuclease 1 by nucleophosmin: impact on tumor biology. *Oncogene*, 33, 2876–2887.
41. Tell, G. and Demple, B. (2015) Base excision DNA repair and cancer. *Oncotarget*, 6, 584–585.
42. Busso, C. S., Iwakuma, T. and Izumi, T. (2009) Ubiquitination of mammalian AP endonuclease (APE1) regulated by the p53-MDM2 signaling pathway. *Oncogene*, 28, 1616–1625.
43. Huang, E., Qu, D., Zhang, Y., Venderova, K., Haque, M. E., Rousseaux, M. W., Slack, R. S., Woulfe, J. M. and Park, D. S. (2010) The role of Cdk5-mediated apurinic/apryrimidinic endonuclease 1 phosphorylation in neuronal death. *Nat. Cell Biol.*, 12, 563–571.
44. Busso, C. S., Lake, M. W. and Izumi, T. (2010) Posttranslational modification of mammalian AP endonuclease (APE1). *Cell. Mol. Life Sci.*, 67, 3609–3620.
45. Yoshida, A., Urasaki, Y., Waltham, M., et al. (2003) Human apurinic/apryrimidinic endonuclease (Ape1) and its N-terminal truncated form (AN34) are involved in DNA fragmentation during apoptosis. *J. Biol. Chem.*, 278, 37768–37776.
46. Roychoudhury, S., Nath, S., Song, H., et al. (2017) Human apurinic/apryrimidinic endonuclease (APE1) is acetylated at DNA damage sites in chromatin, and acetylation modulates its DNA repair activity. *Mol. Cell. Biol.*, 37, e00401–e00416.
47. Lirussi, L., Antoniali, G., Vascotto, C., et al. (2012) Nucleolar accumulation of APE1 depends on charged lysine residues that undergo acetylation upon genotoxic stress and modulate its BER activity in cells. *Mol. Biol. Cell*, 23, 4079–4096.
48. Burra, S., Marasco, D., Malfatti, M. C., Antoniali, G., Virgilio, A., Esposito, V., Demple, B., Galeone, A. and Tell, G. (2019) Human AP endonuclease (Ape1) activity on telomeric G4 structures is modulated by acetylable lysine residues in the N-terminal sequence. *DNA Repair (Amst.)*, 73, 129–143.
49. Sobol, R. W., Horton, J. K., Kühn, R., Gu, H., Singhal, R. K., Prasad, R., Rajewsky, K. and Wilson, S. H. (1996) Requirement of mammalian DNA polymerase-beta in base-excision repair. *Nature*, 379, 183–186.
50. Sung, J. S., DeMott, M. S. and Demple, B. (2005) Long-patch base excision DNA repair of 2-deoxyribonolactone prevents the formation of DNA-protein cross-links with DNA polymerase beta. *J. Biol. Chem.*, 280, 39095–39103.
51. Wilson, S. H. and Kunkel, T. A. (2000) Passing the baton in base excision repair. *Nat. Struct. Mol. Biol.*, 7, 176–178.

52. Almeida, K. H. and Sobol, R. W. (2007) A unified view of base excision repair: lesion-dependent protein complexes regulated by post-translational modification. *DNA Repair (Amst.)*, 6, 695–711.
53. Allinson, S. L., Sleeth, K. M., Matthewman, G. E. and Dianov, G. L. (2004) Orchestration of base excision repair by controlling the rates of enzymatic activities. *DNA Repair (Amst.)*, 3, 23–31.
54. Déry, U. and Masson, J. Y. (2007) Twists and turns in the function of DNA damage signaling and repair proteins by post-translational modifications. *DNA Repair (Amst.)*, 6, 561–577.
55. Fan, J. and Wilson, D. M., III. (2005) Protein-protein interactions and posttranslational modifications in mammalian base excision repair. *Free Radic. Biol. Med.*, 38, 1121–1138.
56. Vascotto, C., Fantini, D., Romanello, M., et al. (2009) APE1/Ref-1 interacts with NPM1 within nucleoli and plays a role in the rRNA quality control process. *Mol. Cell. Biol.*, 29, 1834–1854.
57. Khodyreva, S. N., Prasad, R., Ilina, E. S., Sukhanova, M. V., Kutuzov, M. M., Liu, Y., Hou, E. W., Wilson, S. H. and Lavrik, O. I. (2010) Apurinic/aprimidinic (AP) site recognition by the 5'-dRP/AP lyase in poly(ADP-ribose) polymerase-1 (PARP-1). *Proc. Natl. Acad. Sci. U. S. A.*, 107, 22090–22095.
58. Prasad, R., Dyrkheeva, N., Williams, J. and Wilson, S. H. (2015) Mammalian base excision repair: functional partnership between PARP-1 and APE1 in AP-site repair. *PLoS One*, 10, e0124269.
59. Alseth, I., Eide, L., Pirovano, M., Rognes, T., Seeberg, E. and Bjørås, M. (1999) The *Saccharomyces cerevisiae* homologues of endonuclease III from *Escherichia coli*, Ntg1 and Ntg2, are both required for efficient repair of spontaneous and induced oxidative DNA damage in yeast. *Mol. Cell. Biol.*, 19, 3779–3787.
60. Blaisdell, J. O. and Wallace, S. S. (2001) Abortive base-excision repair of radiation-induced clustered DNA lesions in *Escherichia coli*. *Proc. Natl. Acad. Sci. U. S. A.*, 98, 7426–7430.
61. Friedberg, E. C., Meira, L. B. and Cheo, D. L. (1997) Database of mouse strains carrying targeted mutations in genes affecting cellular responses to DNA damage. *Mutat. Res.*, 383, 183–188.
62. Gros, L., Ishchenko, A. A., Ide, H., Elder, R. H. and Saparbaev, M. K. (2004) The major human AP endonuclease (APE1) is involved in the nucleotide incision repair pathway. *Nucleic Acids Res.*, 32, 73–81.
63. Timofeyeva, N. A., Koval, V. V., Ishchenko, A. A., Saparbaev, M. K. and Fedorova, O. S. (2011) Lys98 substitution in human AP endonuclease 1 affects the kinetic mechanism of enzyme action in base excision and nucleotide incision repair pathways. *PLoS One*, 6, e24063.
64. Ishchenko, A. A., Deprez, E., Maksimenko, A., Brochon, J. C., Tauc, P. and Saparbaev, M. K. (2006) Uncoupling of the base excision and nucleotide incision repair pathways reveals their respective biological roles. *Proc. Natl. Acad. Sci. U. S. A.*, 103, 2564–2569.
65. Gelin, A., Redrejo-Rodríguez, M., Laval, J., Fedorova, O. S., Saparbaev, M. and Ishchenko, A. A. (2010) Genetic and biochemical characterization of human AP endonuclease 1 mutants deficient in nucleotide incision repair activity. *PLoS One*, 5, e12241.
66. Daviet, S., Couvé-Privat, S., Gros, L., Shinozuka, K., Ide, H., Saparbaev, M. and Ishchenko, A. A. (2007) Major oxidative products of cytosine are substrates for the nucleotide incision repair pathway. *DNA Repair (Amst.)*, 6, 8–18.
67. Redrejo-Rodríguez, M., Vigouroux, A., Mursalimov, A., et al. (2016) Structural comparison of AP endonucleases from the exonuclease III family reveals new amino acid residues in human AP endonuclease 1 that are involved in incision of damaged DNA. *Biochimie*, 128–129, 20–33.
68. Kim, K., Biade, S. and Matsumoto, Y. (1998) Involvement of flap endonuclease 1 in base excision DNA repair. *J. Biol. Chem.*, 273, 8842–8848.
69. Klungland, A. and Lindahl, T. (1997) Second pathway for completion of human DNA base excision-repair: reconstitution with purified proteins and requirement for DNase IV (FEN1). *EMBO J.*, 16, 3341–3348.
70. Ischenko, A. A. and Saparbaev, M. K. (2002) Alternative nucleotide incision repair pathway for oxidative DNA damage. *Nature*, 415, 183–187.
71. Ide, H., Tedzuka, K., Shimizu, H., Kimura, Y., Purmal, A. A., Wallace, S. S. and Kow, Y. W. (1994) Alpha-deoxyadenosine, a major anoxic radiolysis product of adenine in DNA, is a substrate for *Escherichia coli* endonuclease IV. *Biochemistry*, 33, 7842–7847.
72. Jorgensen, T. J., Furlong, E. A. and Henner, W. D. (1988) Gamma endonuclease of *Micrococcus luteus*: action on irradiated DNA. *Radiat. Res.*, 114, 556–566.
73. Lesiak, K. B. and Wheeler, K. T. (1990) Formation of alpha-deoxyadenosine in polydeoxynucleotides exposed to ionizing radiation under anoxic conditions. *Radiat. Res.*, 121, 328–337.
74. Dizdaroglu, M., Laval, J. and Boiteux, S. (1993) Substrate specificity of the *Escherichia coli* endonuclease III: excision of thymine- and cytosine-derived lesions in DNA produced by radiation-generated free radicals. *Biochemistry*, 32, 12105–12111.
75. Ishchenko, A. A., Ide, H., Ramotar, D., Nevinsky, G. and Saparbaev, M. (2004) Alpha-anomeric deoxynucleotides, anoxic products of ionizing radiation, are substrates for the endonuclease IV-type AP endonucleases. *Biochemistry*, 43, 15210–15216.
76. Abad, J. P. and Villasante, A. (1999) The 3' non-coding region of the *Drosophila melanogaster* HeT-A telomeric retrotransposon contains sequences with propensity to form G-quadruplex DNA. *FEBS Lett.*, 453, 59–62.
77. Moyzis, R. K., Buckingham, J. M., Cram, L. S., Dani, M., Deaven, L. L., Jones, M. D., Meyne, J., Ratliff, R. L. and Wu, J. R. (1988) A highly conserved repetitive DNA sequence, (TTAGGG)_n, present at the telomeres of human chromosomes. *Proc. Natl. Acad. Sci. U. S. A.*, 85, 6622–6626.
78. de Lange, T. (2005) Shelterin: the protein complex that shapes and safeguards human telomeres. *Genes Dev.*, 19, 2100–2110.
79. Oganessian, L. and Karlseder, J. (2009) Telomeric armor: the layers of end protection. *J. Cell Sci.*, 122, 4013–4025.
80. Huppert, J. L. (2008) Four-stranded nucleic acids: structure, function and targeting of G-quadruplexes. *Chem. Soc. Rev.*, 37, 1375–1384.
81. Fleming, A. M. and Burrows, C. J. (2013) G-quadruplex folds of the human telomere sequence alter the site reactivity and reaction pathway of guanine oxidation compared to duplex DNA. *Chem. Res. Toxicol.*, 26, 593–607.
82. Zhou, J., Liu, M., Fleming, A. M., Burrows, C. J. and Wallace, S. S. (2013) NEIL3 and NEIL1 DNA glycosylases remove oxidative damages from quadruplex DNA and exhibit preferences for lesions in the telomeric sequence context. *J. Biol. Chem.*, 288, 27263–27272.
83. Zhou, J., Fleming, A. M., Averill, A. M., Burrows, C. J. and Wallace, S. S. (2015) The NEIL glycosylases remove oxidized guanine lesions from telomeric and promoter quadruplex DNA structures. *Nucleic Acids Res.*, 43, 4039–4054.
84. Zhou, J., Chan, J., Lambelé, M., Yusufzai, T., Stumpff, J., Opresko, P. L., Thali, M. and Wallace, S. S. (2017) NEIL3 repairs telomere damage during S phase to secure chromosome segregation at mitosis. *Cell Rep.*, 20, 2044–2056.
85. Li, M., Yang, X., Lu, X., et al. (2018) APE1 deficiency promotes cellular senescence and premature aging features. *Nucleic Acids Res.*, 46, 5664–5677.
86. Madlener, S., Ströbel, T., Vose, S., Saydam, O., Price, B. D., Demple, B. and Saydam, N. (2013) Essential role for mammalian apurinic/aprimidinic (AP) endonuclease Ape1/Ref-1 in telomere maintenance. *Proc. Natl. Acad. Sci. U. S. A.*, 110, 17844–17849.
87. Stavnezer, J., Guikema, J. E. and Schrader, C. E. (2008) Mechanism and regulation of class switch recombination. *Annu. Rev. Immunol.*, 26, 261–292.
88. Masani, S., Han, L. and Yu, K. (2013) Apurinic/aprimidinic endonuclease 1 is the essential nuclease during immunoglobulin class switch recombination. *Mol. Cell. Biol.*, 33, 1468–1473.
89. Schrader, C. E., Guikema, J. E., Wu, X. and Stavnezer, J. (2009) The roles of APE1, APE2, DNA polymerase beta and mismatch repair in creating S region DNA breaks during antibody class switch. *Philos. Trans. R. Soc. Lond. B. Biol. Sci.*, 364, 645–652.
90. Guikema, J. E. J., Linehan, E. K., Tsuchimoto, D., Nakabeppu, Y., Strauss, P. R., Stavnezer, J. and Schrader, C. E. (2008) APE1- and APE2-dependent DNA breaks in immunoglobulin class switch recombination. *J. Exp. Med.*, 204, 3295–3295.

91. Akbari, M., Otterlei, M., Peña-Díaz, J., et al. (2004) Repair of U/G and U/A in DNA by UNG2-associated repair complexes takes place predominantly by short-patch repair both in proliferating and growth-arrested cells. *Nucleic Acids Res.*, 32, 5486–5498.
92. Vuong, B. Q., Herrick-Reynolds, K., Vaidyanathan, B., et al. (2013) A DNA break- and phosphorylation-dependent positive feedback loop promotes immunoglobulin class-switch recombination. *Nat. Immunol.*, 14, 1183–1189.
93. Vuong, B. Q. and Chaudhuri, J. (2012) Combinatorial mechanisms regulating AID-dependent DNA deamination: interacting proteins and post-translational modifications. *Semin. Immunol.*, 24, 264–272.
94. Xu, J., Husain, A., Hu, W., Honjo, T. and Kobayashi, M. (2014) APE1 is dispensable for S-region cleavage but required for its repair in class switch recombination. *Proc. Natl. Acad. Sci. U. S. A.*, 111, 17242–17247.
95. Islam, H., Kobayashi, M. and Honjo, T. (2019) Apurinic/apyrimidinic endonuclease 1 (APE1) is dispensable for activation-induced cytidine deaminase (AID)-dependent somatic hypermutation in the immunoglobulin gene. *Int. Immunol.*, 31, 543–554.
96. Gostissa, M., Alt, F. W. and Chiarle, R. (2011) Mechanisms that promote and suppress chromosomal translocations in lymphocytes. *Annu. Rev. Immunol.*, 29, 319–350.
97. Tell, G., Fantini, D. and Quadrioglio, F. (2010) Understanding different functions of mammalian AP endonuclease (APE1) as a promising tool for cancer treatment. *Cell. Mol. Life Sci.*, 67, 3589–3608.
98. Antoniali, G., Lirussi, L., D'Ambrosio, C., et al. (2014) SIRT1 gene expression upon genotoxic damage is regulated by APE1 through nCaRE-promoter elements. *Mol. Biol. Cell*, 25, 532–547.
99. Frossi, B., Antoniali, G., Yu, K., Akhtar, N., Kaplan, M. H., Kelley, M. R., Tell, G. and Pucillo, C. E. M. (2019) Endonuclease and redox activities of human apurinic/apyrimidinic endonuclease 1 have distinctive and essential functions in IgA class switch recombination. *J. Biol. Chem.*, 294, 5198–5207.
100. Fong, Y. W., Cattoglio, C. and Tjian, R. (2013) The intertwined roles of transcription and repair proteins. *Mol. Cell*, 52, 291–302.
101. Fleming, A. M., Ding, Y. and Burrows, C. J. (2017) Oxidative DNA damage is epigenetic by regulating gene transcription via base excision repair. *Proc. Natl. Acad. Sci. U. S. A.*, 114, 2604–2609.
102. Fleming, A. M. and Burrows, C. J. (2017) 8-Oxo-7,8-dihydroguanine, friend and foe: epigenetic-like regulator versus initiator of mutagenesis. *DNA Repair (Amst.)*, 56, 75–83.
103. Dizdaroglu, M. (2012) Oxidatively induced DNA damage: mechanisms, repair and disease. *Cancer Lett.*, 327, 26–47.
104. Kumar, S., Chinnusamy, V. and Mohapatra, T. (2018) Epigenetics of modified DNA bases: 5-methylcytosine and beyond. *Front. Genet.*, 9, 640.
105. Jena, N. R. and Mishra, P. C. (2005) Mechanisms of formation of 8-oxoguanine due to reactions of one and two OH* radicals and the H₂O₂ molecule with guanine: a quantum computational study. *J. Phys. Chem. B*, 109, 14205–14218.
106. Zarakowska, E., Gackowski, D., Foksinski, M. and Olinski, R. (2014) Are 8-oxoguanine (8-oxoGua) and 5-hydroxymethyluracil (5-hmUra) oxidatively damaged DNA bases or transcription (epigenetic) marks? *Mutat. Res. Genet. Toxicol. Environ. Mutagen.*, 764–765, 58–63.
107. Nakabeppu, Y., Tsuchimoto, D., Yamaguchi, H. and Sakumi, K. (2007) Oxidative damage in nucleic acids and Parkinson's disease. *J. Neurosci. Res.*, 85, 919–934.
108. Moreira, P. I., Nunomura, A., Nakamura, M., Takeda, A., Shenk, J. C., Aliev, G., Smith, M. A. and Perry, G. (2008) Nucleic acid oxidation in Alzheimer disease. *Free Radic. Biol. Med.*, 44, 1493–1505.
109. Sliwinski, A., Kwiatkowski, D., Czarny, P., et al. (2016) The levels of 7,8-dihydrodeoxyguanosine (8-oxoG) and 8-oxoguanine DNA glycosylase 1 (OGG1)—a potential diagnostic biomarkers of Alzheimer's disease. *J. Neurol. Sci.*, 368, 155–159.
110. Pan, L., Zhu, B., Hao, W., et al. (2016) Oxidized guanine base lesions function in 8-oxoguanine DNA glycosylase-1-mediated epigenetic regulation of nuclear factor κB-driven gene expression. *J. Biol. Chem.*, 291, 25553–25566.
111. Ba, X. and Boldogh, I. (2018) 8-Oxoguanine DNA glycosylase 1: beyond repair of the oxidatively modified base lesions. *Redox Biol.*, 14, 669–678.
112. Tornaletti, S. (2005) Transcription arrest at DNA damage sites. *Mutat. Res.*, 577, 131–145.
113. Allgayer, J., Kitsera, N., Bartelt, S., Epe, B. and Khobta, A. (2016) Widespread transcriptional gene inactivation initiated by a repair intermediate of 8-oxoguanine. *Nucleic Acids Res.*, 44, 7267–7280.
114. Ramon, O., Sauvaigo, S., Gasparutto, D., Faure, P., Favier, A. and Cadet, J. (1999) Effects of 8-oxo-7,8-dihydro-2'-deoxyguanosine on the binding of the transcription factor Sp1 to its cognate target DNA sequence (GC box). *Free Radic. Res.*, 31, 217–229.
115. Hailer-Morrison, M. K., Kotler, J. M., Martin, B. D. and Sugden, K. D. (2003) Oxidized guanine lesions as modulators of gene transcription. Altered p50 binding affinity and repair shielding by 7,8-dihydro-8-oxo-2'-deoxyguanosine lesions in the NF-κappaB promoter element. *Biochemistry*, 42, 9761–9770.
116. Moore, S. P., Toomire, K. J. and Strauss, P. R. (2013) DNA modifications repaired by base excision repair are epigenetic. *DNA Repair (Amst.)*, 12, 1152–1158.
117. Perillo, B., Ombra, M. N., Berton, A., et al. (2008) DNA oxidation as triggered by H3K9me2 demethylation drives estrogen-induced gene expression. *Science*, 319, 202–206.
118. Pastukh, V., Roberts, J. T., Clark, D. W., Bardwell, G. C., Patel, M., Al-Mehdi, A. B., Borchert, G. M. and Gillespie, M. N. (2015) An oxidative DNA “damage” and repair mechanism localized in the VEGF promoter is important for hypoxia-induced VEGF mRNA expression. *Am. J. Physiol. Lung Cell. Mol. Physiol.*, 309, L1367–L1375.
119. Fleming, A. M., Zhu, J., Ding, Y. and Burrows, C. J. (2017) 8-Oxo-7,8-dihydroguanine in the context of a gene promoter G-quadruplex is an on-off switch for transcription. *ACS Chem. Biol.*, 12, 2417–2426.
120. Pan, L., Hao, W., Zheng, X., Zeng, X., Ahmed Abbasi, A., Boldogh, I. and Ba, X. (2017) OGG1–DNA interactions facilitate NF-κB binding to DNA targets. *Sci. Rep.*, 7, 43297.
121. Mabley, J. G., Pacher, P., Deb, A., Wallace, R., Elder, R. H. and Szabó, C. (2005) Potential role for 8-oxoguanine DNA glycosylase in regulating inflammation. *FASEB J.*, 19, 290–292.
122. Li, G., Yuan, K., Yan, C., et al. (2012) 8-Oxoguanine-DNA glycosylase 1 deficiency modifies allergic airway inflammation by regulating STAT6 and IL-4 in cells and in mice. *Free Radic. Biol. Med.*, 52, 392–401.
123. Fleming, A. M., Zhu, J., Ding, Y., Esders, S. and Burrows, C. J. (2019) Oxidative modification of guanine in a potential Z-DNA-forming sequence of a gene promoter impacts gene expression. *Chem. Res. Toxicol.*, 32, 899–909.
124. Zhu, J., Fleming, A. M. and Burrows, C. J. (2018) The RAD17 promoter sequence contains a potential tail-dependent G-quadruplex that downregulates gene expression upon oxidative modification. *ACS Chem. Biol.*, 13, 2577–2584.
125. Redstone, S. C. J., Fleming, A. M. and Burrows, C. J. (2019) Oxidative modification of the potential G-quadruplex sequence in the PCNA gene promoter can turn on transcription. *Chem. Res. Toxicol.*, 32, 437–446.
126. Fleming, A. M., Zhu, J., Howpay Manage, S. A., and Burrows, C. J. (2019) Human NEIL3 gene expression regulated by epigenetic-like oxidative DNA modification. *J. Am. Chem. Soc.*, 141, 11036–11049.
127. Fleming, A. M., Zhu, J., Ding, Y., Visser, J. A., Zhu, J. and Burrows, C. J. (2018) Human DNA repair genes possess potential G-quadruplex sequences in their promoters and 5'-untranslated regions. *Biochemistry*, 57, 991–1002.
128. Gautier, C. (2000) Compositional bias in DNA. *Curr. Opin. Genet. Dev.*, 10, 656–661.
129. Forneris, F., Binda, C., Vanoni, M. A., Mattevi, A. and Battaglioli, E. (2005) Histone demethylation catalysed by LSD1 is a flavin-dependent oxidative process. *FEBS Lett.*, 579, 2203–2207.
130. Boldogh, I., Hajas, G., Aguilera-Aguirre, L., Hegde, M. L., Radak, Z., Bacs, A., Sur, S., Hazra, T. K. and Mitra, S. (2012) Activation of ras

- signaling pathway by 8-oxoguanine DNA glycosylase bound to its excision product, 8-oxoguanine. *J. Biol. Chem.*, 287, 20769–20773.
131. Vohhodina, J., Harkin, D. P. and Savage, K. I. (2016) Dual roles of DNA repair enzymes in RNA biology/post-transcriptional control. *Wiley Interdiscip. Rev. RNA*, 7, 604–619.
 132. Jobert, L. and Nilsen, H. (2014) Regulatory mechanisms of RNA function: emerging roles of DNA repair enzymes. *Cell. Mol. Life Sci.*, 71, 2451–2465.
 133. Antoniali, G., Malfatti, M. C. and Tell, G. (2017) Unveiling the non-repair face of the base excision repair pathway in RNA processing: a missing link between DNA repair and gene expression? *DNA Repair (Amst)*, 56, 65–74.
 134. Tell, G., Wilson, D. M., III and Lee, C. H. (2010) Intrusion of a DNA repair protein in the RNome world: is this the beginning of a new era? *Mol. Cell. Biol.*, 30, 366–371.
 135. Poletto, M., Vascotto, C., Scognamiglio, P. L., Lirussi, L., Marasco, D. and Tell, G. (2013) Role of the unstructured N-terminal domain of the hAPE1 (human apurinic/aprimidinic endonuclease 1) in the modulation of its interaction with nucleic acids and NPM1 (nucleophosmin). *Biochem. J.*, 452, 545–557.
 136. Chohan, M., Mackedenski, S., Li, W. M. and Lee, C. H. (2015) Human apurinic/aprimidinic endonuclease 1 (APE1) has 3' RNA phosphatase and 3' exoribonuclease activities. *J. Mol. Biol.*, 427, 298–311.
 137. Zhang, C. and Peng, G. (2015) Non-coding RNAs: an emerging player in DNA damage response. *Mutat. Res. Rev. Mutat. Res.*, 763, 202–211.
 138. D'Adda di Fagnana, F. (2014) A direct role for small non-coding RNAs in DNA damage response. *Trends Cell Biol.*, 24, 171–178.
 139. Su, M., Wang, H., Wang, W., Wang, Y., Ouyang, L., Pan, C., Xia, L., Cao, D. and Liao, Q. (2018) LncRNAs in DNA damage response and repair in cancer cells. *Acta Biochim. Biophys. Sin. (Shanghai)*, 50, 433–439.
 140. Poletto, M., Lirussi, L., Wilson, D. M., III and Tell, G. (2014) Nucleophosmin modulates stability, activity, and nucleolar accumulation of base excision repair proteins. *Mol. Biol. Cell*, 25, 1641–1652.
 141. Di Maso, V., Avellini, C., Crocè, L. S., et al. (2007) Subcellular localization of APE1/Ref-1 in human hepatocellular carcinoma: possible prognostic significance. *Mol. Med.*, 13, 89–96.
 142. Nunomura, A., Moreira, P. I., Castellani, R. J., Lee, H. G., Zhu, X., Smith, M. A. and Perry, G. (2012) Oxidative damage to RNA in aging and neurodegenerative disorders. *Neurotox. Res.*, 22, 231–248.
 143. Förstemann, K. and Lingner, J. (2005) Telomerase limits the extent of base pairing between template RNA and telomeric DNA. *EMBO Rep.*, 6, 361–366.
 144. Kahl, G. (2015) *DNA–RNA hybrid. The Dictionary of Genomics, Transcriptomics and Proteomics*. The Dictionary of Genomics, Transcriptomics and Proteomics Science, pp. 1–1.
 145. Hamperl, S. and Cimprich, K. A. (2014) The contribution of co-transcriptional RNA:DNA hybrid structures to DNA damage and genome instability. *DNA Repair (Amst)*, 19, 84–94.
 146. Brambati, A., Colosio, A., Zardoni, L., Galanti, L. and Liberi, G. (2015) Replication and transcription on a collision course: eukaryotic regulation mechanisms and implications for DNA stability. *Front. Genet.*, 6, 166.
 147. Sassa, A., Yasui, M., and Honma, M. (2019) Current perspectives on mechanisms of ribonucleotide incorporation and processing in mammalian DNA. *Genes Environ.*, 41, 3.
 148. Williams, J. S. and Kunkel, T. A. (2014) Ribonucleotides in DNA: origins, repair and consequences. *DNA Repair (Amst)*, 19, 27–37.
 149. Koh, K. D., Balachander, S., Hesselberth, J. R. and Storici, F. (2015) Ribose-seq: global mapping of ribonucleotides embedded in genomic DNA. *Nat. Methods*, 12, 251–257.
 150. Hovatter, K. R. and Martinson, H. G. (1987) Ribonucleotide-induced helical alteration in DNA prevents nucleosome formation. *Proc. Natl. Acad. Sci. U. S. A.*, 84, 1162–1166.
 151. Potenski, C. J. and Klein, H. L. (2014) How the misincorporation of ribonucleotides into genomic DNA can be both harmful and helpful to cells. *Nucleic Acids Res.*, 42, 10226–10234.
 152. Kind, B., Wolf, C., Engel, K., Rapp, A., Cristina Cardoso, M. and Lee-Kirsch, M. A. (2018) Single cell gel electrophoresis for the detection of genomic ribonucleotides. *Methods Mol. Biol.*, 1672, 311–318.
 153. Meroni, A., Nava, G. M., Sertic, S., Plevani, P., Muzi-Falconi, M. and Lazzaro, F. (2018) Measuring the levels of ribonucleotides embedded in genomic DNA. *Methods Mol. Biol.*, 1672, 319–327.
 154. Li, Z., Zhang, H. X., Li, Y., et al. (2019) Method for quantification of ribonucleotides and deoxyribonucleotides in human cells using (trimethylsilyl)diazomethane derivatization followed by liquid chromatography-tandem mass spectrometry. *Anal. Chem.*, 91, 1019–1026.
 155. Zhou, Z.-X., Williams, J. S. and Kunkel, T. A. (2018) Studying ribonucleotide incorporation: strand-specific detection of ribonucleotides in the yeast genome and measuring ribonucleotide-induced mutagenesis. *J. Vis. Exp.*, 58020.
 156. Jinks-Robertson, S. and Klein, H. L. (2015) Ribonucleotides in DNA: hidden in plain sight. *Nat. Struct. Mol. Biol.*, 22, 176–178.
 157. Gombolay, A. L., Vannberg, F. O. and Storici, F. (2019) Ribose-Map: a bioinformatics toolkit to map ribonucleotides embedded in genomic DNA. *Nucleic Acids Res.*, 47, e5.
 158. Clausen, A. R., Lujan, S. A., Burkholder, A. B., et al. (2015) Tracking replication enzymology in vivo by genome-wide mapping of ribonucleotide incorporation. *Nat. Struct. Mol. Biol.*, 22, 185–191.
 159. Daigaku, Y., Keszthelyi, A., Müller, C. A., Miyabe, I., Brooks, T., Retkute, R., Hubank, M., Nieduszynski, C. A. and Carr, A. M. (2015) A global profile of replicative polymerase usage. *Nat. Struct. Mol. Biol.*, 22, 192–198.
 160. Reijns, M. A., Rabe, B., Rigby, R. E., et al. (2012) Enzymatic removal of ribonucleotides from DNA is essential for mammalian genome integrity and development. *Cell*, 149, 1008–1022.
 161. Nick McElhinny, S. A., Kumar, D., Clark, A. B., Watt, D. L., Watts, B. E., Lundström, E. B., Johansson, E., Chabes, A. and Kunkel, T. A. (2010) Genome instability due to ribonucleotide incorporation into DNA. *Nat. Chem. Biol.*, 6, 774–781.
 162. Joyce, C. M. (1997) Choosing the right sugar: how polymerases select a nucleotide substrate. *Proc. Natl. Acad. Sci. U. S. A.*, 94, 1619–1622.
 163. Brown, J. A. and Suo, Z. (2011) Unlocking the sugar “steric gate” of DNA polymerases. *Biochemistry*, 50, 1135–1142.
 164. Nick McElhinny, S. A., Watts, B. E., Kumar, D., Watt, D. L., Lundström, E. B., Burgers, P. M., Johansson, E., Chabes, A. and Kunkel, T. A. (2010) Abundant ribonucleotide incorporation into DNA by yeast replicative polymerases. *Proc. Natl. Acad. Sci. U. S. A.*, 107, 4949–4954.
 165. Marasco, M., Li, W., Lynch, M. and Pikaard, C. S. (2017) Catalytic properties of RNA polymerases IV and V: accuracy, nucleotide incorporation and rNTP/dNTP discrimination. *Nucleic Acids Res.*, 45, 11315–11326.
 166. Vaisman, A. and Woodgate, R. (2018) Ribonucleotide discrimination by translesion synthesis DNA polymerases. *Crit. Rev. Biochem. Mol. Biol.*, 53, 382–402.
 167. Clausen, A. R., Zhang, S., Burgers, P. M., Lee, M. Y. and Kunkel, T. A. (2013) Ribonucleotide incorporation, proofreading and bypass by human DNA polymerase δ . *DNA Repair (Amst)*, 12, 121–127.
 168. Rossi, M. L. and Bambara, R. A. (2006) Reconstituted Okazaki fragment processing indicates two pathways of primer removal. *J. Biol. Chem.*, 281, 26051–26061.
 169. Chiu, H. C., Koh, K. D., Evich, M., Lesiak, A. L., Germann, M. W., Bongiorno, A., Riedo, E. and Storici, F. (2014) RNA intrusions change DNA elastic properties and structure. *Nanoscale*, 6, 10009–10017.
 170. Koh, K. D., Chiu, H. C., Riedo, E. and Storici, F. (2015) Measuring the elasticity of ribonucleotide(s)-containing DNA molecules using AFM. *Methods Mol. Biol.*, 1297, 43–57.
 171. Evich, M., Spring-Connell, A. M., Storici, F. and Germann, M. W. (2016) Structural impact of single ribonucleotide residues in DNA. *ChemBiochem*, 17, 1968–1977.
 172. Klein, H. L. (2017) Genome instabilities arising from ribonucleotides in DNA. *DNA Repair (Amst)*, 56, 26–32.

173. Fu, I., Smith, D. J. and Broyde, S. (2019) Rotational and translational positions determine the structural and dynamic impact of a single ribonucleotide incorporated in the nucleosome. *DNA Repair (Amst.)*, 73, 155–163.
174. Meroni, A., Mentegari, E., Crespan, E., Muzi-Falconi, M., Lazzaro, F. and Podestà, A. (2017) The incorporation of ribonucleotides induces structural and conformational changes in DNA. *Biophys. J.*, 113, 1373–1382.
175. Sparks, J. L., Chon, H., Cerritelli, S. M., Kunkel, T. A., Johansson, E., Crouch, R. J. and Burgers, P. M. (2012) RNase H2-initiated ribonucleotide excision repair. *Mol. Cell*, 47, 980–986.
176. Rydberg, B. and Game, J. (2002) Excision of misincorporated ribonucleotides in DNA by RNase H (type 2) and FEN-1 in cell-free extracts. *Proc. Natl. Acad. Sci. U. S. A.*, 99, 16654–16659.
177. Hiller, B., Achleitner, M., Glage, S., Naumann, R., Behrendt, R. and Roers, A. (2012) Mammalian RNase H2 removes ribonucleotides from DNA to maintain genome integrity. *J. Exp. Med.*, 209, 1419–1426.
178. Cerritelli, S. M. and Crouch, R. J. (2009) Ribonuclease H: the enzymes in eukaryotes. *FEBS J.*, 276, 1494–1505.
179. Lazzaro, F., Novarina, D., Amara, F., et al. (2012) RNase H and postreplication repair protect cells from ribonucleotides incorporated in DNA. *Mol. Cell*, 45, 99–110.
180. Pizzi, S., Sertic, S., Orcesi, S., Cereda, C., Bianchi, M., Jackson, A. P., Lazzaro, F., Plevani, P. and Muzi-Falconi, M. (2015) Reduction of hRNase H2 activity in Aicardi-Goutières syndrome cells leads to replication stress and genome instability. *Hum. Mol. Genet.*, 24, 649–658.
181. Crow, Y. J., Leitch, A., Hayward, B. E., et al. (2006) Mutations in genes encoding ribonuclease H2 subunits cause Aicardi-Goutières syndrome and mimic congenital viral brain infection. *Nat. Genet.*, 38, 910–916.
182. Rabe, B. (2013) Aicardi-Goutières syndrome: clues from the RNase H2 knock-out mouse. *J. Mol. Med. (Berl.)*, 91, 1235–1240.
183. Brzostek-Racine, S., Gordon, C., Van Scoy, S. and Reich, N. C. (2011) The DNA damage response induces IFN. *J. Immunol.*, 187, 5336–5345.
184. Tsukiasahi, M., Baba, M., Kojima, K., Himeda, K., Takita, T. and Yasukawa, K. (2019) Construction and characterization of ribonuclease H2 knockout NIH3T3 cells. *J. Biochem.*, 165, 249–256.
185. Uehara, R., Cerritelli, S. M., Hasin, N., Sakhuja, K., London, M., Iranzo, J., Chon, H., Grinberg, A. and Crouch, R. J. (2018) Two RNase H2 mutants with differential rNMP processing activity reveal a threshold of ribonucleotide tolerance for embryonic development. *Cell Rep.*, 25, 1135–1145.e5.
186. Mottaghi-Dastjerdi, N., Soltany-Rezaee-Rad, M., Sepehrizadeh, Z., Roshandel, G., Ebrahimifard, F. and Setayesh, N. (2015) Identification of novel genes involved in gastric carcinogenesis by suppression subtractive hybridization. *Hum. Exp. Toxicol.*, 34, 3–11.
187. Aden, K., Bartsch, K., Dahl, J., et al. (2019) Epithelial RNase H2 maintains genome integrity and prevents intestinal tumorigenesis in mice. *Gastroenterology*, 156, 145.e19–159.e19.
188. Hiller, B., Hoppe, A., Haase, C., et al. (2018) Ribonucleotide excision repair is essential to prevent squamous cell carcinoma of the skin. *Cancer Res.*, 78, 5917–5926.
189. Sayrac, S., Vengrova, S., Godfrey, E. L. and Dalgaard, J. Z. (2011) Identification of a novel type of spacer element required for imprinting in fission yeast. *PLoS Genet.*, 7, e1001328.
190. Brown, J. A., Fiala, K. A., Fowler, J. D., Sherrer, S. M., Newmister, S. A., Duym, W. W. and Suo, Z. (2010) A novel mechanism of sugar selection utilized by a human X-family DNA polymerase. *J. Mol. Biol.*, 395, 282–290.
191. Ruiz, J. F., Juárez, R., García-Díaz, M., Terrados, G., Picher, A. J., González-Barrera, S., Fernández de Henestrosa, A. R. and Blanco, L. (2003) Lack of sugar discrimination by human Pol mu requires a single glycine residue. *Nucleic Acids Res.*, 31, 4441–4449.
192. Martin, M. J., Garcia-Ortiz, M. V., Esteban, V. and Blanco, L. (2013) Ribonucleotides and manganese ions improve non-homologous end joining by human Polμ. *Nucleic Acids Res.*, 41, 2428–2436.
193. Nick McElhinny, S. A. and Ramsden, D. A. (2003) Polymerase mu is a DNA-directed DNA/RNA polymerase. *Mol. Cell. Biol.*, 23, 2309–2315.
194. Lujan, S. A., Williams, J. S., Clausen, A. R., Clark, A. B. and Kunkel, T. A. (2013) Ribonucleotides are signals for mismatch repair of leading-strand replication errors. *Mol. Cell*, 50, 437–443.
195. Storici, F., Bebenek, K., Kunkel, T. A., Gordenin, D. A. and Resnick, M. A. (2007) RNA-templated DNA repair. *Nature*, 447, 338–341.
196. Shen, Y., Nandi, P., Taylor, M. B., Stuckey, S., Bhadsavle, H. P., Weiss, B. and Storici, F. (2011) RNA-driven genetic changes in bacteria and in human cells. *Mutat. Res.*, 717, 91–98.
197. Shen, Y., Koh, K. D., Weiss, B. and Storici, F. (2011) Mismatched rNMPs in DNA are mutagenic and are targets of mismatch repair and RNases H. *Nat. Struct. Mol. Biol.*, 19, 98–104.
198. Williams, J. S., Lujan, S. A. and Kunkel, T. A. (2016) Processing ribonucleotides incorporated during eukaryotic DNA replication. *Nat. Rev. Mol. Cell Biol.*, 17, 350–363.
199. Williams, J. S., Smith, D. J., Marjavaara, L., Lujan, S. A., Chabes, A. and Kunkel, T. A. (2013) Topoisomerase 1-mediated removal of ribonucleotides from nascent leading-strand DNA. *Mol. Cell*, 49, 1010–1015.
200. Capranico, G., Marinello, J. and Chillemi, G. (2017) Type I DNA topoisomerases. *J. Med. Chem.*, 60, 2169–2192.
201. Cho, J. E. and Jinks-Robertson, S. (2018) Topoisomerase I and genome stability: the good and the bad. *Methods Mol. Biol.*, 1703, 21–45.
202. Williams, J. S. and Kunkel, T. A. (2018) Studying topoisomerase 1-mediated damage at genomic ribonucleotides. *Methods Mol. Biol.*, 1703, 241–257.
203. Sekiguchi, J. and Shuman, S. (1997) Site-specific ribonuclease activity of eukaryotic DNA topoisomerase I. *Mol. Cell*, 1, 89–97.
204. Potenski, C. J., Niu, H., Sung, P. and Klein, H. L. (2014) Avoidance of ribonucleotide-induced mutations by RNase H2 and Srs2-Exo1 mechanisms. *Nature*, 511, 251–254.
205. Kim, N., Huang, S. N., Williams, J. S., Li, Y. C., Clark, A. B., Cho, J. E., Kunkel, T. A., Pommier, Y. and Jinks-Robertson, S. (2011) Mutagenic processing of ribonucleotides in DNA by yeast topoisomerase I. *Science*, 332, 1561–1564.
206. Li, F., Wang, Q., Seol, J. H., Che, J., Lu, X., Shim, E. Y., Lee, S. E. and Niu, H. (2019) Apn2 resolves blocked 3' ends and suppresses Top1-induced mutagenesis at genomic rNMP sites. *Nat. Struct. Mol. Biol.*, 26, 155–163.
207. Zimmermann, M., Murina, O., Reijns, M. A. M., et al. (2018) CRISPR screens identify genomic ribonucleotides as a source of PARP-trapping lesions. *Nature*, 559, 285–289.
208. Lindsey-Boltz, L. A., Kemp, M. G., Hu, J. and Sancar, A. (2015) Analysis of ribonucleotide removal from DNA by human nucleotide excision repair. *J. Biol. Chem.*, 290, 29801–29807.
209. Reardon, J. T. and Sancar, A. (2005) Nucleotide excision repair. *Prog. Nucleic Acid Res. Mol. Biol.*, 79, 183–235.
210. Vaisman, A., McDonald, J. P., Huston, D., Kuban, W., Liu, L., Van Houten, B. and Woodgate, R. (2013) Removal of misincorporated ribonucleotides from prokaryotic genomes: an unexpected role for nucleotide excision repair. *PLoS Genet.*, 9, e1003878.
211. Cai, Y., Geacintov, N. E. and Broyde, S. (2014) Ribonucleotides as nucleotide excision repair substrates. *DNA Repair (Amst.)*, 13, 55–60.
212. Randerath, K., Reddy, R., Danna, T. F., Watson, W. P., Crane, A. E. and Randerath, E. (1992) Formation of ribonucleotides in DNA modified by oxidative damage in vitro and in vivo. Characterization by 32P-postlabeling. *Mutat. Res.*, 275, 355–366.
213. Kuznetsov, N. A., Koval, V. V., Zharkov, D. O., Nevinsky, G. A., Douglas, K. T. and Fedorova, O. S. (2005) Kinetics of substrate recognition and cleavage by human 8-oxoguanine-DNA glycosylase. *Nucleic Acids Res.*, 33, 3919–3931.
214. Yamagata, Y. (2011) Structural basis for the recognition and removal of damaged bases from DNA by a DNA repair enzyme, 3-methyladenine DNA glycosylase from *Escherichia coli*. *Nihon Kessho Gakkaishi*, 39, 303–308.
215. Fromme, J. C., Bruner, S. D., Yang, W., Karplus, M. and Verdine, G. L. (2003) Product-assisted catalysis in base-excision DNA repair. *Nat. Struct. Biol.*, 10, 204–211.

216. Malfatti, M. C., Henneke, G., Balachander, S., Koh, K. D., Newnam, G., Uehara, R., Crouch, R. J., Storici, F. and Tell, G. (2019) Unlike the *Escherichia coli* counterpart, archaeal RNase H1 cannot process ribose monophosphate abasic sites and oxidized ribonucleotides embedded in DNA. *J. Biol. Chem.*, 294, 13061–13072.
217. Berglund, A. K., Navarrete, C., Engqvist, M. K., Hoberg, E., Szilagyi, Z., Taylor, R. W., Gustafsson, C. M., Falkenberg, M. and Clausen, A. R. (2017) Nucleotide pools dictate the identity and frequency of ribonucleotide incorporation in mitochondrial DNA. *PLoS Genet.*, 13, e1006628.
218. Kreisel, K., Engqvist, M. K. M. and Clausen, A. R. (2017) Simultaneous mapping and quantitation of ribonucleotides in human mitochondrial DNA. *J. Vis. Exp.*, 56551.
219. Moss, C. F., Dalla Rosa, I., Hunt, L. E., et al. (2017) Aberrant ribonucleotide incorporation and multiple deletions in mitochondrial DNA of the murine MPV17 disease model. *Nucleic Acids Res.*, 45, 12808–12815.
220. Forslund, J. M. E., Pfeiffer, A., Stojković, G., Wanrooij, P. H. and Wanrooij, S. (2018) The presence of rNTPs decreases the speed of mitochondrial DNA replication. *PLoS Genet.*, 14, e1007315.
221. Wanrooij, P. H., Engqvist, M. K. M., Forslund, J. M. E., Navarrete, C., Nilsson, A. K., Sedman, J., Wanrooij, S., Clausen, A. R. and Chabes, A. (2017) Ribonucleotides incorporated by the yeast mitochondrial DNA polymerase are not repaired. *Proc. Natl. Acad. Sci. U. S. A.*, 114, 12466–12471.
222. Leguisamo, N. M., Gloria, H. C., Kalil, A. N., Martins, T. V., Azambuja, D. B., Meira, L. B. and Saffi, J. (2017) Base excision repair imbalance in colorectal cancer has prognostic value and modulates response to chemotherapy. *Oncotarget*, 8, 54199–54214.
223. Shah, F., Logsdon, D., Messmann, R. A., Fehrenbacher, J. C., Fishel, M. L. and Kelley, M. R. (2018) Exploiting the Ref-1-APE1 node in cancer signaling and other diseases: from bench to clinic. *npj Precis. Oncol.*, 1.
224. Yuan, C. L., He, F., Ye, J. Z., et al. (2017) APE1 overexpression is associated with poor survival in patients with solid tumors: a meta-analysis. *Oncotarget*, 8, 59720–59728.
225. Kumar, M., Shukla, V. K., Misra, P. K. and Raman, M. J. (2018) Dysregulated expression and subcellular localization of base excision repair (BER) pathway enzymes in gallbladder cancer. *Int. J. Mol. Cell. Med.*, 7, 119–132.
226. Di Maso, V., Mediavilla, M. G., Vascotto, C., Lupo, F., Baccarani, U., Avellini, C., Tell, G., Tiribelli, C. and Crocè, L. S. (2015) Transcriptional up-regulation of APE1/Ref-1 in hepatic tumor: role in hepatocytes resistance to oxidative stress and apoptosis. *PLoS One*, 10, e0143289.
227. Sun, Z., Zhu, Y., Aminbuhe, Fan, Q., Peng, J. and Zhang, N. (2018) Differential expression of APE1 in hepatocellular carcinoma and the effects on proliferation and apoptosis of cancer cells. *Biosci. Trends*, 12, 456–462.
228. Jiang, Y., Zhou, S., Sandusky, G. E., Kelley, M. R. and Fishel, M. L. (2010) Reduced expression of DNA repair and redox signaling protein APE1/Ref-1 impairs human pancreatic cancer cell survival, proliferation, and cell cycle progression. *Cancer Invest.*, 28, 885–895.
229. Juhnke, M., Heumann, A., Chirico, V., et al. (2017) Apurinic/apyrimidinic endonuclease 1 (APE1/Ref-1) overexpression is an independent prognostic marker in prostate cancer without TMPRSS2:ERG fusion. *Mol. Carcinog.*, 56, 2135–2145.
230. Hong, J., Chen, Z., Peng, D., Zaika, A., Revetta, F., Washington, M. K., Belkhir, A. and El-Rifai, W. (2016) APE1-mediated DNA damage repair provides survival advantage for esophageal adenocarcinoma cells in response to acidic bile salts. *Oncotarget*, 7, 16688–16702.
231. Qing, Y., Li, Q., Ren, T., et al. (2015) Upregulation of PD-L1 and APE1 is associated with tumorigenesis and poor prognosis of gastric cancer. *Drug Des. Devel. Ther.*, 9, 901–909.
232. Silva, L. P., Santana, T., Sedassari, B. T., de Sousa, S. M., Sobral, A. P. V., Freitas, R. A., Barboza, C. A. G. and de Souza, L. B. (2017) Apurinic/apyrimidinic endonuclease 1 (APE1) is overexpressed in malignant transformation of salivary gland pleomorphic adenoma. *Eur. Arch. Otorhinolaryngol.*, 274, 3203–3209.
233. Yang, X., Peng, Y., Jiang, X., et al. (2018) The regulatory role of APE1 in epithelial-to-mesenchymal transition and in determining EGFR-TKI responsiveness in non-small-cell lung cancer. *Cancer Med.*, 7, 4406–4419.
234. Wen, X., Lu, R., Xie, S., Zheng, H., Wang, H., Wang, Y., Sun, J., Gao, X. and Guo, L. (2016) APE1 overexpression promotes the progression of ovarian cancer and serves as a potential therapeutic target. *Cancer Biomark.*, 17, 313–322.
235. Sheng, Q., Zhang, Y., Wang, R., Zhang, J., Chen, B., Wang, J., Zhang, W. and Xin, X. (2012) Prognostic significance of APE1 cytoplasmic localization in human epithelial ovarian cancer. *Med. Oncol.*, 29, 1265–1271.
236. Kakolyris, S., Kaklamanis, L., Engels, K., Turley, H., Hickson, I. D., Gatter, K. C. and Harris, A. L. (1997) Human apurinic endonuclease 1 expression in a colorectal adenoma-carcinoma sequence. *Cancer Res.*, 57, 1794–1797.
237. Lou, D., Zhu, L., Ding, H., Dai, H. Y. and Zou, G. M. (2014) Aberrant expression of redox protein Ape1 in colon cancer stem cells. *Oncol. Lett.*, 7, 1078–1082.
238. Noike, T., Miwa, S., Soeda, J., Kobayashi, A. and Miyagawa, S. (2008) Increased expression of thioredoxin-1, vascular endothelial growth factor, and redox factor-1 is associated with poor prognosis in patients with liver metastasis from colorectal cancer. *Hum. Pathol.*, 39, 201–208.
239. Chen, T., Liu, C., Lu, H., Yin, M., Shao, C., Hu, X., Wu, J. and Wang, Y. (2017) The expression of APE1 in triple-negative breast cancer and its effect on drug sensitivity of olaparib. *Tumour Biol.*, 39, 1010428317713390.
240. Abdel-Fatah, T. M., Perry, C., Moseley, P., Johnson, K., Arora, A., Chan, S., Ellis, I. O. and Madhusudan, S. (2014) Clinicopathological significance of human apurinic/apyrimidinic endonuclease 1 (APE1) expression in oestrogen-receptor-positive breast cancer. *Breast Cancer Res. Treat.*, 143, 411–421.
241. Wang, Q., Xiao, H., Luo, Q., Li, M., Wei, S., Zhu, X., Xiao, H. and Chen, L. (2016) Low APE1/Ref-1 expression significantly correlates with MGMT promoter methylation in patients with high-grade gliomas. *Int. J. Clin. Exp. Pathol.*, 9, 9562–9568.
242. Hudson, A. L., Parker, N. R., Khong, P., et al. (2018) Glioblastoma recurrence correlates with increased APE1 and polarization toward an immuno-suppressive microenvironment. *Front. Oncol.*, 8, 314.
243. Sengupta, S., Mantha, A. K., Song, H., Roychoudhury, S., Nath, S., Ray, S. and Bhakat, K. K. (2016) Elevated level of acetylation of APE1 in tumor cells modulates DNA damage repair. *Oncotarget*, 7, 75197–75209.
244. Marasco, D., Tell, G., Poletto, M., Damante, G., Loreto, C. Di., Poletto, E. and Puglisi, F. (2012) Acetylation on critical lysine residues of apurinic/apyrimidinic endonuclease 1 (APE1) in triple-negative breast cancers. *Biochem. Biophys. Res. Commun.*, 424, 34–39.
245. Ding, J., Fishel, M. L., Reed, A. M., McAdams, E., Czader, M. B., Cardoso, A. A. and Kelley, M. R. (2017) Ref-1/APE1 as a transcriptional regulator and novel therapeutic target in pediatric T-cell leukemia. *Mol. Cancer Ther.*, 16, 1401–1411.
246. Poletto, M., Malfatti, M. C., Dorjsuren, D., et al. (2016) Inhibitors of the apurinic/apyrimidinic endonuclease 1 (APE1)/nucleophosmin (NPM1) interaction that display anti-tumor properties. *Mol. Carcinog.*, 55, 688–704.
247. Fan, X., Wen, L., Li, Y., Lou, L., Liu, W. and Zhang, J. (2017) The expression profile and prognostic value of APE/Ref-1 and NPM1 in high-grade serous ovarian adenocarcinoma. *APMIS*, 125, 857–862.
248. Kalitin, N. N., Chernykh, Y. B. and Buravtsova, I. V. (2017) Comparative analysis of quantitative parameters of expression of the retinoic acid nuclear receptor RARα gene and APE1/YB-1/MDR1 pattern genes in patients with newly detected multiple myeloma. *Bull. Exp. Biol. Med.*, 164, 90–94.
249. Fishel, M. L., Colvin, E. S., Luo, M., Kelley, M. R. and Robertson, K. A. (2010) Inhibition of the redox function of APE1/Ref-1 in myeloid leu-

- kemia cell lines results in a hypersensitive response to retinoic acid-induced differentiation and apoptosis. *Exp. Hematol.*, 38, 1178–1188.
250. Abbotts, R., Jewell, R., Nsengimana, J., et al. (2014) Targeting human apurinic/apyrimidinic endonuclease 1 (APE1) in phosphatase and tensin homolog (PTEN) deficient melanoma cells for personalized therapy. *Oncotarget*, 5, 3273–3286.
 251. Liang, W., Wei, X., Li, Q., et al. (2017) MicroRNA-765 enhances the anti-angiogenic effect of CDDP via APE1 in osteosarcoma. *J. Cancer*, 8, 1542–1551.
 252. Dai, N., Qing, Y., Cun, Y., et al. (2018) miR-513a-5p regulates radiosensitivity of osteosarcoma by targeting human apurinic/apyrimidinic endonuclease. *Oncotarget*, 9, 25414–25426.
 253. Dziaman, T., Banaszekiewicz, Z., Roszkowski, K., et al. (2014) 8-Oxo-7,8-dihydroguanine and uric acid as efficient predictors of survival in colon cancer patients. *Int. J. Cancer*, 134, 376–383.
 254. Abdel-Fatah, T. M., Albarakati, N., Bowell, L., et al. (2013) Single-strand selective monofunctional uracil-DNA glycosylase (SMUG1) deficiency is linked to aggressive breast cancer and predicts response to adjuvant therapy. *Breast Cancer Res. Treat.*, 142, 515–527.
 255. Azambuja, D. B., Leguisamo, N. M., Gloria, H. C., Kalil, A. N., Rhoden, E. and Saffi, J. (2018) Prognostic impact of changes in base excision repair machinery in sporadic colorectal cancer. *Pathol. Res. Pract.*, 214, 64–71.
 256. Lange, S. S., Takata, K. and Wood, R. D. (2011) DNA polymerases and cancer. *Nat. Rev. Cancer*, 11, 96–110.
 257. Wang, X., Hickey, R. J., Malkas, L. H., et al. (2011) Elevated expression of cancer-associated proliferating cell nuclear antigen in high-grade prostatic intraepithelial neoplasia and prostate cancer. *Prostate*, 71, 748–754.
 258. Malkas, L. H., Herbert, B. S., Abdel-Aziz, W., et al. (2006) A cancer-associated PCNA expressed in breast cancer has implications as a potential biomarker. *Proc. Natl. Acad. Sci. U. S. A.*, 103, 19472–19477.
 259. Abdel-Fatah, T. M., Russell, R., Albarakati, N., et al. (2014) Genomic and protein expression analysis reveals flap endonuclease 1 (FEN1) as a key biomarker in breast and ovarian cancer. *Mol. Oncol.*, 8, 1326–1338.
 260. Nikolova, T., Christmann, M. and Kaina, B. (2009) FEN1 is overexpressed in testis, lung and brain tumors. *Anticancer Res.*, 29, 2453–2459.
 261. Chen, X., Legrand, A. J., Cuniffe, S., Hume, S., Poletto, M., Vaz, B., Ramadan, K., Yao, D. and Dianov, G. L. (2018) Interplay between base excision repair protein XRCC1 and ALDH2 predicts overall survival in lung and liver cancer patients. *Cell. Oncol. (Dordr.)*, 41, 527–539.
 262. Sun, D., Urrabaz, R., Nguyen, M., Marty, J., Stringer, S., Cruz, E., Medina-Gundrum, L. and Weitman, S. (2001) Elevated expression of DNA ligase I in human cancers. *Clin. Cancer Res.*, 7, 4143–4148.
 263. Wyatt, M. D. and Wilson, D. M., III. (2009) Participation of DNA repair in the response to 5-fluorouracil. *Cell. Mol. Life Sci.*, 66, 788–799.
 264. Vodenkova, S., Jiraskova, K., Urbanova, M., et al. (2018) Base excision repair capacity as a determinant of prognosis and therapy response in colon cancer patients. *DNA Repair (Amst.)*, 72, 77–85.
 265. Chaim, I. A., Nagel, Z. D., Jordan, J. J., Mazzucato, P., Ngo, L. P. and Samson, L. D. (2017) In vivo measurements of interindividual differences in DNA glycosylases and APE1 activities. *Proc. Natl. Acad. Sci. U. S. A.*, 114, E10379–E10388.
 266. Hu, J., Liu, M. H., Li, Y., Tang, B. and Zhang, C. Y. (2018) Simultaneous sensitive detection of multiple DNA glycosylases from lung cancer cells at the single-molecule level. *Chem. Sci.*, 9, 712–720.
 267. Köberle, B., Koch, B., Fischer, B. M. and Hartwig, A. (2016) Single nucleotide polymorphisms in DNA repair genes and putative cancer risk. *Arch. Toxicol.*, 90, 2369–2388.
 268. Ray, D. and Kidane, D. (2016) Gut microbiota imbalance and base excision repair dynamics in colon cancer. *J. Cancer*, 7, 1421–1430.
 269. Kiwerska, K. and Szyfter, K. (2019) DNA repair in cancer initiation, progression, and therapy—a double-edged sword. *J. Appl. Genet.*, 60, 329–334.
 270. Liu, J., Zheng, B., Li, Y., Yuan, Y. and Xing, C. (2019) Genetic polymorphisms of DNA repair pathways in sporadic colorectal carcinogenesis. *J. Cancer*, 10, 1417–1433.
 271. Miyaishi, A., Osawa, K., Osawa, Y., et al. (2009) MUTYH Gln324His gene polymorphism and genetic susceptibility for lung cancer in a Japanese population. *J. Exp. Clin. Cancer Res.*, 28, 10.
 272. Zhang, Y., He, B. S., Pan, Y. Q., Xu, Y. Q. and Wang, S. K. (2011) Association of OGG1 Ser326Cys polymorphism with colorectal cancer risk: a meta-analysis. *Int. J. Colorectal Dis.*, 26, 1525–1530.
 273. Lai, C. Y., Hsieh, L. L., Tang, R., Santella, R. M., Chang-Chieh, C. R. and Yeh, C. C. (2016) Association between polymorphisms of APE1 and OGG1 and risk of colorectal cancer in Taiwan. *World J. Gastroenterol.*, 22, 3372–3380.
 274. Gu, D., Wang, M., Zhang, Z. and Chen, J. (2010) Lack of association between the hOGG1 Ser326Cys polymorphism and breast cancer risk: evidence from 11 case-control studies. *Breast Cancer Res. Treat.*, 122, 527–531.
 275. Ali, K., Mahjabeen, I., Sabir, M., Mehmood, H. and Kayani, M. A. (2015) OGG1 mutations and risk of female breast cancer: meta-analysis and experimental data. *Dis. Markers*, 2015, 690878.
 276. Ramaniuk, V. P., Nikitchenko, N. V., Savina, N. V., Kuzhir, T. D., Rolevich, A. I., Krasny, S. A., Sushinsky, V. E. and Goncharova, R. I. (2014) Polymorphism of DNA repair genes OGG1, XRCC1, XPD and ERCC6 in bladder cancer in Belarus. *Biomarkers*, 19, 509–516.
 277. Smal, M. P., Kuzhir, T. D., Savina, N. V., Nikitchenko, N. V., Rolevich, A. I., Krasny, S. A. and Goncharova, R. I. (2018) BER gene polymorphisms associated with key molecular events in bladder cancer. *Exp. Oncol.*, 40, 288–298.
 278. Stanczyk, M., Sliwinski, T., Cuchra, M., Zubowska, M., Bielecka-Kowalska, A., Kowalski, M., Szmaj, J., Mlynarski, W. and Majsterek, I. (2011) The association of polymorphisms in DNA base excision repair genes XRCC1, OGG1 and MUTYH with the risk of childhood acute lymphoblastic leukemia. *Mol. Biol. Rep.*, 38, 445–451.
 279. Gotoh, N., Saitoh, T., Takahashi, N., et al. (2018) Association between OGG1 S326C CC genotype and elevated relapse risk in acute myeloid leukemia. *Int. J. Hematol.*, 108, 246–253.
 280. Jiraskova, K., Hughes, D. J., Brezina, S., et al. (2019) Functional polymorphisms in DNA repair genes are associated with sporadic colorectal cancer susceptibility and clinical outcome. *Int. J. Mol. Sci.*, 20, 97.
 281. Przybyłowska, K., Kabzinski, J., Sygut, A., Dziki, L., Dziki, A. and Majsterek, I. (2013) An association selected polymorphisms of XRCC1, OGG1 and MUTYH gene and the level of efficiency oxidative DNA damage repair with a risk of colorectal cancer. *Mutat. Res.*, 745–746, 6–15.
 282. Zhou, X., Wei, L., Jiao, G., Gao, W., Ying, M., Wang, N., Wang, Y. and Liu, C. (2015) The association between the APE1 Asp148Glu polymorphism and prostate cancer susceptibility: a meta-analysis based on case-control studies. *Mol. Genet. Genomics*, 290, 281–288.
 283. Mattar, M. A. M., Zekri, A. R. N., Hussein, N., Morsy, H., Esmat, G., and Amin, M. A. (2018) Polymorphisms of base-excision repair genes and the hepatocarcinogenesis. *Gene*, 675, 62–68.
 284. Hadi, M. Z., Coleman, M. A., Fidelis, K., Mohrenweiser, H. W. and Wilson, D. M. III. (2000) Functional characterization of Ape1 variants identified in the human population. *Nucleic Acids Res.*, 28, 3871–3879.
 285. Hsieh, W. C., Lin, C., Chen, D. R., et al. (2017) Genetic polymorphisms in APE1 Asp148Glu(rs3136820) as a modifier of the background levels of abasic sites in human leukocytes derived from breast cancer patients and controls. *Breast Cancer*, 24, 420–426.
 286. Dai, Z. J., Wang, X. J., Kang, A. J., et al. (2014) Association between APE1 single nucleotide polymorphism (rs1760944) and cancer risk: a meta-analysis based on 6,419 cancer cases and 6,781 case-free controls. *J. Cancer*, 5, 253–259.
 287. Kiuru, A., Lindholm, C., Heinävaara, S., et al. (2008) XRCC1 and XRCC3 variants and risk of glioma and meningioma. *J. Neurooncol.*, 88, 135–142.
 288. Li, Y., Li, S., Wu, Z., et al. (2013) Polymorphisms in genes of APE1, PARP1, and XRCC1: risk and prognosis of colorectal cancer in a Northeast Chinese population. *Med. Oncol.*, 30, 505.
 289. Nissar, S., Sameer, A. S., Rasool, R., Chowdri, N. A. and Rashid, F. (2015) Polymorphism of the DNA repair gene XRCC1 (Arg194Trp) and its role in colorectal cancer in Kashmiri population: a case control study. *Asian Pac. J. Cancer Prev.*, 16, 6385–6390.

290. Meng, Q., Wang, S., Tang, W., *et al.* (2017) XRCC1 mediated the development of cervical cancer through a novel Sp1/Krox-20 switch. *Oncotarget*, 8, 86217–86226.
291. Sarkaria, J. N., Kitange, G. J., James, C. D., Plummer, R., Calvert, H., Weller, M. and Wick, W. (2008) Mechanisms of chemoresistance to alkylating agents in malignant glioma. *Clin. Cancer Res.*, 14, 2900–2908.
292. Visnes, T., Grube, M., Hanna, B. M. F., Benitez-Buelga, C., Cázares-Körner, A. and Helleday, T. (2018) Targeting BER enzymes in cancer therapy. *DNA Repair (Amst.)*, 71, 118–126.
293. Li, B., Song, T. N., Wang, F. R., Yin, C., Li, Z., Lin, J. P., Meng, Y. Q., Feng, H. M. and Jing, T. (2019) Tumor-derived exosomal HMGB1 promotes esophageal squamous cell carcinoma progression through inducing PD1+ TAM expansion. *Oncogenesis*, 8, 17.
294. Gao, Q., Wang, S., Chen, X., *et al.* (2019) Cancer-cell-secreted CXCL11 promoted CD8+ T cells infiltration through docetaxel-induced-release of HMGB1 in NSCLC. *J. Immunother. Cancer*, 7, 42.
295. Liu, Y., Prasad, R., and Wilson, S. H. (2010) HMGB1: roles in base excision repair and related function. *Biochim. Biophys. Acta.*, 1799, 119–130.
296. Paudel, Y. N., Angelopoulou, E., Piperi, C., Balasubramaniam, V. R. M. T., Othman, I. and Shaikh, M. F. (2019) Enlightening the role of high mobility group box 1 (HMGB1) in inflammation: updates on receptor signalling. *Eur. J. Pharmacol.*, 858, 172487.
297. Tang, D., Kang, R., Zeh, H. J. and Lotze, M. T. (2011) High-mobility group box 1, oxidative stress, and disease. *Antioxid. Redox Signal.*, 14, 1315–1335.
298. Yu, Y., Tang, D. and Kang, R. (2015) Oxidative stress-mediated HMGB1 biology. *Front. Physiol.*, 6: 93.
299. Sheller-Miller, S., Urrabaz-Garza, R., Saade, G. and Menon, R. (2017) Damage-associated molecular pattern markers HMGB1 and cell-free fetal telomere fragments in oxidative-stressed amnion epithelial cell-derived exosomes. *J. Reprod. Immunol.*, 123, 3–11.
300. Buoncervello, M., Borghi, P., Romagnoli, G., Spadaro, F., Belardelli, F., Toschi, E. and Gabriele, L. (2012) Apicidin and docetaxel combination treatment drives CTCFL expression and HMGB1 release acting as potential antitumor immune response inducers in metastatic breast cancer cells. *Neoplasia*, 14, 855–867.
301. Malhotra, V. (2013) Unconventional protein secretion: an evolving mechanism. *EMBO J.*, 32, 1660–1664.
302. Frye, B. C., Halfter, S., Djudjaj, S., *et al.* (2009) Y-box protein-1 is actively secreted through a non-classical pathway and acts as an extracellular mitogen. *EMBO Rep.*, 10, 783–789.
303. Russo, D., Arturi, F., Bulotta, S., Pellizzari, L., Filetti, S., Manzini, G., Damante, G. and Tell, G. (2001) Ape1/Ref-1 expression and cellular localization in human thyroid carcinoma cell lines. *J. Endocrinol. Invest.*, 24, RC10–RC12.
304. Bobola, M. S., Blank, A., Berger, M. S., Stevens, B. A. and Silber, J. R. (2001) Apurinic/apyrimidinic endonuclease activity is elevated in human adult gliomas. *Clin. Cancer Res.*, 7, 3510–3518.
305. Puglisi, F., Barbone, F., Tell, G., *et al.* (2002) Prognostic role of Ape/Ref-1 subcellular expression in stage I–III breast carcinomas. *Oncol. Rep.*, 9, 11–17.
306. Bendtsen, J. D., Jensen, L. J., Blom, N., Von Heijne, G. and Brunak, S. (2004) Feature-based prediction of non-classical and leaderless protein secretion. *Protein Eng. Des. Sel.*, 17, 349–356.
307. Park, M. S., Lee, Y. R., Choi, S., Joo, H. K., Cho, E. J., Kim, C. S., Park, J. B., Jo, E. K. and Jeon, B. H. (2013) Identification of plasma APE1/Ref-1 in lipopolysaccharide-induced endotoxemic rats: implication of serological biomarker for an endotoxemia. *Biochem. Biophys. Res. Commun.*, 435, 621–626.
308. Choi, S., Lee, Y. R., Park, M. S., *et al.* (2013) Histone deacetylases inhibitor trichostatin A modulates the extracellular release of APE1/Ref-1. *Biochem. Biophys. Res. Commun.*, 435, 403–407.
309. Lee, Y. R., Kim, K. M., Jeon, B. H. and Choi, S. (2015) Extracellularly secreted APE1/Ref-1 triggers apoptosis in triple-negative breast cancer cells via RAGE binding, which is mediated through acetylation. *Cancer Res.*, 76, 4422–4422.
310. Nath, S., Roychoudhury, S., Kling, M. J., Song, H., Biswas, P., Shukla, A., Band, H., Joshi, S. and Bhakat, K. K. (2017) The extracellular role of DNA damage repair protein APE1 in regulation of IL-6 expression. *Cell. Signal.*, 39, 18–31.
311. Pascut, D., Sukowati, C. H. C., Antoniali, G., *et al.* (2019) Serum AP-endonuclease 1 (sAPE1) as novel biomarker for hepatocellular carcinoma. *Oncotarget*, 10, 383–394.
312. Kuilman, T., Michaloglou, C., Vredeveld, L. C., Douma, S., van Doorn, R., Desmet, C. J., Aarden, L. A., Mooi, W. J. and Peeper, D. S. (2008) Oncogene-induced senescence relayed by an interleukin-dependent inflammatory network. *Cell*, 133, 1019–1031.
313. Tanner, K. and Gottesman, M. M. (2015) Beyond 3D culture models of cancer. *Sci. Transl. Med.*, 7, 283ps9.
314. Abbott, A. (2003) Cell culture: biology's new dimension. *Nature*, 424, 870–872.
315. Leushacke, M. and Barker, N. (2014) Ex vivo culture of the intestinal epithelium: strategies and applications. *Gut*, 63, 1345–1354.
316. Ohta, Y. and Sato, T. (2014) Intestinal tumor in a dish. *Front. Med. (Lausanne)*, 1, 14.
317. Cristobal, A., van den Toorn, H. W. P., van de Wetering, M., Clevers, H., Heck, A. J. R. and Mohammed, S. (2017) Personalized proteome profiles of healthy and tumor human colon organoids reveal both individual diversity and basic features of colorectal cancer. *Cell Rep.*, 18, 263–274.
318. Van De Wetering, M., Francies, H. E., Francis, J. M., *et al.* (2015) Prospective derivation of a living organoid biobank of colorectal cancer patients. *Cell*, 161, 933–945.
319. Drost, J., van Boxtel, R., Blokzijl, F., *et al.* (2017) Use of CRISPR-modified human stem cell organoids to study the origin of mutational signatures in cancer. *Science*, 358, 234–238.
320. Francies, H. E., Barthorpe, A., McLaren-Douglas, A., Barendt, W. J. and Garnett, M. J. (2019) Erratum to: drug sensitivity assays of human cancer organoid cultures. *Methods Mol. Biol.*, 1576, 353.
321. Codrich, M., Comelli, M., Malfatti, M. C., *et al.* (2019) Inhibition of APE1-endonuclease activity affects cell metabolism in colon cancer cells via a p53-dependent pathway. *DNA Repair (Amst.)*, 82, 102675.
322. Li, T., Wernersson, R., Hansen, R. B., *et al.* (2017) A scored human protein-protein interaction network to catalyze genomic interpretation. *Nat. Methods*, 14, 61–64.

open

Architecture of The Human Ape1 Interactome Defines Novel Cancers Signatures

Dilara Ayyildiz^{1,4}, Giulia Antoniali^{1,4}, Chiara D'Ambrosio^{2,4}, Giovanna Mangiapane¹, Emiliano ¹, Andrea Scaloni², ^{1*} & Silvano ^{3*}

APE1 is essential in cancer cells due to its central role in the Base Excision Repair pathway of DNA lesions and in the transcriptional regulation of genes involved in tumor progression/chemoresistance. Indeed, APE1 overexpression correlates with chemoresistance in more aggressive cancers, and APE1 protein-protein interactions (PPIs) specifically modulate different protein functions in cancer cells. Although important, a detailed investigation on the nature and function of protein interactors regulating APE1 role in tumor progression and chemoresistance is still lacking. The present work was aimed at analyzing the APE1-PPI network with the goal of defining bad prognosis signatures through systematic bioinformatics analysis. By using a well-characterized HeLa cell model stably expressing a flagged APE1 form, which was subjected to extensive proteomics analyses for immunocaptured complexes from different subcellular compartments, we here demonstrate that APE1 is a central hub connecting different subnetworks largely composed of proteins belonging to cancer-associated communities and/or involved in RNA- and DNA-metabolism. When we performed survival analysis in real cancer datasets, we observed that more than 80% of these APE1-PPI network elements is associated with bad prognosis. Our findings, which are hypothesis generating, strongly support the possibility to infer APE1-interactomic signatures associated with bad prognosis of different cancers; they will be of general interest for the future definition of novel predictive disease biomarkers. Future studies will be needed to assess the function of APE1 in the protein complexes we discovered. Data are available via ProteomeXchange with identifier PXD013368.

Alteration of DNA repair mechanisms is an important hallmark of cancer cells, and plays a role both in the onset of an initial cancerous phenotype and in tumor progression. Tumor cells can develop drug resistance through repair mechanisms that counteract the DNA damage induced by chemotherapy or radiotherapy^{1,2}. Thus, specific DNA repair inhibitors are often combined with DNA-damaging agents to improve therapy efficacy. Emerging evidences in tumor biology suggest that: i) protein-protein interactions (PPIs) specifically modulate both canonical and non-canonical roles of DNA repair enzymes; ii) RNA processing pathways participate in DNA-Damage Response (DDR); iii) defects in the above-mentioned regulatory mechanisms are associated with cancer genomic instability³. Very recent studies clearly show that many DNA repair proteins are associated with those involved in RNA metabolism, proving a role of their interactome network in undertaking non-canonical functions affecting gene expression in tumors. In addition, novel studies have shown that interaction of DDR components and miRNA biogenesis process is linked to cancer development². In the context of these emerging lines, we already demonstrated the crucial role that enzymes belonging to the base excision DNA repair (BER) pathway play⁴. In particular, we showed that the essential BER enzyme apurinic/apyrimidinic endonuclease 1 (APE1), which is encoded by the *APEX1* gene, contributes to the regulation of oxidative stress responses and to the expression of chemoresistance genes *via* unsuspected functions in RNA metabolism^{4–8}. The involvement of this protein in RNA processing events^{9–11}, including miRNA expression, was recently unraveled by our group using a limited

¹Laboratory of Molecular Biology and DNA repair, Department of Medicine, University of Udine, p.le M. Kolbe 4, 33100, Udine, Italy. ²Proteomics and Mass Spectrometry Laboratory, Institute for the Animal Production System in the Mediterranean Environment (ISPAAM), National Research Council (CNR) of Italy, via Argine 1085, 80147, Naples, Italy. ³Bioinformatics Core Facility, Centre for Integrative Biology (CIBIO), University of Trento, via Sommarive 18, 38123, Povo (Trento), Italy. ⁴These authors contributed equally: Dilara Ayyildiz, Giulia Antoniali and Chiara D'Ambrosio. *email: gianluca.tell@uniud.it; silvano.piazza@unitn.it

unbiased functional proteomic approach⁴. However, the reduced characterization of APE1 interaction with proteins involved in miRNA processing, *e.g.* NPM1, hnRNP, PRP19, SFPQ and p53¹², strongly limited our complete understanding of this phenomenon and of its functional relevance in cancer biology, thus hampering a further translation of these findings into therapy.

It is well known that the different functions of APE1 may depend on its interacting partners^{13,14}; for example, an alteration of its interaction networks has been reported to play a significant role in BER impairment. A recent hypothesis also suggests that APE1 functional dysregulation may impact on the RNome expression and, thus, on the expression of target genes playing a relevant role in the pathology onset⁴. Since several cancer-associated APE1 variants present mutations in the endonuclease domain, exhibiting only mild nuclease defects *in vitro*^{15–17}, we hypothesize that APE1 non-canonical functions associated with its overexpression and/or an altered expression of its protein interacting partners should be related to cancer promotion. A proof of concept for the relevance of APE1 PPIs in cancer biology is represented by the paradigmatic example of the APE1-nucleophosmin 1 (NPM1) interaction, as ascertained by us¹⁸. NPM1 is a multifunctional protein that controls cell growth and genome stability through a mechanism either involving nucleolar-cytoplasmic shuttling or a fine modulation of the whole BER pathway^{11,19}. Recently, an important role for NPM1 in miRNA biology, associated with cancer development, was outlined^{20–22}. Abnormal cytoplasmic APE1 and NPM1 levels were associated with the oncogenic progression and chemoresistance of HGSC (high-grade serous ovarian adenocarcinoma), a prediction of a poor prognosis therein^{23,24}, and a dysregulation of the BER and miR-221/222 processing pathways in AML cells^{18,25}. The efficacy of novel APE1/NPM1 interaction inhibitors, which sensitize cancer cells to chemotherapy agents, supports the translational importance of these findings²⁶. These results further support the hypothesis that an alteration of other APE1 PPIs may be causally involved in cancer development and chemoresistance.

Prompted by these observations, the present work was aimed at: i) implementing the already known APE1-PPI network using a more efficient functional proteomics approach, and ii) defining the association of the APE1-PPI network with the modulation of tumor progression and chemoresistance through a systematic bioinformatics analysis of the Cancer Genome Atlas (TCGA) datasets. To this purpose, we used HeLa cells as a general and well-characterized cancer cell model to generate novel disease hypotheses and molecular diagrams. Having a well-characterized cell model is essential when using unbiased strategies, such as genomics and proteomics, in order to easily interpret data and generate novel assumptions. In this context, few years ago, we developed a specific HeLa cell line stably expressing a flagged tagged APE1 form for selective and efficient protein complex immunocapture^{4,17,26,27}. This cell line, and its corresponding products, were characterized in both cancer and genotoxic damage response contexts by means of different holistic approaches, including genomics, transcriptomics and proteomics^{4,12}. In this study, we wanted to improve our previous interactomic analyses by taking advantage of more sensitive mass spectrometry technologies, which were here applied to the analysis of extracts from different subcellular compartments. Resulting data were analysed by bioinformatics in a dedicated translational perspective. Our findings support the possibility to infer APE1 interactomic signatures associated with bad prognosis of different cancers and will be of general interest for the definition of novel predictive biomarker signatures of cancers.

Results

Proteomic characterization of the APE1-PPI network. With this work, we wanted to study the relevance of APE1-PPIs in cancer using an unbiased functional proteomic approach in order to expand the number of known APE1 PPIs, as derived from studies from this and other groups^{4,12}. To this purpose, we used HeLa cells stably expressing the APE1 FLAG-tagged protein¹² (WT), which were here managed to optimize the isolation of APE1-PPI complexes through co-immunoprecipitation experiments (Figs. 1 and 2A). Differently from our previous investigations¹², APE1-interacting protein complexes were isolated from either the whole cell lysate, or nuclear- and cytoplasmic-enriched subcellular fractions. Then, resulting protein mixtures were resolved by SDS-PAGE, and corresponding gel lanes were cut into parallel gel portions that were further subjected to proteomic analysis. As control experiments, we applied the same proteomic procedure to a cell clone stably transfected with the empty scramble vector (SCR) (Figs. 1 and 2A). As additional negative control experiments, nuclear and cytoplasmic cell extracts from HeLa cells expressing APE1 FLAG-tagged were co-immunoprecipitated with a resin lacking the anti-FLAG antibody to exclude any additional background (Fig. 2A, res). Western blotting analysis showed an APE1 enrichment in co-immunoprecipitated material from nuclear, cytoplasmic and total cell extracts of a HeLa cell clone stably expressing the flagged protein (Fig. 2A). In order to check for the quality of the immunoprecipitated materials, nucleophosmin 1 (NPM1) was used as a known APE1 interactor prior to further proteomic analysis^{12,18,19,28}. By using this approach, a number of proteins were identified in APE1-FLAG co-immunoprecipitates from the above-mentioned whole-cell lysate and corresponding subcellular fractions (Supplementary Table S1 and Table S2). After careful filtration for false positives identified in the corresponding control (SCR and res) samples, 62, 31 and 394 proteins were identified as potential APE1 interactors in the whole-cell lysate, nuclear fraction and cytoplasmic fractions, respectively, which accounted for 455 non-redundant proteins. A poor overlapping of components from different extracts was observed, qualitatively confirming the preparation specificity (Fig. 2B). Various molecules (*i.e.* FEN1, hnRNPK, NPM1, PABPC1, SFPQ and XRCC1) were already described as APE1-interacting partners in other studies from this^{4,12} and other groups^{24,29,30}, confirming the good quality of our analysis. The following proximity ligation assays were then successfully carried out to validate the identified APE1-interacting proteins within cells: i) SFPQ (splicing factor, proline- and glutamine-rich), DHX9 (DEAH-box helicase 9) and hnRNPK (heterogeneous nuclear ribonucleoprotein K) in HeLa cells (Fig. 2C and Supplementary Figs. S1 and S2); ii) hnRNPA2/B1 in the JHH-6 hepatocellular carcinoma cell line³¹ (Supplementary Fig. S1B); iii) SFPQ in the A549 lung cancer cell line (Supplementary Fig. S1C)³². The above-mentioned APE1-binding partners list was then added with additional proteins (*n* = 80) deriving from previous APE1-focused interactomic investigations⁴ to yield a final list of APE1-PPI elements (*n* = 535), which

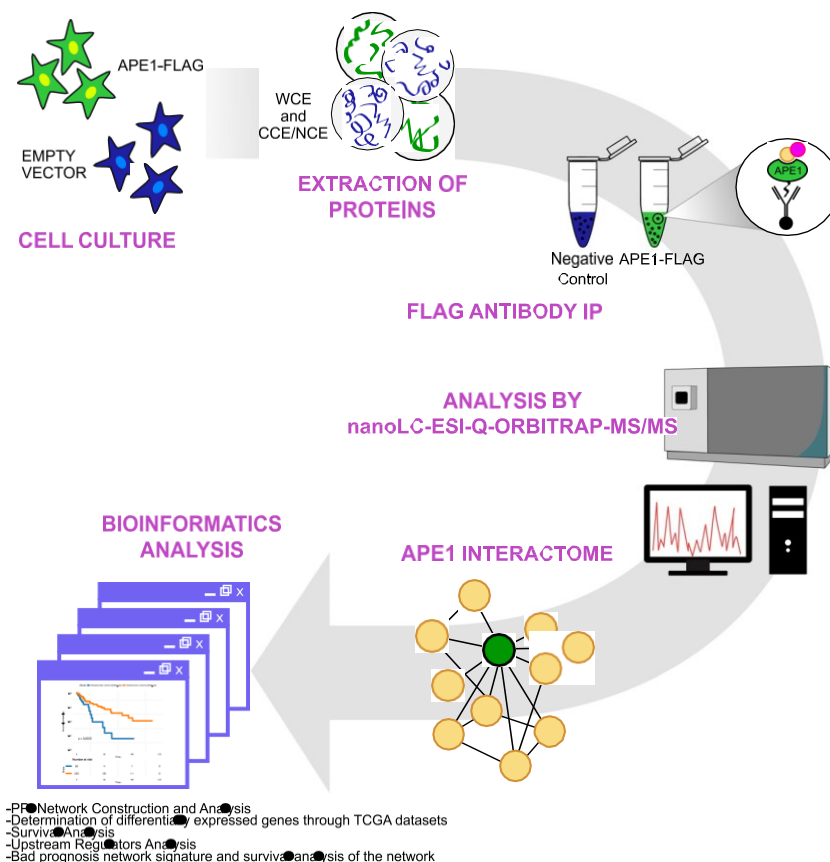


Figure 1. Schematic experimental pipeline used in this study. Schematic representation of the workflow for ascertaining APE1-interacting proteins by proteomic experiments. Whole-cell lysates (WCE), or nuclear (NCE) and cytoplasmic (CCE) extracts were prepared from the 3 × APE1 FLAG-tagged expressing cells or control cells transformed with an empty vector (SCR). M2 antibodies against the FLAG peptide were used for co-immunoprecipitation of the above cell lysates. As additional control experiment, identical cell extracts from HeLa cells expressing 3 × APE1 FLAG-tagged were also co-immunoprecipitated with a resin lacking the FLAG antibody (res). The resulting bound proteins were digested with trypsin and analyzed by nanoLC-ESI-Q-Orbitrap-MS/MS. By comparison with proteins identified in the control co-immunoprecipitation experiments, we removed contaminant proteins from components identified in WCE, NCE and CCE; the resulting APE1-interacting partners were further added of additional proteins binding to APE1 ($n = 80$) from previous studies⁴, and finally subjected to bioinformatics analysis.

were associated with 531 non-redundant genes. The large size of this inventory (containing direct as well as indirect protein-binding partners) was rationalized based on the multiple biological functions/activities in which APE1 has been associated (redox control, transcriptional activity, DNA and RNA metabolism), and its localization in various subcellular districts. This condition is similar to the one recently reported for two APE1 protein interactors, namely XRCC6 and XRCC5, which have been similarly demonstrated to bind both to RNA/DNA as well as to about 300 proteins³³. Other examples of proteins having hundreds of interactors (as deduced by a single immunocapture experiment) are already present in the scientific literature^{34–37}. On the other hand, this final list, of direct or indirect APE1-binding partners, contained about 100 proteins whose capability to interact (directly or indirectly) with APE1 was already ascertained by different experimental approaches (Supplementary Table S3). The above-mentioned protein inventory was then subjected to bioinformatics analysis to establish a PPI-network associated with APE1 (Fig. 1); then, we linked this analysis to additional cancer/biological databases with the aim to provide a more complete picture of the APE1 biological roles in both cancer and cellular biology.

APE1-PPI network construction and analysis. The APE1-interacting partners from this and other investigations ($n = 535$) were used to establish the APE1-PPI network. Direct and/or indirect interactions between these molecules were retrieved by the InWeb_InBioMap web tool, which is a large data compendium for high-quality PPI networks. Afterwards, the undirected PPI network, representing the interactome of APE1, was constructed with 511 nodes (24 proteins were not recognized by the tool) and 3934 edges (Fig. 3A). The resulting network was visualized and analyzed by using the Cytoscape software and its packages³⁸. The initial analysis of the network was carried out by performing functional enrichment analysis for terms belonging to the “Gene Ontology - Biological Process” database, using the ClueGO tool with standard parameters to identify enriched pathways on the basis of the network’s gene frequency in each pathway ($n = 383$, 75%). Based on this analysis, 109 genes were enriched in the group of pathways called “DNA metabolic process” (7.4% genes per group), 90 genes

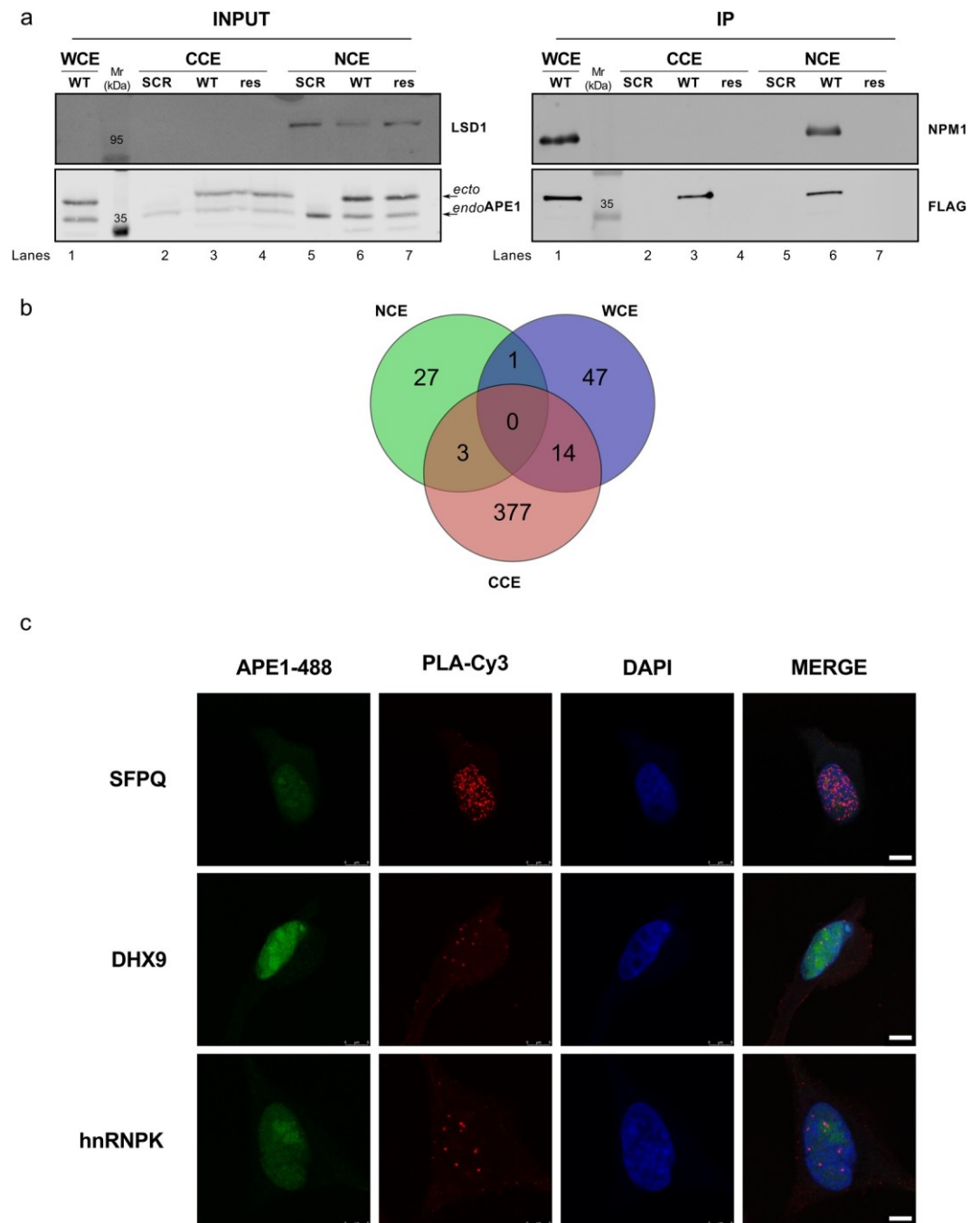


Figure 2. Proteomic characterization of the APE1 interactome. **(A)** Representative Western blotting to confirm APE1 pulldown in the co-immunoprecipitation experiment. Western blotting analysis was performed on total HeLa cell clone extracts (INPUT) and on co-immunoprecipitated material (IP) with specific antibodies for APE1 and FLAG. The endogenous (*endo*) and ectopic (*ecto*) form of the APE1 protein is visible. The resulting material was tested for the occurrence of NPM1, a known APE1 interactor. LSD1 was used to probe nuclear enrichment. SCR, HeLa cell clone transfected with empty vector; WT, HeLa cell clone expressing APE1-FLAG tagged protein; res, co-immunoprecipitated with a resin lacking the FLAG antibody; WCE, whole cell extract; NCE, nuclear cell extract; CCE, cytoplasmic cell extract. **(B)** Venn diagram showing APE1-interacting partners identified in whole-cell lysates (WCE), or nuclear (NCE) and cytoplasmic (CCE) extracts. **(C)** Nucleoplasmic interaction between APE1 and three identified interactors. HeLa cells were seeded on a glass coverslip and the PLA reaction was carried out using anti-APE1, anti-SFPQ, anti-DHX9 and anti-hnRNPk antibodies. APE1 localization was detected by using an anti-APE1 antibody and visualized in green. Confocal microscopy analysis highlighted the presence of distinct fluorescent red dots (PLA signals) indicating the occurrence of *in vivo* interaction between APE1 and its protein partners. DAPI staining was used as a reference for the nuclei. See also Supplementary Figs. S1 and S2 for negative controls. Bars, 8 μ M.

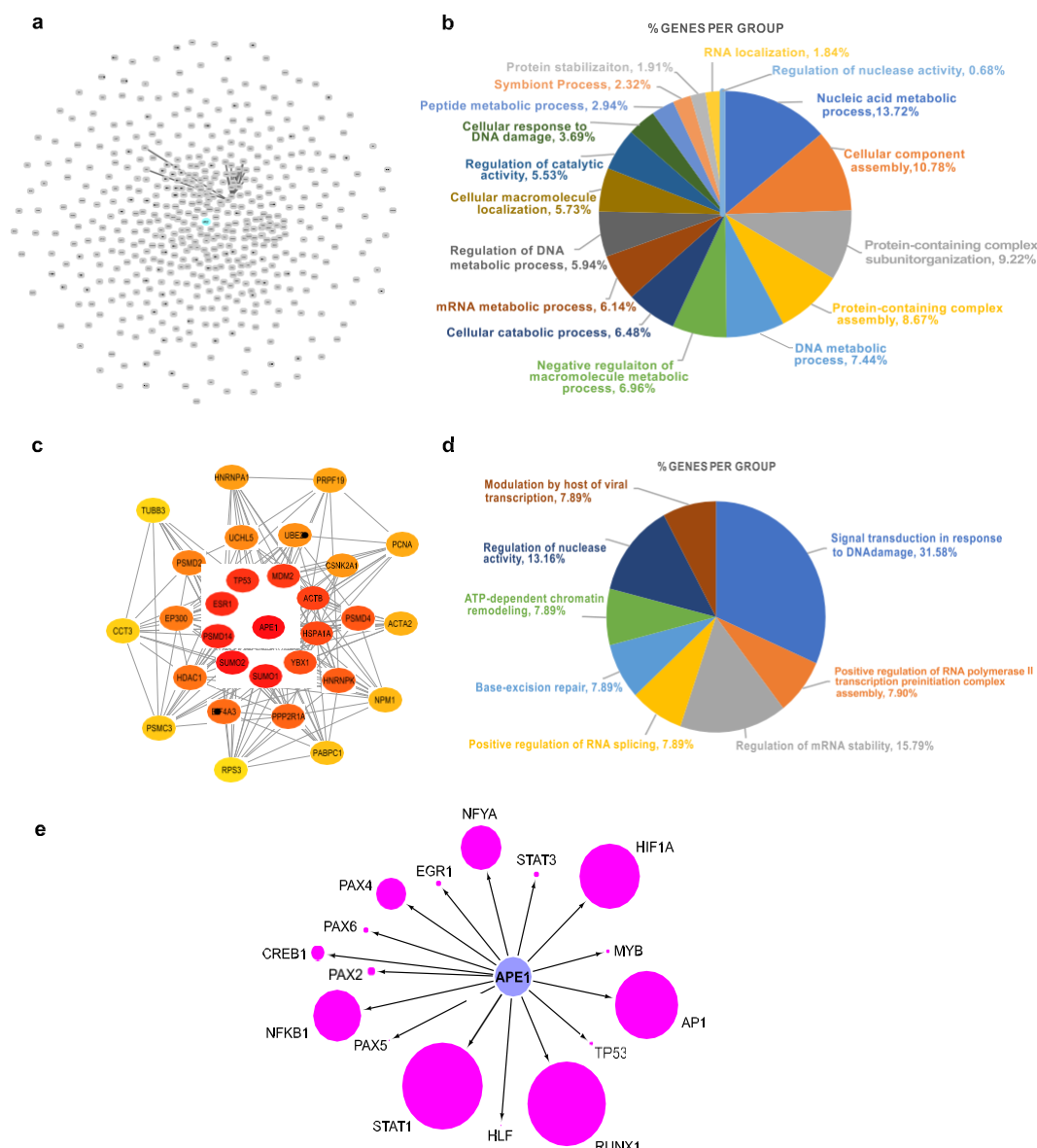


Figure 3. Bioinformatics characterization of the APE1 interactome. **(A)** Global APE1 Protein-Protein Interaction Network. **(B)** Functional annotation of the global network based on Gene Ontology - Biological Process terms ($p < 0.05$). In the pie chart, the percentage of the proteins/genes enriched in the group of pathways is shown. **(C)** Top 30 hubs of the APE1-PPI network, based on global metric, betweenness centrality. Color shades represent the significance of the hub, with red color as the most significant and yellow color as the least. **(D)** Functional annotation of the Top 30 hubs based on Gene Ontology - Biological Process terms ($p < 0.05$). In the pie chart, the percentage of the genes enriched in the group of pathways is shown. **(E)** Transcriptional regulatory network of the APE1 interactome. Node size represents the number of putative binding sites identified by the LASAGNA-Search 2.0 tool in the promoters (-2500 , -1 nt from the TSS) of the APE1 interactome genes for 16 transcription factors that are modified by APE1 redox activity or use APE1 as a co-factor.

were enriched in the group of pathways called “mRNA metabolic process” (6.1% genes per group), 54 genes were enriched in the group of pathways called “DNA damage response” (3.7% genes per group) and 27 genes were enriched in the group of pathways called “RNA localization” (1.8% genes per group) (Fig. 3B and Supplementary Table S4). These results clearly confirmed the involvement of APE1 and its interacting partners in processes involved in RNA (with particular emphasis on mRNA), DNA and protein metabolism/stability, supporting our previous findings^{4,12}.

The complex PPI-network containing 511 nodes was then studied in order to focus on its most important elements; this was done through a hub analysis based on global metric, betweenness centrality. In graph theory, betweenness centrality is a measure of centrality in a graph based on the shortest paths; therefore, it represents the degree to which nodes stand between each other. As a result, the top 30 hub nodes were identified and

extracted from the main APE1-PPI network as hub-subnetworks (Fig. 3C). This hub module was then analyzed with ClueGO to understand the specific roles of these genes in biological processes (Fig. 3D and Supplementary Table S4). The predominant enrichment was observed for: i) 12 hub genes involved in the group of pathways named “signal transduction in response to DNA damage” (31.6% genes per group); ii) 6 hub genes enriched in the group of pathways called “regulation of mRNA stability” (15.8% genes per group); iii) 3 central hub genes (HSPA1A, PRPF19 and PSMD4) involved in the group of pathways related to “positive regulation of RNA splicing”, confirming previous interactomic results⁴. Globally, these results indicate the significant involvement of the APE1-PPI network in RNA and DNA metabolism, showing that APE1 acts as the central hub connecting different subnetworks with diverse functions.

Role of APE1 in the transcriptional regulation of the APE1-PPI network. Among its multifunctional biological roles, APE1 is also known as transcriptional and post-transcriptional regulator. On the one hand, APE1 can exert its nuclear redox control function on several transcription factors (TFs), modulating their activity and, hence, gene expression³⁹. On the other hand, it can also act at the RNA level through its ability in binding to transcripts, thus affecting corresponding stability and processing^{4,10}. Therefore, we can hypothesize that APE1 may contribute to gene expression regulation of elements of its own PPI. In order to check whether APE1 could be involved in the former activity, we performed a TFBS motif discovery analysis with the LASAGNA-Search 2.0 tool⁴⁰ on the promoters of the above-mentioned 531 genes representing the APE1 interactome. This allowed to verify and quantify the presence of enriched putative binding sites for more than a hundred TFs (Supplementary Table S5). In particular, we identified putative sites for 16 TFs that are known to be stimulated by the APE1 redox activity or to regulate gene expression by using APE1 as a co-factor (e.g. AP1, NF- κ B1, HIF1 α and members of the STAT family) (Fig. 3E). Some of these TF binding sites (e.g. PAX5 sites) were not highly abundant in the obtained results but, since they are known to regulate gene expression in a tissue-specific manner, we believe that the HeLa cell model used in the present work could not represent the most suitable one to study their effect. We also compared the list of APE1-PPI partners identified in the present work with that of the RNA molecules bound by APE1 ($n = 1015$), which we previously had defined through RIP-seq experiments^{4,12}; this analysis demonstrated that 42 genes, that interact with APE1 at the transcript level, are also part of the APE1-PPI (p -value = 0.01, Supplementary Fig. S3). We finally integrated these data with the results of a microarray differential gene expression profiling analysis performed in siAPE1 HeLa cells¹². Interestingly, we found that 55 genes, belonging to the APE1-PPI network, were differentially expressed (absolute log fold change ≥ 1 , adj. p -value ≤ 0.05), as well as 45 other transcripts originating from the RIP-seq experiment, globally accounting for 95 unique genes (p -value = 0.0001, Supplementary Fig. S3). Altogether, these results strongly support the possibility that APE1 may contribute to the regulation of the expression of the majority of its own PPI genes.

Correlation between APE1 and its protein-binding partners at the gene expression level. Correlated expression of differently associated genes is often observed being a common feature and an important booster of the transformation process⁴¹, even though a perfect correlation of gene expression at mRNA and protein levels is not always observed⁴². However, data described in the previous section provided interesting evidences suggesting that the integration of proteomic and transcriptomic data, correlated by common biological functions, may highlight the potential involvement of subsets of genes in neoplastic transformation.

In order to understand if a relationship between APE1 and its protein interaction partners may be observed also at the gene expression level, we analyzed the corresponding correlations in the Genomic Data Commons (GDC) RNA-Seq tumor database. In more than 11,000 tumor sample datasets, we observed that the gene expression correlation between APE1 and its PPI-network elements is higher (p -value $< 10^{-15}$) than that with respect to: (i) all the genes, (ii) random-gene datasets (PPI size) or (iii) random genes vs the APE1-PPI network (Fig. 4A,B). By using the same dataset, gene expression data for the genes coding the 531 interactors of APE1 were obtained for 33 different tumor types described in TCGA (Supplementary Table S6) as well as for the associated normal tissues. Further analyses were performed across the top 11 TCGA cancer datasets having the highest number of bad prognostic genes (see below) that were up- and down-regulated ($p < 0.05$, absolute log fold change > 1) (Figs. 4C, 5 and Supplementary Table S6). According to the results of the differential gene expression analysis, more than half of the APE1 interactors were found to be differentially expressed in many datasets (Fig. 4). The gene expression of APE1 across these datasets was used to calculate the Pearson correlation existing between APE1 and its interactors. A very high percentage of differentially expressed genes (DEGs) in those datasets was found to have significant ($p < 0.05$) correlation with APE1 gene expression (Fig. 4C). Altogether, these results demonstrated the existence of a very strong orchestration in the expression of APE1 and of its interacting proteins in the aforementioned cancer types, suggesting the existence of common pathways of transcriptional regulation for APE1-PPIs in cancer development.

Upstream regulators analysis. With the aim of ascertaining the role of these gene modules in more detail, an upstream regulators analysis was performed using the TRANSPATH tool within the geneXplain 4.11 web platform. For each TCGA cancer dataset, the list of significant DEGs was analyzed, and the three molecules having the lowest Ranks sum were retained (Table 1) as the ones having the best probability of being the master regulators of that network. These results strengthened, on the one hand, the general role of the modules in RNA and DNA repair mechanisms. In fact, XRCC6 (master regulator of 5 datasets) and DDB1 (master regulator of 3 datasets) are proteins associated with the DNA repair process^{43,44}. YBX1, another highly represented master regulator (KIRC, KIRP and PAAD), is known to act as both an RNA- and a DNA-binding protein, as well as being involved in miRNA processing⁴⁵. However, what really equated all these regulators was their role in the apoptotic, proliferative and resistance pathways, as shown in Table 1. We also evaluated the correlation of the expression profiles

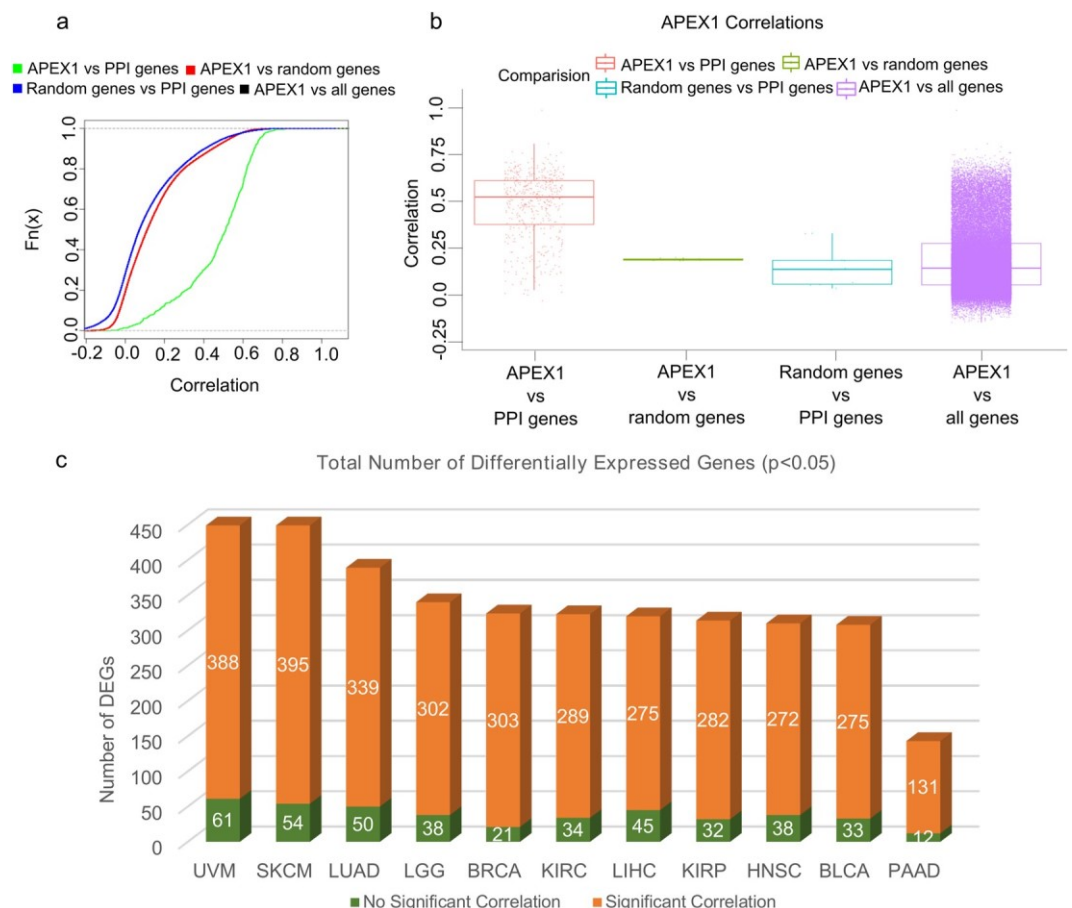


Figure 4. Differential gene expression and correlation analysis of APE1-interacting partners in the TCGA datasets. **(A)** Empirical cumulative distribution function (ECDF). Empirical cumulative distribution curves of the correlation of the gene expression profiles of APE1 and APE1-PPI network genes in the TCGA datasets or in the control groups. Green line: APEX1 expression versus the PPI network genes; red line: APEX1 expression versus 100 sets with the same size of the PPI gene set composed by random genes; blue line: 100 random genes expression versus the PPI network genes; black line: APEX1 expression versus all genes. Note that the black line is nearly superimposed to the red line and, for this reason, almost hidden by it. **(B)** Box-plots of the same data. The average correlations for all the control groups are statistically significantly different ($p < 0.005$) with respect to the APEX1-PPI correlation. **(C)** Total number of differentially expressed genes ($p < 0.05$, absolute log fold change difference > 1) across the top 11 TCGA datasets having the highest number of up- and down-regulated genes. In the bar chart, the number of genes having significant correlation (absolute (PCC) > 0.6 , $p < 0.05$) with the expression of APE1 is shown in orange, while the others are shown in green.

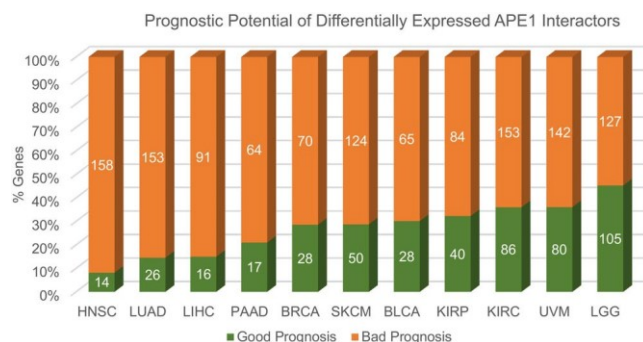


Figure 5. Survival analysis of APE1-interacting partners in the TCGA datasets. For each cancer type, bar plots represent the percentages and the total number of genes having significant ($p < 0.05$) bad or good prognosis, shown in orange and green color, respectively.

Dataset	Top1	Top1 Bibliography	Gene Symbol Description	Top2	Top2 Bibliography	Gene Symbol Description	Top3	Top3 Bibliography	Gene Symbol Description
HNSC	XRCC6	(1) (2) (3)	X-ray repair cross-complementing protein 6	PRKDC	(1) (2) (3)	Protein kinase, DNA-activated, catalytic subunit	TERF2	(1) (2) (3)	Telomeric repeat binding factor 2
KIRC	PRKCD	(1) (2) (3)	Protein kinase C delta type	PPP1CB	(2)	Protein phosphatase 1 catalytic subunit beta	YBX1	(1) (2) (3)	Y-Box binding protein 1
LUAD	PRKN	(2)	Parkin RBR E3 ubiquitin protein ligase	HDAC2	(1) (2) (3)	Histone deacetylase 2	XRCC6	(1) (2) (3)	X-ray repair cross-complementing protein 6
UVM	SMYD2	(1) (2) (3)	SET and MYND domain containing 2	KDM1A	(1) (2) (3)	Lysine demethylase 1A	XRCC5	(1) (2)	X-ray repair cross-complementing protein 5
LGG	SETD7	(1) (2) (3)	SET domain containing 7, histone lysine methyltransferase	KDM1A	(1) (2) (3)	Lysine demethylase 1A	CUL1	(1) (2)	Cullin-1
SKCM	DDB1	(1) (2) (3)	Damage specific DNA binding protein 1	PTP4A3	(1) (2) (3)	Protein tyrosine phosphatase 4A3	XRCC6	(1) (2) (3)	X-ray repair cross-complementing protein 6
LIHC	PRKN	(2)	Parkin RBR E3 ubiquitin protein ligase	HDAC2	(1) (2) (3)	Histone deacetylase 2	XRCC6	(1) (2) (3)	X-ray repair cross-complementing protein 6
KIRP	YBX1	(1) (2) (3)	Y-Box binding protein 1	PTP4A3	(1) (2) (3)	Protein tyrosine phosphatase 4A3	TCF21	(1) (2) (3)	Transcription factor 21
BRCA	DDB1	(1) (2) (3)	Damage specific DNA binding protein 1	XRCC6	(1) (2) (3)	X-ray repair cross-complementing protein 6	IDE	(1) (2)	Insulin-degrading enzyme
BLCA	DDB1	(1) (2) (3)	Damage specific DNA binding protein 1	XRCC5	(1) (2)	X-ray repair cross-complementing protein 5	TRIM28	(1) (2) (3)	Tripartite motif containing 28
PAAD	YBX1	(1) (2) (3)	Y-Box binding protein 1	ACTL6A	(1) (2)	Actin-like protein 6A	HNRNPK	(1) (2) (3)	Heterogeneous nuclear ribonucleoprotein K

Table 1. APE1-PPI bad prognostic signatures top regulators analysis. GeneXplain identification of the Top 3 putative master regulators (ranked by ascending Ranks sum) of bad prognostic genes in the 11 selected TCGA cancer datasets. Numbers in brackets refer to the presence of bibliographic evidence associating upstream regulators with proliferation (1), apoptosis (2) and resistance (3), respectively. For TCGA abbreviations, see Supplementary Table S6; for all the references Supplementary Table S7.

of APEX1 and of these regulators in each bad prognostic network (Fig. 6 and Supplementary Figs. S4–S11, data is represented according to a color code).

Afterwards, upstream regulators analysis was performed also on the global APE1-PPI network to widen our understanding of its functions. The resulting top 10 master regulators are provided in Supplementary Table S8. Interestingly, we observed that some of these master regulators (i.e. NUA1, KDM1A, UBE2D1, RBX1 and UBE2M) were known to be associated with the p53 signaling pathway^{46–51}.

Definition of a bad-prognostic APE1 signature in cancers. With the aim of evaluating the real impact of APE1-interacting partners in TCGA cancer datasets, survival analyses were performed using the RTCGA Bioconductor package. The genes that were differentially expressed in a statistically significant manner ($p < 0.05$, absolute log fold change > 1) between tumor and normal tissues were analyzed; Kaplan-Meier plots were obtained for each gene in each dataset, allowing to define good and bad prognosis gene signatures on a per cancer basis (Supplementary Table S4). The distribution of the genes with respect to significant good or bad prognosis ($p < 0.05$) in those cancer datasets is represented in Fig. 5.

In order to focus our attention on the most relevant cancer types, we based our bioinformatic analysis on the eleven datasets having the highest number of bad prognostic genes. Among those, we were interested in particular in liver (LIHC)^{52–56}, lung (LUAD)^{57–60} and pancreatic (PAAD)^{61–65} cancer datasets, as the essential role of APE1 in the tumorigenic processes of these cancer types is already well established. Notably, the LUAD dataset was the third having the highest number of bad prognostic genes ($n = 153$). We then represented these genes as a subnetwork of the APE1-PPI network having correlation information with the following color code: green for significant positive correlation ($PCC > 0.6$), red for significant negative correlation ($PCC < -0.6$) and grey for no correlation (Fig. 6A). In the network, the top 3 master regulators were also represented with diamond-shaped nodes. Afterwards, we specifically studied the survival outcomes of patients with high or low expression of the bad prognosis signature, using the median log fold change value of the genes in the network. The Kaplan-Meier plot (Fig. 6B) clearly shows that high expression of the genes in the bad prognostic network was associated with significant ($p < 0.0001$) lower survival probability. The biological processes dominantly enriched in this network were as follows: nucleic acid metabolism, protein transporters and arrangements to form complex subunits that have polymerized to generate fiber-shaped structures (Fig. 6C and Supplementary Table S4).

Because of the strong interest in APE1 as a prognostic factor in liver^{52–56} and pancreatic cancers^{61–63}, we applied the same representation also to the LIHC (Fig. 6D–F) and PAAD datasets (Fig. 6G–I) with a total number of 91 and 64 bad prognostic genes, respectively. The bad prognostic signatures in these networks highlighted again a significant involvement of DNA- and RNA-related pathways (Figs. 6F–I; Supplementary Table S4). In

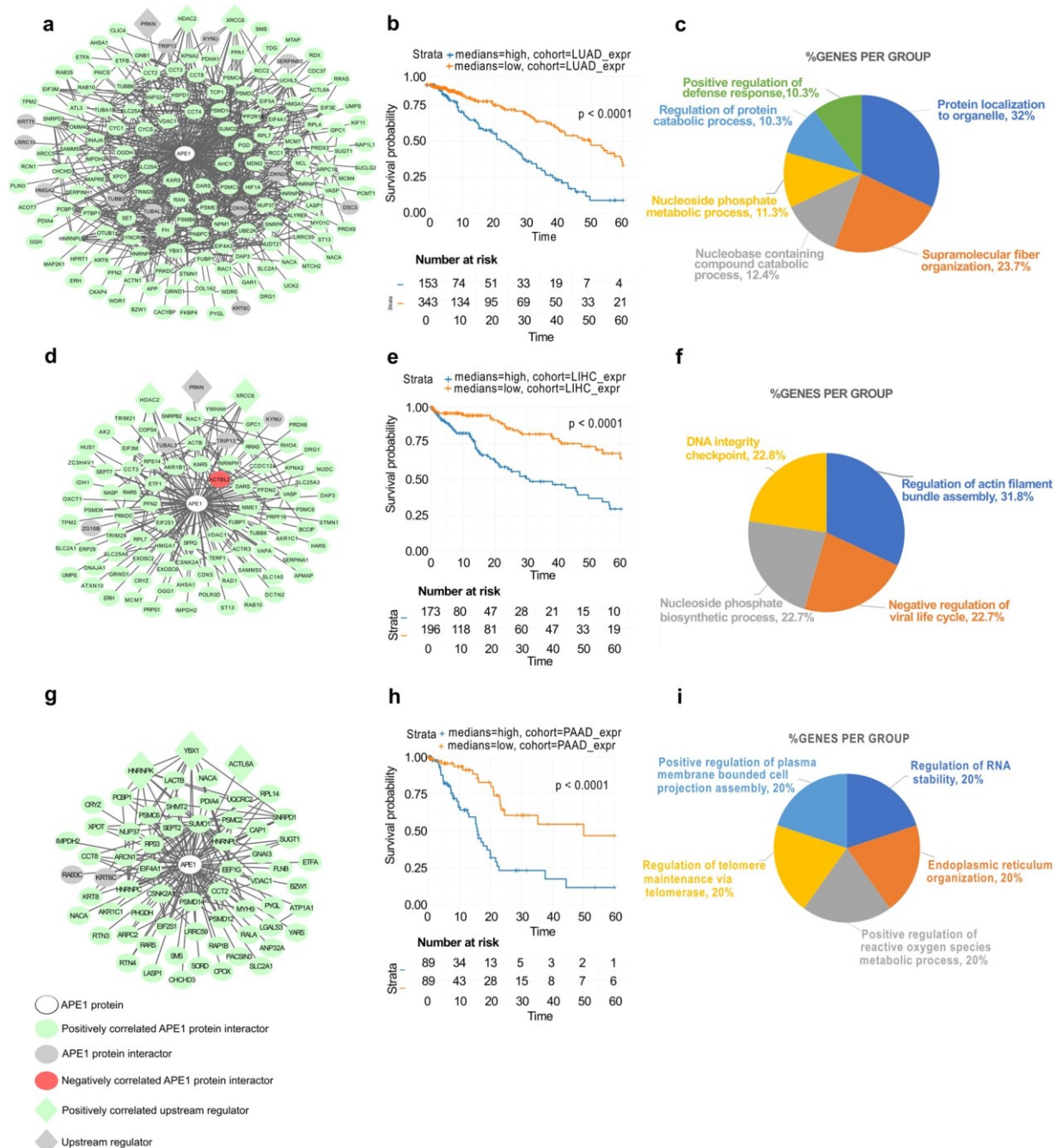


Figure 6. The most relevant cancer-specific prognostic subnetworks in the APE1 interactome. (**A,D,G**) Bad Prognosis networks of the LUAD (**A**), LIHC (**D**) and PAAD (**G**) datasets formed by the protein interactors of APE1. Circular nodes represent the interactors of APE1, while diamond nodes represent the top 3 upstream regulators of the network. APE1 is symbolized with the white color as the central node. Significant negatively correlated nodes are symbolized with the red color ($PCC < -0.6$), while the nodes having significant positive correlation ($PCC > 0.6$) are symbolized with the green color. Upstream regulators are symbolized with the purple color and the rest of the nodes are symbolized with the grey color. (**B,E,H**) Survival probability of the patients having high and low median expression of the gene signatures forming the overall networks, as represented by Kaplan-Meier plots. (**C,F,I**) Functional annotation of the Bad Prognosis networks based on Gene Ontology - Biological Process terms ($p < 0.05$). In the pie chart, the percentage of the genes enriched in the pathways is given next to the enriched terms.

general, the results of survival analysis emphasized the importance of the APE1-PPI network for real clinical data. Specifically, 84.3% of the genes ($n = 451$) present in the APE1-PPI network was associated with bad prognosis in one or more cancer datasets.

APE1-inhibitors sensitize cancer cells to mitochondrial toxicant Rotenone. In order to refine our study and to provide an additional level to the functional characterization of APE1-PPI, we finally performed a comparative bioinformatics analysis to define the cellular localization of DEGs, as obtained from the LIHC, LUAD and PAAD datasets. As shown in Fig. 7A, 24.4% of the DEGs in LIHC, 21.4% of the DEGs in LUAD and 16.8% of the DEGs in PAAD represented APE1-PPIs that can also localize to mitochondria. Interestingly, 89.7%, 90.4% and 62.5% of these DEGs were observed to be upregulated in the corresponding TCGA datasets. The mitochondrial compartments and expression trends associated with these DEGs are shown in Fig. 7B.

With the aim to support APE1 involvement in mitochondrial functionality, we performed a caspase activity assay upon treatment with Compound #3, an APE1 endonuclease inhibitor⁶⁶, in combination with rotenone, a well-known mitochondrial respiratory chain inhibitor⁶⁷. HeLa cells were treated with different concentrations of Compound #3 in the presence/absence of rotenone (at the doses of 0.5 μ M and 5 μ M) for 24 h (Fig. 7C) (Supplementary Fig. S12). HeLa cells treated with the combination of both compounds resulted more sensitive to apoptosis, demonstrating the existence of a synthetic lethality relation between APE1 and mitochondrial activity, which may be further explored for designing novel anticancer strategies.

Discussion

The multifunctional DNA repair protein APE1 is a central enzyme in the BER pathway, and it has also been involved in the regulation of cellular response to genotoxic damage via direct and indirect mechanisms. In addition to the primary roles of APE1 in DNA damage repair, emerging evidences indicate that APE1 may also control RNA metabolism processes and thus gene expression^{4,13,68}. In order to better clarify these novel functional aspects, we used well-established systems biology methods as optimal procedures to dissect/identify newly arising roles and possible mechanisms involving APE1. In this study, we focused on interactomic information obtained from previous studies^{4,12} as well as from novel experiments, which were performed using sensitive mass spectrometry technologies applied to the analysis of subcellular compartments. This allowed defining a final list containing 535 APE1-PPI elements that were finally subjected to a deep bioinformatics investigation.

Starting from this comprehensive list of proteins, the identification of direct and/or indirect interactions among APE1-binding partners was deduced, and a direct/indirect PPI network representing the global interactome of APE1 was constructed. This network, which was composed of 511 nodes and 3934 edges, retained a level of complexity that hampered the full understanding of the specific properties of each node. Therefore, a hub analysis was accomplished to define the top 30 nodes that were crucial for the communication of the whole network. Specifically, hub analysis was performed on betweenness centrality, a global metric that determines the involvement of each node in the information flow within the network. As a consequence, this method allowed the identification of the most informative proteins (hubs) for optimized therapeutic targeting in specific tumors (based on further bioinformatic analyses reported below). Among the most important hubs, APE1, SUMO1, SUMO2, TP53, ESR1, MDM2, PSMD4 and ACTB are worth mentioning (Fig. 3C). The resulting hub module was then analyzed with the Cytoscape plugin ClueGO to understand the role of these proteins in biological processes; the obtained results pointed to the involvement of these proteins mainly in DNA damage, mRNA stability and RNA splicing (Fig. 3D and Supplementary Table S4), indicating how these pathways were intertwined through the central role of APE1.

These data corroborated an emerging evidence in tumor biology; in fact, many DNA repair proteins are associated with those involved in RNA metabolism, thus proving a substantial role of the corresponding interactome networks in determining their non-canonical functions, which impact on gene expression in tumor cells³. These considerations emphasized the importance of understanding the regulatory behavior of APE1-interacting partners in various cancer datasets. To achieve this, the differential expression profiles and the gene expression correlations of APE1 and its interacting partners were calculated through the analysis of 33 TCGA datasets. The top 11 datasets with the highest number of differentially expressed genes, together with their correlation information, are represented as a bar chart in Fig. 4C. A very high percentage of differentially expressed genes was observed to have a significant prognostic potential, which was indicative for the relevance of these gene sets for related cancers (Fig. 5). These 11 gene sets were then subjected to survival analysis for a better understanding of their role according to a clinical perspective. LIHC, LUAD and PAAD networks, which were composed of bad prognostic genes in high percentages, confirmed previous studies on the important role of APE1 in these cancers^{52–55,57–65}. Kaplan-Meier estimation was used to calculate survival probability associated with these genes; the ones having significantly lower survival prognosis ($p < 0.05$) were used to create cancer-specific PPI subnetworks (Fig. 6 and Supplementary Figs. S4–S11). These cancer-specific bad prognostic network signatures unveiled potential protein interactor targets to be further probed by novel therapeutic approaches.

In addition, the top 11 datasets were used to perform the upstream regulators analysis for wider understanding of the regulatory events acting on the gene sets and the top 3 master regulator genes, as well as their involvement in the apoptotic, proliferative and resistance pathways, were characterized. Out of 11 datasets, XRCC6 was found to be one of the top 3 master regulators in 5 datasets (*i.e.* HNSC, LUAD, LIHC, SKCM and BRCA), together with its interacting partner XRCC5, which was the master regulator of 2 datasets (UVM and BLCA). XRCC6 and XRCC5 are coding the proteins Ku70 and Ku80, which form a molecular heterodimer involved in the initial step of the non-homologous end joining (NHEJ) pathway. Ring-shaped Ku complex directs DNA-dependent protein kinase catalytic subunit (DNA PKcs coded by PRKDC/XRCC7) to the DNA ends, and triggers its kinase activity for DNA repair⁶⁹. Interestingly, PRKDC was found among APE1 interactors as a component having a high correlation and bad survival prognosis in various datasets. It was previously reported that genetic variants of PRKDC play an important role in splicing regulation, causing mRNA instability⁷⁰. PRKDC and XRCC6 play an important role in the suppression of chromosomal rearrangements and in the maintenance of genome integrity, along with a significant function in the recognition and repair of double strand breaks⁷⁰. Therefore, their roles were studied in various cancers, such as breast^{71,72}, glioma⁷³, renal⁷⁴, hepatocellular^{75,76}, digestive⁷⁷, bladder⁷⁸ and lung⁷⁰ cancer.

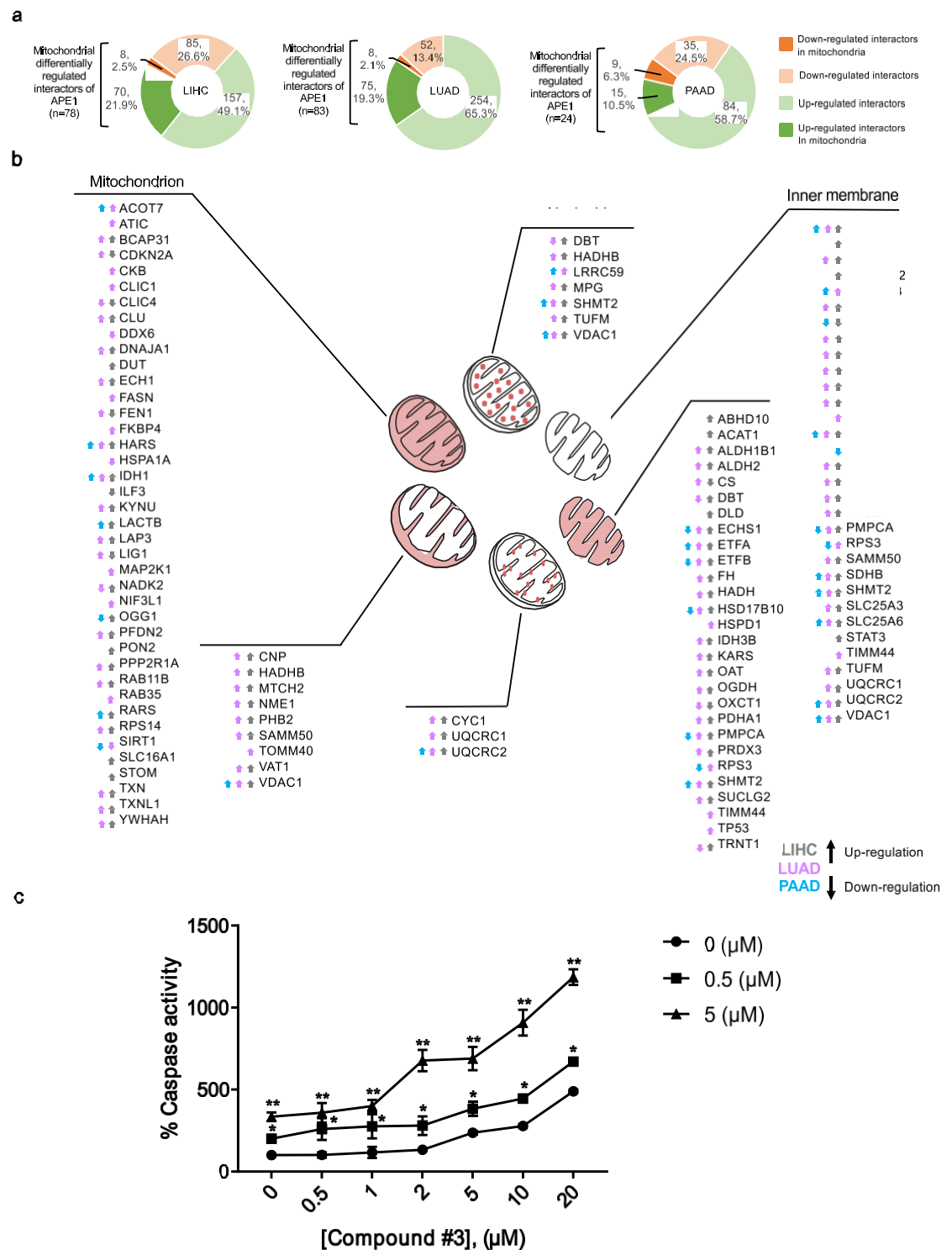


Figure 7. Differentially expressed APE1-PPIs in LIHC, LUAD and PAAD datasets point to the relevance of mitochondrial pathways impairment in cancer. **(A)** Differentially expressed APE1 interactors with mitochondrial localization. The colour codes are as follows: bright green colour for up-regulated DEGs that can localize to mitochondria, bright orange colour for down-regulated DEGs that can localize to mitochondria, light green and light orange colours for up- and down-regulated DEGs that do not localize to mitochondria, respectively. **(B)** Localization of DEGs in the mitochondrial compartments. Specific mitochondrial sub-compartmentalization of DEGs is shown. For each location, the global expression trend and dataset information is given with arrow and colour codes. Upside arrow represents up-regulation, while downside arrow represents down-regulation. The colour of the arrows represents the datasets as follows: grey colour for LIHC, purple colour for LUAD and blue colour for PAAD. **(C)** Inhibition of APE1 endonuclease activity in combination with treatment with rotenone sensitizes HeLa cells to apoptosis. Cells were treated with Compound #3 in the absence or presence of rotenone (0.5 and 5 μM), for 24h. The Apo-ONE assay was used to quantify relative levels of

apoptosis. The activities of caspases 3/7 were examined using a fluorescence-based assay. Data were normalized on untreated cells and represent the means \pm SD of three independent experiments. Asterisks represent a significant difference with respect to cells treated with Compound #3 alone. Data were evaluated statistically by two-tails Studentt-test.

On the other hand, Ku complex is known to interact with RECQL4 and to form a macromolecular assembly promoting NHEJ. A well-known RECQL4-binding partner, namely DDB1⁷⁹, was found to be one of the top 3 master regulators of 3 datasets (SKCM, BLCA and BRCA). DDB1 has been reported to be involved in the damage recognition step of the BER pathway⁸⁰, and to be correlated with a high risk when down-regulated in head and neck squamous cell carcinoma⁸¹. The oncogenic transcriptional factor of RECQL4, namely YB1 (coded by YBX1), was here recognized as an interacting partner of APE1 and a master regulator observed in KIRC, KIRP and PAAD datasets. YB1 was found to be overexpressed in various cancer types and frequently associated with poor outcome and chemotherapy resistance^{82,83}. It has also been reported to act as both an RNA- and DNA-binding protein, and as a component involved in miRNA processing^{45,84}. These findings underline the important involvement of APE1-centered prognostic networks mainly in DNA repair, with the association of RNA metabolism in various cancer types.

Among the remaining top regulators identified in this study, we also found some important genes that might give some clues about the general involvement of the APE1 interactome in the p53 signaling pathway. In particular, some of the top 10 master regulators that were associated with the p53 signaling pathway (*i.e.* NUA1, KDM1A, UBE2D1, RBX1 and UBE2M) deserved particular attention. For example, NUA1 is known to be involved in DNA damage response by phosphorylating p53 and participating in the transcriptional regulation of the *CDKN1A* promoter⁴⁶. Since NUA1 is phosphorylated by AKT⁴⁷, it has been hypothesized that this protein could be involved in acting between ATR and CDKN1A in response to low doses of UV irradiation⁴⁸. Analogously, the master regulator KDM1A (LSD1) was hypothesized to be a potential therapeutic target for the estrogen-regulated type I endometrial cancer because of its crucial role in the LSD1/cyclin D1/PI3K/AKT feedback loop⁴⁹. On the other hand, Zhou and colleagues recently reported that UBE2D1 facilitated the growth of hepatocellular carcinoma *in vitro* and *in vivo* by decreasing the p53 protein level in an ubiquitin-dependent manner⁵⁰. Interestingly, the master regulators UBE2M and RBX1 were also reported to have up-regulation together with other neddylation enzymes to highlight overexpression of the neddylation pathway in HCC⁵¹. In conclusion, our analysis of the global network indicated the relation of APE1 and its interactors with DNA repair mechanisms, and the possible involvement of the p53 signaling pathway, as confirmed by the identification of p53 binding sites among the significantly enriched TFBS located in the promoters of APE1-PPI genes. However, what associated the highest number of top regulators was their role in the apoptotic, proliferative and resistance pathways.

In order to further characterize the LIHC, LUAD and PAAD TCGA datasets, the corresponding DEGs were examined also considering their subcellular locations. As a result, 24.4% of DEGs in LIHC, 21.4% of DEGs in LUAD and 16.8% of DEGs in PAAD datasets pointed to the involvement of APE1-PPIs in mitochondria functionality (Fig. 7). For example, the bad prognostic gene *VDAC1* (voltage dependent anion channel 1), which is a multifunctional mitochondrial protein and an important regulator of cancer cell fate through its metabolic and energetic functions^{85,86}, was commonly up-regulated in all 3 datasets. Similarly, many other mitochondria-resident APE1-PPIs were found to be commonly up-regulated in the analyzed datasets. Among these, it is worth mentioning: (i) *SHMT2* (serine hydroxymethyltransferase), that mainly localizes to the matrix, nucleoid and inner membranes, and is known to be targeted by c-myc for cell survival, with various studies confirming its bad prognostic power in different cancer types^{87–91}; (ii) pro-apoptotic protein *SLC25A6* (mitochondrial ADP/ATP carrier-3, *AAC3*)^{92,93}; (iii) ROS regulating respiratory complex III protein *UQCRC2* (ubiquinol-cytochrome c reductase complex core protein 2)⁹⁴; (iv) respiratory complex II protein *SDHB* (succinate dehydrogenase B)⁹⁵; (v) fatty acid β -oxidation proteins *ETFA* (electron transfer flavoprotein subunit alpha)^{96,97} and *ACAA2* (acetyl-CoA acyltransferase 2)⁹⁸; (vi) bad prognostic multifunctional *LGALS3* (galectin-3) protein⁹⁹; (vii) autoimmunity protein *HARS* (histidyl-tRNA synthetase)¹⁰⁰; (viii) oxidative damage control protein *IDH1* (isocitrate dehydrogenase 1)¹⁰¹. Additional matrix proteins were found being up-regulated in LIHC and LUAD, while down-regulated in PAAD; they included fatty acid β -oxidation proteins *ECHS1* (enoyl coenzyme A hydratase short chain 1)¹⁰² and *ETFB* (electron transfer flavoprotein subunit beta)¹⁰³, multifunctional protein *17 β -HSD10* (17 β -hydroxysteroid dehydrogenase type 10, encoded by *HSD17B10*)¹⁰⁴ and mitochondrial protein processor *PMPCA* (mitochondrial-processing peptidase subunit alpha)¹⁰⁵. The relevance of APE1 function within mitochondria in tumor cells has recently been highlighted by our¹⁰⁶ and other publications¹⁰⁷, emphasizing a pivotal role for APE1 in mitochondrial-mediated signalling in cancer cells, thus opening new perspectives in cancer therapy.

Testing on a limited set of APE1-interacting partners, we previously observed that the APE1-interactome is dynamically regulated during genotoxic stress conditions⁴ with an enrichment of proteins involved in BER, while losing interaction with typical proteins involved in RNA metabolism. It would be interesting to extend this study to the whole APE1-PPI network described here. On the same track, it would be interesting to specifically evaluate the contribution of DNA and RNA molecules in modulating the APE1-PPI network dynamics. Information on the latter aspects may be obtained by characterizing the APE1-interactome before and upon the enzymatic removal of RNA and DNA. In conclusion and for the sake of clarity, we must state that this work is hypothesis generating and future studies will be needed to assess the function of APE1 in the protein complexes we discovered. Our current work is actually focused along these lines.

Materials and Methods

Cell line and materials. Inducible HeLa cell clones silenced for endogenous APE1 and reconstituted with the ectopic FLAG-tagged APE1 form were used¹¹. HeLa cell clones were grown in Dulbecco's modified Eagle's medium (Invitrogen, Monza, Italy) supplemented with 10% v/v fetal bovine serum (Euroclone, Milan, Italy), 100 U/ml penicillin, 10 µg/ml streptomycin sulphate, 3 µg/ml blasticidin, 100 µg/ml zeocine, 400 µg/ml geneticin (Invitrogen), and cultured in a humidified incubator containing a 5% CO₂ atmosphere, at 37 °C. For inducible APE1-shRNA experiments, doxycycline (1 µg/ml) (Sigma-Aldrich, St. Louis, MO) was added to the cell culture medium and cells were grown for 10 days. JHH-6 cells (undifferentiated hepatocellular carcinoma)³¹ were cultured in William's medium E (Sigma-Aldrich), while A549 (adenocarcinomic human alveolar basal epithelial cells)³² cells were cultured in RPM1 (Euroclone); both cell cultures were supplemented with 10% v/v fetal bovine serum, 100 U/ml penicillin, 10 µg/ml streptomycin sulphate. All cell lines were tested for mycoplasma contamination (N-GARDE Mycoplasma PCR Reagent, Euroclone).

Preparation of cell extracts and co-immunoprecipitation. Immunoprecipitation studies were carried out with whole cell extracts, and nuclear or cytoplasmic subfractions of HeLa cell clones as already reported^{11,108} (see Supplementary Material and Methods for details).

Immunofluorescence confocal and Proximity Ligation analyses. Immunofluorescence procedures and Proximity Ligation Assay (PLA) (Duolink, Sigma-Aldrich) were carried out as described earlier⁴. PLA was performed following the manufacturer's instructions. Cells were visualized through a Leica TCS SP8 confocal system (Leica Microsystems GmbH, Germany). See Supplementary Material and Methods for the list of the antibodies used.

Antibodies used and Western blotting analysis. For Western blotting analyses, cell lysates were resolved on 12% T SDS-PAGE, transferred onto nitrocellulose membranes (AmershamTM ProtranTM, GE Healthcare) and probed with the indicated antibodies (see Supplementary Material). The corresponding secondary antibodies labeled with IR-Dye (anti-rabbit IgG IRDye 680 and anti-mouse IgG IRDye 800) were used. Detection was performed with the Odyssey CLx Infrared imaging system (LI-COR GmbH, Germany). Protein bands were quantified using Odyssey software (Image Studio 5.0). Original uncropped images of western blots used in this study can be found in Supplementary Fig. S13.

Proteomic analysis. Immunopurified proteins from whole, nuclear and cytoplasmic cell extracts of HeLa cell clones expressing ectopic APE1 FLAG-tagged protein or stably transfected with the empty vector¹² (SCR) were analyzed in parallel by 12% T SDS-PAGE. As additional control experiment, identical cell extracts from HeLa cells expressing APE1 FLAG-tagged were also co-immunoprecipitated with a resin lacking the FLAG antibody (res). After staining with colloidal Coomassie blue, whole gel lanes from all samples were cut into 12 slices, minced and washed with water. Corresponding proteins were separately *in-gel* reduced, S-alkylated with iodoacetamide and digested with trypsin, as previously reported¹⁰⁹ and subjected to mass spectrometry analysis as detailed in Supplementary Material and Methods. A careful filtration for false positives ascertained in control samples (SCR and res) from whole, nuclear or cytoplasmic cell extracts allowed identifying APE1-binding proteins in APE1-FLAG co-immunoprecipitates from the corresponding cell extracts.

APE1-PPI network construction. The gene list of APE1-interacting partners was used to construct the corresponding PPI network by defining the interactions between the partners using the InWeb_InBioMap tool, applying the suggested parameters¹¹⁰. The APE1-PPI network was represented as an undirected graph (*i.e.*, nodes and edges symbolize proteins and interactions between them, respectively), and it was visualized via Cytoscape (v3.6.1)³⁸. The network enrichment analysis was performed using the ClueGO tool, using standard parameters¹¹¹. The hubs of the network were obtained by using the Cytohubba tool based on the global metric, betweenness centrality¹¹².

Transcription factor binding sites discovery. The FASTA-formatted sequences corresponding to the promoters (−2500, −1 nt from the TSS) of the 531 genes of the APE1 interactome were recovered using the “getfasta” command of the BEDTools toolset¹¹³. Sequences were analyzed using the LASAGNA-Search 2.0 tool to identify the presence of enriched transcription factor binding sites (TFBS); the matrix-derived model that used JASPAR CORE matrices was selected and the positions of the 145 TF models available were mapped for every promoter (Cutoff p-value: 0.001). For each promoter, the top10 results were then identified and used to provide the global counts of each TFBS in the analyzed dataset. Finally, the putative binding sites for TFs that underwent APE1 redox activity or that played their regulatory activity using APE1 as co-factor were represented as a network using Cytoscape, with node size corresponding to the number of identified binding sites.

Tumor datasets and differential gene expression analysis. The differential gene expression results from TCGA and normal datasets (GTEx data) for the genes encoding the proteins present in the APE1-PPI network were obtained via the GDC data portal hub (<https://portal.gdc.cancer.gov/>, last accessed July 2018). The RUVSeq package inside the R/Bioconductor environment was used to eliminate the batch effect coming from the combination of two data sources¹¹⁴. In order to better estimate the differentially expressed genes between the tumor and the normal corresponding datasets, we obtained “in-silico empirical” negative controls, *i.e.*, the least significantly DE genes based on a first-pass DE analysis performed prior to RUVg normalization¹¹⁴. Empirical Distribution analysis, Pearson correlations and Kolmogorov-Smirnov analyses were performed between the gene

expression profiles of APE1 and APE1-PPI elements in cancer patients or in the control groups using the *stats* package inside the R/Bioconductor environment. In particular, we compared the correlations of APE1 expression vs the PPI network genes expression with respect to: a) APE1 expression vs 100 sets with the same size of the PPI genes set composed by random genes; b) 100 random genes expressions vs the PPI network genes; c) APE1 expression vs all genes.

The analyses of the differentially expressed genes based on GO-CC (Gene Ontology-Cellular Component) was performed using the DAVID annotation tool¹¹⁵.

Survival analysis. For each TCGA dataset, differentially expressed genes (multiple correction adjustment using the Benjamini-Hochberg method, $p < 0.05$; absolute log fold change difference ≥ 1) corresponding to an interacting partner of APE1 were used to perform survival analysis. Kaplan-Meier plots were drawn using the R/TCGA Bioconductor package¹¹⁶, which uses maximally selected rank statistics (maxstat) to determine the optimal cutpoint for continuous variables. Division of the samples was done within the 30–70% percentile range of gene expression by the optimal cutpoint value. The Benjamini-Hochberg method was used for p-value correction of Kaplan-Meier plots.

Upstream regulators analysis. The set of genes corresponding to APE1 interactors having significant differential expression and significant bad survival prognosis was used to define cancer specific bad prognostic subnetworks of APE1 for the top 11 TCGA datasets. For each subnetwork, putative master regulators were identified by the TRANSPATH database (5.1.1.1)¹¹⁷ through the geneXplain platform (geneXplain web edition 4.11)¹¹⁸. Identified regulators (max radius: 4; Score cutoff: 0.2; FDR cutoff: 0.05; Z-score cutoff: 1.0) were sorted ascendingly based on the Ranks sum, reflecting a combination of sorting by Score and by Z-score. Upon sorting by Score from the biggest values to the lowest, a rank was assigned to the molecules (the molecule with the highest Score had rank 1). Upon independent sorting by Z-Score from the biggest values to the lowest, a rank was assigned to the molecules (the molecule with the highest Z-score had rank 1). Afterwards, for each molecule, the ranks upon sorting by Score and upon sorting by Z-Score were summed up, and the Ranks Sum was generated. The lower the Ranks sum, the more interesting the candidate molecule was, with good Score and good Z-score values. The same analysis was also repeated on the APE1-PPI network regardless of any differential expression analysis, survival probability and cancer type.

Caspase-3 activity assay. Caspase 3/7 activity levels were measured in a fluorescence-based assay using the Apo-One® Homogeneous Caspase 3/7 assay (Promega Corp., WI, USA). Assays were performed according to the manufacturer's recommendations. Four-thousands cells were plated onto black 96-well plates and the day after cells were treated with Compound #3⁶⁶ in the presence/absence of rotenone (R8875, Sigma-Aldrich) (0.5 μ M and 5 μ M), for 24 h. Fluorescence was measured at 521 nm by using a multi-well plate reader (Enspire 2300 Multilabel Reader, PerkinElmer). The values were standardized to wells containing media alone.

Data availability

The mass spectrometry proteomics data have been deposited to the ProteomeXchange Consortium via the PRIDE¹¹⁹ partner repository with the dataset identifier PXD013368. Reviewer account details: Username: reviewer03955@ebi.ac.uk Password: Rh2r9CaX.

Received: 12 May 2019; Accepted: 16 December 2019;

Published online: 08 January 2020

References

- Hein, N., Hannan, K. M., George, A. J., Sanij, E. & Hannan, R. D. The nucleolus: an emerging target for cancer therapy. *Trends Mol. Med.* **19**, 643–54 (2013).
- Hanahan, D. & Weinberg, R. A. Hallmarks of cancer: the next generation. *Cell* **144**, 646–74 (2011).
- Wickramasinghe, V. O. & Venkitaraman, A. R. RNA Processing and Genome Stability: Cause and Consequence. *Mol. Cell* **61**, 496–505 (2016).
- Antoniali, G. *et al.* Mammalian APE1 controls miRNA processing and its interactome is linked to cancer RNA metabolism. *Nat. Commun.* **8**, 797 (2017).
- Malfatti, M. C. *et al.* Abasic and oxidized ribonucleotides embedded in DNA are processed by human APE1 and not by RNase H2. *Nucleic Acids Res.* **45**, 11193–11212 (2017).
- Vohhodina, J., Harkin, D. P. & Savage, K. I. Dual roles of DNA repair enzymes in RNA biology/post-transcriptional control. *Wiley Interdiscip. Rev. RNA* **7**, 604–619 (2016).
- Jobert, L. & Nilsen, H. Regulatory mechanisms of RNA function: emerging roles of DNA repair enzymes. *Cell. Mol. Life Sci.* **71**, 2451–2465 (2014).
- Abbotts, R. *et al.* Targeting human apurinic/apyrimidinic endonuclease 1 (APE1) in phosphatase and tensin homolog (PTEN) deficient melanoma cells for personalized therapy. *Oncotarget* **5**, 3273–3286 (2014).
- Beraquist, B. R., McNeill, D. R. & Wilson, D. M. Characterization of abasic endonuclease activity of human Ape1 on alternative substrates, as well as effects of ATP and sequence context on AP site incision. *J. Mol. Biol.* **379**, 17–27 (2008).
- Barnes, T. *et al.* Identification of Apurinic/apyrimidinic endonuclease 1 (APE1) as the endoribonuclease that cleaves c-myc mRNA. *Nucleic Acids Res.* **37**, 3946–3958 (2009).
- Vascotto, C. *et al.* APE1/Ref-1 interacts with NPM1 within nucleoli and plays a role in the rRNA quality control process. *Mol. Cell Biol.* **29**, 1834–54 (2009).
- Vascotto, C. *et al.* Genome-wide analysis and proteomic studies reveal APE1/Ref-1 multifunctional role in mammalian cells. *Proteomics* **9**, 1058–74 (2009).
- Antoniali, G., Lirussi, L., Poletto, M. & Tell, G. Emerging roles of the nucleolus in regulating the DNA damage response: the noncanonical DNA repair enzyme APE1/Ref-1 as a paradigmatic example. *Antioxid. Redox Signal.* **20**, 621–639 (2014).
- Tell, G. & Demple, B. Base excision DNA repair and cancer. *Oncotarget* **6**, 584–585 (2015).

- 15 Kim, W.-C. *et al.* Characterization of the endoribonuclease active site of human apurinic/apyrimidinic endonuclease 1. *J. Mol. Biol.* **411**, 960–971 (2011).
- 16 Illuzzi, J. L. *et al.* Functional assessment of population and tumor-associated APE1 protein variants. *PLoS One* **8**, e65922 (2013).
- 17 Lirussi, L. *et al.* APE1 polymorphic variants cause persistent genomic stress and affect cancer cell proliferation. *Oncotarget* **7**, 26293–26306 (2016).
- 18 Vascotto, C. *et al.* Functional regulation of the apurinic/apyrimidinic endonuclease 1 by nucleophosmin: impact on tumor biology. *Oncogene* **33**, 2876–2887 (2014).
- 19 Poletto, M. *et al.* Role of the unstructured N-terminal domain of the hAPE1 (human apurinic/apyrimidinic endonuclease 1) in the modulation of its interaction with nucleic acids and NPM1 (nucleophosmin). *Biochem. J.* **452**, 545–557 (2013).
- 20 Zou, Q. *et al.* The human nucleophosmin 1 mutation A inhibits myeloid differentiation of leukemia cells by modulating miR-10b. *Oncotarget* **7**, 71477–71490 (2016).
- 21 Wang, K., Zhang, S., Weber, J., Baxter, D. & Galas, D. J. Export of microRNAs and microRNA-protective protein by mammalian cells. *Nucleic Acids Res.* **38**, 7248–7259 (2010).
- 22 Havelange, V. *et al.* Implications of the miR-10 family in chemotherapy response of NPM1-mutated AML. *Blood* **123**, 2412–2415 (2014).
- 23 Londero, A. P. *et al.* Expression and prognostic significance of APE1/Ref-1 and NPM1 proteins in high-grade ovarian serous cancer. *Am. J. Clin. Pathol.* **141**, 404–414 (2014).
- 24 Fan, X. *et al.* The expression profile and prognostic value of APE/Ref-1 and NPM1 in high-grade serous ovarian adenocarcinoma. *APMIS* **125**, 857–862 (2017).
- 25 Rommer, A. *et al.* Overexpression of primary microRNA 221/222 in acute myeloid leukemia. *BMC Cancer* **13**, 364 (2013).
- 26 Poletto, M. *et al.* Inhibitors of the apurinic/apyrimidinic endonuclease 1 (APE1)/nucleophosmin (NPM1) interaction that display anti-tumor properties. *Mol. Carcinog.* **55**, 688–704 (2016).
- 27 Barchiesi, A., Wasilewski, M., Chacinska, A., Tell, G. & Vascotto, C. Mitochondrial translocation of APE1 relies on the MIA pathway. *Nucleic Acids Res.* **43**, 5451–5464 (2015).
- 28 Fantini, D. *et al.* Critically lysine residues within the overlooked N-terminal domain of human APE1 regulate its biological functions. *Nucleic Acids Res.* **38**, 8239–56 (2010).
- 29 Cristini, A., Groh, M., Kristiansen, M. S. & Gromak, N. RNA/DNA Hybrid Interactome Identifies DXH9 as a Molecular Player in Transcriptional Termination and R-Loop-Associated DNA Damage. *Cell Rep.* **23**, 1891–1905 (2018).
- 30 Farg, M. A., Konopka, A., Soo, K. Y., Ito, D. & Atkin, J. D. The DNA damage response (DDR) is induced by the C9orf72 repeat expansion in amyotrophic lateral sclerosis. *Hum. Mol. Genet.* **26**, 2882–2896 (2017).
- 31 Fujise, K. *et al.* Integration of hepatitis B virus DNA into cells of six established human hepatocellular carcinoma cell lines. *Hepato gastroenterology* **37**, 457–460 (1990).
- 32 Foster, K. A., Oster, C. G., Mayer, M. M., Averv, M. L. & Audus, K. L. Characterization of the A549 cell line as a type II pulmonary epithelial cell model for drug metabolism. *Exp. Cell Res.* **243**, 359–366 (1998).
- 33 Abbasi, S. & Schild-Poulter, C. Mapping the Ku Interactome Using Proximity-Dependent Biotin Identification in Human Cells. *J. Proteome Res.* **18**, 1064–1077 (2019).
- 34 Shchepachev, V. *et al.* Defining the RNA interactome by total RNA-associated protein purification. *Mol. Syst. Biol.* **15**, e8689 (2019).
- 35 Moreira, P. I. *et al.* Nucleic acid oxidation in Alzheimer disease. *Free. Radic. Biol. Med.* **44**, 1493–1505 (2008).
- 36 Li, Y. *et al.* The N-cadherin interactome in primary cardiomyocytes as defined using quantitative proximity proteomics. *J. Cell. Sci.* **132** (2019).
- 37 Arifuzzaman, M. *et al.* Large-scale identification of protein-protein interaction of *Escherichia coli* K-12. *Genome Res.* **16**, 686–691 (2006).
- 38 Shannon, P. *et al.* Cytoscape: a software environment for integrated models of biomolecular interaction networks. *Genome Res.* **13**, 2498–2504 (2003).
- 39 Li, M. & Wilson, D. M. Human apurinic/apyrimidinic endonuclease 1. *Antioxid. Redox Signal.* **20**, 678–707 (2014).
- 40 Lee, C. & Huang, C.-H. LASAGNA-Search: an integrated web tool for transcription factor binding site search and visualization. *BioTechniques* **54**, 141–153 (2013).
- 41 Maurizio, E. *et al.* Translating Proteomic Into Functional Data: An High Mobility Group A1 (HMGA1) Proteomic Signature Has Prognostic Value in Breast Cancer. *Mol. Cell Proteom.* **15**, 109–123 (2016).
- 42 Vogel, C. & Marcotte, E. M. Insights into the regulation of protein abundance from proteomic and transcriptomic analyses. *Nat. Rev. Genet.* **13**, 227–232 (2012).
- 43 Wittschleben, B. O., Iwai, S. & Wood, R. D. DDB1-DDB2 (xeroderma pigmentosum group E) protein complex recognizes a cyclobutane pyrimidine dimer, mismatches, apurinic/apyrimidinic sites, and compound lesions in DNA. *J. Biol. Chem.* **280**, 39982–9 (2005).
- 44 Sugawara, K. Molecular mechanisms of DNA damage recognition for mammalian nucleotide excision repair. *DNA Repair. (Amst.)* **44**, 110–117 (2016).
- 45 Wu, S.-L. *et al.* Genome-wide analysis of YB-1-RNA interactions reveals a novel role of YB-1 in miRNA processing in glioblastoma multiforme. *Nucleic Acids Res.* **43**, 8516–8528 (2015).
- 46 Hou, X. *et al.* A new role of NIAK1: directly phosphorylating p53 and regulating cell proliferation. *Oncogene* **30**, 2933–2942 (2011).
- 47 Suzuki, A. *et al.* Identification of a novel protein kinase mediating Akt survival signaling to the ATM protein. *J. Biol. Chem.* **278**, 48–53 (2003).
- 48 Esteve-Puig, R. *et al.* A mouse model uncovers LKB1 as an UVB-induced DNA damage sensor mediating CDKN1A (p21WAF1/CIP1) degradation. *PLoS Genet.* **10**, e1004721 (2014).
- 49 Chen, C. *et al.* LSD1 sustains estrogen-driven endometrial carcinoma cell proliferation through the PI3K/AKT pathway via demethylating H3K9 of cyclin D1. *Int. J. Oncol.* **50**, 942–952 (2017).
- 50 Zhou, C., Bi, F., Yuan, J., Yang, F. & Sun, S. Gain of UBE2D1 facilitates hepatocellular carcinoma progression and is associated with DNA damage caused by continuous IL-6. *J. Exp. Clin. Cancer Res.* **37**, 290 (2018).
- 51 Yu, J. *et al.* Overactivated neddylation pathway in human hepatocellular carcinoma. *Cancer Med.* (2018).
- 52 Cheng, T.-L. *et al.* Induction of apurinic endonuclease 1 overexpression by endoplasmic reticulum stress in hepatoma cells. *Int. J. Mol. Sci.* **15**, 12442–12457 (2014).
- 53 Yang, Z. & Zhao, J. Effect of APE1 and XRCC1 gene polymorphism on susceptibility to hepatocellular carcinoma and sensitivity to cisplatin. *Int. J. Clin. Exp. Med.* **8**, 9931–9936 (2015).
- 54 Di Maso, V. *et al.* Transcriptional Up-Regulation of APE1/Ref-1 in Hepatic Tumor: Role in Hepatocytes Resistance to Oxidative Stress and Apoptosis. *PLoS ONE* **10**, e0143289 (2015).
- 55 Sun, Z. *et al.* Differential expression of APE1 in hepatocellular carcinoma and the effects on proliferation and apoptosis of cancer cells. *Biosci. Trends* **12**, 456–462 (2018).
- 56 Pascut, D. *et al.* Serum AP-endonuclease 1 (sAPE1) as novel biomarker for hepatocellular carcinoma. *Oncotarget* **10**, 383–394 (2018).
- 57 Zhang, S. *et al.* Serum APE1 as a predictive marker for platinum-based chemotherapy of non-small cell lung cancer patients. *Oncotarget* **7**, 77482–77494 (2016).

- 38 Yu, S.-N. *et al.* Evaluation of Prediction of Polymorphisms of DNA Repair Genes on the Efficacy of Platinum-Based Chemotherapy in Patients With Non-Small Cell Lung Cancer: A Network Meta-Analysis. *J. Cell. Biochem.* **118**, 4782–4791 (2017).
- 39 Thakur, S., Dhiman, M. & Mantha, A. K. APE1 modulates cellular responses to organophosphate pesticide-induced oxidative damage in non-small cell lung carcinoma A549 cells. *Mol. Cell. Biochem.* **441**, 201–216 (2018).
- 40 Lu, G.-S., Li, M., Xu, C.-X. & Wang, D. APE1 stimulates EGFR-TKI resistance by activating Akt signaling through a redox-dependent mechanism in lung adenocarcinoma. *Cell Death Dis.* **9**, 1111 (2018).
- 41 Jiang, Y., Zhou, S., Sandusky, G. E., Kelley, M. R. & Fishel, M. L. Reduced expression of DNA repair and redox signaling protein APE1/Ref-1 impairs human pancreatic cancer cell survival, proliferation, and cell cycle progression. *Cancer Invest.* **28**, 885–95 (2010).
- 42 Cardoso, A. A. *et al.* APE1/Ref-1 regulates STAT3 transcriptional activity and APE1/Ref-1-STAT3 dual-targeting effectively inhibits pancreatic cancer cell survival. *PLoS One* **7**, e47462 (2012).
- 43 Logsdon, D. P. *et al.* Regulation of HIF1 α under Hypoxia by APE1/Ref-1 Impacts CA9 Expression: Dual Targeting in Patient-Derived 3D Pancreatic Cancer Models. *Mol. Cancer Ther.* **15**, 2722–2732 (2016).
- 44 Shah, F. *et al.* APE1/Ref-1 knockdown in pancreatic ductal adenocarcinoma - characterizing gene expression changes and identifying novel pathways using single-cell RNA sequencing. *Mol. Oncol.* **11**, 1711–1732 (2017).
- 45 Logsdon, D. P. *et al.* Blocking HIF signaling via novel inhibitors of CA9 and APE1/Ref-1 dramatically affects pancreatic cancer cell survival. *Sci. Rep.* **8**, 13759 (2018).
- 46 Rai, G. *et al.* Synthesis, biological evaluation, and structure-activity relationships of a novel class of apurinic/aprimidinic endonuclease 1 inhibitors. *J. Med. Chem.* **55**, 3101–12 (2012).
- 47 Höglinger, G. U. *et al.* Dysfunction of mitochondrial complex I and the proteasome: interactions between two biochemical deficits in a cellular model of Parkinson's disease. *J. Neurochem.* **86**, 1297–1307 (2003).
- 48 Tell, G., Wilson, D. M. 3rd & Lee, C. H. Intrusion of a DNA repair protein in the RNome world: is this the beginning of a new era? *Mol. Cell Biol.* **30**, 366–71 (2010).
- 49 Karran, P. DNA double strand break repair in mammalian cells. *Curr. Opin. Genet. Dev.* **10**, 144–150 (2000).
- 50 Singh, A., Singh, N., Behera, D. & Sharma, S. Role of polymorphic XRCC6 (Ku70)/XRCC7 (DNA-PKcs) genes towards susceptibility and prognosis of lung cancer patients undergoing platinum based doublet chemotherapy. *Mol. Biol. Rep.* **45**, 253–261 (2018).
- 51 He, W. *et al.* The Ku70 -1310C/G promoter polymorphism is associated with breast cancer susceptibility in Chinese Han population. *Mol. Biol. Rep.* **39**, 577–583 (2012).
- 52 Nasiri, M., Saadat, I., Omidvari, S. & Saadat, M. Genetic variation in DNA repair gene XRCC7 (G6721T) and susceptibility to breast cancer. *Gene* **505**, 195–197 (2012).
- 53 Wang, L.-E. *et al.* Polymorphisms of DNA repair genes and risk of glioma. *Cancer Res.* **64**, 5560–5563 (2004).
- 54 Hirata, H. *et al.* Polymorphisms of DNA repair genes are associated with renal cell carcinoma. *Biochem. Biophys. Res. Commun.* **342**, 1058–1062 (2006).
- 55 Hsieh, Y.-H. *et al.* DNA double-strand break repair gene XRCC7 genotypes were associated with hepatocellular carcinoma risk in Taiwanese males and alcohol drinkers. *Tumour Biol.* **36**, 4101–4106 (2015).
- 56 Li, Z. *et al.* Genetic polymorphism of DNA base-excision repair genes (APE1, OGG1 and XRCC1) and their correlation with risk of lung cancer in a Chinese population. *Arch. Med. Res.* **42**, 226–34 (2011).
- 57 Yang, M.-D. *et al.* Predictive role of XRCC5/XRCC6 genotypes in digestive system cancers. *World J. Gastrointest. Oncol.* **3**, 175–181 (2011).
- 58 Wang, S.-Y. *et al.* Genetic variants of the XRCC7 gene involved in DNA repair and risk of human bladder cancer. *Int. J. Urol.* **15**, 534–539 (2008).
- 59 Lu, H. *et al.* Cell cycle-dependent phosphorylation regulates RECQL4 pathway choice and ubiquitination in DNA double-strand break repair. *Nat. Commun.* **8**, 2039 (2017).
- 60 Spivak, G. Nucleotide excision repair in humans. *DNA Repair. (Amst.)* **36**, 13–18 (2015).
- 61 Han, P. *et al.* Reduced mRNA expression of nucleotide excision repair genes in lymphocytes and risk of squamous cell carcinoma of the head and neck. *Carcinogenesis* **38**, 504–510 (2017).
- 62 Stein, U. *et al.* YB-1 facilitates basal and 5-fluorouracil-inducible expression of the human major vault protein (MVP) gene. *Oncogene* **24**, 3606–3618 (2005).
- 63 Wu, J., Stratford, A. L., Astanehe, A. & Dunn, S. E. YB-1 is a Transcription/Translation Factor that Orchestrates the Oncogenome by Hardwiring Signal Transduction to Gene Expression. *Transl. Oncogenomics* **2**, 49–65 (2007).
- 64 Suresh, P. S., Tsutsumi, R. & Venkatesh, T. YBX1 at the crossroads of non-coding transcriptome, exosomal, and cytoplasmic granular signaling. *Eur. J. Cell Biol.* **97**, 163–167 (2018).
- 65 Shoshan-Barmatz, V., Ben-Hail, D., Admoni, L., Krelm, Y. & Tripathi, S. S. The mitochondrial voltage-dependent anion channel 1 in tumor cells. *Biochim. Biophys. Acta* **1848**, 2547–2575 (2015).
- 66 Arif, T., Vasilkovskiy, L., Refaely, Y., Konson, A. & Shoshan-Barmatz, V. Silencing VDAC1 Expression by siRNA Inhibits Cancer Cell Proliferation and Tumor Growth *In Vivo*. *Mol. Ther. Nucleic Acids* **3**, e159 (2014).
- 67 Woo, C. C., Chen, W. C., Teo, X. Q., Radda, G. K. & Lee, P. T. H. Downregulating serine hydroxymethyltransferase 2 (SHMT2) suppresses tumorigenesis in human hepatocellular carcinoma. *Oncotarget* **7**, 53005–53017 (2016).
- 68 Zhang, L. *et al.* Prognostic and therapeutic value of mitochondrial serine hydroxyl-methyltransferase 2 as a breast cancer biomarker. *Oncol. Rep.* **36**, 2489–2500 (2016).
- 69 Wang, B. *et al.* Mitochondrial serine hydroxymethyltransferase 2 is a potential diagnostic and prognostic biomarker for human glioma. *Clin. Neurol. Neurosurg.* **154**, 28–33 (2017).
- 70 Lee, G. Y. *et al.* Comparative oncogenomics identifies PSMB4 and SHMT2 as potential cancer driver genes. *Cancer Res.* **74**, 3114–3126 (2014).
- 71 Antonov, A. *et al.* Bioinformatics analysis of the serine and glycine pathway in cancer cells. *Oncotarget* **5**, 11004–11013 (2014).
- 72 Zamora, M., Granell, M., Mampel, T. & Viñas, O. Adenine nucleotide translocase 3 (ANT3) overexpression induces apoptosis in cultured cells. *FEBS Lett.* **563**, 155–160 (2004).
- 73 Gallerne, C. *et al.* The fourth isoform of the adenine nucleotide translocator inhibits mitochondrial apoptosis in cancer cells. *Int. J. Biochem. Cell Biol.* **42**, 623–629 (2010).
- 74 Aguilera-Aguirre, L. *et al.* Mitochondrial dysfunction increases allergic airway inflammation. *J. Immunol.* **183**, 5379–5387 (2009).
- 75 Saxena, N. *et al.* SDHB-Deficient Cancers: The Role of Mutations That Impair Iron Sulfur Cluster Delivery. *J. Natl. Cancer Inst.* **108** (2016).
- 76 Muller, F. L., Liu, Y. & Van Remmen, H. Complex III releases superoxide to both sides of the inner mitochondrial membrane. *J. Biol. Chem.* **279**, 49064–49073 (2004).
- 77 Toogood, H. S., Levs, D. & Scrutton, N. S. Dynamics driving function: new insights from electron transferring flavoproteins and partner complexes. *FEBS J.* **274**, 5481–5504 (2007).
- 78 Miltiadou, D. *et al.* Variants in the 3' untranslated region of the ovine acetyl-coenzyme A acyltransferase 2 gene are associated with dairy traits and exhibit differential allelic expression. *J. Dairy Sci.* **100**, 6285–6297 (2017).
- 79 Wang, H. *et al.* LGALS3 Promotes Treatment Resistance in Glioblastoma and Is Associated with Tumor Risk and Prognosis. *Cancer Epidemiol. Biomarkers Prev.* **28**, 760–769 (2019).

- 10 Freist, W., Verhey, J. F., Rühlmann, A., Gauss, D. H. & Arnez, J. G. Histidyl-tRNA synthetase. *Biol. Chem.* **380**, 623–646 (1999).
- 11 Khurshed, M. *et al.* IDH1-mutant cancer cells are sensitive to cisplatin and an IDH1-mutant inhibitor counteracts this sensitivity. *FASEB J.* **fi201800547R** (2018).
- 12 Zhu, X.-S. *et al.* Attenuation of enoyl coenzyme A hydratase short chain 1 expression in gastric cancer cells inhibits cell proliferation and migration *in vitro*. *Cell. Mol. Biol. Lett.* **19**, 576–589 (2014).
- 13 Ruiz-Pinto, S. *et al.* Exome array analysis identifies ETFB as a novel susceptibility gene for anthracycline-induced cardiotoxicity in cancer patients. *Breast Cancer Res. Treat.* **167**, 249–256 (2018).
- 14 Yang, S.-Y. *et al.* Roles of 17 β -hydroxysteroid dehydrogenase type 10 in neurodegenerative disorders. *J. Steroid Biochem. Mol. Biol.* **143**, 460–472 (2014).
- 15 Ioshi, M. *et al.* Mutations in the substrate binding glycine-rich loop of the mitochondrial processing peptidase- α protein (PMPCA) cause a severe mitochondrial disease. *Cold Spring Harb. Mol. Case Stud.* **2**, a000786 (2016).
- 16 Codrich, M. *et al.* Inhibition of APE1-endonuclease activity affects cell metabolism in colon cancer cells via a p53-dependent pathway. *DNA Repair. (Amst.)* **82**, 102675 (2019).
- 17 Li, M. *et al.* Human AP endonuclease/redox factor APE1/ref-1 modulates mitochondrial function after oxidative stress by regulating the transcriptional activity of NRF1. *Free. Radic. Biol. Med.* **53**, 237–248 (2012).
- 18 Antoniali, G., Marcuzzi, F., Casarano, E. & Tell, G. Cadmium treatment suppresses DNA polymerase δ catalytic subunit gene expression by acting on the p53 and Sp1 regulatory axis. *DNA Repair. (Amst.)* **35**, 90–105 (2015).
- 19 Spreafico, A. *et al.* A proteomic study on human osteoblastic cells proliferation and differentiation. *Proteomics* **6**, 3520–3532 (2006).
- 20 Li, T. *et al.* A scored human protein-protein interaction network to catalyze genomic interpretation. *Nat. Methods* **14**, 61–64 (2017).
- 21 Bindea, G. *et al.* ClueGO: a Cytoscape plug-in to decipher functionally grouped gene ontology and pathway annotation networks. *Bioinformatics* **25**, 1091–1093 (2009).
- 22 Chin, C.-H. *et al.* cytoHubba: identifying hub objects and sub-networks from complex interactome. *BMC Syst. Biol.* **8**, S11 (2014).
- 23 Quinlan, A. R. & Hall, I. M. BEDTools: a flexible suite of utilities for comparing genomic features. *Bioinformatics* **26**, 841–842 (2010).
- 24 Risso, D., Ngai, J., Speed, T. P. & Dudoit, S. Normalization of RNA-seq data using factor analysis of control genes or samples. *Nat. Biotechnol.* **32**, 896–902 (2014).
- 25 Huang, D. W., Sherman, B. T. & Lempicki, R. A. Systematic and integrative analysis of large gene lists using DAVID bioinformatics resources. *Nat. Protoc.* **4**, 44–57 (2009).
- 26 Kosinski, M. & Biecek, P. *RTCGA: The Cancer Genome Atlas Data Integration. R package version 1.8.0*, <https://rtcga.github.io/RTCGA>.
- 27 Krull, M. *et al.* TRANSPATH: an information resource for storing and visualizing signaling pathways and their pathological aberrations. *Nucleic Acids Res.* **34**, D546–551 (2006).
- 28 Kolpakov, F., Poroikov, V., Selivanova, G. & Kel, A. GeneXplain — Identification of Causal Biomarkers and Drug Targets in Personalized Cancer Pathways. *J. Biomol. Tech.* **22**, S16 (2011).
- 29 Perez-Riverol, Y. *et al.* The PRIDE database and related tools and resources in 2019: improving support for quantification data. *Nucleic Acids Res.* **47**, D442–D450 (2019).

Acknowledgements

Authors thank Gianfranco Novi for technical assistance, Prof. Alexander Kel and the geneXplain team for the generous help in the upstream analysis, and Prof. Alessandro Quattrone for the support from the CIBIO Core Facilities scientific research. This work was supported by grants from Associazione Italiana per la Ricerca sul Cancro (AIRC) (IG19862) to G. Tell and from Regione Campania, PO FESR 2014–2020 – Obiettivo specifico 1.2 - “Manifestazione di interesse per la realizzazione di Technology Platform nell’ambito della lotta alle patologie oncologiche” for the project “Sviluppo di approcci terapeutici innovativi per patologie neoplastiche resistenti ai trattamenti (SATIN)” to A.S. This work was supported by grants from Associazione Italiana per la Ricerca sul Cancro (AIRC) (IG19862) to G. Tell, and Programma Operativo Regionale Campania FESR 2014–2020, asse 1 OO.SS. 1.2.2/1.1.2 (SATIN - Sviluppo di approcci terapeutici innovativi per patologie neoplastiche resistenti ai trattamenti) to A. Scaloni.

Author contributions

G.T. designed and conceived the study and supervised the experiments; G.A. performed most of the wet lab experiments, analyzed the data and critically contributed to the interpretation of the results; G.M. performed the PLA analysis on JHH6 cell line; G.A., C.D.A. and A.S. carried out the proteomic analysis; D.A., E.D., S.P. performed the bioinformatics analysis of all the proteomics and genomics datasets; G.T., D.A., S.P. and G.A. mainly wrote the manuscript; E.D. and A.S. provided critical comments and suggestions and contributed to the interpretation of the results and writing of the manuscript. All authors critically read and approved the final version of the manuscript.

Competing interests

The authors declare no competing interests.

Additional information

Supplementary information is available for this paper at <https://doi.org/10.1038/s41598-019-56981-z>.

Correspondence and requests for materials should be addressed to G.T. or S.P.

Reprints and permissions information is available at www.nature.com/reprints.

Publisher’s note Springer Nature remains neutral with regard to jurisdictional claims in published maps and institutional affiliations.



Open Access This article is licensed under a Creative Commons Attribution 4.0 International License, which permits use, sharing, adaptation, distribution and reproduction in any medium or format, as long as you give appropriate credit to the original author(s) and the source, provide a link to the Creative Commons license, and indicate if changes were made. The images or other third party material in this article are included in the article's Creative Commons license, unless indicated otherwise in a credit line to the material. If material is not included in the article's Creative Commons license and your intended use is not permitted by statutory regulation or exceeds the permitted use, you will need to obtain permission directly from the copyright holder. To view a copy of this license, visit <http://creativecommons.org/licenses/by/4.0/>.

© The Author(s) 2020